The role of NKR-P1:Clr family interactions in murine cytomegalovirus infection

by

Oscar Alberto Aguilar

A thesis submitted in conformity with the requirements
for the degree of Doctor of Philosophy
Department of Immunology
University of Toronto

The role of the NKR-P1:Clr family interactions in murine cytomegalovirus infection

Oscar A. Aguilar
Doctor of Philosophy

Department of Immunology
University of Toronto

Abstract

Natural killer (NK) cells play a key role in innate immunity by detecting alterations in self and non-self ligands *via* paired NK cell receptors (NKR). Here, an MHC-I-independent NK cell recognition mechanism that involves modulation of NKR-P1:Clr receptor-ligand function upon mouse cytomegalovirus (MCMV) infection is characterized. Expression of host "self" Clr-b ligand is rapidly lost on MCMV-infected cells, invoking "missing-self" NK recognition. Cross-species viral infections using rodent fibroblasts suggest this response is evolutionarily conserved. Active viral infection is necessary for Clr-b loss, as inactivated virus and innate signalling agonists fail to elicit Clr-b downregulation. Clr-b loss is partially blocked by cycloheximide, suggesting early viral or nascent host proteins are required for Clr-b downregulation.

Further investigation using CD3ζ/NKR-P1 reporter cell assays identified a novel Clr-b-independent MCMV-encoded decoy immunoevasin, m12, that directly engages the paired NKR-P1A/B/C receptor clade. Thus, MCMV m12 is the first physiological ligand for the prototypical NK1.1 orphan receptors (NKR-P1B/C). MCMV m12 restrains NK effector function by directly engaging the inhibitory NKR-P1B receptor. However, m12 also interacts with the activating NKR-P1A/C receptors to counterbalance m12 decoy function. Independent structural analyses

reveal that m12 is IgV-like and sequesters a large surface area of the C-type lectin-like NKR-P1 protein via a "polar claw" docking mechanism. Polymorphisms in, and ablation of, the viral m12 protein and host NKR-P1B/C alleles impact NK cell responses *in vivo*. This work identifies the long-sought foreign ligand for this key immunoregulatory NKR family and reveal how it controls the evolutionary balance of immune recognition during host-pathogen interplay.

Additional work provides evidence that the MCMV m153 immunoevasin stabilizes host Clr-b surface levels. In contrast, infections using m153-deficient MCMV mutants show exacerbated Clr-b downregulation. Importantly, enhanced Clr-b loss by MCMV Δm153-mutant infection is reversed by exogenous m153 complementation. Intracellular m153 localization suggests the Clr-b stabilization effect may be indirect. This is confirmed by m153 tetramer staining of dendritic cells, and *in vivo* analyses showing that Δm153 MCMV exhibits enhanced virulence, in an Nkrp1b/Clrb-independent manner. Thus, m153 may bind an activating immunoreceptor. Together, these data demonstrate that the NKR-P1:Clr recognition axis is subverted by multiple MCMV immune evasion strategies.

Dedication

A las hijas y los hijos de guerra. To the lives that were robbed of an opportunity to thrive due to violence, not only in Latin America, but also throughout the world. To my ancestors who have suffered for centuries (Cuzcatlecos, Pipiles, Mayas, y Lencas), who recently suffered a brutal military dictatorship from 1930-1990's, and importantly, to the future generations who continue to experience ongoing violence. Algun dia, este mundo va cambiar.

Acknowledgments

First and foremost, I would like to thank Prof. James Carlyle for giving me the opportunity to work in his laboratory. I realize that he was taking a risk on a student with very little immunology training. I am truly thankful for the support that was given since day 1, from giving me the freedom to pursue any scientific question in the lab, throwing money into expensive experiments, and encouraging my scientific development. Importantly, for also being supportive of all the extra-curricular activities I was involved in – these activities kept me sane and provided me with motivation that I channeled into my work. An important lesson that I will be taking with me, is that you taught me to *challenge* authority – this was a valuable lesson because it is not often you will find a mentor who will push you to push *them*, but Jim, you did and this has made me a more confident scientist. Also, thank you for encouraging the participation at conferences, the places we have visited are memories that I will always be grateful for – especially NK2016 (Sicily) and ICI2016 (Melbourne) – we showed the international community what Canadian Immunology is capable of! I wish you, and your family nothing but the best.

Secondly, Dr. David (David Allan). You were an incredible mentor throughout my studies, and an inspiring scientist. Your level-headed approach not only to science, but also during personal troubles were instrumental in navigating this experience. All those late nights discussing science, troubleshooting, and supporting my crazy ideas were great learning experiences. Your ability to produce great quality data is something that I always strived for, and although I am not at your level yet – I hope to get there one day.

Next, I would like to state that none of the work in this thesis would have been possible without collaborations with scientists around the world. Importantly, the ones we picked up along the way. There are four laboratories that I would like to highlight here (in chronological order). First, Prof. Stipan Jonjić, thank you for welcoming me into your laboratory back in November of 2012 and giving me the opportunity to engage in this fruitful collaboration. I also thank the entire lab, but in particular, Branka, Astrid, Eddie, Dijana, and Johanna. Secondly, Prof. Andrew Makrigiannis, thank you for welcoming me into your lab numerous times over the years, and especially during that crucial (and hectic) time when you were relocating your lab. I also thank the entire "Mak lab" for the science talks and great laughs, specially Dr. Munir Rahim – you were supportive from our first interaction and I learned a great deal from you, and Dr. Megan Tu – you were instrumental in the final stretch, and I truly appreciate your modesty, although I still owe you at least a coffee! Third, Prof. Margulies and Dr. Tiluhun for key reagents and ongoing collaborations. Last but not least, Dr. Richard Berry and Prof. Jamie Rossjohn – Richard, thank you for *forcing* us to collaborate with you, this has been an incredible experience and I'm grateful for the scientific discussions, projects, and for the laughs we shared over drinks overlooking the Mediterranean and in Melbourne. Prof. Rossjohn, thank you for your support – your support of my work was truly inspiring, and confirmed that we were right in *fighting* to get our work out.

I thank all the organizations that supported me as a young scientist. This includes funding agencies: NSERC for awarding me a PGS-D scholarship, and CIHR and BWF for funding our scientific pursuits. Importantly, I want to also thank the societies who provided a welcoming and supportive environment: the Canadian Immunologists (CSI), the North American Immunologists (AAI), and the NK biologists (SNI).

I am also truly grateful to the entire Department of Immunology at the University of Toronto. This includes my committee members, Prof. Alberto Martin and Prof. Stephen Girardin, whose advice during meetings was key in steering me throughout my studies. Also, the professors who I had the pleasure to work with: Prof. Watts, Prof. Philpott, and Prof. Rast. Thank you to all the faculty members (and post-doctoral fellows) who also offered encouragement and advice. I also thank the department for awarding me the Miller Award, I am truly humbled by this. A special thanks to IGSA and the graduate students of the department (too many to name here). I have always been proud to be a colleague to so many inspiring people – I wish you all the best!

To the Carlyle lab family. Jason, thank you for making sure I was involved in IGSA and providing a welcoming ambience throughout the department from the beginning. Tina, for maintenance of the lab and making sure we had proper regular celebrations for our achievements. Mobin, for reminding me why it is important to excel in science, specifically what it means for students coming from war-torn countries. Ali, for providing a great sense of humor and making work (and home) an enjoyable experience. Linda, for the laughs and making sure that I remain grounded by highlighting my defects. Anuisa, for the laughs, energy, and making time to hang out with us boring graduate students, we always knew you had better things to do, but we appreciated your company. Tyler, for the stories and laughs and unique perspective. William, for laughing at my lame jokes. Natacha, for reminding me that I need to practice my French more often, and pushing me to be a better mentor. Peter, for being supportive from the beginning, the insightful discussions on NK cell biology, and for providing me with refuge in my times of need. Miho, for always being there through the good and the bad and for your help during these times – whether it be with personal or with scientific ones. Also, for the 10-minutes laughing sessions. Now, onto team Aruz: Dr. Mesci, thank you for being enjoyable to work with and making sure we had a good laugh throughout our days. It was a pleasure to work with you, but it's been an even greater pleasure to be your friend. You are a great husband and father and can't wait to see what your son achieves! Jaehun, thank you for putting a smile on my face in the worst of times, for the help in the lab whenever I was overwhelmed, and for always making yourself available when beer and wings were involved. To my trainees: Tim, not only were you my first student in the lab, but you were also my teacher. The m12 story would not have been possible without your insights from the RNA-Seq experiments. Jacky, you were exceptional at SALO and proved to be exceptional in the lab, thank you for making sure I stayed sane and providing the lab with a pleasant atmosphere. Isabella, I thank you for pushing me, and making sure I was on my "A" game by challenging me scientifically. Also, thank you for the delicious Caipirinhas and Brigadeiros! Collectively, I wish everyone who has pipetted at S206B the very best in their future endeavours!

I want to thank the various people at Sunnybrook who made the work possible, and enjoyable. This includes the SRI flow facility (Gisele, Geneve, Courtney and Vincent), the Genomics Core (Yutaka), admin staff (Sue, Melanie), and support staff (Neil, Aaron, Damien, Ronald, and David). A special thanks to all the friends at SRI – especially those who were instrumental in creating the soon to be contender to Barcelona FC and Real Madrid, *Sunnybrook FC*. There are too many members to name here but a special thanks to the core (Chris, Christian, Nathan, Elizabeth, Michael, Lily, Kabir, Ashton, Kogulan, Mahmoud, Kevin, and Yacine). These soccer sessions provided much needed exercise and I look forward to seeing how influential this movement becomes. Also, Annabelle, thank you for being yourself and for the joyful company you provide, along with the delicious treats.

To everyone who welcomed me into their lives and communities during my non-scientific endeavours, offering distinct perspectives, while sharing in so many great experiences. This includes the people at Let's Talk Science who were always supportive of my vision for Immunology day, and providing me with the necessary resources. To all the grad students (and some post-docs) who helped run Immunology Day while I was the coordinator. A very special thanks to LTS members involved in the Sandy Lake initiative (Julie, Shannon, Peter, Zoe, Elsa, Adam, Caitlin, and Olivia), and most important, to the beautiful Sandy Lake First Nation community for welcoming us and teaching us so much about *life*. I am humbled and grateful for this experience. Gary and Starsky, I carry the honour you granted me to the heart and cannot thank you enough. I hope to return and give back in a greater capacity. Lastly, to a special group of people who I will hold dear forever: the SALO community, who provided so much during the toughest times of the PhD. A special thanks to Francisco, Camilla, Avila, Kate, Diego, Jacky, Madelaine, Alex, and the rest of students and tutors/mentors. SALO was always the highlight of my weeks – and this would not have been possible without the many people who were involved in making it what it was. Francisco, thank you for teaching me the importance of feeling "uncomfortable" during discussions – this is how progress is truly advanced. You were also the one who taught me that there is absolutely nothing wrong with writing a long acknowledgment section, because nobody achieves a PhD in isolation, this is due to numerous individuals who have contributed in different degrees at different stages along the way.

My love for science would not have been possible without the support of people who first gave me the opportunity to do research. This was my MSc supervisor, Prof. Ken Storey. Thank you for taking a chance on a bike technician working at Canadian Tire. Thank you to the Storey lab who demonstrated that you can do great science, while having fun in the lab. Going back, this takes me to the first person who advocated for me to be given such an opportunity, this is Dr. Tarek Abd El Halim, who at the time was my lab partner in undergraduate lab classes – thank you for your friendship at every step of the way. You have always been an inspiration to me.

Very special thanks also to Madelaine Cahuas and the entire Cahuas and Sandu family. You were all like a family for me in Toronto, and I have many memories which I will forever cherish. Not only did you provide delightful conversation, incredible feasts filled with laughter, but also welcomed me like one of your own. I wish you all the very best and will always love you all. Madelaine, a very special thank you for your love and support, for the times you forced me out of the lab, for taking care of me, the vacations, the delicious meals, the laughs, the parties, the music, the conquered Netflix series, the sharing of experiences and dreams, the activism, the analyses, etc... I can go forever… you taught me a great deal and inspired me to be a better person. Thank you for all the wonderful memories – you truly made the PhD a much more pleasant experience. Otra cosa, siempre recuerda que somos ¡*ganadores*! *Abrazos*.

Now, a la *familia*. I cannot thank everyone in my family enough for everything they have done, and will have to keep it short and sweet. To my parents, thank you for sacrificing everything you had back in El Salvador so that your sons could have an opportunity in Canada. Thank you for pushing me to pursue an *education*, your teachings will live on through us, and will be passed on to future generations. Tío Salvador aka tío Chamba, thank you for teaching me that laughter is the best medicine. My brothers, Orlando y Juan, thank you for always providing me with the support I needed throughout the years, for having my back, for believing in me, and for "holding it down" in la casita when I left the nest. *Hermanos*, you have motivated me in more ways you will ever know. My nephews, Alejandro y Xavier, you two have been a source of inspiration during the toughest times, know that the sacrifices that I have made have been with

you in mind. Megan, for the support, laughs and welcoming us into your *family*. Abuelita Carmen, gracias por ser la persona que eres y por tener ese gran corazón, your loving and understanding nature is the reason why your sons, daughters, and grandchildren have such patient, loving, and giving characters. My brother Moises, the story of your life has also been source for my perseverance – it is a reality for many Salvadoreños, and it has kept me motivated throughout my studies – not only for you, but for all those children from Sivar that never received the opportunities I was given.

Thank you to the rest of the Aguilar and Alfaro family, all my tíos, tías, primos y primas in Chicago, Miami, Montreal, Kingston, Ottawa, and El Salvador: you all know who you are. Importantly, for the family members that are no longer with us - from the family members we lost during the war: abuelita Ofelia y tío Jorge; and others that left us since (abuelo Bonifacio y varios tíos): you will always live through us. Importantly, during my PhD, we lost several pillars of the family: abuelo Valeriano, tío Juan, and recently, tío Manuel y tío Fermin. I have to highlight nuestro tío Manuel for taking care of la familia during the some of the most turbulent times of our lives. Tío, you consistently showed me to lead by example, and I'm doing my best to follow your lead. Tío Fermin, thank you for teaching me to enjoy life, and to remain humble. A todos, thank you for showing us to appreciate life and to above all else take care of each other, *la familia siempre es primero*. *Gracias por sus ejemplos, sacrificios y sus enseñanzas*.

A la cherada con raíces en la colonia El Sauce in Soyapango! Nunca me olvido de ustedes – un gran saludo y gracias por siempre hacerme sentir como si nunca me fui. Yo nunca me olvidaré de dónde vengo y cargo el orgullo Soyapaneco, Salvadoreño, y Cuzcatleco dondequiera que ande.

Lastly, I would like to thank all the artists that kept me company while conducting the experiments. Some special thanks to Larcenist, Pescozada, Joaquin Santos, Conflikto Armado, DaInkPusha/Most, Kinto Sol, Immortal Technique, Calle 13, Nas, Lupe Fiasco, and of course, Silvio Rodriguez. Also, Óscar Martínez, and many other journalists whose writing and analysis is a voice of hope in El Salvador, and the world.

In case I have missed anyone, please accept my humble apologies and be sure to call me out on it.

Table of Contents

List of Tables

List of Figures

List of Appendices

List of Abbreviations

ACK	ammonium-chloride-potassium
ActD	actinomycin D
ADCC	antibody-dependent cellular cytotoxicity
AICL	activation induced C-type lectin
AIDS	acquired immunodeficiency syndrome
AIM2	absent in melanoma 2
AIRL	antibody-induced redirected lysis
ADP	adenosine di-phosphate
AMP	adenosine mono-phosphate
APC	allophycocyanin
ATP	adenosine tri-phosphate
β_2m	beta-2-microglobulin
CD	cluster of differentiation
CHX	clycoheximide
cDNA	complementary DNA
Clec	C-type lectin
CLP	common lymphoid progenitor
Clr	C-type lectin-related
CMV	cytomegalovirus
CPRG	chlorophenol-red-β-D-galactopyranoside
CTL	C-type lectin
DAI	DNA-dependent activator of IFN-regulatory factors
DC	dendritic cell
DNA	deoxyribonucleic acid
DR	death receptor
dsDNA	double-stranded DNA
E	early
EC	extracellular
ECTV	ectromelia virus

EGFP	enhanced green fluorescent protein
ER	endoplasmic reticulum
FcR	Fc receptor
GFP	green fluorescent protein
gp	glycoprotein
HCMV	human cytomegalovirus
HIV	human immunodeficiency virus
HHR	hammerhead ribozyme
IE	immediate early
IFN	interferon
IFN-I	type I interferon
IFNAR	interferon-α receptor
Ig	immunoglobulin
IL	interleukin
ILC	innate lymphoid cell
IP	immunoprecipitation
IRF	interferon regulatory factor
ITAM	immunoreceptor tyrosine-based activation motif
ITIM	immunoreceptor tyrosine-based inhibition motif
ITSM	immunoreceptor tyrosine-based switch motif
KACL	keratinocyte-associated C-type lectin
KIR	killer immunoglobulin-like receptor
KLR	killer lectin-like receptor
L	late
LAK	lymphokine-activated killer
LCMV	lymphocytic choriomeningitis virus
LLT1	lectin-like transcript-1
LPS	lipopolysaccharide
LRC	leukocyte receptor complex
LTi	lymphoid tissue inducer
mAb	monoclonal antibody

MCMV	mouse cytomegalovirus
MEF	mouse embryonic fibroblast
MFI	mean fluorescence intensity
MHC	major histocompatibility complex
MICA/B	MHC class I polypeptide-related gene A/B
MIEP	major immediate early promoter
MOI	multiplicity of infection
mRNA	messenger RNA
NCR	natural cytotoxicity receptor
NFAT	nuclear factor of activated T-cells
NK	natural killer
NKC	natural killer gene complex
NKG2	natural killer group 2
Nkp46	natural killer cell protein of 46 kDa
NKR	natural killer receptor
NKR-P1	natural killer receptor protein-1
NLR	Nod-like receptor
NLRP	NLR family, pyrin containing
Nod	nucleotide-binding oligomerization domain
Ocil	osteoclast inhibitory lectin
PAMP	pathogen associated molecular pattern
PE	phycoerythrin
OD	optical density
ORF	open reading frame
PAA	phosphonoacetic acid
PCR	polymerase chain reaction
PFU	plaque forming unit
PKR	protein kinase R
PRR	pattern recognition receptor
qPCR	quantitative PCR
Rae-1	retinoic acid early-inducible protein-1

RAET	retinoic acid inducible transcript
RCMV	rat cytomegalovirus
RCTL	rat cytomegalovirus C-type lectin
REF	rat embryonic fibroblasts
RNA	ribonucleic acid
RPKM	reads per kilobase of transcript per million mapped reads
RT	reverse transcription
SDS-PAGE	sodium docecyl sulphate polyacrylamide gel electrophoresis
SLAM	signaling lymphocytic activation molecule
SNP	single nucleotide polymorphism
STAT	signal transducer and activator of transcription
SG	salivary gland
SPR	surface plasmon resonance
TC	tissue culture
TLR	Toll-like receptor
TM	transmembrane
TNF-α	tumour necrosis factor-α
TRAIL	TNF-related apoptosis-induced ligand
UL16	unique-long 16
ULBP	UL16 binding-protein
UV	ultraviolet
VV	vaccinia virus
WB	western blot
WT	wildtype

List of Publications

1. **Aguilar OA***, Berry R*, Rahim MMA, Reichel JJ, Lau TNH, Tanaka M, Fu Z, Balaji G, Popović B, Tu MM, Kirkham CL, Mahmoud AB, Mesci A, Krompotić A, Allan DSJ, Makrigiannis AP, Jonjić S, Rossjohn J, Carlyle JR. A viral immunoevasin controls innate immunity by targeting the prototypical natural killer cell receptor family. *Cell*. 2017 Mar 23;169(1):58-71.e14.
   *Equal contribution

2. **Aguilar OA**, Hadj-Moussa H, Storey KB. Freeze-responsive regulation of MEF2 proteins and downstream gene networks in muscle of the wood frog, Rana sylvatica. In press in *J Therm Biol.*

3. Kirkham CL, **Aguilar OA**, Yu T, Tanaka M, Mesci A, Chu KL, Fine JH, Mossman KL, Bremner R, Allan DSJ, Carlyle JR. Interferon-dependent induction of Clr-b during MCMV infection protects bystander cells from NK cells via NKR-P1B-mediated inhibition. 2017. *J Innate Immun*. 2017 Mar 14.

4. Allan DSJ, Cerdeira AS, Ranjen A, Kirkham CL, **Aguilar OA**, Tanaka M, Childs RW, Dunbar CE, Strominger JL, Kopcow HD, Carlyle JR. Transcriptome analysis reveals similarities between human blood $CD3^{-}CD56^{bright}$ cells and mouse $CD127^{+}$ innate lymphoid cells. In press in *Sci Rep*.

5. Rahim MM, Wight A, Mahmoud AB, **Aguilar OA**, Lee SH, Vidal SM, Carlyle JR, Makrigiannis AP. Expansion and Protection by a Virus-Specific NK Cell Subset Lacking Expression of the Inhibitory NKR-P1B Receptor during Murine Cytomegalovirus Infection. *J Immunol*. 2016 Sep 15;197(6):2325-37.

6. **Aguilar OA**, Hadj-Moussa H, Storey KB. Regulation of SMAD transcription factors during freezing in the freeze tolerant wood frog, Rana sylvatica. *Comp Biochem Physiol B Biochem Mol Biol*. 2016 Nov;201:64-71.

7. Zhang Y, **Aguilar OA**, Storey KB. Transcriptional activation of muscle atrophy promotes cardiac muscle remodeling during mammalian hibernation. *PeerJ*. 2016 Aug 11;4:e2317.

8. **Aguilar OA**, Mesci A, Ma J, Chen P, Kirkham CL, Hundrieser J, Voigt S, Allan DS, Carlyle JR. Modulation of Clr Ligand Expression and NKR-P1 Receptor Function during Murine Cytomegalovirus Infection. *J Innate Immun*. 2015;7(6):584-600.

9. Chen P*, **Aguilar OA***, Rahim MM, Allan DS, Fine JH, Kirkham CL, Ma J, Tanaka M, Tu MM, Wight A, Kartsogiannis V, Gillespie MT, Makrigiannis AP, Carlyle JR. Genetic investigation of MHC-independent missing-self recognition by mouse NK cells using an in vivo bone marrow transplantation model. *J Immunol*. 2015 Mar 15;194(6):2909-18.
   * Equal contribution

10. Allan DS, Kirkham CL, **Aguilar OA**, Qu LC, Chen P, Fine JH, Serra P, Awong G, Gommerman JL, Zúñiga-Pflücker JC, Carlyle JR. An in vitro model of innate lymphoid cell function and differentiation. *Mucosal Immunol*. 2015 Mar;8(2):340-51.

11. Karimi MA, **Aguilar OA**, Zou B, Bachmann MH, Carlyle JR, Baldwin CL, Kambayashi T. A truncated human NKG2D splice isoform negatively regulates NKG2D-mediated function. *J Immunol*. 2014 Sep 15;193(6):2764-71.

12. Williams KJ, Wilson E, Davidson CL, **Aguilar OA**, Fu L, Carlyle JR, Burshtyn DN. Poxvirus infection-associated downregulation of C-type lectin-related-b prevents NK cell inhibition by NK receptor protein-1B. *J Immunol*. 2012 May 15;188(10):4980-91.

13. Chen P, Bélanger S, **Aguilar OA**, Zhang Q, St-Laurent A, Rahim MM, Makrigiannis AP, Carlyle JR. Analysis of the mouse 129-strain Nkrp1-Clr gene cluster reveals conservation of genomic organization and functional receptor-ligand interactions despite significant allelic polymorphism. *Immunogenetics*. 2011 Oct;63(10):627-40.

List of Conference Presentations

Invited Oral Presentations

1. **Aguilar OA**, Rahim MMA, Reichel JJ, Berry R, Lau TNH, Tanaka M, Tu MM, Kirkham CL, Mesci A, Mahmoud AB, Popović B, Krmpotić A, Rossjohn J, Allan DSJ, Makrigiannis AP, Jonjić S, and Carlyle JR. The mouse cytomegalovirus m12 glycoprotein controls innate immune recognition by direct engagement of the NKR-P1B and NKR-P1C (NK1.1) receptors. NK2016: 16th Meeting of the Society for Natural Immunity. Taormina, Sicily, Italy. October 2-6, 2016

2. **Aguilar OA**, Rahim MMA, Richel J, Lau T, Samaniego J, Sampaio I, Krmpotić A, Jonjić S, Makrigiannis A, Allan DSJ, and Carlyle JR. Identification of two MCMV immunoevasins that modulate NK cell recognition via the NKR-P1B:Clr-b axis. ICI2016: Meeting of the International Congress of Immunology. Melbourne, Victoria, Australia. August 21-26, 2016.

3. **Aguilar OA**, Rahim MMA, Reichel J, Lau T, Samaniego J, Sampaio I, Krmpotić A, Jonjić S, Makrigiannis A, Allan DSJ, and Carlyle JR. Identification of two MCMV immunoevasins that modulate NK cell recognition via the NKR-P1B:Clr-b axis. CSI2016: 29th Annual Meeting of the Canadian Society for Immunology. Ottawa, Ontario, Canada. April 1-4, 2016.

4. **Aguilar OA**, Samaniego J, Sampaio I, Lau T, Rahim MMA, Popović B, Krmpotić A, Makrigiannis A, Jonjić S, Allan DSJ, and Carlyle JR. Identification of two MCMV immunoevasins that modulate NK cell recognition via the NKR-P1B:Clr-b axis. CSI2015: 28th Annual Meeting of the Canadian Society for Immunology. Winnipeg, MB, Canada. June 4-7, 2015.

5. **Aguilar OA**, Mesci A, Ma J, Chen P, Allan DSJ, and Carlyle JR. Regulation of the Inhibitory NK cell ligand, Clr-b, in response to cytomegalovirus infection. CSI2014: 27th Annual Meeting of the Canadian Society for Immunology. Quebec, QC, Canada. March 6-9, 2014.

Poster Presentations

1. **Aguilar OA**, Rahim MMA, Sampaio IS, Samaniego JD, Popović B, Tilahun M, Krmpotić A, Margulies DH, Allan DSJ, Makrigiannis AP, Jonjić S, and JR Carlyle. The m153 gene product stabilizes expression of the inhibitory NKR-P1B ligand, Clr-b, during mouse cytomegalovirus infection. CSI2017: 30th Meeting of the Canadian Society for Immunology. Banff, AB, Canada. April 7-10, 2017.

2. **Aguilar OA**, Rahim MMA, Sampaio IS, Samaniego JD, Popović B, Tilahun M, Krmpotić A, Margulies DH, Allan DSJ, Makrigiannis AP, Jonjić S, and JR Carlyle. The m153 gene product stabilizes expression of the inhibitory NKR-P1B ligand, Clr-b, during

mouse cytomegalovirus infection. NK2016: 16th Meeting of the Society for Natural Immunity. Taormina, Sicily, Italy. October 2-6, 2016.

3. **Aguilar OA**, Rahim MMA, Reichel J, Lau T, Samaniego J, Sampaio I, Krmpotić A, Jonjić S, Makrigiannis A, Allan DSJ, and Carlyle JR. Identification of two MCMV immunoevasins that modulate NK cell recognition via the NKR-P1B:Clr-b axis. AAI2016: Immunology 2016, Annual Meeting of the American Association of Immunologists. Seattle, WA, USA, May 13-17, 2016.

4. **Aguilar OA**, Rahim MMA, Reichel J, Lau T, Samaniego J, Sampaio I, Krmpotić A, Jonjić S, Makrigiannis A, Allan DSJ, and Carlyle JR. Identification of two MCMV immunoevasins that modulate NK cell recognition via the NKR-P1B:Clr-b axis. CSI2016: 29th Annual Meeting of the Canadian Society for Immunology. Ottawa, Ontario, Canada. April 1-4, 2016.

5. **Aguilar OA**, Samaniego J, Sampaio I, Lau T, Rahim MMA, Popović P, Krmpotić A, Makrigiannis A, Jonjić S, Allan DSJ, and JR Carlyle. Identification of two MCMV immunoevasins that modulate NK cell recognition via the NKR-P1B:Clr-b axis. CSI2015: 28th Annual Meeting of the Canadian Society for Immunology. Winnipeg, MB, Canada. June 4-7, 2015.

6. **Aguilar OA**, Samaniego J, Sampaio I, Lau T, Rahim MMA, Popović P, Krmpotić A, Makrigiannis A, Jonjić S, Allan DSJ, and JR Carlyle. Identification of two MCMV immunoevasins that modulate NK cell recognition via the NKR-P1B:Clr-b axis. NK2015: 15th Meeting of the Society for Natural Immunity. Montebello, Quebec, Canada. May 2-6, 2015.

7. **Aguilar OA**, Mesci A, Ma J, Chen P, Allan DSJ, James R. Carlyle. Regulation of the Inhibitory NK cell ligand, Clr-b, in response to cytomegalovirus infection. CSI2014: 27th Annual Meeting of the Canadian Society for Immunology. Quebec, QC, Canada. March 6-9, 2014.

Chapter 1

Introduction

Oscar A. Aguilar

This work has not been published.

1.1 Innate Immunity and NK cells

1.1.1 Innate Immunity

The immune system is a complex biological network of molecules and specialized cells whose function is to distinguish between "self" and "non-self/altered-self." Immunity is commonly classified in terms of the innate and adaptive immune systems, largely due to the ability to *innately* detect and eliminate pathogens, or to *adapt* specific resistance to the pathogen through a rigorous selection process ensuring clonal antigen-specific B and T cell receptors are generated by genetic rearrangement of V-D-J elements (Murphy et al., 2012). Microbes in the environment are constantly challenging us; however, we only occasionally become ill. This is largely due to the efficacy of the innate immune system that keeps pathogens at bay, and is achieved via germline-encoded pattern recognition receptors (PRR) capable of detecting pathogen/microbe/danger-associated molecular patterns (PAMP/MAMP/DAMP).

Engagement of these PRR initiates an immune response, resulting in the production of type-I interferons (IFNαβ), pro-inflammatory cytokines, and chemotactic molecules that serve to recruit specialized cells, each with a unique arsenal of immune functions, such as dendritic cells, macrophages, neutrophils, and natural killer (NK) cells. Collectively, these provide the basis of the innate immune response, which is critical for initial control of pathogenic insults, and also functions to prime the adaptive immune response.

1.1.2 Natural Killer Cells

NK cells are innate immune lymphocytes responsible for patrolling, detecting, and eliminating infectious/pathological cells. Their discovery dates back to the 1970's when a subset of splenocytes was identified that was capable of killing tumour cells *in vitro* independently of T cells (which at the time were thought to be the only cells capable of cytotoxicity); thus, due to their ability to "naturally" kill target cells, they were termed natural killer cells (Kiessling et al., 1975a; Kiessling et al., 1975b). It is now accepted that NK cells are capable of eliminating infected, transformed, antibody-coated, transplanted, and otherwise "stressed" cells (Lanier, 2005). Their effectors functions include: (i) cell-mediated cytotoxicity, either through the release of pre-formed cytotoxic granules (containing granzymes and perforin), or by induction of apoptosis through TNF family ligand-receptor interactions (i.e., FasL:Fas [TNFSF6:TNFRSF6], TRAIL:TRAILR1/2 [CD253:DR4/5; TNFSF10:TNFRSF10A/B]); and (ii) secretion of

cytokines, notably IFN-γ and TNF-α, which initiate and promote T_H1 adaptive immune responses (Lanier, 2005; Vivier et al., 2008). They consist of 2-10% of the total lymphocyte pool, depending on anatomical location and the immunological state of an individual (Vivier et al., 2008).

Although originally considered to be innate immune cells, there have been recent revelations that suggest NK cells actually demonstrate "adaptive-like" characteristics, including a requirement for education, the display of self/non-self antigen-specific receptors, and the ability to generate augmented effector and memory features (Cooper et al., 2009; Kim et al., 2005; Sun and Lanier, 2011). This feature was first described using liver NK cells, whereby upon sensitization to allergen, adoptive transfer of these NK cells resulted in an allergic contact hypersensitivity response (Cerwenka and Lanier, 2016; O'Leary et al., 2006; Paust and von Andrian, 2011). However, the receptor(s) involved remain somewhat elusive. Since then, a single antigen-specific receptor that is capable of eliciting NK cell memory during MCMV infection has been described in detail. This is the same receptor responsible for eliciting MCMV-resistance in C57Bl/6 (B6) mice, specifically, the stimulatory Ly49H receptor that directly engages the viral decoy ligand, m157 (Arase et al., 2002; Lee et al., 2001; Smith et al., 2002; Sun et al., 2009). Here, upon MCMV infection, Ly49H+ NK cells proliferate (Dokun et al., 2001), and small subset of them become memory NK cells that, upon transfer to naïve newborn mice, deliver more robust NK cell responses to MCMV infection *in vivo* (Sun et al., 2009).

1.1.3 NK Cell Development and Education

NK cells were initially considered to be innate immune cells due to their ability to rapidly respond to stimuli without prior sensitization. It was also thought that there were three main cell types under the lymphoid lineage umbrella; i.e., T, B, and NK cells. Recently, however, there have been numerous studies suggesting that NK cells are one (cytotoxic) subset of innate lymphoid cells (ILC), the remainder of which are helper subsets, much like T cells. These populations have been grouped into three groups (ILC1/2/3) according to their lineage development and function. Group-1 ILC include cytotoxic NK cells, as well as non-cytotoxic Th1-like ILC1 (IFN-γ producers), and are important in protecting against intracellular pathogens, such as viruses and bacteria (Spits et al., 2016; Walker et al., 2013; Zook and Kee, 2016). Group-2 ILC (ILC2) produce Th2-like cytokines (IL-4,5,13) that help to fight helminth infections and

are important in wound healing and allergy (Walker et al., 2013; Zook and Kee, 2016). Group-3 ILC include lymphoid-tissue-inducer (LTi) cells, which are crucial for the development of secondary lymphoid tissues, in addition to $NCR1^+$ and $NCR1^-$ ILC3 subsets (IL-22/17 producers), which play important roles in gut epithelial border integrity and maintenance of a healthy gut microbial (commensal) environment (Walker et al., 2013; Zook and Kee, 2016). Interestingly, there are also striking parallels between ILC and T cell subsets characterized by master regulator transcription factor expression and function (Vivier et al., 2016). As such, it has recently become clear that NK cells are synonymous with cytotoxic $CD8^+$ T cells (T-bet, Eomes), ILC1 with T_H1 $CD4^+$ T cells (T-bet), ILC2 with T_H2 $CD4^+$ T cells (GATA3), and ILC3 with T_H22 and T_H17 $CD4^+$ T cells (RORγt) (Zook and Kee, 2016).

ILC development predominantly occurs in the bone marrow, however some of these lineages can also arise in other tissues (including thymus, lymph nodes, liver, and gut); whether they develop *in situ* or undergo lineage differentiation and maturation at these sites remains to be determined (Sun and Lanier, 2011). All ILC arise from a common lymphoid progenitor (CLP), which also gives rise to T and B cells. The transcription factor networks subsequently involved in ILC development are currently being investigated; however, Id2 is required for ILC development, to suppress E-protein function that is essential for T and B cell devleopment (De Obaldia and Bhandoola, 2015; Vivier et al., 2016). NK cells subsequently require the transcription factors, Nfil3, T-bet, and Eomes, in addition to environmental cues, such as the cytokine IL-15, and educational ligand engagement through cognate NK cell receptors (Bando and Colonna, 2016; De Obaldia and Bhandoola, 2015; Sun and Lanier, 2011; Vivier et al., 2016; Zook and Kee, 2016). Tracing NK cell versus ILC1 development can be difficult at the earliest stages due to a paucity of stage-specific markers; nonetheless, the earliest progenitors can be distinguished from CLP based on a $CD122^+CD127^+$ but NKR^- phenotype (Sun and Lanier, 2011). NK cells later begin to express typical NK cell receptors, of which the inhibitory NKR-P1B, bifunctional 2B4 (CD244), and stimulatory NKR-P1C (NK1.1) and NKG2D receptors are among the first to be expressed, followed by the inhibitory and activating Ly49 receptors, gain of intermediate CD11b levels, loss of CD27, and terminal acquisition of KLR-G1 (Sun and Lanier, 2011; Zook and Kee, 2016).

With respect to human NK cells, the cognate germline-encoded NK cell receptors specific for major histocompatibility class-I (MHC-I) ligands are not evolutionarily conserved,

because human NK cells utilize Ig-like KIR instead of the lectin-like Ly49 receptors, while, the cytotoxic machinery factors are largely conserved (Rab27, perforin, granzymes, and many transcription factors) (Vivier et al., 2016). As such, there also exist other discrepancies between lineage receptor expression between human and mouse NK cells. For instance, mouse NK cells from C57BL/6 (B6) mice are commonly characterized by expression of the activating NK1.1 receptor (*Klrb1c*; NKR-P1C^{B6}) and lack of T lineage markers (i.e., NK1.1^{+}CD3^{-}) (Glimcher et al., 1977; Koo and Peppard, 1984; Ryan et al., 1992), whereas the closest NK1.1 homolog in humans is NKR-P1A (*KLRB1*; CD161), which is inhibitory in nature and only expressed on a subset of NK cells and some T cells (Lanier, 2005); notably, this variegated expression pattern and function suggest a closer homology to the rodent inhibitory NKR-P1B receptor (Klrb1b; which is also NK1.1^{+} in some inbred mouse strains, such as Swiss-NIH, SJL, FVB, and CD-1). Consequently, human NK cells are instead characterized by bimodal expression of CD56 (NCAM1), CD16 (FcγRIII), and a lack of T cell markers (i.e., CD56^{bright}CD16^{-}CD3^{-} or CD56^{dim}CD16^{+}CD3^{-}). Despite this differential nomenclature, there exist some markers that are more conserved, such as the NKp46/*NCR1* receptor, which is also expressed on some ILC subsets (Serafini et al., 2015; Spits et al., 2016; Walker et al., 2013).

NK cells, like other lymphoid cells, need to be properly "educated" in order to ensure self-tolerance and self-regulated effector function. Although the precise mechanisms are not fully understood, several models have been described. It was long known that NK cells from MHC-I-deficient $\beta_2m^{-/-}$ mice were tolerant to 'self' and thus functionally hyporesponsive to MHC-I-deficient target cells (Liao et al., 1991), thus highlighting the importance of programmed educational signaling via the inhibitory MHC-I-specific Ly49 receptors (Kim et al., 2005). Indeed, it was elegantly shown that NK cells bearing self MHC-I-specific receptors (e.g., Ly49C/I^{+} and/or NKG2A^{+} in B6 mice) were functionally responsive to activating stimuli and more capable of eliciting effector cytotoxicity and cytokine production; thus, it was argued that NK cells are "licensed" to kill during development by self-MHC-I-specific receptors (via a signal also known as arming), and that this checkpoint 'stimulus' resulted in NK cell maturation to full effector function (Kim et al., 2005). Alternatively, the disarming model argues that the presence of variegated self-MHC-I-specific inhibitory receptors prevents chronic over-stimulation through uniform stimulatory receptors, synonymous with the phenomenon of T cell 'anergy' to ensure self-tolerance (Raulet and Vance, 2006). Recently, the rheostat model has also

been proposed and argues that NK cells can actually be educated and re-educated based upon their predominant microenvironments and the integrated or net sum of tolerizing signals (both stimulatory and inhibitory), thus resembling a tunable rheostat (Hoglund and Brodin, 2010; Raulet and Vance, 2006; Sun and Lanier, 2011). Importantly, the overarching interpretation of these results depends upon the experimental model utilized and the immune status of the host. In inflammatory settings (and in IL-2 lymphokine-activated killer (LAK) cell culture *in vitro*), NK cell responses cannot necessarily be predicted entirely based upon their level of education *in vivo*, and indeed cytokines and other immune and stromal cells can influence their functionality. An example of this is in the context of MCMV infection, whereby the "unlicensed/uneducated" NK cells are highly responsive to infection (Orr et al., 2010).

1.1.4 NK Cell Recognition and Cognate Receptors

NK cells are tightly regulated via the integration of signals from stimulatory and inhibitory cell surface receptors delivered upon engagement of cognate ligands on target cells under surveillance. On healthy cells, such a balanced combination of stimulatory and inhibitory ligand expression permits NK cells to be educated and tolerant to self, such that the regulatory signals dominate (**Fig 1.1**) (Lanier, 2005; Raulet and Vance, 2006). Furthermore, although MHC-I molecules have been well established as being a dominant class of self ligands, there are also numerous MHC-I-independent ligands that similarly inhibit NK cells, although our understanding of these are more limited. In inflammatory settings, such as during stress, in cancer or during viral infection, two mechanisms of NK cell recognition take place. Firstly, target cells can increase expression of basal stimulatory ligands, resulting in increased engagement of activating receptors, a process known as "induced-self recognition" (**Fig. 1.1**, right). Secondly, target cells can downregulate inhibitory ligands, such as MHC-I molecules, thereby resulting in disinhibition, a process termed "missing-self recognition" (**Fig. 1.1**, left). In most physiological scenarios, these two processes take place simultaneously, and it is the collective integration of these signals that dictates whether an NK cell will elicit an cytotoxic response towards a target cell or disengage and move on (Lanier, 2005; Raulet and Vance, 2006).

NK cells express an extensive repertoire of germline-encoded NK cell receptors (NKR). These receptors are classified into two main structural forms, immunoglobulin (Ig)-like and C-type lectin (CTL)-like. Interestingly, they are also largely encoded within two concentrated

Figure 1.1

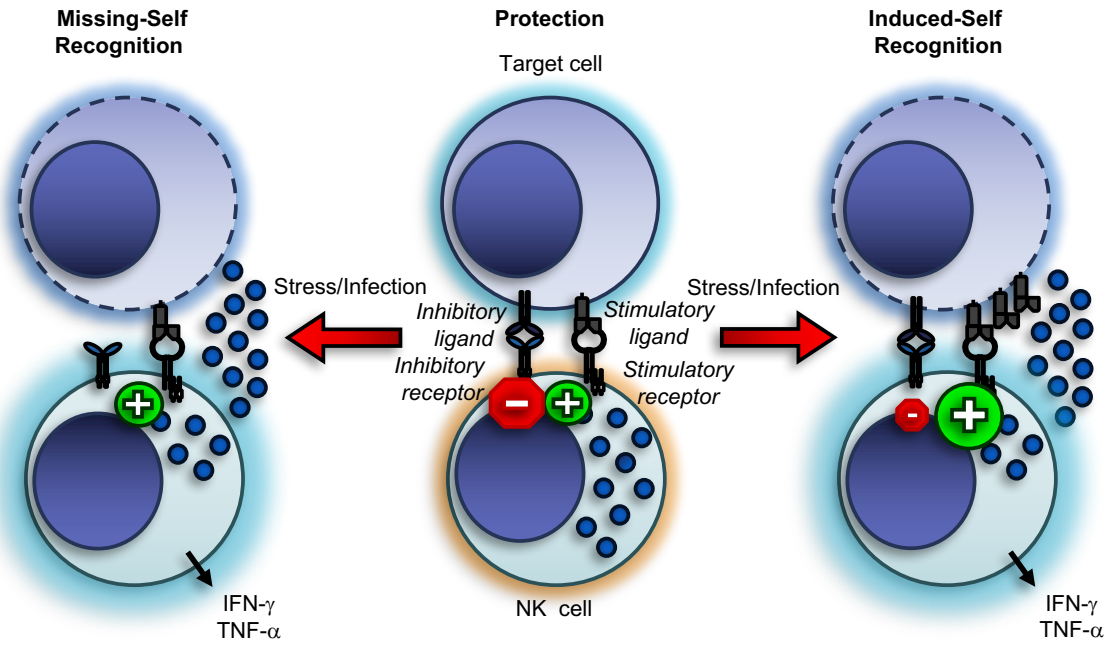

Figure 1.1. Regulation of NK cell activation through NK receptor engagement. NK cells are educated to be self-tolerant during development such that there is a balance between inhibitory and stimulatory signals upon interacting with a healthy cell (center). Upon infection, stress, or transformation, a target cell can either downregulate inhibitory ligands and/or upregulate stimulatory ligand expression resulting in missing-self or induced-self NK cell recognition, respectively (left an right panels). This activation leads secretion of cytokines and cytotoxic granules.

genomic regions, the leukocyte receptor cluster (LRC) and the natural killer gene complex (NKC). The best described NKR are the classical MHC-Ia-specific receptors, which in humans are encoded in the LRC on human chromosome 19 and are termed the killer-cell Ig-like receptors (KIR) (Lanier, 2005). In rodents, the functional homologs are the CTL-like Ly49 receptors found within the NKC on mouse chromosome 6 (**Fig. 1.2A**) (Lanier, 2005). Although structurally distinct, they likely evolved convergently to serve the same key functional role in NK cell education and target cell recognition during pathological circumstances (Lanier, 2005; Raulet and Vance, 2006; Raulet et al., 2001). Importantly, while inhibitory Ly49 and KIR receptors primarily bind self-MHC-I, stimulatory isoforms also exist, such as KIR(2/3D)S and Ly49D/H.

Also located within the NKC is the CD94/NKG2 family. These NKR are also CTL-like and consist of the divergent NKG2D activating homodimer, and the more closely related inhibitory NKG2A and activating NKG2C/E receptors, which form heterodimers with the conserved CD94 subunit (Lanier, 2005). NKG2D recognizes MHC-I-related stress-induced ligands, which in humans consist of the MICA/B, ULBP1-6, and RAET1 isoforms, whereas in mice the ligands include the Rae-1α-ε, Mult1, and H60a/b/c isoforms (Raulet, 2003). The inhibitory CD94/NKG2A and activating CD94/NKG2C/E heterodimers interact with non-classical MHC-Ib molecules, HLA-E in humans and Qa1 in mice (Braud et al., 1998; Raulet, 2003; Vance et al., 2009; Vance et al., 1999). Interesting, although these are functionally paired receptors, they bind the same or similar ligands (classical MHC-Ia leader peptides loaded onto HLA-E/Qa1), although peptide specificity and affinity may differ during infection and stress. Notably, these paired receptors have non-overlapping expression in mice and humans (Beziat et al., 2012; Malmberg et al., 2012; Vance et al., 1999; Vance et al., 1998). Due to the differences between NKG2D and CD94/NKG2A/C/E, researchers often exclude NKG2D from this family.

Other NKR not detailed above include the natural cytotoxicity receptor (NCR) family (consisting of NKp46/*NCR1*, NKp44/*NCR2*, and NKp30/*NCR3*), the signaling lymphocyte activation molecule (SLAM) family (SLAMF1/CD150, SLAMF4/2B4/CD244, CRACC, SLAMF3/Ly9/CD229, SLAMF5/CD84, and SLAMF6/Ly108/NTBA), and the prototypical natural killer cell receptor protein-1 (NKR-P1) family of receptors, amongst others (see **Table 1.1**) (Lanier, 2005; Raulet and Vance, 2006; Vivier et al., 2008).

Figure 1.2

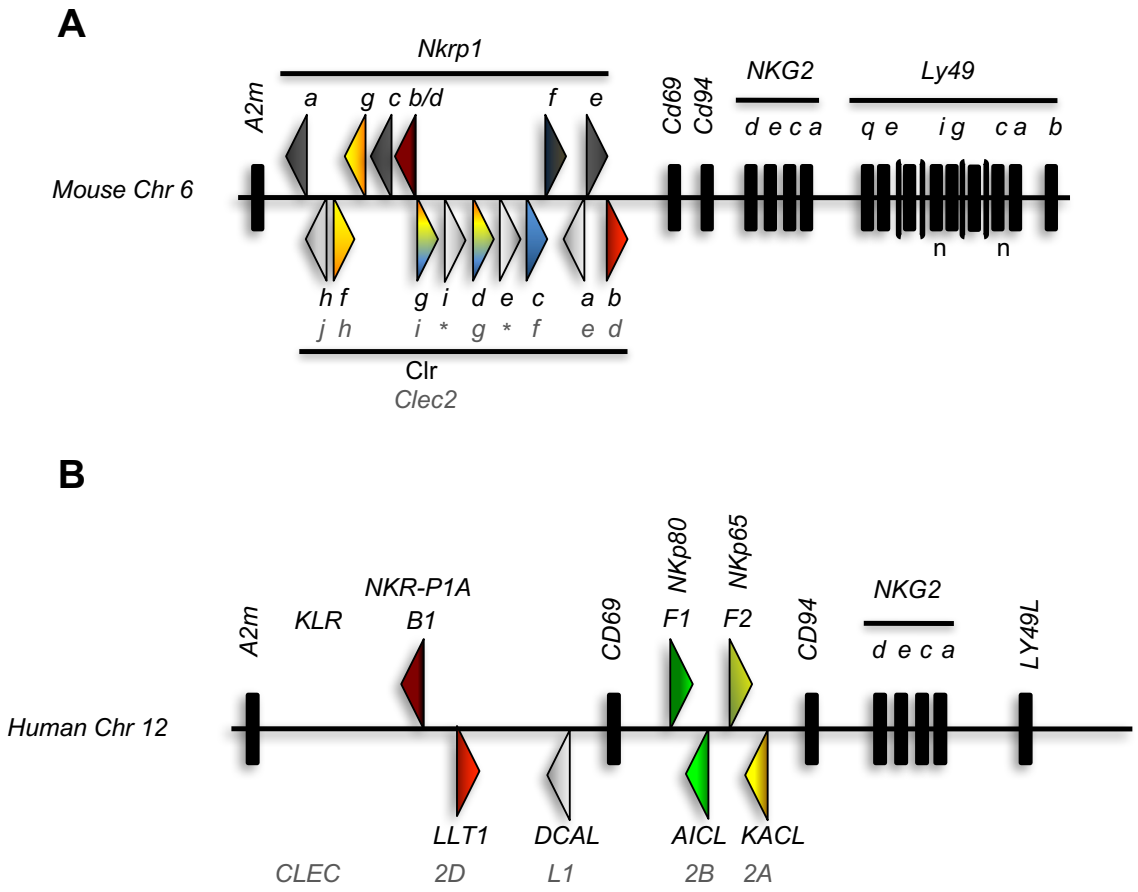

Figure 1.2. The mouse and human Natural Killer Gene Complex (NKC). (**A**) The mouse NKC located on chromosome 6 demonstrating the varying genes including the Nkrp1, Nkg2, and Ly49 families (from left to right). The Nkrp1 region includes the Clr ligand genes and highlights gene orientation and alternate names. (**B**) The human NKC on chromosome 12.

Table 1.1. List of mouse NK cell receptors and their known ligands

Receptors	Ligands	Function	References
Ly49 Family			
Ly49A	H-2D^{d,k,p}, H-2^{f,q}, H-2M3	–	(Andrews et al., 2012; Orr and Lanier, 2011)
Ly49C	H-2K^{b,d}, D^{d,k}	–	(Orr and Lanier, 2011)
Ly49D	H-2D^{d}, Hm1-C4	+	(Orr and Lanier, 2011)
Ly49E	Urokinase plasminogen activator (UPA)	–	(Orr and Lanier, 2011)
Ly49F	H-2K^{d}	–	(Hanke et al., 1999; Orr and Lanier, 2011)
Ly49G2	H-2D^{d,k,d,b}	–	(Hanke et al., 1999; Orr and Lanier, 2011)
Ly49H	MCMV m157	+	(Arase et al., 2002; Smith et al., 2002)
Ly49I	H-2K^{b,d,k}, D^{d}	–	(Arase et al., 2002; Orr and Lanier, 2011; Smith et al., 2002)
Ly49J	Unknown	–	
NKG2 Family			
NKG2A/CD94	Qa-1	–	(Vance et al., 1998)
NKG2C/CD94	Qa-1	+	(Vance et al., 1999)
NKG2D	Rae-1, Mult-1, H60	+	(Carayannopoulos et al., 2002; Cerwenka et al., 2000; Diefenbach et al., 2003)
NKG2E/CD94	Qa-1	+	(Vance et al., 1999)
NKR-P1 Family			
NKR-P1A	? (MCMV m12)	+	(This thesis)
NKR-P1B	Clr-b (MCMV m12)	–	(Carlyle et al., 2004; Iizuka et al., 2003)
NKR-P1C	? (MCMV m12)	+	(This thesis)
NKR-P1F	Clr-c, Clr-d, Clr-g	+	(Chen et al., 2011; Iizuka et al., 2003)
NKR-P1G	Clr-f, Clr-d, Clr-g	–	(Chen et al., 2011)
SLAM Family			
2B4/CD244	SLAMF2/CD48	+/–	(Schwartzberg et al., 2009; Veillette, 2006)
SLAMF3/Ly9	SLAMF3		(Schwartzberg et al., 2009; Veillette, 2006)
SLAMF5/CD84	SLAMF5		(Schwartzberg et al., 2009; Veillette, 2006)
SLAMF6/Ly108	SLAMF6	+/–	(Schwartzberg et al., 2009; Veillette, 2006)
SLAMF7/CRACC	SLAMF7/CD319		(Schwartzberg et al., 2009; Veillette, 2006)

Ig-like Receptors			
NKp46	Viral hemagglutinin	+	(Jarahian et al., 2011)
DNAM-1/CD226	PVR, Nectin-2	+	(Bottino et al., 2003; Tahara-Hanaoka et al., 2004)
Tactile/CD96	PVR	+/–	(Chan et al., 2014; Fuchs et al., 2004)
Tigit	PVR, Nectin-2	–	(Yu et al., 2009)

1.1.5 The NKR-P1 Receptors and Clr ligands

The NKR-P1 family of NK cell receptors are type-II transmembrane C-type lectin-like proteins, distantly related to and genetically linked to the Ly49 receptors in the NKC. Historically, this family represents the very first marker selectively expressed on NK cells, originally discovered using polyclonal C3H anti-CE mouse NK1 alloantigen-specific antisera, and later redefined more specifically using NK1.1 mAb (Glimcher et al., 1977; Koo and Peppard, 1984). The NK1.1 mAb (PK136) was subsequently used to determine an NK1.1 alloantigen, the NKR-P1C activating receptor in B6 mice (Ryan et al., 1992). Since then, additional NKR-P1 family members have been identified, consisting of both stimulatory and inhibitory receptor isoforms. In mice, this includes three stimulatory (NKR-P1A/*Klrb1*a, NKR-P1C/*Klrb1c*, and NKR-P1F/*Klrb1f*), two inhibitory (NKR-P1B/D/*Klrb1b* and NKR-P1G/*Klrb1g*) receptors, and one pseudogene (NKR-P1E/*Klrb1-ps1*) (Carlyle et al., 2008; Kirkham and Carlyle, 2014; Mesci et al., 2006; Plougastel et al., 2001b; Yokoyama and Plougastel, 2003). Interestingly, the ligands for these receptors, the Clr/*Clec2* family, are genetically linked and interspersed amongst the NKR-P1 genes themselves, likely to ensure co-inheritance and preserve MHC-I-independent self tolerance (Carlyle et al., 2004; Carlyle et al., 2008; Chen et al., 2011; Iizuka et al., 2003). The first identified member, Clr-b/Ocil, was first described to play a role in bone morphogenesis, whereby it inhibited osteoclast formation (Zhou et al., 2001; Zhou et al., 2002). Contemporaneously, a family of genes centromeric to *Cd69* in the NKC was identified and termed the C-type lectin-related (Clr) gene products, encoded by the *Clec2* genes (Plougastel et al., 2001a; Plougastel et al., 2001b). Thus, the Clr nomenclature became more commonly used, and Ocil became synonymous with Clr-b. Subsequently, it was determined that the NKR-P1B inhibitory receptor recognized Clr-b/*Clec2d*, the NKR-P1F putative stimulatory receptor interacts with Clr-c,d,g/*Clec2f*,*g*,*i*, while the putative inhibitory NKR-P1G receptor binds Clr-d,f,g/*Clec2g*,*h*,*i*, (Carlyle et al., 2004; Chen et al., 2011; Iizuka et al., 2003). Nevertheless, the stimulatory NKR-P1A and NKR-P1C isoforms, along with some Clr family members, remain

orphan receptors/ligands until now (**Table 1.1**). This conserved genetic linkage has also been observed in the rat NKR-P1:Clr system, although the nomenclature and gene content are not orthologous, due to a more complex Clr repertoire, yet a simplified NKR-P1 organization (Kveberg et al., 2011; Kveberg et al., 2009; Kveberg et al., 2015). Upon first inspection, humans appear to have lost the activating NKR-P1 paralogs, and thus contain a single inhibitory receptor, NKR-P1A (CD161/*KLRB1*) (Lanier et al., 1994), which interacts with its genetically linked ligand, LLT1/*CLEC2D* (Aldemir et al., 2005; Rosen et al., 2005). Interestingly, humans also have two additional receptors, NKp65/*KLRF2* and NKp80/*KLRF1*, which are also C-type lectin-like proteins with genetically linked NKC-encoded ligands, KACL/*CLEC2A* and AICL/*CLEC2B*, respectively (Spreu et al., 2010; Welte et al., 2006). While these genes are situated telomeric to *CD69*, unlike the rodent NKR-P1-Clr cluster, they have been hypothesized to represent divergent homologs to the rodent stimulatory NKR-P1 genes (Bartel et al., 2013) (**Fig. 1.2B**).

Although the NKR-P1 receptors were originally thought to be NK cell-specific, they are now known to be expressed by a number of immune cell subsets. For instance, invariant natural killer T (NKT) cells, mucosal-associated invariant T (MAIT) cells, ILC subsets, γδ T cell subsets, some conventional $CD4^+$ T cells, and activated $CD8^+$ T cells all express NK1.1 and/or related NKR-P1 family members (Bezman et al., 2012; Zhang et al., 2012). Similarly, NKR-P1B has also been detected on a minor subset of NKT cells, and in most ILC subsets at the transcript level (Allan et al., 2015; Aust et al., 2009). Interestingly, NKR-P1G is expressed on a subset of intestinal αβ and γδ T cells (intraepithelial lymphocytes, IEL) (Leibelt et al., 2015). The expression of other NKR-P1 isoforms remains less well known, due to a paucity of reagents (Aust et al., 2009). However, *Nkrp1/Klrb1* transcripts can be found in NK cells and other lymphocytes, including ILC, where NK1.1 expression is low on ILC1 and some ILC3 (Spits et al., 2016); on the other hand, *Nkrp1b/Klrb1b* transcripts are detected in all ILC subsets (Allan et al., 2015).

The intracellular signaling events that take place upon NKR-P1 ligation have been described using immobilized NK1.1 mAb. NKR-P1C cross-linking on B6 NK cells results in antibody-induced redirected lysis (AIRL) and secretion of IFN-γ (Arase et al., 1996; Karlhofer and Yokoyama, 1991). Importantly, the stimulatory NKR-P1 receptors lack a consensus immunoreceptor tyrosine-based activation motif (ITAM). However, NKR-P1C contains a

charged transmembrane (TM) amino acid (Asp, D) residue to facilitate association with the FcRγ adaptor molecule (Arase et al., 1997), which in turn contains an ITAM, and thus NKR-P1C ligation leads to Syk tyrosine kinase recruitment and activation of cytotoxicity (Arase et al., 1996; Karlhofer and Yokoyama, 1991). Importantly, the NK1.1 alloantigen was originally shown to be expressed on B6, CE, NZB, C58, Ma/My, ST, and SJL mouse NK cells, but not BALB/c, AKR, CBA, C3H, DBA, or 129 NK cells (Koo and Peppard, 1984). Subsequently, it was demonstrated that in the Swiss-NIH and SJL strains, the NK1.1 mAb cross-reacts with the inhibitory NKR-P1B receptor (Carlyle et al., 1999; Kung et al., 1999). Interestingly, NK1.1 cross-linking using LAK cells from heterozygous hybrid (B6xSw)F1 mice revealed that inhibitory NKR-P1B signals could abrogate stimulatory NKR-P1C signals upon co-ligation, whereas CD16 (FcγRIII) stimulation was only partially reduced (Carlyle et al., 1999). NKR-P1B lacks a charged TM amino acid residue, instead possessing a cytoplasmic immunoreceptor tyrosine-based inhibition motif (ITIM), which recruits the SHP-1 phosphatase upon ligation (Carlyle et al., 1999; Kung et al., 1999).

The full expression patterns of the Clr ligands remain to be thoroughly investigated. The most well described family member is Clr-b, ligand for the inhibitory NKR-P1B/D alleles. It is broadly expressed on hematopoietic cells, and other cell types such as fibroblasts, but commonly downregulated on cancerous, stressed, and virally-infected cells (Carlyle et al., 2004; Fine et al., 2010; Voigt et al., 2007; Williams et al., 2012). It has also been shown to play a role in "missing-self" recognition of normal cells during BM transplantation, and tumour immune evasion in the Eμ-cmyc spontaneous lymphoma model (Chen et al., 2015; Rahim et al., 2015). Thus, its expression pattern overlaps and parallels that of MHC-I, and Clr-b provides an MHC-I-independent mechanism for self-nonself discrimination and NK cell recognition of "healthy-self" versus "missing-self/altered-self" targets. In fact, *Clec2d* transcripts have been found in a number of tissues except in the brain and eye (Zhang et al., 2012). Cell surface expression of other Clr family members remains largely unknown, due to lack of available reagents. However, transcript data indicates that Clr-g/*Clec2i*, similarly to Clr-b/*Clec2d*, can be detected in a number of hematopoietic cell subsets, albeit at lower levels (Zhang et al., 2012). Clr-c/*Clec2f* was only sparsely detected at low levels in lymphoid tissues, the gonads, the intestine, and the tongue, whereas Clr-d/*Clec2g* was also detected at low levels in lymphoid compartments, but more uniquely in the eye (Zhang et al., 2012). Interestingly, Clr-f/*Clec2h* is highly expressed in

intestinal (and kidney) epithelial cells, whereas it has been show to play a role in immunosurveillance mediated via the NKR-P1G inhibitory receptor found on intestinal IEL subsets (Leibelt et al., 2015). Clr-a/*Clec2e*, on the other hand, has uniquely restricted expression within the gut epithelium, with a "missing-self" expression pattern that reciprocates polyI;C-inducible Clr-f expression, suggesting they may be represent a paired ligand regulation system; however, the function of Clr-a and any cognate receptors remain to be determined (Rutkowski et al., 2016). Thus, although some Clr ligands have both overlapping and unique paired recognition (inhibitory/stimulatory NKR-P1) receptors, which conceptually highlights an important facet of a balanced/integrated NK cell recognition system, Clr expression patterns are variable, regulated, and may play a role in both broad and/or tissue/cell-specific self-nonself discrimination. Notably, additional Clr family members have also been identified but not yet studied, such as Clr-h/*Clec2j*, and three pseudogenes (Clr-e/*Clec2-ps1*, Clr-i/*Clec2-ps2* and Clr-j/*Clec2-ps3*). Importantly, whether or not Clr proteins can also function as receptors themselves, capable of intracellular 'reverse' signaling upon engagement, also remains to be investigated.

1.1 Cytomegalovirus

Most of the introductory information presented in this subsection has been extensively reviewed elsewhere in the book chapter "Murine Cytomegalovirus and Other Herpesviruses", as part of "The Mouse in Biomedical research, 7th Edition, 2007 (Shellam et al., 2007).

1.2.1 β-herpesviruses: Cytomegalovirus

Cytomegaloviruses belong to the *β-herpesvirinae* subfamily of *Herpesviridae*, and have been isolated from human, mouse, rats, guinea pigs, as well as non-human primates. They exhibit host-specific tropisms, have the ability to establish acute, chronic (persistent) and latent (hidden) infections, and are generally asymptomatic in immunocompetent hosts. The term *cytomegalia*, was coined due to the phenotypic intranuclear inclusions and cellular enlargements that were initially observed in infected tissues, which were later shown to be transferable by inoculation of homogenates into healthy animals. Murine cytomegalovirus (MCMV) was first isolated in 1954 by Margaret Smith (Smith, 1954), and since then, has become one of the most

widely studied viral infection models in mice. Two years later, human cytomegalovirus (HCMV) isolates were identified (Smith, 1956).

Since then, MCMV has served as an important model with which to study human CMV (HCMV) infection, due to the similarities seen in tissue tropism, genetic complement of the virus, and observed viral pathogenesis. The importance of studying MCMV infections has recently become more apparent, due to the increased awareness of the pathogenesis of CMV infection in immunocompromised hosts. There have been many reports that describe HCMV as being a leading cause of mortality and morbidity in HIV/AIDS patients, solid organ or bone marrow transplant patients, cancer patients undergoing chemotherapy, and nascent CMV infection can cause severe congenital defects in newborns (Tsutsui et al., 2005). Recent advances in the field of virology have enabled researchers to generate a plethora of tools to study MCMV infection *in vitro* and *in vivo*. Due to restricted host-specificity, HCMV cannot be studied in rodents; however, MCMV can serve as a valuable model in studying CMV-associated disease pathology, host immune responses, and immune evasion mechanisms. In this respect, the virus and the co-evolution of host-pathogen interactions can teach us many important facets of generalized innate and adaptive immunity; what is deemed important to the virus must also be important for host immunity.

1.2.2 CMV structure and viral replication

Cytomegaloviruses are large double-stranded DNA (dsDNA) viruses, comprised of four morphologically distinct elements, which include the genomic core, an icosahedral capsid, the tegument protein matrix, and a lipid bilayer envelope. The viral genome itself is located as part of the core within the capsid, as a large linear dsDNA element. The tegument or viral matrix contains some pre-formed proteins that are required for DNA replication and host immune evasion (Kalejta, 2008). The envelope is a lipid bilayer containing viral glycoproteins essential for attachment and viral entry into the host cell. Together, the virion size is approximately 230 nM in diameter (Shellam et al., 2007).

CMV genomes are amongst the largest viral genomes, being >200 kb in size (Shellam et al., 2007). The genome of MCMV Smith strain is ~230 kb (230,278 bp) in size (Rawlinson et al., 1996), a size that is comparable to other known CMV, including HCMV and RCMV (Chee et al., 1990; Ettinger et al., 2012; Vink et al., 2000). The MCMV genome contains ~170 open reading

frames (termed *m01-m170*); however, in recent years, additional spliced genes, as well as virally encoded miRNA, have been discovered (Dolken et al., 2007; Juranic Lisnic et al., 2013). The MCMV envelope is mainly composed of lipids obtained from the intracellular membranes of host cells, in addition to a number of glycoproteins, such as gB, gL, gH, and gO. These glycoproteins are essential for viral entry into the host cell, in particular gB (Little et al., 1981). Infection is initiated upon binding of receptors on susceptible cells, resulting in fusion of the viral envelope with the host cell plasma membrane, thereby releasing the capsid into the cytoplasm, whereby it is transported via microtubules to enter the nucleus through the nuclear pores. Subsequently, the transcription of viral genes, replication of viral DNA, and assembly of viral genomes into capsids all take place in the nucleus of the host cell. Although the MCMV genome is a linear dsDNA molecule, upon replication, the termini fuse via a 3'-nucleotide extension, resulting in DNA replication by the rolling-circle method (Marks and Spector, 1984). Host DNA synthesis is inhibited by ≥95% within 10-12 hours post-infection (h.p.i.) (Moon et al., 1976). These circular intermediates are formed within ~2h of infection, and replication takes place between 8-16 h.p.i (Misra et al., 1978; Moon et al., 1976; Muller et al., 1978; Muller and Hudson, 1977).

All herpesviruses have three temporal gene expression categories, α, β, and γ, corresponding to the immediate early (IE), early (E), and late (L) phases of viral replication, respectively. The IE/α genes are the first to be transcribed and are regulated by the major IE promoter (MIEP), and do not require *de novo* protein synthesis for transcription (Dorsch-Hasler et al., 1985). Three IE/α genes have been identified in MCMV, termed *ie1*, *ie2*, and *ie3*, where *ie1* and *ie3* are downstream of the MIEP and actually represent splice variants differing in their last exon usage, while *ie2* is transcribed from a different promoter in the opposite direction and is not essential for *in vitro* or *in vivo* replication (Dorsch-Hasler et al., 1985; Keil et al., 1987; Messerle et al., 1992; Messerle et al., 1991). IE/α gene expression activates E/β genes, many of which encode viral immunoevasins, while others are required for L/γ gene expression. Entry into L/γ phase requires DNA replication, and occurs about 16 h.p.i.; most of these latter gene products encode structural proteins (Shellam et al., 2007).

Capsid proteins are synthesized in the cytoplasm, but get transported back into the nucleus, whereupon viral genomic DNA gets packaged into capsids that are then transported through the nuclear membrane, acquiring their primary envelope as they bud from the nucleus.

The egress of the nascent virions is not very well understood; however, observations from α-herpesviruses suggest that the capsids merge with the endoplasmic reticulum (ER), acquiring tegument proteins while transiting through the ER/Golgi network, the finally acquire a mature envelope upon egress via the secretory pathway (Shellam et al., 2007).

1.3 Host-Pathogen Interactions with CMV

1.3.1 Pathogenesis and Host Responses to CMV

CMV infection in immunocompetent hosts is usually asymptomatic, and is typically not associated with serious tissue damage. In mice, however, this depends on a number of factors, including the viral dose, the mouse strain, and the source of virus. For instance, MCMV can be either passaged *in vivo* (usually in BALB/c mice), where the virus is isolated from natural salivary gland (SG) reservoirs, or it can be passaged *in vitro* from tissue culture (TC) supernatants, where it is propagated in mouse embryonic fibroblast (MEF) monolayers. Generally, TC-derived MCMV is less virulent than SG-isolated virus, likely due to a requirement for the latter of a full *in vivo* replication cycle, including selection for host immune evasion genes, maintenance of pathogenesis factors, and SG homing and viral productivity genes. In addition, it is possible that crude SG extracts may contain inflammatory cytokines and higher order aggregates of viral particles with cellular debris (Krmpotic et al., 2003). Upon *in vivo* infection, the virus is disseminated to various organs, including the kidney, liver, and spleen (Sweet, 1999), but it is quickly cleared in all tissues, with the exception of the SG (Krmpotic et al., 2003). This viral spreading is largely mediated via circulating infected innate immune cells, such as monocytes (Daley-Bauer et al., 2014).

The scenario is very different in immunocompromised individuals. HCMV is one of the leading causes of opportunistic infection amongst AIDS patients, and can result in a number of clinical manifestations, including pneumonitis, hepatitis, retinitis, colitis, and encephalitis (Krmpotic et al., 2003). It can also be very harmful to individuals with an immature immune system. HCMV can be transmitted transplacentally from mother to fetus, to her newborn during birth, or through breast-feeding (Krmpotic et al., 2003). Such infections can result in morbidity, mortality, and mental retardation in congenitally infected infants (Krmpotic et al., 2003;

Reddehase, 2002; Sweet, 1999). Many of these pathologies are recapitulated with MCMV infection of immunocompromised and neonatal mice (Krmpotic et al., 2003; Sweet, 1999).

Acute CMV infection is initially controlled by the combined efforts between the innate and adaptive immune systems. NK cells play a pivotal role in early resistance to and control of infection, and are instrumental in priming the adaptive immune response. Many mechanisms have been implicated in CMV control, discussed in detail below in section 1.3.5.

Despite efficient control by NK cells, T cells are also necessary for the resolution of infection and establishing latency. Early experiments demonstrated that adoptive transfer of CMV-primed T cells was protective in sublethally γ-irradiated hosts infected with MCMV (Reddehase et al., 1988; Reddehase et al., 1985). These antiviral effects are largely attributed to $CD8^+$ T cells, with only minimal control by $CD4^+$ T cells (Krmpotic et al., 2003; Sweet, 1999). T cell immunotherapy efficacy has also been demonstrated in clinical HCMV infections in immunocompromised patients after BM transplantation (Riddell et al., 1992). These $CD8^+$ T cells undergo expansion of CMV Ag-specific effectors, followed by a contraction phase upon viral clearance (Hou et al., 1994). Interestingly, during latency, some of these $CD8^+$ T cells undergo memory inflation, a process where over time, there is an accumulation of Ag-specific T cells with an effector-memory T_{EM} cell phenotype (Klenerman and Oxenius, 2016). Intriguingly, many of these T_{EM} cells have TCR specificities for IE1 peptides (Klenerman and Oxenius, 2016; Reddehase, 2002). It is thought that this may be due to constant Ag exposure during latency; however, understanding why these cells do not display an exhausted phenotype (as seen in cancer, HIV, and LCMV infection) would have novel therapeutic potential.

Although $CD4^+$ T cells are not as important in clearing MCMV infection in the periphery, they are crucial in viral elimination in the salivary glands, thus limiting horizontal transfer (Jonjic et al., 1989; Walton et al., 2011). This is largely due to IFN-γ production (and to a lesser extent TNF-α). Antibodies against MCMV can be generated as early as 3-5 d.p.i. for IgM and 5-7 d.p.i. for IgG (Lawson et al., 1988). Although these antibodies are not crucial for clearance of acute infection, they are important in limiting re-emergence of virus and secondary infection (Jonjic et al., 1994).

Following resolution of acute CMV infection, the virus enters its latency stage, where no virions are detected; however, copies of the CMV genome remain in certain cells. Indeed, selective viral gene expression can be detected in certain tissues, such as expression of *ie1*, but

not *ie3*, E/β or L/γ genes (Kurz and Reddehase, 1999). The cells and tissues that harbour these viral copies are not very well understood, although the spleen, salivary glands, liver, lungs, and kidneys have been implicated (Krmpotic et al., 2003). Viral latency is efficiently controlled by the immune system, yet homeostatic disturbances can result in viral reactivation, such as is seen in AIDS patients and in immunocompromised transplant patients.

1.3.2 Immune Evasion

The intricate relationship between CMV and their host is exemplified by the co-evolution of genes involved in anti-viral immunity and viral immune evasion. CMV are notoriously known for encoding genes that evade various facets of immune recognition, termed immunoevasins (see **Table 1.2**).

Table 1.2. List of MCMV-encoded immunoevasin genes

Gene	Target	Function	Reference
m04/ gp34	MHC-I	Inhibitory: Escorts MHC-I to cell surface to inhibit NK cells. Stimulatory: Certain strains have evolved Ly49 receptors to recognize m04 in H-2-dependent manner	(Babic et al., 2010; Kielczewska et al., 2009; Kleijnen et al., 1997; Pyzik et al., 2011)
m06/ gp48	MHC-I	Re-routes MHC-I/β_2m complexes for degradation	(Reusch et al., 1999)
m18	CK2	Recruits CK2 and limits HDAC3 activity – however, this results in upregulation of *Raet1* transcripts	(Greene et al., 2016)
m20.1	PVR	Retains PVR ligand expression to block DNAM-1 activation	(Lenac Rovis et al., 2016)
M27	STAT2	Downregulates STAT2 resulting in interference with type-I (IFN-αβ) and type-II (IFN-γ) signaling	(Zimmermann et al., 2005)
M33 (GPCR Homologue)	Heterotrimeric $G_{q/11}$ proteins	Promotes viral dissemination, particularly in the salivary gland. Stimulates CREB transcriptionally through PLC-β and PKC signaling	(Davis-Poynter et al., 1997; Sherrill et al., 2009)
M45	RIP1/3	Inhibits DAI/ZBP-1 induced NFκB activation by interacting with RIP1/3	(Rebsamen et al., 2009)
M78	unknown	Important for viral replication in the lungs an salivary glands	(Davis-Poynter et al., 2016)

M83/M84	unknown	HCMV UL83 homologs; inhibit IFI16 cytDNA sensor to block IRF3 activation	(Li et al., 2013a)
MCK-2 (m129-m131); chemokine homologue	gH/gL complex	Forms part of the virion and influences host tropism, including infection of macrophages. Increases viral spreading to salivary gland.	(Jordan et al., 2011; Wagner et al., 2013)
m138 (Fc receptor homologue, fcr-1)	NKG2DL: Mult-1, H60, Rae-1ε; CD80 (B7-1)	Targets NKG2D ligands as well as the co-stimulatory molecule CD80 for lysosomal degradation	(Arapovic et al., 2009a; Arapovic et al., 2009b; Lenac et al., 2006; Mintern et al., 2006)
m142/m143	PKR	Bind/inactivate dsRNA/PKR to inhibit eIF2α phosphorylation/translation	(Child et al., 2006; Valchanova et al., 2006)
m144	unknown	Inhibits NK cell activation through an unknown receptor	(Farrell et al., 1997)
m145	Mult-1	Prevents NKG2D activation by limiting Mult1 cell surface expression	(Krmpotic et al., 2005)
m147.5	CD86	Downregulates expression of the co-stimulatory molecule CD86	(Loewendorf et al., 2004)
m152/gp40	MHC-I Rae-1	Inhibits MHC-I and Rae-1 cell surface expression to modulate T and NK cell recognition	(Krmpotic et al., 2002; Lodoen et al., 2003; Ziegler et al., 1997)
m154	CD48	Prevents 2B4/CD244 activation by degrading its ligand, CD48	(Zarama et al., 2014)
m155	H60	Prevents NKG2D activation by limiting H60 cell surface expression	(Hasan et al., 2005)
m157	$Ly49H^{B6}$, I^{129}	Recognized by the stimulatory $Ly49H^{B6}$ receptor ($CMV1^{r}$); also engages the inhibitory $Ly49I^{129}$ receptor, and some Ly49C alleles, to inhibit NK cells	(Arase et al., 2002; Corbett et al., 2011; Smith et al., 2002)
m166	TRAIL-DR	Restricts TRAIL-DR expression leading to suppressed apoptosis	(Verma et al., 2014)

1.3.3 General Immune Evasion Mechanisms

Among known immune evasion strategies in MCMV, the M27 gene product is known to abrogate type-I IFN responses by disrupting downstream STAT2 signaling, and M45 fulfills an anti-apoptotic role by interfering with NFκB activation via RIP1 association (Rebsamen et al., 2009; Zimmermann et al., 2005). In addition, the MCMV m142/m143 gene products prevent eIF2α phosphorylation and translational arrest by binding dsRNA and inactivating PKR (Child

et al., 2006; Valchanova et al., 2006). The M83/M84 gene products are homologs of HCMV UL83, a tegument protein that inhibits IRF3 activation via the IFI16 cytosolic DNA sensor (Li et al., 2013a), thus it is possible that these genes have similar functions. MCMV also encodes a viral CC chemokine, or virokine, named MCK-2 (m129-m131) that is crucial for viral dissemination and salivary gland titres (Wagner et al., 2013). Reciprocally, the MCMV M33 and M78 genes encode G-protein-coupled receptor homologs that function like chemokine receptors to promote viral dissemination (Melnychuk et al., 2005).

1.3.4 Evasion of Adaptive Immunity

Adaptive immune responses are actively targeted during CMV infection. MCMV interferes with cytotoxic T cell recognition by utilizing the m06 (gp48) and the m152 (gp40) gene products to downregulate MHC-I molecules, thereby preventing viral antigen presentation to the T cell receptor (Pinto et al., 2006; Reusch et al., 1999; Ziegler et al., 1997). Additionally, MCMV encodes genes that target the NKG2D-ligands, which directly engage the stimulatory receptor NKG2D expressed on activated $CD8^+$ T cells and NK cells. For instance, Mult1 is targeted by both m138 (fcr-1) and m145, while H60 is targeted by m138 and m155 (Arapovic et al., 2009a; Hasan et al., 2005; Krmpotic et al., 2005; Lenac et al., 2006). Interestingly, in addition to downregulating MHC-I molecules, m152 also retains the Rae-1 family of NKG2D-ligands (Rae-1α/β/γ/δ/ε) (Arapovic et al., 2009b). Furthermore, the MCMV m138 and m147.5 gene products downregulate CD80 (B7.1) and CD86 (B7.2), respectively, to interfere with T cell co-stimulation and thereby increase viral persistence (Loewendorf et al., 2004; Mintern et al., 2006). However, preventing cell surface expression is not the only mechanism CMV viruses use to evade recognition. For instance, MCMV utilizes the m04 gene product to associate with MHC-I alleles at the cell surface, presumably masking presentation of viral peptides, and likely to inhibit NK cells, as outlined below (Kleijnen et al., 1997).

1.3.5 Innate Immune Evasion and Role of NK cells in MCMV Recognition

The importance of NK cells in controlling CMV infections has long been appreciated. In fact, in a clinical case study, a patient with a deficiency in NK cells (and some myeloid cells) was found to suffer from a high incidence of recurring herpesvirus infections, in particular CMV

infections (Biron et al., 1989). As stated above, during acute CMV infection, NK cells play a pivotal role in controlling the infection and priming the adaptive immune response. In B6 mice infected with MCMV, NK cell activation can be detected as early as 1 d.p.i (Bezman et al., 2012). These responses include cytokine production as well as effector cytotoxicity. Importantly, NK cell cytotoxic functions are more vital for the control of viral replication, as evident from infection in *Prf*$^{-/-}$ and *Ifng*$^{-/-}$ mice in comparison to wild-type B6 mice (Parikh et al., 2015).

Despite the swift recognition of viral infection, MCMV still manages to escape NK cell detection using a variety of mechanisms, each of which tells us something about normal NK cell immune recognition mechanisms. The first viral gene product that was identified to inhibit NK cell function directly was the MHC-I homologue, m144 (Farrell et al., 1997); however, how m144 achieves this remains elusive, as no m144 receptor has been identified. The C57BL/6 strain of mice was long known to be MCMV-resistant, due to evolutionary acquisition of the *Cmv1* locus. Subsequent investigations demonstrated that the *Cmv1*^{r} gene encoded the stimulatory Ly49H^{B6} receptor (Brown et al., 2001; Dokun et al., 2001; Lee et al., 2001), and that the Ly49H^{B6} receptor directly engaged the MCMV m157 glycoprotein, also an MHC-I homologue (Arase et al., 2002). Thus, the Ly49H:m157 interaction dominantly controls MCMV resistance in B6 mice, and was later shown to be important in the expansion and generation of long-lived memory NK cells that efficiently control recurrent infection (Sun et al., 2009). However, this was only half the story, as certain mouse strains also encode inhibitory Ly49C/I receptors that directly bind the m157 decoy ligand, including Ly49I^{129}, thereby explaining how and why MCMV evolved the m157 immunoevasin (Arase et al., 2002). Interestingly, most wild-derived MCMV isolates encode polymorphic m157 variants that evade Ly49H-dependent stimulatory recognition, and passage of MCMV encoding m157 capable of engaging Ly49H results in loss-of-function MCMV immune escape mutants that lose m157 expression; thus, the dominant effect of Ly49H is sufficient to evolutionarily select viral mutants during *in vivo* infection (Corbett et al., 2011; Voigt et al., 2003). Thus, the Ly49C,I,H:m157 axis was the first to demonstrate host-pathogen co-evolution involving an NK cell receptor family and a viral immunoevasin. Nonetheless, many additional non-redundant viral genes have since been identified to be involved in subversion of NK cell responses.

Unlike T cells, which require activation to express the NKG2D receptor, resting NK cells natively express NKG2D; therefore, the non-redundant arsenal of immunoevasins that actively

prevent NKG2D-ligand expression also serve to evade NK cell recognition – this includes m138 (Mult1, H60), m145 (Mult1), m152 (Rae-1α-ε), and m155 (H60) (Krmpotic et al., 2002). In contrast, the downregulation of MHC-I molecules by m06 and m152 serves to induce "missing-self" recognition via the inhibitory Ly49 receptors. Thus, when m04 (gp34) was discovered to bind MHC-I molecules and escort them to the cell surface, it was postulated that m04 evolved as a decoy escort protein to inhibit NK cells (Kleijnen et al., 1997). This has since been confirmed using m04-deficient MCMV (Δm04); however, epistatic H-2 (MHC-I) haplotype-dependent phenotypes were subsequently observed to negatively impact viral fitness (Babic et al., 2010; Desrosiers et al., 2005). Subsequently, it was found that certain mouse strains encode stimulatory Ly49 receptors that recognize certain m04-modified MHC-I alleles, including Ly49P activating receptor recognition of H-2D^k (Desrosiers et al., 2005; Kielczewska et al., 2009; Pyzik et al., 2011). These findings thus reveal striking complexity to host-pathogen co-evolution and NK cell receptor recognition of CMV immunoevasins. The Ly49:MHC-I:m04 interaction has since been revealed to be additionally dependent on an additional MCMV gene product, m169 (MAT), further extending this complexity.

In recent years, four additional families of NK cell receptors have been implicated in CMV-mediated immune evasion. In 2014, the MCMV m154 glycoprotein was shown to hinder MHC-I-independent CD48 ligand cell surface expression to prevent engagement via the 2B4/CD244/SLAMF4 activating (ITSM-bearing) receptor, thereby averting NK cell responses (Zarama et al., 2014). Additionally, the MCMV m166 gene product was discovered to suppress expression of the TRAIL-DR, thus similarly preventing NK cell effector function (Verma et al., 2014). Recently, MCMV m20.1 was found to downregulate PVR/CD155, a ligand for the stimulatory DNAM-1/CD226 receptor, inhibitory TIGIT receptor, and CD96 on NK cells (Lenac Rovis et al., 2016). Interestingly, in the rat model, the RCMV-English isolate encodes a spliced C-type lectin-like gene product, *rctl* (spliced transcripts are uncommon in herpesviruses) (Voigt et al., 2001). It was further demonstrated that the RCTL gene product directly engaged certain inhibitory NKR-P1B alleles, and to a lesser extent, activating NKR-P1A receptor alleles, on NK cells *in vitro*, in turn modulating strain-dependent RCMV virulence *in vivo* (Voigt et al., 2007).

1.4 Hypothesis

In the current thesis, I sought to shed light on the complexity of NK cell responses elicited through the NKR-P1B:Clr-b recognition axis during MCMV infection, with an ultimate goal of identifying MCMV immunoevasins that modulated NKR-P1B receptor function or Clr-b ligand expression and function. Given that RCMV-English has evolved an immunoevasin to subvert NK recognition by engaging the rNKR-P1B receptor, I hypothesized that similar mechanisms may exist between MCMV and the mouse NKR-P1 homologs; in addition, the mechanisms underlying the striking regulation of Clr-b during MCMV and RCMV infection suggest that CMV gene products or immunoevasins may also regulate ligand expression and/or function. It is anticipated that the findings outlined in this thesis will also shed light on interactions between HCMV and the human NKR-P1 homologs, in particular the NKR-P1A inhibitory receptor (KLRB1/CD161), and possibly the divergent NKp80 and NKp65 activating receptors (KLR-F1/2).

Chapter 2

Modulation of Clr Ligand Expression and NKR-P1 Receptor Function during Murine Cytomegalovirus Infection

Oscar A. Aguilar, Aruz Mesci, Jaehun Ma, Peter Chen, Christina L. Kirkham, Joachim Hundrieser, Sebastian Voigt, David S.J. Allan, James R. Carlyle

Experiments were designed and conducted by O.A.A. and A.M. with guidance from D.S.J.A and J.R.C. Figures 2.9, 2.13, and 2.14 were generated by A.M. Assistance with experiments from J.M. and C.L.K. BWZ reporter assays were conducted with the guidance of P.C. and A.M. The Clr-11 mAb, HT29, was generated in the former lab of Prof. Kurt Wonigeit (Hanover) and provided by J.H. RCMV viruses and REF cells were provided by S.V. This project was funded by grants to J.R.C.

This work was published in the *Journal of Innate Immunity*. 2015; 7(6):584-600.
https://doi.org/10.1159/000382032

2 MCMV Infection modulates NKR-P1B:Clrb Interactions

2.1 Abstract

Viruses are known to induce pathological cellular states that render infected cells susceptible or resistant to immune recognition. Here, we characterize an MHC-I-independent NK cell recognition mechanism that involves modulation of inhibitory NKR-P1B:Clr-b receptor-ligand interactions in response to mouse cytomegalovirus (MCMV) infection. We demonstrate that mouse Clr-b expression on healthy cells is rapidly lost at the cell surface and transcript levels in a time-dependent, dose-dependent manner upon MCMV infection. In addition, cross-species infections using rat cytomegalovirus (RCMV) infection of mouse fibroblasts and MCMV infection of rat fibroblasts suggests that this response is conserved during host-pathogen interactions. Active viral infection appears to be necessary for Clr-b loss, as cellular stimulation using UV-inactivated whole virus or agonists of many innate pattern recognition receptors (PRR) failed to elicit efficient Clr-b downregulation. Notably, Clr-b loss could be partially blocked by titrated cycloheximide treatment, suggesting that early viral or nascent host proteins are required for Clr-b downregulation. Interestingly, reporter cell assays suggest that MCMV may encode a novel Clr-b-independent immunoevasin that functionally engages the NKR-P1B receptor. Together, these data suggest that Clr-b modulation is a conserved innate host cell response to virus infection that is subverted by multiple CMV immune evasion strategies.

2.2 Introduction

Natural killer (NK) cells are innate cytotoxic lymphocytes capable of recognizing pathological target cells via multiple germline-encoded receptor-ligand interactions. They can detect and eliminate cancerous, virus-infected, transplanted, antibody-opsinized, and “stressed” cells (Lanier, 2005). Their effector function is tightly regulated by receptor-ligand interactions, inhibitory or stimulatory in nature, which are collectively integrated to enable target cell recognition (Lanier, 2005; Raulet and Vance, 2006). These interactions follow the tenets of “missing-self” and “induced-self” recognition (Karre et al., 1986) respectively, which allow NK cells to be self-tolerant yet responsive to “altered-self” pathologies and “non-self” foreign

entities (Raulet and Vance, 2006). Initially, missing-self recognition was shown to be dependent on the expression of polymorphic MHC class I (MHC-I) molecules (Karre et al., 1986), recognized by inhibitory self-MHC-I-specific receptors (rodent Ly49 or human KIR). More recently, however, numerous receptors have been identified that recognize non-MHC-I ligands (Kumar and McNerney, 2005).

In rodents, most NK cell receptors consist of type-II transmembrane C-type lectin-like proteins encoded within the NK gene complex (NKC). These include the Ly49 receptors that recognize classical MHC-I molecules, the CD94/NKG2 heterodimeric receptors that recognize non-classical MHC-I molecules, the NKG2D homodimer that recognizes MHC-I-related stress-induced ligands, and the NKR-P1 receptors that recognize other genetically linked C-type lectin-related (Clr) proteins (Carlyle et al., 2008; Kirkham and Carlyle, 2014).

At least five members are known to exist in the mouse NKR-P1 family, three predicted stimulatory isoforms (NKR-P1A,C,F), and two inhibitory isoforms (NKR-P1B,G) (Carlyle et al., 2008; Mesci et al., 2006). NKR-P1C, which encodes the well-known NK1.1 antigen in the B6 mouse strain, directly stimulates NK cell function. Yet, similar to NKR-P1A, NKR-P1C remains an orphan receptor. On the other hand, the NKR-P1F and NKR-P1G receptors recognize an overlapping yet distinct set of ligands, whereby NKR-P1F recognizes Clr-c,d,g, and NKR-P1G recognizes Clr-d,f,g in reporter cell assays (Chen et al., 2011; Kveberg et al., 2011). Recently, it was shown that NKR-P1G and Clr-f play an important role in mucosal immunity (Leibelt et al., 2015), and that the NKR-P1F/G receptors are expressed and functional on rat NK cells (Kveberg et al., 2015). The remaining receptor, NKR-P1B, and its likely allelic variant, NKR-P1D, recognize Clr-b (a.k.a., Ocil/*Clec2d*) (Carlyle et al., 2004; Iizuka et al., 2003). Clr-b expression is quite broad and mirrors MHC-I expression on hematopoietic cells, yet it is commonly downregulated during cellular pathologies, including on cancerous cell lines (Carlyle et al., 2004; Fine et al., 2010), in response to genotoxic stress (Carlyle et al., 2004; Fine et al., 2010), and during viral infection (Ettinger et al., 2012; Voigt et al., 2007; Williams et al., 2012). Regarding the latter, mouse Clr-b and rat Clr-11 expression are rapidly lost at both the transcript and protein levels during poxvirus (Vaccinia virus, VV; Ectromelia virus, ECTV) and rat cytomegalovirus (RCMV-E; MHV8) infection, respectively (Ettinger et al., 2012; Voigt et al., 2007; Williams et al., 2012).

Cytomegaloviruses (CMV) are members of the *Betaherpesvirinae* sub-family and are highly species-specific, possessing restricted host tropisms and requirements for productive infection. They are double-stranded DNA viruses with large genomes (≥200kb) that frequently accommodate numerous immunoevasin genes. While CMV infections are generally asymptomatic in immune-competent hosts, uncontrolled infections can occur in immunocompromised individuals and in newborns, where infection can lead to severe complications and congenital defects. NK cells play a pivotal role in responding to and controlling acute CMV infections, and as such, considerable co-evolution at this host-pathogen interface has led to reciprocal strategies to maintain balance (Lanier, 2008). In fact, numerous CMV-encoded immunoevasin genes are known to modulate NK cell receptor-ligand interactions and effector function. MCMV encodes stealth proteins (m138, m145, m152, m155) that prevent induced-self maturation of NKG2D ligands (Mult1, Rae-1, H60), cloaking ligands (m04, m06) that regulate MHC-I recognition by T and NK cells, at least one MHC-like decoy ligand (m157) that is directly recognized by host NK cell receptors (inhibitory Ly49I; stimulatory Ly49H), and presumably others (e.g., m144) (Arase et al., 2002; Krmpotic et al., 2005; Lee et al., 2001; Lenac et al., 2006; Lodoen et al., 2003; Lodoen et al., 2004). In addition, the English isolate of rat CMV (RCMV-E) encodes an immunoevasin, RCTL, that targets the rat NKR-P1B:Clr-11 axis during host-pathogen interactions *in vivo* (Voigt et al., 2007; Voigt et al., 2001).

Here, we demonstrate that there is striking evolutionary conservation in the host cell response to pathogen-induced regulation of Clr/*Clec2d* expression. Both mouse Clr-b (*Clec2d*) and rat Clr-11 (*Clec2d11*) are acutely modulated at the transcript and protein levels in response to reciprocal cross-species MCMV or RCMV infection of rat or mouse host cells, respectively. Downregulation of Clr-b requires live virus infection, as it does not occur using whole inactivated virus, nor using simple agonists of innate pattern recognition receptor (PRR) pathways. Moreover, loss of cell surface Clr-b can be partially blocked by inhibition of nascent protein synthesis and the ubiquitin-proteasome degradation pathway, but not using inhibitors of late viral replication. We also provide evidence of a novel Clr-b-independent immunoevasin capable of engaging the mouse NKR-P1B receptor upon MCMV infection of fibroblasts *in vitro*.

2.3 Materials and Methods

2.3.1 Cells

NIH3T3 fibroblast and J774A.1 monocyte-like cells were obtained from American Type Culture Collection (ATCC). Wild-type C57BL/6 (WT B6) mouse embryonic fibroblasts (MEF) were obtained from T.W. Mak (University of Toronto, Canada). Cells were cultured in complete DMEM-HG, supplemented with 2mM glutamine, 100U/mL penicillin, 100µg/mL streptomycin, 50µg/mL gentamicin, 110µg/mL sodium pyruvate, 50µM 2-mercaptoethanol, 10mM HEPES, and 10-20% FCS.

2.3.2 Virus infections

MCMV (Smith strain) was provided by Dr. A. Makrigiannis (University of Ottawa, Canada). MCMV-GFP was provided by Dr. S. Vidal (McGill University, Canada) and has been previously described (Henry et al., 2000). Wild-type RCMV-English (RCMV-E) and a ΔRCTL-mutant have been previously described (Voigt et al., 2007). Viruses were passaged on MEF or REF fibroblast monolayers. Plaque assays were used to determine viral titers as described (Brune et al., 2001), without centrifugation during infection. For *in vitro* infections, fibroblasts were seeded to subconfluent monolayers, virus was added (multiplicity of infection, MOI~0.5 PFU/cell), then cells were centrifuged at 800x*g* for 30 minutes at 37ºC (effective MOI~10 PFU/cell with centrifugation), and incubated at 37ºC, 5% CO_2 for the indicated times.

2.3.3 RNA isolation, cDNA synthesis, and qRT-PCR

Total RNA was isolated using a mirVana RNA isolation kit (LifeTechnologies), and reverse transcription reactions were carried out using Superscript III cDNA synthesis kits (LifeTechnologies). Quantitative real-time RT-PCR was performed on a CFX-96 Real-Time PCR detection System (BioRad) using 20-50 ng of cDNA, Sso-Fast EvaGreen Supermix (BioRad), and gene-specific primers designed using Primer-Blast (www.ncbi.nlm.nih.gov/tools/primer-blast), selected to span at least one intron and possess minimal reactivity with other genes (*Clec2d*/Clr-b: 5'-AGC TCC TCA GCT CTG AGA TGT GTG, 5'- AGG GGA GAT GGT TCC GTG CCT TT; *Tbp*: 5'-AGA GCC ACG GAC AAC TGC GTT G, 5'-CTG GGA AGC CCA ACT TCT GCA C). Data were analyzed using CFX Manager software (BioRad).

2.3.4 Flow cytometry

Cells were stained in flow buffer (HBSS, 0.5% BSA, 0.03% NaN_3) on ice with primary

mAb for 25-30 minutes, or secondary streptavidin (SA) conjugates for 15-20 minutes, washed between incubations, then analyzed using a FACSCalibur flow cytometer (BD Biosciences). Cells were gated by FSC/SSC, and propidium iodide exclusion for viability. Data was analyzed using FlowJo software (Treestar). Biotinylated 4A6 mAb (mClr-b; rat IgMκ) and R3A8 mAb (rClr-11, RCMV-E RCTL; mouse IgMκ) were described previously (Carlyle et al., 2004; Mesci and Carlyle, 2007). Biotin-conjugated mAb specific for H-2K^{b}D^{b} (28-8-6, mouse IgG2aκ), H-2D^{q}L^{q} (KH117, mouse IgG2aκ) were purchased from BD Pharmingen; purified mouse pan-Rae-1 mAb (186107, rat IgG2a) was purchased from R&D Systems; CD71 mAb (RI7 217.1.4) was purchased from eBioscience; SA-APC was purchased from LifeTechnologies; all other mAb and secondary reagents were purchased from BD Biosciences, e-Bioscience, or LifeTechnologies. HT29 mAb was developed in the laboratory of Dr. K. Wonigeit (Hannover Medical School). Briefly, intraperitoneal alloimmunization was performed using NKC-congenic LEW donor (Clr-11^{LEW}) splenocytes into LEW.TO-NKC recipient rats (Clr-11TO); hybridoma supernatants were screened by indirect immunofluorescence and flow cytometry for expression on LEW-strain IL-2 lymphokine-activated killer (NK-LAK) cells, but not LEW.TO-NKC NK-LAK cells, and 293 cells transfected with Clr-11^{LEW} but not Clr-11TO.

2.3.5 BWZ reporter cell assays

BWZ.CD3ζ/NKR-P1B$^{B6/129}$ reporter cells were generated as described (Chen et al., 2011; Mesci and Carlyle, 2007). Stimulator cells (mock or MCMV-infected fibroblasts) were cultured in flat 96-well plates in 3-fold dilutions, then reporter cells ($5x10^4$/well) were added and co-cultures were incubated overnight at 37ºC. Purified blocking antibody was added at 10 μg/ml. Control reporter cells were stimulated with 10 ng/ml PMA plus 0.5 μM ionomycin. Cells were washed, resuspended in 100 μL of 1X CPRG buffer (90 mg/L chlorophenol-red-β-D-galactopyranoside (Roche), 9 mM $MgCl_2$, 0.1% NP-40, in PBS), incubated at room temperature, then analyzed using a Varioskan microplate reader (Thermo Scientific), using $OD_{595-655}$.

2.3.6 Agonists, Inhibitors, and Cytokines

Various TLR, NLR, and RLR agonists were obtained from Invivogen (San Diego, CA). Additional NLR agonists were provided by Dr. D.J. Philpott (University of Toronto, Canada).

3',5'-c-di-AMP was purchased from Invivogen and 2',5-3,5'-cGAMP was purchased from Biolog (Bremen, Germany). Actinomycin D (ActD), cycloheximide (CHX), phosphonoacetic acid (PAA), cytosine arabinoside (AraC), AMP, ADP, ATP, and nigericin were purchased from Sigma-Aldrich (St. Louis, MO, USA). All reagents were dissolved in DMSO, water, serum-free DMEM, or PBS according to manufacturer's directions. Cells were treated for 24 hours with reagents or solvent controls in parallel.

2.3.8 Statistical Analysis

Data were analyzed using GraphPad Prism 5, employing either a paired Student's two-tailed t-test, or one-way or two-way ANOVA, with Bonferroni correction, where applicable (see Figure legends). All graphs show mean values ±SEM; *$p<0.05$, **$p<0.01$, ***$p<0.001$. All data are representative of at least three independent experiments.

2.4 Results

2.4.1 MCMV infection promotes cell-intrinsic mClr-b downregulation *in vitro*

We have previously shown that RCMV-E infection of rat embryonic fibroblasts (REF cells) results in a rapid loss of the rat Clr-b homologue, rClec2d11 (rClr-11), by 24 hours post-infection (h.p.i.) (Voigt et al., 2007). To extend these observations to MCMV infection of mouse fibroblasts, we infected mouse NIH3T3 fibroblasts with purified MCMV-Smith virus (MOI of 0.5 PFU/cell by plaque assay; effective MOI~10 with centrifugal enhancement) and assessed Clr-b cell surface expression. As shown in **Figure 2.1A/B**, mClr-b was temporally regulated during MCMV infection, with a pronounced loss by 6-24 h.p.i. However, the use of wild-type MCMV could not discern whether mClr-b downregulation was a direct or an indirect consequence of virus infection at the single cell level.

Consequently, we repeated NIH3T3 infections using a recombinant MCMV-GFP virus that ectopically expresses enhanced GFP driven by an immediate-early (IE) CMV promoter (Henry et al., 2000). The MCMV-GFP was generated previously by homologous integration of EGFP under the control of a native MCMV *ie1/3* gene promoter into MCMV-Smith (VR-194), between the *ie1/3* and *ie2* genes, and proximal to the native *ie1/3* enhancer elements. It does not appear to exhibit any differences in growth kinetics in cell culture *in vitro*, or in infected salivary

Figure 2.1

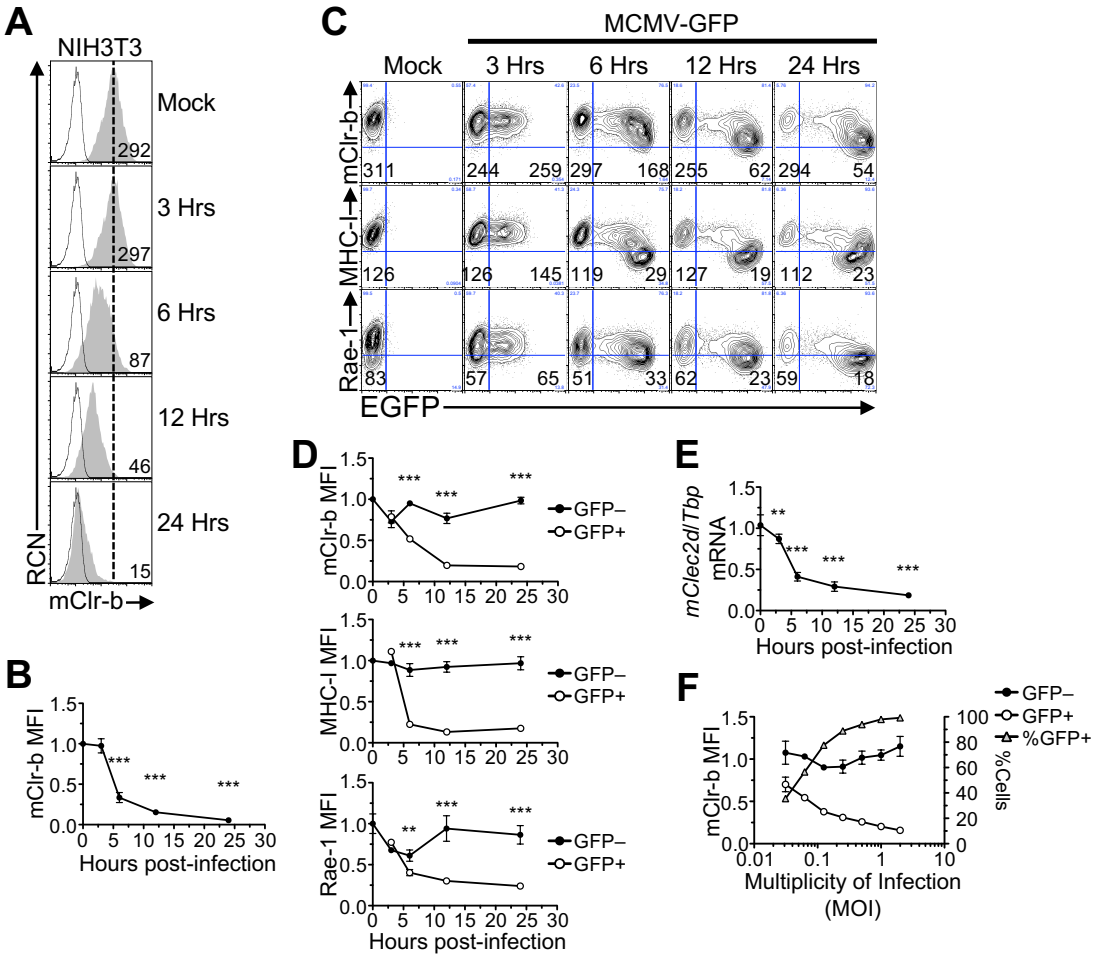

Figure 2.1. MCMV infection promotes rapid Clr-b downregulation. (**A**) NIH3T3 cells were infected with MCMV-Smith virus at an MOI of 0.5 PFU/cell over a 24h time course and analyzed by flow cytometric analysis for cell surface expression of mClr-b (shaded histogram, 4A6 Clr-b mAb; black line, secondary reagent alone; dotted vertical line, reference for Mock control median fluorescence intensity (MFI) level; numbers indicate MFI values). (**B**) Quantitation of mClr-b MFI levels in (A) normalized to mock control levels. (**C**) Time-course of Clr-b, MHC-I, and Rae-1 expression upon NIH3T3 cell infection using recombinant MCMV-GFP. Numbers represent MFI levels of the respective markers gated on GFP^- (uninfected) or GFP^+ (MCMV-infected) cells. (**D**) Quantitation of mClr-b, MHC-I, and Rae-1 MFI levels on MCMV-GFP-infected cells in (C) normalized to mock controls. (**E**) Transcript levels (*Clec2d*) following MCMV infection (indexed to *Tbp* levels, and normalized relative to Mock controls). (**F**) Quantitation of mClr-b MFI levels and %GFP+ cells upon MCMV-GFP infections at different multiplicity of infection (MOI) ratios analyzed 22 hrs post-infection. Black and white circles represent GFP^- and GFP^+ cell subsets (corresponding with left Y-axis) and gray triangles represent $\%GFP^+$ cells (right Y-axis). Graphs show mean±SEM. Experiments were analyzed using ANOVA with Bonferroni post-hoc analysis; *p<0.05, **p<0.01, ***p<0.001. All data are representative of at least three independent experiments.

glands *in vivo* (Henry et al., 2000). As shown in **Figure 2.1C,D**, MCMV-GFP infections distinguished infected (GFP^+) from uninfected (GFP^-) cells as early as 3 h.p.i., with prominent mClr-b loss ensuing by 6-24 h.p.i. In parallel, we examined cell surface expression of MHC-I ligands for the Ly49 receptors ($H\text{-}2^q$) and Rae-1 ligands for the NKG2D receptor (**Fig. 2.1C,D**). Similar to mClr-b, MHC-I and Rae-1 levels were also reduced by 6-24 h.p.i. (**Fig. 2.1C,D**), likely due to the action of several known MCMV-encoded immunoevasins (e.g., m04, m06, m138, m145, m152, m155) (Krmpotic et al., 2005; Lanier, 2008; Lenac et al., 2006; Lodoen et al., 2003; Lodoen et al., 2004; Wagner et al., 2002). As a control, MCMV-GFP infection had no effect on cell surface levels of the transferrin receptor (CD71, **Fig. 2.2**). Importantly, the restricted loss of mClr-b on infected (GFP^+) cells suggests that this response occurs by an MCMV infection-dependent cell-intrinsic mechanism.

Notably, experiments using MCMV culture supernatants revealed a pronounced upregulation of Clr-b surface expression on uninfected (GFP^-) "bystander" cells, likely mediated by soluble factors such as interferons (Kirkham et al., 2017); however, this bystander mClr-b upregulation was not observed using purified virus, which only promoted infection-dependent mClr-b downregulation (**Fig. 2.1C,D**). In addition, similar losses of mClr-b expression on the infected GFP^+ but not uninfected GFP^- subsets were also observed for several cell types, including primary WT B6 MEF and adult ear fibroblasts (AEF), S17 bone marrow stromal cells, J774 and RAW264.7 monocyte/macrophage cells, and fetal ILC-like MNK-3 cells (Mesci, 2011).

It has previously been shown that RCMV-E infection of rat fibroblasts results in a loss of rClr-11 at both the transcript and cell surface protein levels (Voigt et al., 2007). Similarly, quantitative real-time RT-PCR analysis of MCMV-infected mouse NIH3T3 fibroblasts revealed that mClr-b surface protein downregulation was mirrored by a time-dependent loss of mClr-b (*Clec2d*) transcripts by 6-24 h.p.i. (normalized to *Tbp*; **Fig. 2.1E**). Interestingly, similar losses were observed for other mouse mClr family members, including mClr-a/c/f/g (*Clec2e*/*f*/*h*/*i*; **Fig. 2.3**). Titration of MCMV infections using 2-fold MOI dilutions demonstrated that mClr-b loss correlated with viral dosage, and was restricted to infected GFP^+ cells (**Fig. 2.1F**). Collectively, these results indicate that MCMV promotes an infection-dependent cell-intrinsic loss of mClr-b (*Clec2d*) at the transcript and cell surface protein levels.

Figure 2.2

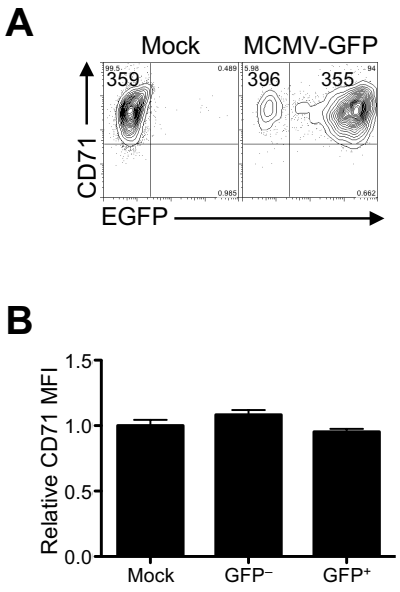

Figure 2.2. Cell surface expression of CD71 (Transferrin Receptor) is unaltered during MCMV Infection. NIH3T3 cells were infected with MCMV-GFP (MOI of 0.5 PFU/cell) and analyzed by flow cytometry 24 h.p.i. using APC-conjugated anti-mouse CD71 mAb. (**A**) Representative flow plots of uninfected and infected NIH3T3. The numbers in the gates corresponds to the CD71 MFI. (**B**) Quantitation of CD71 expression in mock-infected and infected populations normalized to mock levels. Graph shows mean±SEM of normalized MFI values in (A). Data is representative of at least three independent experiments.

Figure 2.3

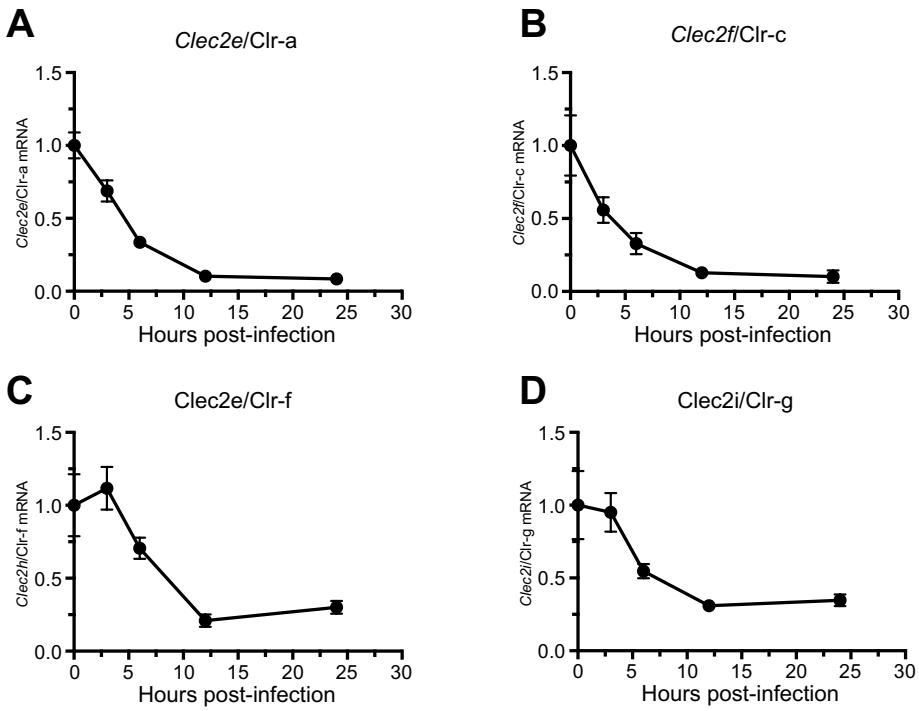

Figure 2.3. Transcript expression of Clr members during MCMV infection. (**E**) Transcript levels of (**A**) *Clec2a*/Clr-a, (**B**) *Clec2f*/Clr-c, (**C**) *Clec2e*/Clr-f, and (**D**) *Clec2i*/Clr-g following MCMV infection (indexed to *Tbp* levels, and normalized relative to Mock controls).

2.4.2 MCMV-mediated mClr-b downregulation is partially blocked by translational inhibition

Since mClr-b downregulation was triggered early in the MCMV replication cycle, and only in infected cells, we next assessed the contribution of *de novo* gene expression to mClr-b downregulation. To this end, we repeated MCMV infections in the presence of transcriptional, translational, and viral replication inhibitors. It is important to note that some of these inhibitors can also prevent host gene expression and/or induce cellular stress responses, resulting in mClr-b downregulation in the absence of infection. In addition, cell surface Clr-b exhibits fast turnover kinetics, with a half-life of about 3 hrs (**Fig. 2.4**). Thus, we titrated these chemicals where possible to minimize the extent of mClr-b downregulation by chemical treatment alone, then tested their ability to block MCMV-mediated mClr-b downregulation.

As shown in **Figure 2.5A,B**, UV-inactivated MCMV failed to promote mClr-b downregulation on NIH3T3 cells. As expected, MHC-I and Rae-1 levels did not change using UV-inactivated MCMV (**Fig. 2.5A,B**) (Tokuyama et al., 2011), suggesting that active or productive viral infection are required for MCMV-mediated loss of mClr-b, MHC-I and Rae-1 ligands. In contrast, inhibition of transcription and immediate early (α) gene expression using actinomycin D (ActD) resulted in a substantial loss of basal mClr-b surface expression (even on Mock and uninfected GFP^- cells; **Fig. 2.5C,D**). This implies either that mClr-b undergoes rapid turnover in the absence of nascent transcripts (blocked by ActD; **Fig. 2.4**), or that ActD may also promote stress-mediated mClr-b downregulation (Fine et al., 2010; Williams et al., 2012). Thus, we attempted to titrate ActD levels to achieve only partial Clr-b loss, while maintaining partial inhibition of immediate early genes; however, such an optimal dose was not possible, making inferences on immediate early gene blockade inconclusive (**Fig. 2.5**).

MCMV early (β) gene expression can be inhibited using the translational inhibitor, cycloheximide (CHX). Notably, pre-treatment of NIH3T3 cells with a low dose of CHX alone caused some basal mClr-b loss on uninfected cells (compare Mock DMSO versus CHX; **Fig. 2.5C,D; Fig. 2.4**). Interestingly, however, CHX treatment rendered the expression profiles of infected (GFP^+) versus uninfected (GFP^-) cells nearly indistinguishable (**Fig. 2.5C,D**), suggesting that CHX was sufficient to prevent MCMV infection-mediated loss of mClr-b. Notably, higher CHX doses blocked mClr-b expression on uninfected cells, similar to ActD treatment (**Fig. 2.6**). Similarly, MHC-I and Rae-1 downregulation, mediated by known early

Figure 2.4

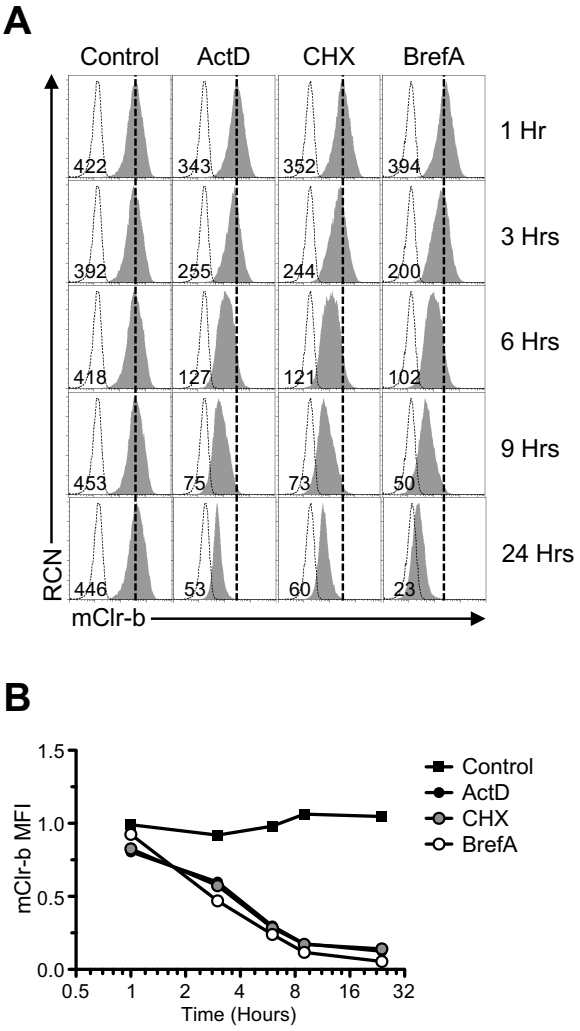

Figure 2.4. Kinetic studies reveal that mClr-b on mouse fibroblasts has a short half-life. (**A**) NIH3T3 cells were treated with inhibitors of transcription, translation, and golgi maturation; actinomycin D (ActD, 10 nM), cycloheximide (CHX, 10 μg/ml), and brefaldin A (BrefA, 10 μg/ml) respectively, at different timepoints and stained by flow cytometry using 4A6 mAb. Shaded histograms represents 4A6 staining; black line, secondary reagent alone; dotted vertical line, reference for control MFI level; numbers indicate MFI values. (**B**) Quantitation of mClr-b MFI levels in (A) normalized to mock control levels (mean ± SEM).

Figure 2.5

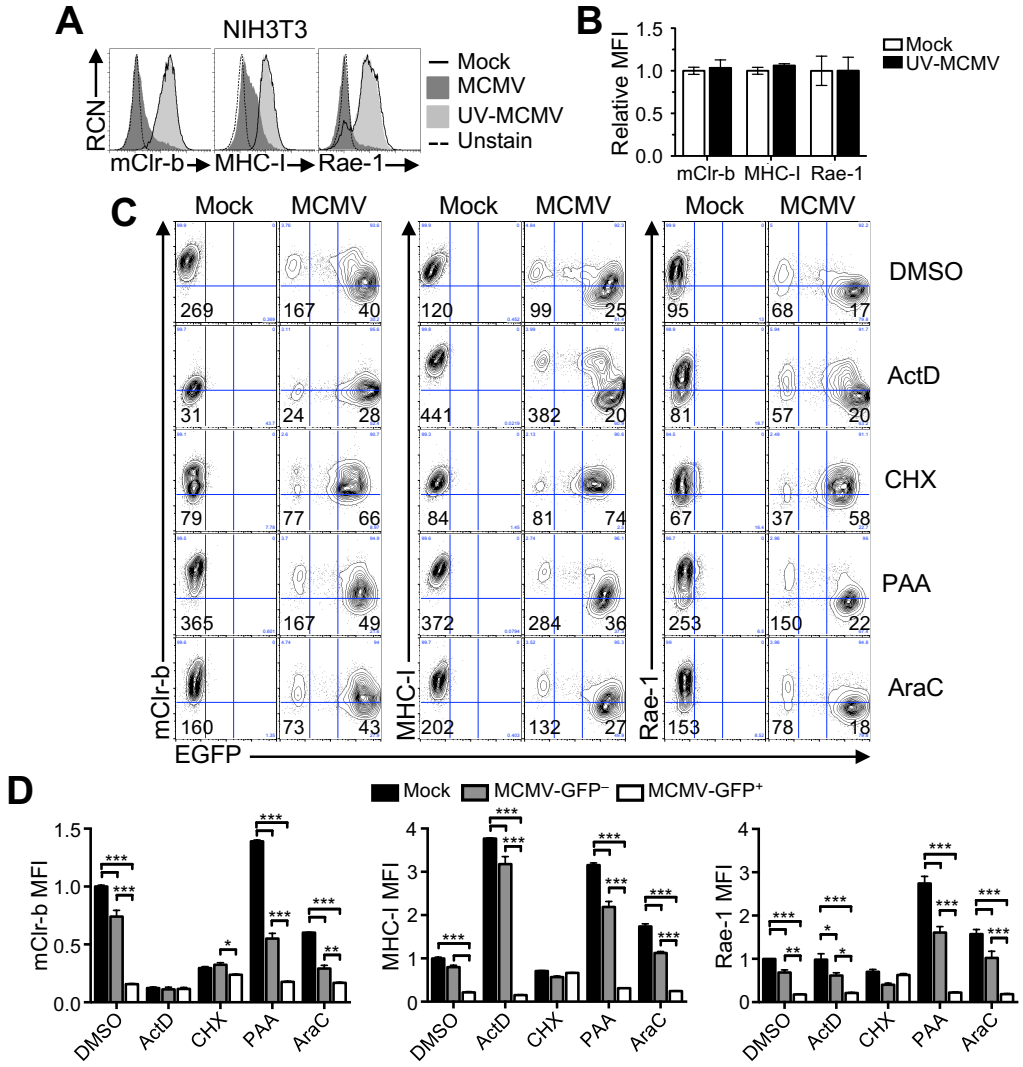

Figure 2.5. MCMV-mediated mouse Clr-b downregulation is prevented by UV-inactivation and inhibition of early viral and host protein synthesis. (**A**) Characterization of mClr-b, MHC-I, and Rae-1 expression upon treatment with UV-inactivated MCMV-GFP. Infected NIH3T3 cells were analyzed for surface expression of mClr-b (4A6 mAb), MHC-I (H-2L^{q}D^{q}), and Rae-1 (α-ε). (**B**) Quantitation of mClr-b, MHC-I, and Rae-1 MFI levels in (B) relative to Mock controls. (**C**) Characterization of mClr-b, MHC-I, and Rae-1 expression upon MCMV-GFP infections in the presence of various chemical inhibitors. NIH3T3 cells were pre-treated with DMSO (control), Actinomycin D (ActD, 10 nM), cycloheximide (CHX, 10 µg/ml), phosphonoacetic acid (PAA, 400 µg/ml), or cytosine arabinoside (AraC, 50 µg/ml), then infected with MCMV-GFP and analyzed by flow cytometry at 24 h.p.i. (**D**) Quantitation of mClr-b, MHC-I, and Rae-1 MFI levels in (C) normalized to DMSO-treated Mock MFI levels. Graphs show mean±SEM. Experiments were analyzed using ANOVA with Bonferroni post-hoc analysis. All data are representative of at least three independent experiments.

Figure 2.6

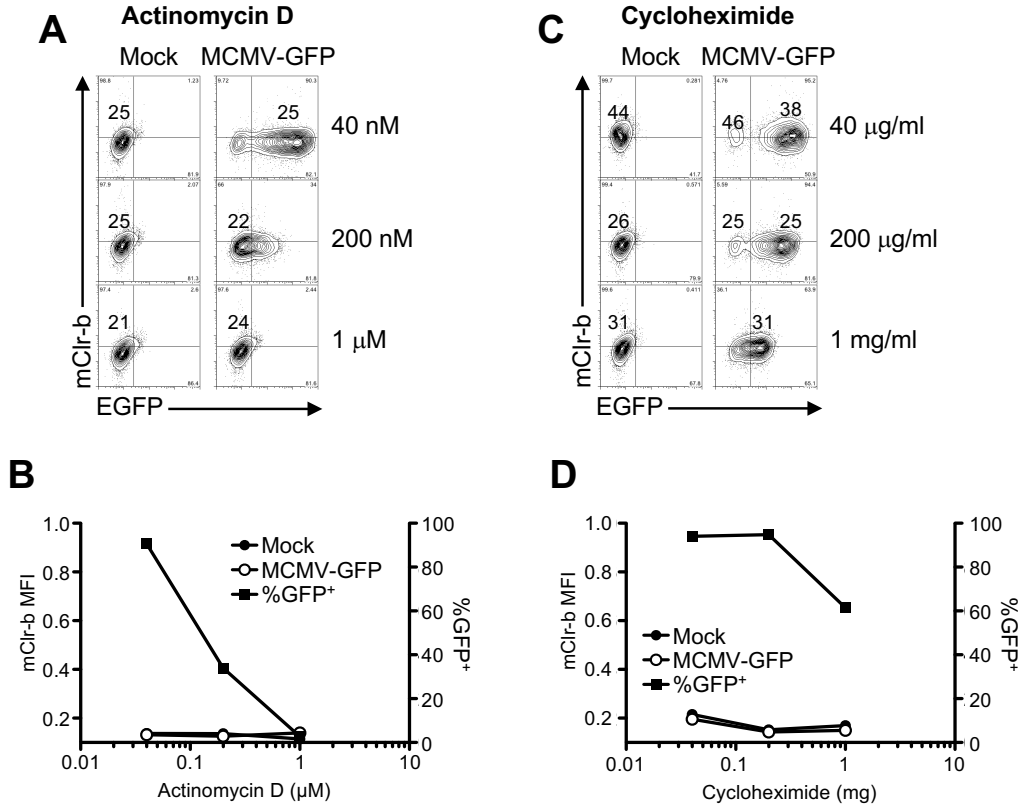

Figure 2.6. Immediate early gene expression is abolished with high doses of ActD or CHX and during MCMV infection. NIH3T3 cells were treated with titrated doses of (**A**) ActD or (**C**) CHX and either mock or MCMV-GFP infected and analyzed for Clr-b expression 24 h.p.i by flow cytometry. Numbers correspond to Clr-b MFI of population. (**B**) and (**D**) Quantitation of mClr-b MFI levels normalized to mock DMSO control levels for A and C, respectively (mean ± SEM). The left Y-axis corresponds to the mClr-b exression (mock and MCMV-GFP infected) whereas the right Y-axis measures the % of GFP+ cells in infected samples. Data is representative of at least three independent experiments.

viral immunoevasin genes, were also blocked by CHX treatment (**Fig. 2.5C,D**). Nonetheless, CHX is capable of inhibiting the translation of both viral immediate/early and host gene products; thus, immediate early to early viral proteins and/or *de novo* cellular protein synthesis appear to be involved in regulating mClr-b expression during infection.

Late (γ) viral gene expression is enhanced by viral genome replication, and can be blocked by viral DNA polymerase inhibitors, such as phosphonoacetic acid (PAA) or cytosine arabinoside (AraC). However, viral replication appeared to be dispensable for MCMV-mediated downregulation of mClr-b, MHC-I, and Rae-1 ligands (**Fig. 2.5C,D**). Collectively, these results suggest that MCMV-mediated Clr-b downregulation requires immediate early to early events in active MCMV infection, but not late events nor viral genome replication *per se*.

We next tested the effects of the proteasomal inhibitor, MG132, on MCMV infection-mediated Clr-b loss, as we previously showed that inhibition of the ubiquitin (Ub)-proteasome degradation pathway could prevent genotoxic stress-mediated Clr-b downregulation (Fine et al., 2010; Williams et al., 2012). As shown in **Fig. 2.7**, MG132 was effective at blocking MCMV-mediated Clr-b loss, albeit incompletely even at high doses. However, MG132 also affects numerous Ub-dependent cellular processes apart from proteasomal degradation, including autophagy and Ub-dependent signaling pathways. These results suggest that the ubiquitin-proteasomal degradation pathway may be partially responsible for Clr-b loss induced by MCMV infection, perhaps by accelerating Clr-b turnover.

2.4.3 RCMV-E-mediated Clr-11 loss and RCTL induction are blocked by CHX treatment

Using new reagents and cell lines, we next more closely examined the requirements for RCMV-E-mediated rClr-11 downregulation and RCTL immunoevasin expression in the rat system. First, we repeated RCMV-E infections using both rat embryonic fibroblasts (REF cells; **Fig. 2.8**) (Voigt et al., 2007), as well as primary rat AEF cells (**Fig. 2.9**). Since R3A8 antibody is dual-specific (cross-reactive for both the RCTL decoy and host rClr-11) (Mesci and Carlyle, 2007; Voigt et al., 2007), we infected REF cells using either wild-type RCMV-E (RCMV WT) or an RCTL-deficient virus (RCMV ΔRCTL) in order to distinguish rClr-11 from RCTL. Interestingly, infections using UV-inactivated RCMV viruses appeared to slightly increase R3A8 staining on REF cells (**Fig. 2.8A,B**), which may be due to weak host rClr-11 induction in the

Figure 2.7

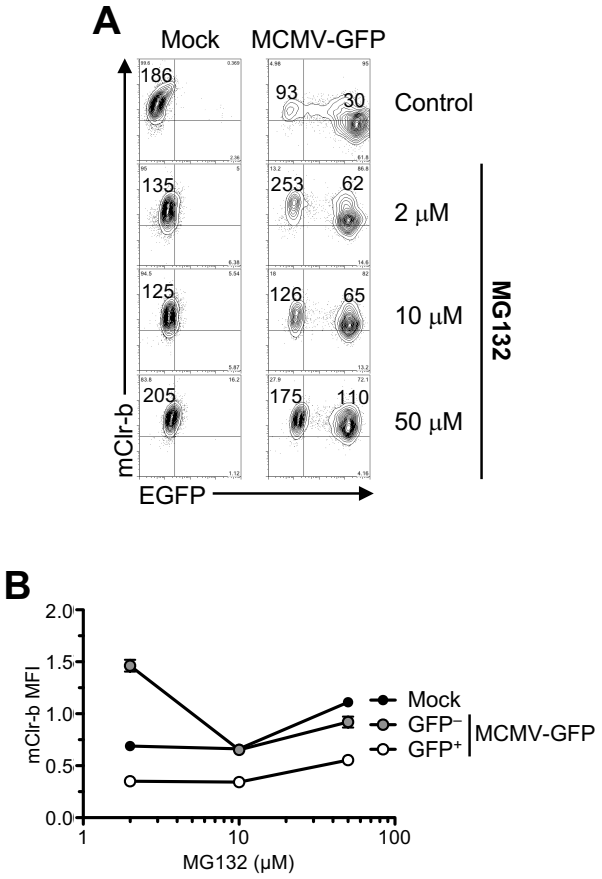

Figure 2.7. Inhibition of ubiquitin-proteosomal degradation pathway partially blocks mClr-b downregulation during MCMV infection. NIH3T3 cells were treated with titrated doses of the proteosomal inhibitor, MG132, and either mock-infected or MCMV-infected and analyzed by flow cytometry 24 h.p.i. (**A**) Representative flow plots of uninfected and infected NIH3T3 stained with 4A6 mAb. The numbers in the gates corresponds to the mClr-b MFI. (**B**) Quantitation of mClr-b expression in mock-infected and MCMV-infected populations normalized to mock DMSO levels. Graph shows mean±SEM of normalized MFI values in (A). Data is representative of at least three independent experiments.

Figure 2.8

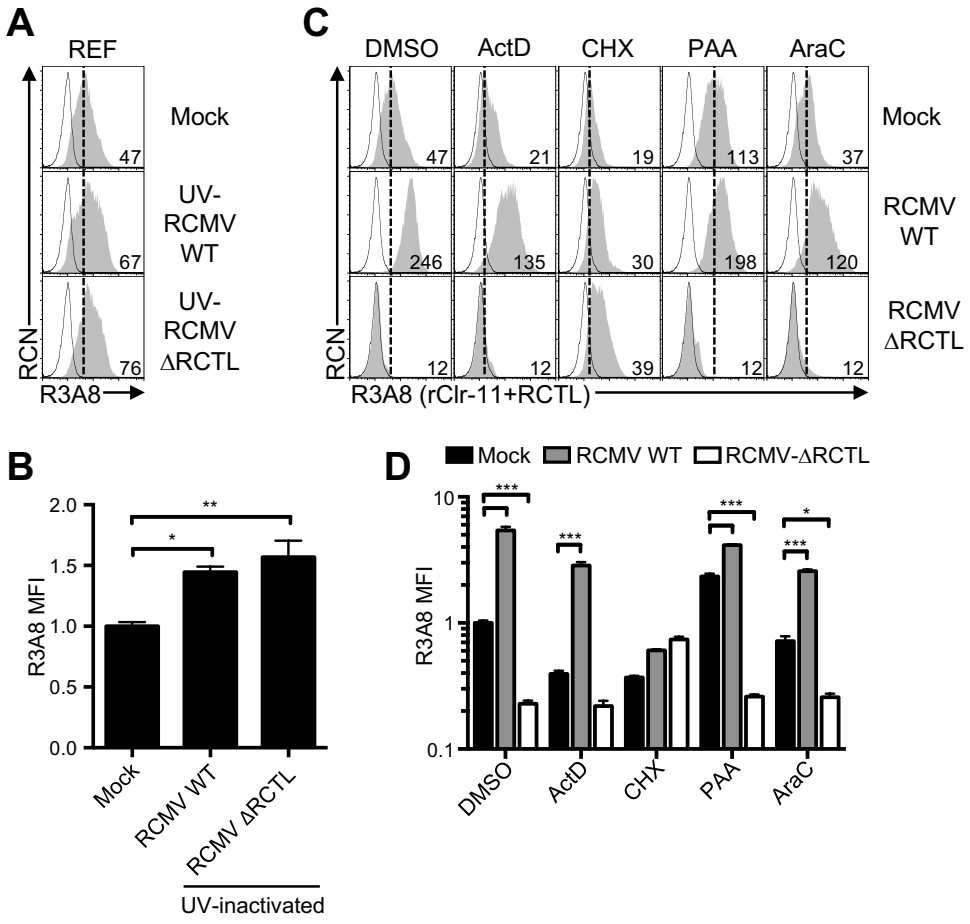

Figure 2.8. RCMV-mediated rClr-11 downregulation and RCTL induction are prevented by UV-inactivation and inhibition of early viral and host protein synthesis. (**A**) Characterization of rClr-11 expression on RCMV-E-infected REF cells upon treatment with UV-inactivated RCMV-E WT or ΔRCTL-mutant virus. Treated cells were analyzed by flow cytometry for rClr-11/RCTL (R3A8 mAb) expression (numbers indicate MFI values). (**B**) Quantitation of R3A8 MFI levels shown in (A) relative to Mock controls. (**C**) Characterization of rClr-11/RCTL (R3A8 mAb) expression upon RCMV-E WT or ΔRCTL-mutant virus infections in the presence of various chemical inhibitors. REF cells were pre-treated with DMSO (control), ActD (10 nM), CHX (10 µg/ml), PAA (400 µg/ml), or AraC (50 µg/ml), then infected with RCMV-E WT or ΔRCTL-mutant virus and analyzed by flow cytometry at 24 h.p.i. for R3A8 expression (shaded histogram, R3A8 rClr-11/RCTL mAb; black line, secondary reagent alone; dotted vertical line, reference for Mock control MFI level; numbers indicate MFI values). **(D**) Quantitation of rClr-11/RCTL (R3A8 mAb) MFI levels in (C) normalized to DMSO-treated Mock control MFI levels. Graphs show mean±SEM. Experiments were analyzed using ANOVA with Bonferroni post-hoc analysis. All data are representative of at least three independent experiments.

Figure 2.9

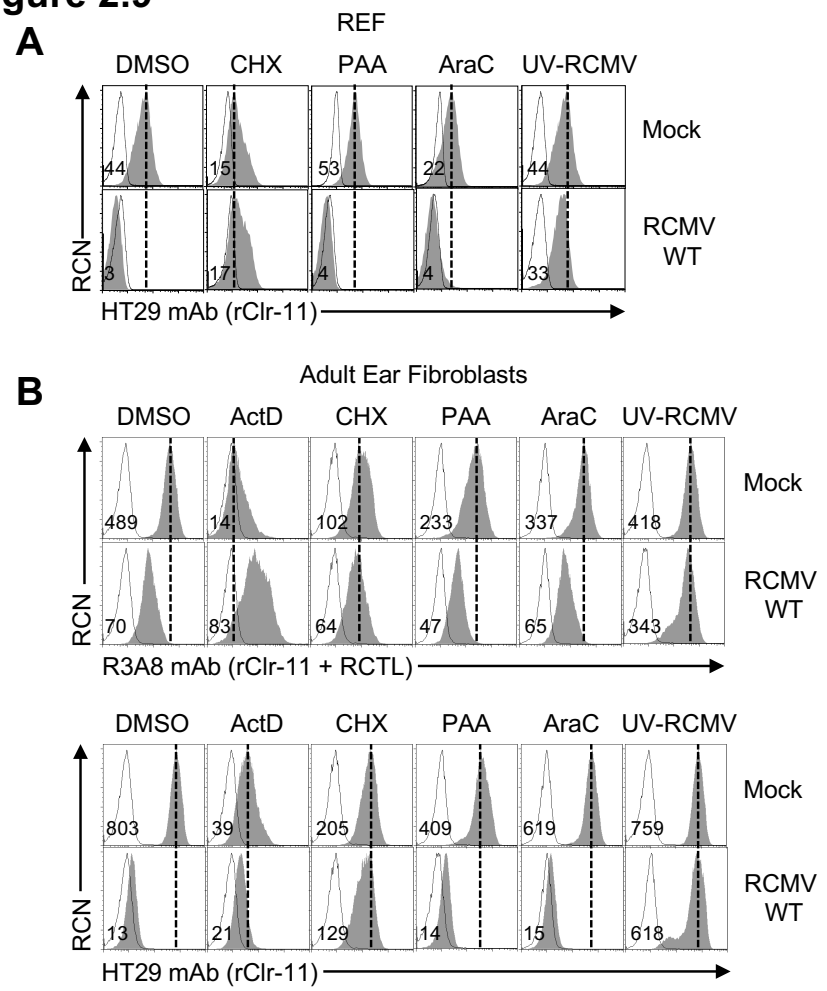

Figure 2.9. Extended analysis of RCMV-mediated rClr-11 downregulation and RCTL induction using RCMV-E WT virus and inhibitor treatments. (**A**) Characterization of rClr-11 (HT29 mAb) expression upon RCMV-E WT virus infection of REF cells in the presence of various chemical inhibitors or using UV-inactivated virus. REF cells were pre-treated with DMSO (control), CHX (10 μg/ml), PAA (400 μg/ml), or AraC (50 μg/ml), then infected with RCMV-E WT virus, or treated with UV-inactivated RCMV-E virus, then analyzed by flow cytometry at 24 h.p.i. Shaded histograms represent HT29 (rClr-11) mAb; black line, secondary reagent alone; dotted vertical line, reference for Mock control MFI level; numbers indicate MFI values. **(B**) Characterization of rClr-11/RCTL (R3A8 mAb, top) or rClr-11 (HT29 mAb, bottom) expression upon RCMV-E WT virus infection of primary rat adult ear fibroblast (AEF) cells in the presence of chemical inhibitors or using UV-inactivated virus. Rat AEF cells were pre-treated with treatments as in A, then infected with RCMV-E WT virus, or treated with UV-inactivated RCMV-E virus, then analyzed by flow cytometry at 24 h.p.i. Shaded histograms represent R3A8 (rClr-11/RCTL) or HT29 (rClr-11) mAb; black line, secondary reagent alone; dotted vertical line, reference for Mock control MFI level; numbers indicate MFI values.

absence of active infection, or perhaps weak cross-reactivity with another unidentified host rClr family member. Nonetheless, RCMV WT infection of REF cells results in an increase in R3A8 staining (due to RCTL), versus Mock-treated control cells (rClr-11 alone; **Fig. 2.8C,D**). In contrast, ΔRCTL-mutant infection of REF cells promotes a loss of R3A8 staining (rClr-11 alone) versus Mock-control cells (rClr-11 alone; **Fig. 2.8C,D**). Taken together, RCTL appears to replace host Clr-11 during RCMV infection. Similar data were observed for rClr-11^{hi} rat AEF cells (**Fig. 2.9**); however, R3A8 staining decreases here due to a much larger loss of rClr-11 not fully compensated by RCTL upregulation. Second, we used a novel rClr-11 mAb, HT29, in parallel with R3A8 mAb; importantly, HT29 mAb does not cross-react with RCTL, yet possesses robust reactivity with rClr-11, allowing us to observe loss of rClr-11 in isolation upon infection of REF and AEF cells using WT RCMV (**Fig. 2.9**).

Next, the effects of inhibitors were examined. Similar to the results in mouse NIH3T3 cells, ActD treatments alone resulted in a substantial infection-independent loss of basal rClr-11 from the cell surface of rat AEF and REF cells, albeit incomplete (compare Mock DMSO versus ActD; **Fig. 2.8C,D; Fig. 2.9**). However, this titrated ActD concentration failed to prevent expression of the *rctl* gene product (RCMV WT versus ΔRCTL-mutant; **Fig. 2.8C,D; Fig. 2.9**). Nor did ActD prevent infection-mediated downregulation of host rClr-11 (Mock versus ΔRCTL-mutant; **Fig. 2.8C,D; Fig. 2.9**). This RCMV-mediated induction of viral RCTL and loss of host rClr-11 were also confirmed using HT29 versus R3A8 mAb (see ActD; **Fig. 2.9**). Notably, as seen in the mouse system, higher ActD doses were required to block RCTL induction upon RCMV-E infection, and these doses completely blocked basal rClr-11 expression on uninfected cells, precluding usage of an optimal ActD dose (**Fig. 2.10**).

Again similar to the mouse system, treatment with a titrated CHX dose resulted in decreased basal rClr-11 cell surface expression (Mock DMSO versus CHX; **Fig. 2.8C,D; Fig. 2.9**). More importantly, however, CHX rendered the R3A8 expression profiles of the two infected populations indistinguishable (RCMV WT versus ΔRCTL-mutant; **Fig. 2.8C,D**), and blocked infection-mediated loss of host rClr-11 visualized using both R3A8 and HT29 mAb (Mock versus RCMV; **Fig. 2.8C,D**; **Fig. 2.9**). These data suggest that CHX is sufficient to prevent both infection-mediated loss of rClr-11, as well as RCTL induction, and are in agreement with previous data suggesting that *rctl* is an early gene (Voigt et al., 2007).

Figure 2.10

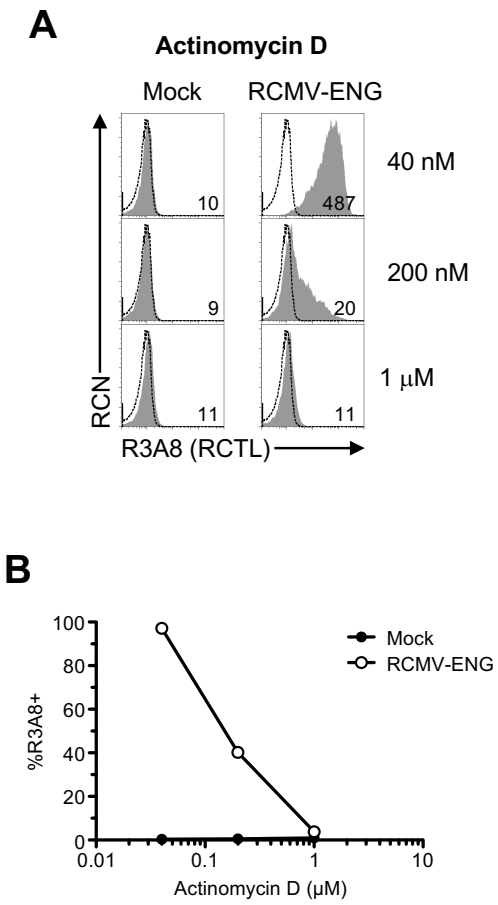

Figure 2.10. High dose of ActD blocks expression of RCTL during RCMV-E infection. (**A**) REFs were treated with titrated doses of ActD and either mock or RCMV-E infected and analyzed for R3A8 (RCTL) expression 24 h.p.i by flow cytometry. Numbers correspond to R3A8 MFI of population. (**B**) Quantitation of %R3A8+ cells in both mock-infected and RCMV-infected treatments for A (mean ± SEM). Data is representative of at least three independent experiments.

Notably, similar to UV-inactivated RCMV (**Fig. 2.8A,B**), the subtle increase in R3A8 staining observed upon RCMV infection in the presence of CHX treatment (using both RCMV WT and ΔRCTL-mutant; **Fig. 2.8C,D**) may result from weak rClr-11 induction in the absence of productive infection (in the presence of CHX), or perhaps weak cross-reactivity with another unidentified host rClr family member; however, this was not observed using another rClr-11 mAb, HT29 (**Fig. 2.9**). Of note, treatments with PAA or AraC were insufficient to prevent rClr-11 downregulation or RCTL induction (**Fig. 2.8C,D; Fig. 2.9A,B**). Collectively, these results demonstrate that only translational inhibition using CHX abrogates RCMV-mediated host rClr-11 downregulation, at the same time preventing RCTL immunoevasin induction. Thus, host rClr-11 downregulation is a phenomenon induced by active RCMV infection, and countered by the *rctl* gene product.

2.4.4 Cross-species CMV infection promotes host mClr-b and rClr-11 downregulation

The similar results obtained using MCMV infection of mouse fibroblasts and RCMV infection of rat fibroblasts prompted us to investigate whether host mClr-b/rClr-11 downregulation was a conserved cellular response to infection, or whether virus-specific (and potentially host-adapted) immunoevasins were involved. Using cross-species infections, host mClr-b expression can also be monitored without RCTL cross-reactivity (using 4A6 mAb), while RCTL expression can be monitored without rClr-11 cross-reactivity (using R3A8 mAb). We thus infected mouse NIH3T3 cells with MCMV or RCMV-E and measured cell surface expression of mClr-b, MHC-I, and Rae-1 (**Fig. 2.11A,B**). Strikingly, mClr-b downregulation was observed using MCMV or RCMV viruses (~15-fold reduction; **Fig. 2.11A,B**); interestingly, however, mClr-b loss was consistently more robust using cross-species RCMV infection. In contrast, MHC-I molecules showed a smaller <2-fold reduction upon cross-species RCMV infection versus a >4-fold reduction using MCMV infection. Rae-1 downregulation was similar using MCMV or RCMV infection (~6-fold reduction; **Fig. 2.11A,B**). To monitor the RCTL immunoevasin in isolation, we also stained infected mouse NIH3T3 cells using the rat-specific R3A8 mAb; as expected, RCTL was only detected using RCMV WT virus (**Fig. 2.11A,B**). Notably, no cross-contamination of the viruses could be detected, and RCMV itself is non-cytopathic in NIH3T3 cells, although it can induce cytomegaly.

Figure 2.11

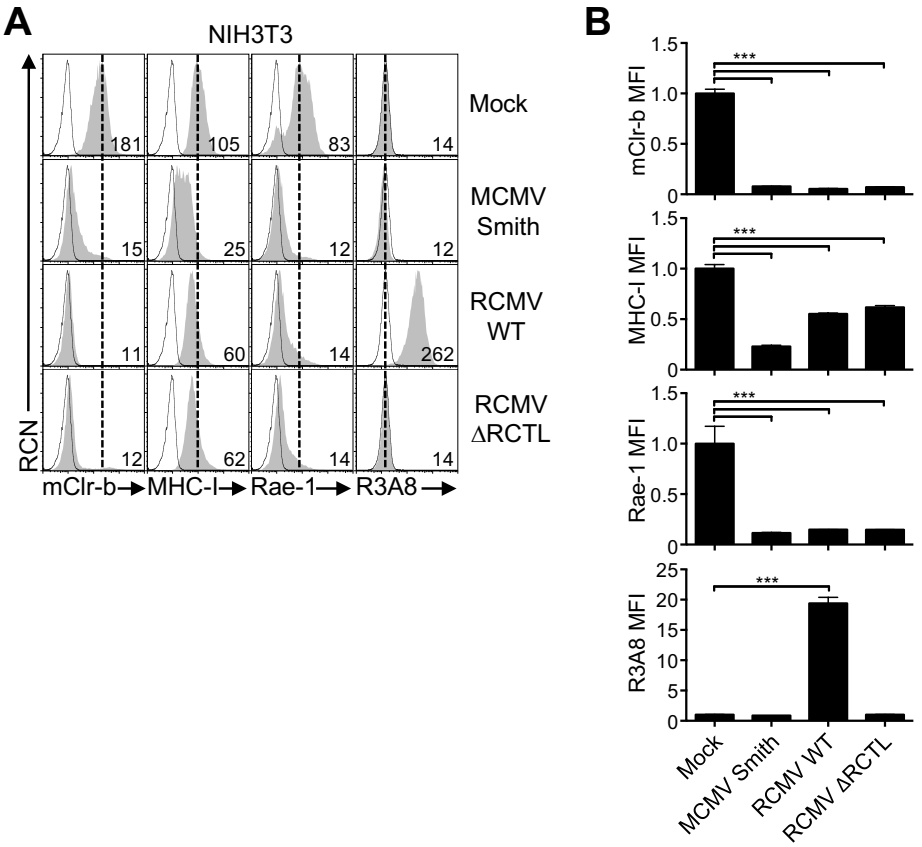

Figure 2.11. Xenogeneic RCMV-E infection promotes mouse Clr-b loss on mouse fibroblasts. (**A**) NIH3T3 were infected with MCMV-Smith or RCMV-E viruses then analyzed by flow cytometry at 24 h.p.i. for mClr-b, MHC-I, Rae-1, and R3A8 (RCTL) expression. Shaded histograms represent primary mAb stain; black line, secondary reagent alone; dotted vertical line, reference for Mock control MFI level; numbers indicate MFI values. (**B**) Quantitation of MFI levels in (A) normalized to Mock control MFI levels. Graphs show mean±SEM. Experiments were analyzed using 1-way ANOVA with Bonferroni post-hoc analysis. All data are representative of at least three independent experiments.

To reciprocate these observations, we infected rat REF cells with RCMV-E or MCMV viruses and measured cell surface expression of rClr-11 (±RCTL) using R3A8 mAb (**Fig. 2.12A,B**). Interestingly, cross-species MCMV infection of REF cells also promoted rClr-11 downregulation (~4-fold); however, as observed for mClr-b using mouse fibroblasts, rClr-11 loss was slightly more robust using RCMV-E virus (ΔRCTL-mutant) versus cross-species MCMV viruses (**Fig. 2.12A,B**). Upon further investigation using MCMV-GFP, the infected (GFP^+) REF cells were observed to downregulate rClr-11 (R3A8) expression, whereas uninfected (GFP^-) REF cells did not (**Fig. 2.12C,D**). These data suggest that host Clr (mClr-b/rClr-11) downregulation is a conserved cellular response to CMV infection, and that RCTL is an RCMV-E-specific immunoevasin.

2.4.5 Modulation of mClr-b by PRR agonists

Both viral and bacterial infections lead to the detection of numerous pathogen/danger-associated molecular patterns (PAMP/DAMP) via host pattern recognition receptors (PRR); such PAMP include both extracellular moieties and intracellular (vesicular or cytosolic) metabolites. Thus, we sought to determine whether CMV-mediated mClr-b downregulation could be recapitulated in isolation upon cellular exposure to defined PAMP, or alternatively if Clr-b loss may require active viral infection. Since whole UV-inactivated CMV is insufficient to promote mClr-b loss, and viral replication is dispensable, yet immediate early to early viral gene expression and/or host protein translation are required, it is likely that intermediates of virus infection, perhaps signaling metabolites, nucleic acids, or unidentified viral gene products, may be required to mimic CMV infection. To this end, we treated cell lines with a panel of known PRR agonists targeting various innate sensing pathways.

Initially, mouse fibroblast cell lines (NIH3T3, MEF) were treated with various PRR agonists targeting Toll-like receptors (TLR1-9), Nod-like receptors (NLR), or cytosolic nucleic acid receptors, including RIG-I-like receptors (RLR) or AIM2-like receptors (ALR) (**Fig. 2.13A,B**). However, no significant mClr-b downregulation comparable to MCMV infection was observed upon treatment of fibroblasts using these PRR agonists, including intracellular double-stranded RNA (polyI:C) and double-stranded immunostimulatory DNA (dsB-DNA) (**Fig. 2.13A,B**). However, upon investigation of known inducers of the Nlrp3 inflammasome, extracellular ATP was the sole metabolite that autonomously downregulated mClr-b on all cell

Figure 2.12

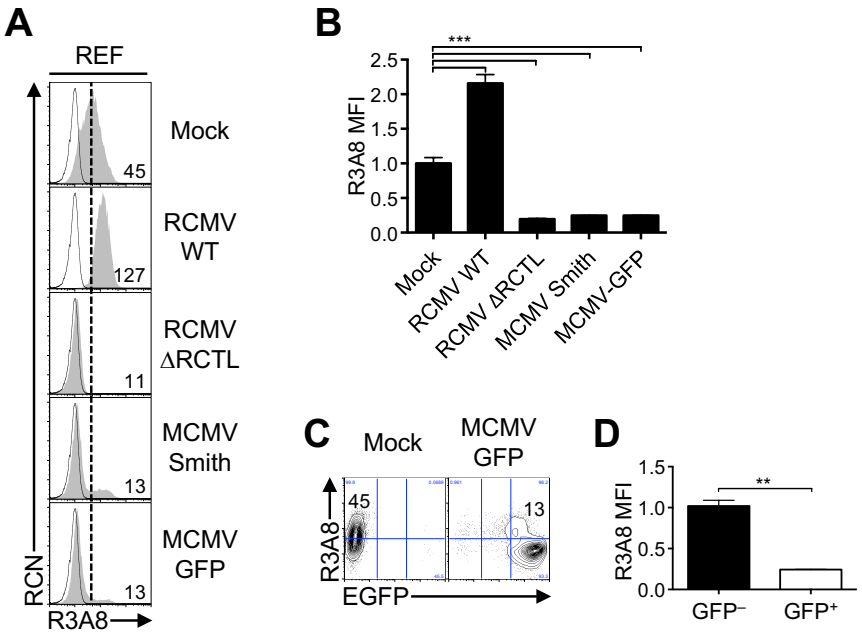

Figure 2.12. Xenogeneic MCMV infection promotes rat Clr-11 loss on rat fibroblasts. (**A**) REF cells were infected with MCMV or RCMV-E viruses and analyzed by flow cytometry at 24 h.p.i. for R3A8 (rClr-11/RCTL) expression. Shaded histograms represent primary R3A8 stain; black line, secondary reagent alone; dotted vertical line, reference for Mock control MFI level; numbers indicate MFI values. (**B**) Quantitation of MFI levels in (A) normalized to Mock control MFI levels. (**C**) Representative R3A8 (rClr-11) flow cytometric analysis of MCMV-GFP-infected REF cells. (**D**) Quantitation of R3A8 MFI levels in (C) gated by MCMV-GFP expression. Graphs show mean ± SEM. Experiments were analyzed using 1-way ANOVA with Bonferroni post-hoc analysis (except D, t-test). All data are representative of at least three independent experiments.

Figure 2.13

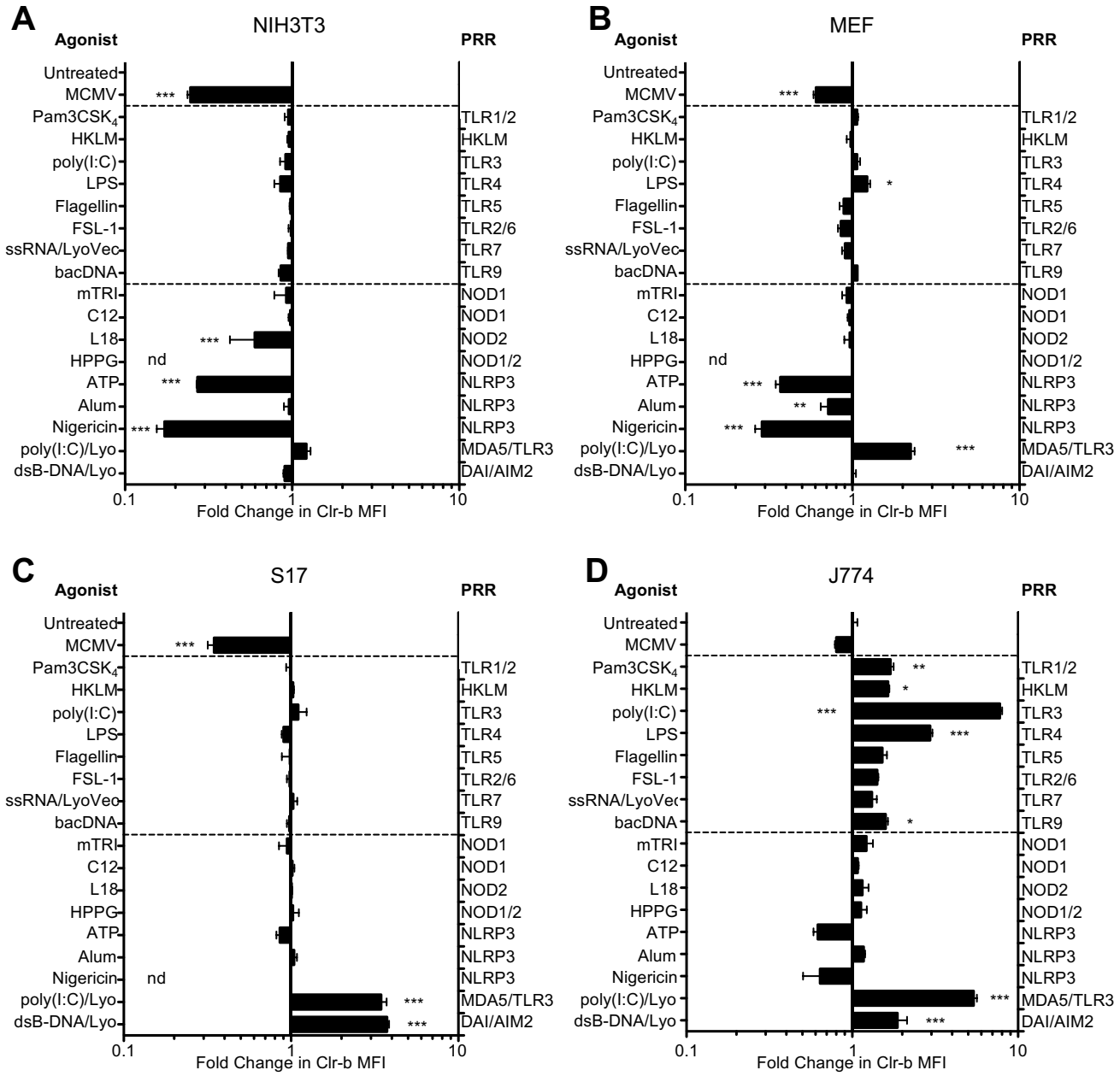
A
NIH3T3
B
MEF
C
S17
D
J774
Agonist
PRR
Untreated
MCMV
Pam3CSK4
HKLM
poly(I:C)
LPS
Flagellin
FSL-1
ssRNA/LyoVec
bacDNA
mTRI
C12
L18
HPPG
ATP
Alum
Nigericin
poly(I:C)/Lyo
dsB-DNA/Lyo
TLR1/2
HKLM
TLR3
TLR4
TLR5
TLR2/6
TLR7
TLR9
NOD1
NOD1
NOD2
NOD1/2
NLRP3
NLRP3
NLRP3
MDA5/TLR3
DAI/AIM2
nd
0.1
1
10
Fold Change in Clr-b MFI

Figure 2.13. Modulation of mouse Clr-b levels on various mouse cell lines treated with simple PRR agonists. (**A**) NIH3T3 cells, (**B**) MEF cells, (**C**) S17 stromal cells, and (**D**) J774 macrophage cells were treated with various PRR agonists then analyzed for mouse Clr-b levels by flow cytometry. Clr-b MFI levels were quantitated relative to untreated cells and represented as fold-change in MFI values. Abbreviations: Pam3CSK4 (synthetic triacylated Pam_3CSK_4 lipoprotein, 1 μg/ml); HKLM (heat-killed *L. monocytogenes*, 10^4); poly(I:C) (100 ng/ml); LPS (lipopolysaccharide, 1 μg/ml); Flagellin (1 μg/ml); FSL-1 (synthetic FSL-1 diacylated lipoprotein, 1 μg/ml); ssRNA/LyoVec (single-stranded RNA complexed with LyoVec, 100 ng/ml); bacDNA (*E.coli* bacterial DNA, 1 μg/ml); mTRI (mTRI-DAP muramyl tripeptide, 1 μg/ml); C12 (acylated iE-DAP dipeptide, 1 μg/ml); L18 (muramyl dipeptide with a C18 fatty acid chain, 1 μg/ml); HPPG (*H. pylori* proteoglycan, 10 μg/ml); ATP (adenosine triphosphate, 25 mM); Alum (aluminum potassium sulphate, 10 μg/ml), Nigericin (50 μM), poly(I:C)/Lyo (poly(I:C) complexed with LyoVec liposomes, 100 ng/ml); dsB-DNA/Lyo (double-stranded B-DNA complexed with LyoVec liposomes, 100 ng/ml), or MCMV-GFP virus. Left labels represent agonist treatments, right labels represent PRR targets of the agonists. Graphs show mean±SEM. Experiments were analyzed using 1-way ANOVA with Bonferroni post-hoc analysis; *$p<0.05$, **$p<0.01$, ***$p<0.001$. All data are representative of at least three independent experiments.

lines, while nigericin (a K^+ ionophore) was effective for some cell lines, and inflammasome activation by alum salts was inconclusive (**Fig. 2.13A,B**). We also tested cyclic dinucleotides (c-di-AMP and c-GAMP), recently shown to serve as bacterial PAMP or second messengers of host cytosolic dsDNA sensing (via cGAS (Ablasser et al., 2013; Li et al., 2013b; Parvatiyar et al., 2012) and the mitochondrial STING sensor); however, we failed to observe any changes in mClr-b expression. In addition, we repeated the above treatments using J774 macrophages (as a hematopoietic immune cell lineage); however, ATP and nigericin treatments were less robust at inducing mClr-b downregulation on these cells (**Fig. 2.13C,D**). Moreover, cytosolic nucleic acids actually promoted mClr-b upregulation on many cells, and numerous PRR agonists induced mClr-b on J774 cells (**Fig. 2.13C,D**). Collectively, these results suggest that single PRR engagement in isolation is not sufficient to mimic MCMV-mediated mClr-b downregulation; however, the role of ATP in promoting mClr-b loss is intriguing (see below).

To further investigate the role of PRR in MCMV-mediated mClr-b downregulation, we obtained mutant fibroblasts deficient in various sensing pathways and infected them with MCMV-GFP, to monitor mClr-b expression on infected versus uninfected cells. Infection of *Ifnar1*$^{-/-}$, *Irf3*$^{-/-}$, *Irf3*$^{-/-}$/*Irf7*$^{-/-}$, and *Tbk1*$^{-/-}$/*Ikke*$^{-/-}$ primary fibroblasts demonstrated that these cells retained mechanisms to downregulate mClr-b upon MCMV-GFP infection (**Fig. 2.14**), albeit to different extents. Similarly, fibroblasts deficient in several innate immune sensors (*Pkr*$^{-/-}$, *RnaseL*$^{-/-}$, *Pkr*$^{-/-}$/*RnaseL*$^{-/-}$, *Asc*$^{-/-}$, *Caspase1*$^{-/-}$, *Nlrp3*$^{-/-}$, *Aim2*$^{-/-}$, *Mavs*$^{-/-}$, and *Dai*/*Zbp1*$^{-/-}$) all retained the ability to downregulate mClr-b upon MCMV-GFP infection (**Fig. 2.14**). It should be noted that initial experiments using primary *Dai/Zbp1*$^{-/-}$ AEF revealed a significant block in mClr-b downregulation by MCMV-GFP; however, this significance was lost upon extended cell culture, suggesting that complex mechanistic redundancy may also be possible. Interestingly, the MCMV-dependent loss of mClr-b on inflammasome mutants (*Asc*$^{-/-}$, *Caspase-1*$^{-/-}$, *Nlrp3*$^{-/-}$, *Aim2*$^{-/-}$) and nucleic acid sensing mutants (*Pkr*$^{-/-}$/*RNaseL*$^{-/-}$, *Mavs*$^{-/-}$, and *Dai*/*Zbp1*$^{-/-}$) suggests that the autonomous action of ATP in promoting mClr-b loss may occur via a distinct mechanism other than inflammasome activation or strict PRR signaling. In other experiments, transduction of NIH3T3 cells using lentiviral shRNA vectors to knockdown Dai/Zbp-1 or Sting expression failed to prevent mClr-b downregulation upon MCMV-GFP infection. Together, these results remain inconclusive, but suggest that there may be redundancy in innate mechanisms that trigger CMV infection-mediated mClr-b downregulation.

Figure 2.14

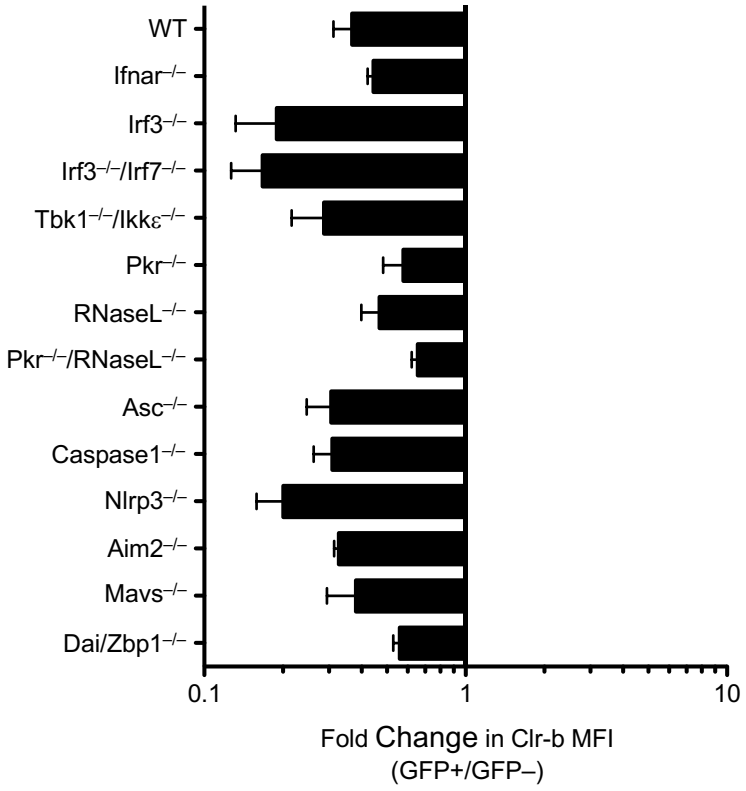

Figure 2.14. Mouse Clr-b downregulation upon MCMV-GFP infection of primary fibroblasts from mice deficient in select genes involved in innate immune recognition. Primary mouse MEF or AEF cells from various mutant mouse strains were infected with MCMV-GFP and analyzed for Clr-b expression 24 h.p.i. by flow cytometry. Fold changes were calculated by ratios of Clr-b MFI levels between infected (GFP^+) versus uninfected ($GFP^–$) cells.

The observation that extracellular ATP induced a potential inflammasome-independent Clr-b loss on a number of cell lines prompted further investigation. To extend this finding, we treated NIH3T3 cells with ATP, ADP, or AMP at various concentrations. Interestingly, Clr-b downregulation was observed above ~5 mM ATP, while ADP and AMP were even more effective at lower doses; notably, the ADP effects were also bimodal, such that Clr-b loss could be titrated out at either low or high doses (**Fig. 2.15**). It should be noted that ATP treatment failed to promote loss of Clr-b nascent transcripts (C.L. Kirkham, unpublished observation), suggesting a mechanism distinct from MCMV infection.

2.4.6 MCMV infection downregulates mClr-b but induces a Clr-b-independent NKR-P1B ligand

To assess the functional consequences of MCMV-mediated mClr-b loss on NKR-P1B receptor recognition, we utilized BWZ reporter cell assays (Chen et al., 2011; Mesci and Carlyle, 2007). Briefly, BWZ.36 cells possess a *LacZ* gene under the control of tandem NFAT enhancer elements, such that TCR-like signals delivered via NKR-P1/CD3ζ-fusion receptors induce β-galactosidase expression, which in turn can be detected spectrophotometrically using a colorimetric substrate, CPRG. Both mAb-dependent and cellular ligand-dependent signals can be measured semi-quantitatively using this assay. Here, BWZ.36 reporter cells bearing a CD3ζ/NKR-P1B chimeric fusion receptor (BWZ.P1B cells) were used to interrogate NKR-P1B-dependent ligand function when incubated with MCMV-infected cells. As previously shown, co-culture of BWZ.P1B reporter cells with titrated doses of NIH3T3 stimulator cells yielded a strong NKR-P1B-dependent response, in comparison to parental BWZ.36 (BWZ–) cells lacking the NKR-P1B receptor (**Fig. 2.16A**). Upon MCMV infection of NIH3T3 stimulator cells, the signal observed for BWZ.P1B reporter cells was greatly diminished, as expected, due to MCMV-mediated mClr-b downregulation (**Fig. 2.16B**). To confirm that the response of uninfected NIH3T3 cells was mClr-b specific, we utilized blocking mClr-b (4A6) mAb to abrogate the NKR-P1B:Clr-b interaction (**Fig. 2.16C**). Interestingly, however, 4A6 mAb failed to block residual NKR-P1B-dependent stimulation of MCMV-infected NIH3T3 cells (**Fig. 2.16D**).

In parallel, we tested whether MCMV infection could induce stimulation of BWZ reporter cells bearing other CD3ζ/NKR-P1-family receptors; however, no signal was observed using reporter cells bearing NKR-P1A, NKR-P1C, NKR-P1F, or NKR-P1G chimeric receptors

Figure 2.15

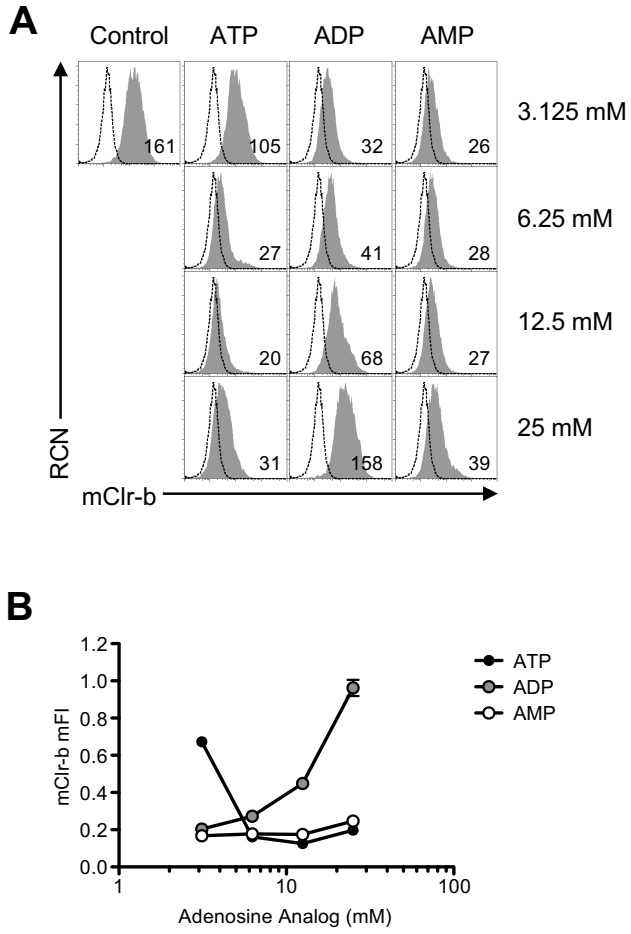

Figure 2.15. Adenosine nucleotide analogs affect mClr-b cell surface expression in mouse fibroblasts. NIH3T3 cells were treated with titrated doses of AMP, ADP, or ATP and analyzed by flow cytometry 24 hrs post-treatment by flow cytometry. (**A**) Representative flow plots of treated NIH3T3. The numbers in the gates corresponds to the mClr-b MFI. (**B**) Quantitation of mClr-b expression in treated populations normalized to untreated controls values. Graph shows mean±SEM of normalized MFI values in (A). Data is representative of at least three independent experiments.

Figure 2.16

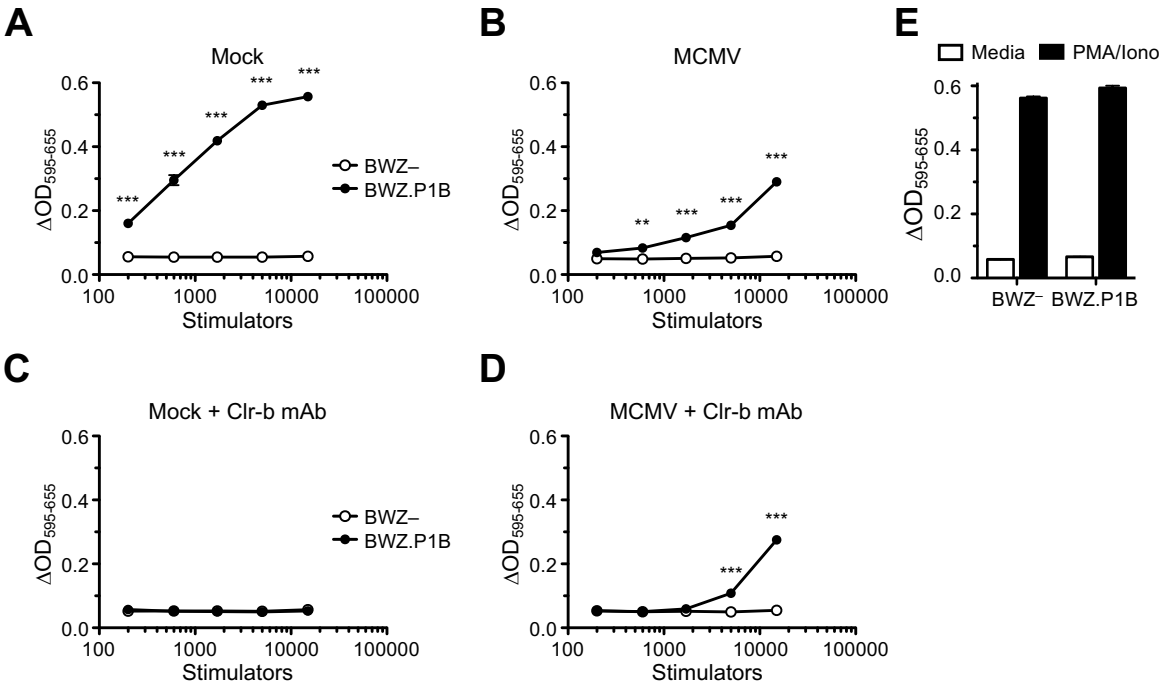

Figure 2.16. BWZ.CD3ζ/NKR-P1B reporter cell analysis of ligand expression on MCMV-infected NIH3T3 fibroblasts. NIH3T3 cells were infected with MCMV at MOI ~0.5 PFU/cell, infection was allowed to proceed overnight (~18 hours), then infected cells were used as stimulator cells upon co-culture with CD3ζ/NKR-P1B receptor-bearing BWZ reporter cells (versus parental BWZ.36 cells), subsequently analyzed for b-galactosidase activity 20h later. Stimulator cell titrations included: (**A**) Mock control NIH3T3 cells; (**B**) MCMV-infected NIH3T3 cells; (**C**) Mock control NIH3T3 cells with 4A6 blocking Clr-b mAb (10 μg/ml), or (**D**) MCMV-infected NIH3T3 cells with blocking 4A6 Clr-b mAb. (**E**) Represents the values of experimental controls (white bars and black bars represent media alone and PMA/ionomycin treatments respectively). White circles represent parental BWZ.36 (BWZ–) cells; black circles represent BWZ cells bearing the CD3ζ/NKR-P1B ectodomain (BWZ.P1B). Graphs show mean±SEM. Experiments were analyzed using ANOVA with Bonferroni post-hoc analysis. All data are representative of at least three independent experiments.

(**Fig. 2.17**). These results suggest that MCMV may encode an immunoevasin that interacts with the mouse NKR-P1B receptor, similar in function to RCTL encoded by RCMV-E.

2.5 Discussion

Previous work has demonstrated that rat Clr-11 transcripts and cell surface expression are rapidly lost in response to RCMV-English infection, yet RCTL functionally replaces rClr-11 as an NKR-P1B ligand (Voigt et al., 2007). In concordance with this, similar findings were reported for mClr-b in a mouse model of orthopoxvirus (VV, ECTV) infection (Williams et al., 2012). Here, we provide evidence for a conserved mechanistic response for both mClr-b and rClr-11 in response to cross-species CMV infection. Studies initiated using MCMV-Smith virus to infect mouse and rat fibroblasts revealed a striking loss of mClr-b, similar to the rClr-11 downregulation observed in REF cells using RCMV-E infection. Further investigation using MCMV-GFP virus revealed that only infected cells (GFP^+), and not uninfected "bystander" cells (GFP^-), downregulate mClr-b/rClr-11 cell surface expression at the single cell level. This effect was observed as early as 6 h.p.i., a time point that represents an early event in the course of CMV infection. Since new infectious MCMV virions are usually produced within 16-24 h.p.i., and given that AraC and PAA treatments used to block late CMV gene expression had no effect on mClr-b downregulation, viral replication appears to be dispensable for mClr-b loss. In addition, attempts to investigate a role for immediate early gene expression were inconclusive, as ActD treatments alone abrogated host mClr-b/rClr-11 expression on uninfected cells.

However, observations using CHX, as well as UV-inactivated whole CMV virions, suggest that interference with immediate early to early viral and/or host gene expression during MCMV infection is sufficient to prevent mClr-b loss, yet active viral infection is necessary to promote mClr-b downregulation. These findings demonstrate a pivotal role of immediate early to early CMV infection events in the initiation of the cellular 'missing-self' Clr-b response. Notably, we have observed a similar response using other viruses *in vitro*, including RNA viruses (A. Mesci and J. Ma, unpublished data); thus, loss of inhibitory Clr is a conserved response to infection by many types of viruses (and cellular pathologies, including genotoxic stress and oncogenic transformation) (Fine et al., 2010; Voigt et al., 2007; Williams et al., 2012). Since both RCMV and MCMV appear to have evolved functional surrogate ligands for NKR-P1B, immunoevasins that counteract the infection-mediated loss of mClr-b/rClr-11, the

Figure 2.17

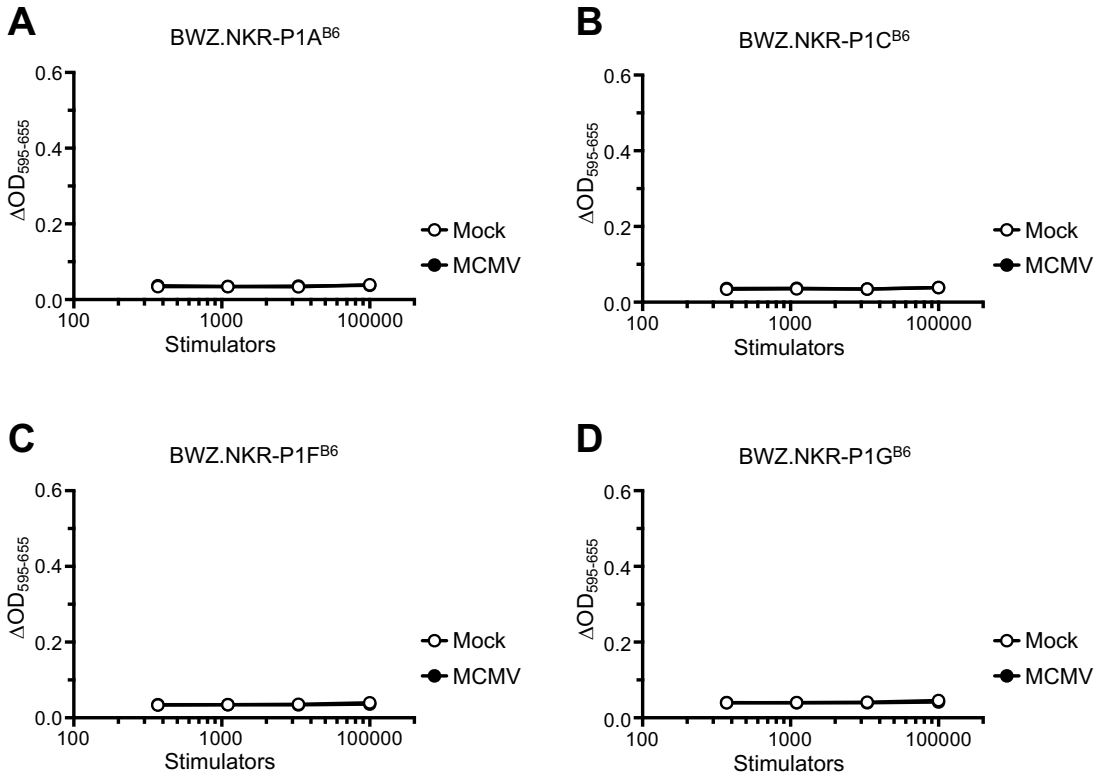

Figure 2.17. BWZ reporter assays using BWZ cells bearing CD3ζ/NKR-P1 fusion receptors co-cultured with MCMV infected fibroblasts. Mock or MCMV-infected NIH3T3 cells were used as stimulators in co-cultures with BWZ reporter cells bearing CD3ζ fusions with (**A**) NKR-P1A, (**B**) NKR-P1C, (**C**) NKR-P1F, and (**D**) NKR-P1G. White circles represent mock-infected cells; black circles represent MCMV-infected cells. Graphs show mean±SEM. Experiments were analyzed using ANOVA with Bonferroni post-hoc analysis. All data are representative of at least two independent experiments.

"missing-self" phenomenon observed may be a host response; however, we cannot rule out a complex role for necessary viral genes in eliciting host Clr downregulation.

On this point, we have attempted here to expand current understanding of the host intracellular innate immune response during CMV infection. We hypothesized that PRR engagement, such as via TLR, NLR, or cytosolic nucleic acid sensors, might mimic the innate immune response to MCMV infection, evident by the observed phenotype of mClr-b downregulation. However, studies using single PRR agonists in isolation, and MCMV-GFP infection studies using mutant fibroblasts, suggest that simple PRR engagement may not be sufficient. These findings are perhaps not entirely surprising, since engagement of some PRR in isolation may be detrimental to the host immune response, in that uninfected bystander cells may become targets recognized by NK cells. A more refined hypothesis hints that viral PAMP or "infection-stress" intermediates may be sensed intracellularly to enable a cell-autonomous "missing-self" mClr-b response in infected cells alone. This response may be opposed in uninfected "bystander" cells by maintaining or even upregulating "healthy-self" NK cell inhibition via mClr-b (e.g., via paracrine cytokines, such as interferons). In fact, plasmid DNA transfection occasionally results in subtle mClr-b loss (on both transfected and untransfected cells), while soluble factors in CMV culture supernatants reproducibly result in mClr-b upregulation on uninfected (GFP^-) cells (Kirkham et al., 2017).

However, our cytosolic PRR agonists also failed to replicate MCMV-mediated mClr-b downregulation. Indeed, a combination of PRR agonists may be required to invoke mClr-b downregulation; for example, signal-1 associated with TLR ligation (e.g., via TLR3,7,8,9), followed by signal-2 associated with inflammasome activation (e.g., via Nlrp3 or AIM2) (Mariathasan et al., 2004). However, attempts to provide TLR stimulation in combination with cytosolic DNA agonists resulted in no alterations in mClr-b expression. Alternatively, cytosolic DNA may be detected by one sensor, yet further processing or signaling intermediates may be generated by another co-factor, such as the synergy observed between cGAS and Ddx41 (Ablasser et al., 2013; Li et al., 2013b; Parvatiyar et al., 2012). Nonetheless, transfection of cyclic-di-AMP or c-GAMP into NIH3T3 cells alone resulted in no changes in mClr-b expression. Hence, our efforts to find a single PRR trigger have proven ineffective.

Another possibility is that signal initiation may occur in the nucleus. Intricate details of interplay during host-pathogen interactions continue to be discovered, such as recent findings

using HCMV, whereby host IFI16 directly recognizes HCMV gDNA, yet HCMV circumvents viral detection via pUL83 (Li et al., 2013a). It remains to be determined whether a nuclear sensor or repressor (host or viral) may be involved in cessation of mClr-b expression, but estimates of surface mClr-b turnover put the half-life at ~3h, in line with the observed rapid CMV-mediated mClr-b loss. Notably, recent results indicate that the MCMV *ie3* (M122) gene product is capable of promoting modest Clr-b downregulation upon transfection, in part by repressing Clr-b/*Clec2d* promoter activity (Kirkham et al., 2017).

Perhaps not surprisingly, cellular responses to stimulation using PRR agonists also appeared to be cell-type specific. For example, responses of J774 macrophages and S17 stromal cells deviated from observations using NIH3T3 and primary fibroblast cell lines, in that mClr-b was found to be upregulated in response to many PRR agonists; however, some of these effects may be due to differential sensitivity to or production of type-I IFN (Kirkham et al., 2017). Nonetheless, even when induced upon MCMV-GFP infection (e.g., J774 macrophages), mClr-b levels still remained lower on infected (GFP^+) versus uninfected (GFP^-) cells. Of relevance, however, rodent Clr induction on hematopoietic cells during infection is reminiscent of observations regarding the closest human homologue, LLT-1 (*CLEC2D*; ligand for human inhibitory NKR-P1A/*KLRB1*); LLT1 is induced at the cell surface upon activation of immune cells (Germain et al., 2011; Rosen et al., 2008; Voigt et al., 2007; Williams et al., 2012). This opposing regulation could be due to differential PRR expression, cell-type specific ligand regulation in immune versus somatic cells, or inherent differences between the mouse and human homologues. Further work is required to elucidate the *in vivo* significance of mClr-b and other *Clec2d* family members with respect to viral infections.

In contrast to other PRR agonists, ATP, and perhaps nigericin (in certain cells), appear to be uniquely capable of invoking mClr-b loss in the absence of other treatments. The significance of this remains unknown, although these compounds may induce signaling events that intersect with pathways that promote mClr-b downregulation, such as cellular transformation or stress responses (Fine et al., 2010). Extracellular ATP and nigericin can induce inflammasome activation (Mariathasan et al., 2004); however, all of the inflammasome-mutant MEF investigated ($Asc^{-/-}$, $Caspase\text{-}1^{-/-}$, $Nlrp3^{-/-}$, $Aim2^{-/-}$) retained the ability to downregulate mClr-b in response to MCMV-GFP infection; therefore, further work is required to decipher the role of

inflammasome activation and the specific role of adenosine phosphates (ATP, ADP, AMP). An intriguing possibility is AMPK, which is regulated by all three forms.

The conserved mClr-b and rClr-11 downregulation observed in response to MCMV and RCMV infection of mouse and rat fibroblasts, along with the observation that cross-species infection and other virus infections promote the same phenotype, suggests that this phenomenon may be an innate host response to viral infection, in order to signal recognition by NK cells. Notably, the mClr-b (*Clec2d*) and rClr-11 (*Clec2d11*) gene products both contain discontinuous hammerhead ribozyme (HHR) motifs in their 3'UTR (Martick et al., 2008; Scott et al., 2009) capable of mediating post-transcriptional regulation of transcript size and abundance *in cis*, akin to micro-RNA (miR)-mediated regulation *in trans*. We and others (L. Horan, unpublished data) have confirmed that the presence of the HHR does affect mRNA stability and abundance; however, whether the HHR provides a constitutive turnover mechanism (to enable rapid shutoff), or if the HHR is differentially regulated under conditions of health versus stress, remain to be resolved. Of note, the human LLT1 (*CLEC2D*) gene product lacks the HHR motif; however, it is still subject to post-transcriptional regulation via alternative splicing (Germain et al., 2010; Martick et al., 2008) (O.A.A., unpublished results).

Importantly, these studies also provide evidence that there is conservation of CMV strategies to subvert NK receptor-ligand interactions, since RCMV-E infection of mouse fibroblasts invokes downregulation of mClr-b, MHC-I molecules, and Rae-1 isoforms. This implies that RCMV-E may encode immunoevasin genes that counter-regulate, retain intracellularly, or facilitate degradation of Clr, MHC-I, and NKG2D ligands, as shown for several MCMV and HCMV gene products. In addition, MCMV is capable of cross-species downregulation of rClr-11, and may encode a viral immunoevasin that functionally engages the mouse NKR-P1B inhibitory receptor, akin to the RCMV-E RCTL gene product that engages rat NKR-P1A/B alleles (Voigt et al., 2007; Voigt et al., 2001). Because MCMV infection stimulated engagement of NKR-P1B-bearing BWZ reporter cells that was not blocked using mClr-b (4A6) mAb, this phenomenon appears to be mClr-b-independent. It has been previously been shown that MCMV encodes gene products that target inhibitory receptors on NK cells by mimicking or stabilizing MHC-I expression (m157, m144, m04) (Arase et al., 2002; Babic et al., 2010; Lanier, 2008). In light of our findings, MCMV may also target MHC-I-independent "missing-self" recognition. Mining the MCMV genome will undoubtedly reveal the nature of this mechanism,

and this work is currently underway, using mutant mice and MCMV strains. Further investigations are also warranted into the expression and modulation of human NKR-P1A:LLT1 (*KLRB1:CLEC2D*) interactions by HCMV and poxviruses (Germain et al., 2011; Rosen et al., 2008; Voigt et al., 2007; Williams et al., 2012). Together, these results further reveal the importance of the NKR-P1:Clr receptor-ligand system in innate self-nonself discrimination, particularly in the context of viral infection.

Chapter 3

The MCMV m12 immunoevasin controls innate immunity by directly engaging the NKR-P1B and NKR-P1C (NK1.1) receptors

Oscar A. Aguilar, Mir Munir A. Rahim, Johanna J. Reichel, Richard Berry, Timothy N.H. Lau, Miho Tanaka, Zhihui Fu, Gautham R. Balaji, Megan M. Tu, Christina L. Kirkham, Aruz Mesci, Ahmad B. Mahmoud, Branka Popović, Astrid Krmpotić, Jamie Rossjohn, David S.J. Allan, Andrew P. Makrigiannis, Stipan Jonjić, James R. Carlyle

O.A.A. designed, performed, and analyzed experiments and identified receptor-ligand interactions. M.M.A.R., M.T., M.M.T., and A.B.M assisted with *in vivo* experiments. J.J.R. generated the m12 mutant and revertant viruses. R.B., G.R.B., and Z.F. generated the purified m12 and NKR-P1 proteins and performed SPR analyses (Figure 3.10). R.B. contributed to manuscript writing. G.R.B. assisted with the structural analysis. T.N.H.L assisted with bioinformatic analysis. C.L.K, A.M., B.P., and A.K. assisted with *in vitro* experiments. D.S.J.A., A.P.M., S.J., J.R., and J.R.C. contributed to the direction of the study. This work was funded by and done in the labs of J.R., A.P.M., S.J., and J.R.C. J.R.C. contributed to the design and interpretation of experiments, project management.

This work plus additional contributions were published in *Cell*. 2017; 169(1):58-71.e14.
http://dx.doi.org/10.1016/j.cell.2017.03.002

3 MCMV m12 immunoevasin subverts NKR-P1 recognition

3.1 Abstract

Natural killer (NK) cells detect alterations in self and non-self ligands via paired NK cell receptors. Murine cytomegalovirus (MCMV) encodes numerous immunoevasins that directly target NK cell receptor-ligand interactions. Here, we identify an MCMV-encoded m02 family member, m12, that restrains NK cell effector function by directly engaging the NKR-P1B inhibitory receptor. Remarkably, m12 also interacts with the prototypical NK1.1 antigen and stimulatory orphan receptor, NKR-P1C. In addition, polymorphisms in m12 and host NKR-P1B/C alleles differentially impact NK cell recognition. Notably, two m12 allelic variants and an m12-deficient virus show differential viral titers *in vivo* upon infection of B6 wild-type but not NKR-P1B-deficient mice. Thus, m12 is a viral decoy that interacts with both inhibitory and stimulatory NKR-P1 receptors, providing insight into innate immune evasion and co-evolution during host-pathogen interactions.

3.2 Introduction

Natural killer (NK) cells are a subset of innate lymphoid cells (ILC) capable of recognizing a diverse array of pathological target cells. As efficient sentinels responsible for the clearance of cancerous, transplanted, antibody-opsonized, virally-infected, and stressed cells, they discriminate between healthy-self, altered-self, and non-self targets through the integration of balanced signals delivered via multiple families of paired germline-encoded NK cell receptors (NKR). Normal cells display abundant expression of self ligands that bind to inhibitory NKR, rendering healthy cells protected (Raulet and Vance, 2006). However, during pathology, two changes occur that render “altered-self” target cells more susceptible to NK recognition: (i) induction of stress-associated self (or pathogen-associated non-self) ligands, which trigger stimulatory NKR, leading to “induced-self” recognition; and/or (ii) loss of self ligands recognized by inhibitory NKR, which disinhibit NK cells, leading to “missing-self” recognition (Raulet and Vance, 2006).

Several NKR families have been described, many of which are grouped together in large genomic regions, such as the natural killer gene complex (NKC) and the leukocyte receptor cluster (LRC). In rodents, most NKR are type-II transmembrane (TM) C-type lectin-like proteins encoded within the NKC. These include the Ly49 (*Klra1*) receptors that mainly recognize classical MHC-Ia molecules, the heterodimeric NKG2/CD94 (*Klrc1/Klrd1*) receptors that bind non-classical MHC-Ib, the homodimeric NKG2D (*Klrk1*) receptor that recognizes MHC-I-related stress-induced ligands, and the NKR-P1 (*Klrb1*) receptors that interact with genetically-linked C-type lectin-related (*Clr/Clec2*) proteins (Kirkham and Carlyle, 2014; Raulet and Vance, 2006). Other NK cell receptors include the immunoglobulin superfamily members, such as the SLAM family receptor, 2B4/CD244 (which recognizes genetically-linked CD48), NKp46 (which recognizes viral antigens and an unidentified host ligand), and the KIR family (responsible for MHC-I recognition in primates) (Raulet and Vance, 2006).

There exist at least five functional mouse NKR-P1 receptors, three stimulatory isoforms (NKR-P1A,C,F) and two inhibitory isoforms (NKR-P1B,G) (Carlyle et al., 2008; Kirkham and Carlyle, 2014). NKR-P1C (which encodes the prototypical NK1.1 antigen in B6 mice) and NKR-P1A are orphan receptors expressed on most NK cells, and stimulate NK cell effector function upon ligation. Interestingly, the NKR-P1F and NKR-P1G subclade of receptors recognize partially overlapping and distinct ligands, whereby both NKR-P1F/G recognize Clr-d,g, NKR-P1F recognizes Clr-c, and NKR-P1G recognizes Clr-f (Chen et al., 2011; Iizuka et al., 2003; Kveberg et al., 2009). The shared ligand pairs may help to balance integrated signals during NK cell education or effector responses, while the unique ligands may contribute to tissue-restricted functions. Recently, Clr-f was shown to be restricted to gut epithelial tissues, where it may be important for mucosal immunosurveillance (Leibelt et al., 2015). Finally, NKR-P1E is a pseudogene, while the remaining NKR-P1B and its divergent NKR-P1D allele (NKR-P1B^{B6}) recognize the broadly-expressed Clr-b ligand (Carlyle et al., 2004). To date, Clr-b has been shown to be involved in missing-self recognition under diverse pathological states, including cancer (Carlyle et al., 2004), genotoxic and cellular stress (Fine et al., 2010), BM transplants (Chen et al., 2015; Rahim et al., 2015), tumour immune escape in a spontaneous cancer model (Chen et al., 2015; Rahim et al., 2015), and virus infection (by both cytomegaloviruses and poxviruses) (Aguilar et al., 2015; Voigt et al., 2007; Williams et al., 2012). In humans, there exists a single NKR-P1A receptor that recognizes the human Clr homologue, LLT1 (*CLEC2D*);

nonetheless, it has recently been postulated that the human NKp80 (*KLRF1*) and NKp65 (*KLRF2*) receptors, which recognize AICL (*CLEC2B*) and KACL (*CLEC2A*), respectively, might represent divergent homologues of the rodent stimulatory NKR-P1 receptors (Bartel et al., 2013; Kirkham and Carlyle, 2014).

Among pathogens recognized by NK cells, cytomegaloviruses (CMV) are a family of *betaherpesvirinae* that demonstrate co-evolution with their natural hosts, likely due to cycles of natural selection for viral versus host fitness. While CMV infections are typically asymptomatic in immunocompetent individuals, immunocompromised patients and newborns are susceptible to severe pathology and congenital defects. CMV possess large dsDNA genomes (>200 kb) that accommodate numerous immunoevasin genes targeting both innate and adaptive immunity. Since early responses to CMV infection are largely NK cell-mediated, these viruses have evolved a diverse array of immunoevasins that directly or indirectly antagonize NK cell function.

Perhaps the best-known example, the MCMV m157 protein binds directly to inhibitory Ly49C/I receptors from certain mouse strains; reciprocally, some mice have counter-evolved a stimulatory Ly49H receptor to directly recognize the m157 evasin, and this recognition dominantly establishes MCMV resistance in B6 mice (Arase et al., 2002; Lee et al., 2001; Smith et al., 2002). In addition, the MHC-I-like m144 protein has been reported to inhibit NK cells in a β_2m-dependent manner via an unidentified NKR (Farrell et al., 1997). Also well known are the non-redundant immunoevasins that retain stimulatory NKG2D-ligands intracellularly to subvert NK cell activation, including m138 (targets Mult1, H60), m145 (Mult1), m152 (Rae-1), and m155 (H60) (Hasan et al., 2005; Krmpotic et al., 2002; Krmpotic et al., 2005; Lenac et al., 2006; Lodoen et al., 2003). Among these, m152 also promotes evasion of T cell responses by downregulating MHC-I, along with m06; alternatively, m04 masks certain MHC-I alleles at the cell surface to avoid T cell recognition (Kleijnen et al., 1997; Reusch et al., 1999; Ziegler et al., 1997), yet these complexes can be recognized by inhibitory Ly49A/G and/or stimulatory Ly49P/L/D2/W alleles (Kielczewska et al., 2009; Pyzik et al., 2011). More recently, other mechanisms of evasion have been reported, including downregulation of TRAIL (by m166) (Verma et al., 2014) and CD48 (by m154) (Zarama et al., 2014). In the rat CMV-English isolate (RCMV-E), a spliced RCTL gene product directly engages the inhibitory rat NKR-P1B, but also weakly interacts with the stimulatory rat NKR-P1A paralog (Voigt et al., 2007). Recently, we

also provided evidence for an unknown MCMV-encoded ligand that targets mouse NKR-P1B (Aguilar et al., 2015).

In this report, we identify the MCMV m02 family member, m12, as a functional decoy ligand that directly engages the mouse NKR-P1B inhibitory receptor and inhibits NK cytotoxicity. Importantly, we also demonstrate that m12 directly interacts with two stimulatory orphan receptors, the prototypical NK1.1 antigen (NKR-P1C), and NKR-P1A. *In vivo* infections using wild-type MCMV (MW97.01 strain), an m12-deficient mutant (Δm12), and a Smith-strain m12-revertant ($m12^{Smith}$) revealed differential viral copy numbers in WT B6 mice that were abrogated in B6.*Nkrp1b*$^{-/-}$ mice. Interestingly, strain-specific allelic polymorphisms in both m12 and host NKR-P1B/C modulated their interactions, suggesting they have co-evolved during host-pathogen interactions. These findings further add to the complexity of MCMV immune evasion mechanisms, and demonstrate an important role for the NKR-P1 family of receptors in NK cell-mediated immunity to infection. Finally, these results identify m12 as the first physiological $NKR\text{-}P1C^{B6}$ ligand, almost 40 years since the discovery of the prototypical NK1.1 antigen (Glimcher et al., 1977).

3.3 Materials and Methods

3.3.1 Animals

C57Bl/6 (B6) mice were purchase from the Jackson Laboratory, FVB/N (FVB) and 129S6 (129) mice were purchased from Charles River. We have previously described the B6.*Nkrp1b*$^{-/-}$ and B6.*Clrb*$^{-/-}$ mice (Chen et al., 2015; Kartsogiannis et al., 2008; Rahim et al., 2015). All animals were maintained according to approved protocols at the respective institutes: Sunnybrook Research Institute, University of Ottawa, and the University of Rijeka.

3.3.2 Cells

NIH3T3, YAC-1 and HEK293T cells were purchased from the American Type and Culture Collection (ATCC). BWZ.36 cells were obtained from N. Shastri (UC Berkeley, Berkeley) (Sanderson and Shastri, 1994). B6 mouse embryonic fibroblasts (MEF) were obtained from T.W. Mak (University of Toronto, Canada). Cells were cultured in complete DMEM-HG, supplemented with 2 mM glutamine, 100 U/mL penicillin, 100 μg/ml streptomycin, 50 μg/mL

gentamicin, 110 μg/mL sodium pyruvate, 50 μM 2-mercaptoethanol, 10 mM HEPES, and 10 % FCS. Cells were maintained in incubator at 37°C, 5% CO_2.

3.3.3 Viruses and infections

MCMV (Smith strain), MCMV-GFP, and MW97.01 (BAC-generated strain) have all been previously described (Henry et al., 2000; Wagner et al., 1999). The MCMV K181 strain was provided by Dr. Michael G. Brown (University of Virginia). The Δm12 virus and revertant viruses were constructed using BAC technology that has previously been described (Wagner and Koszinowski, 2004). For *in vitro* infections, mouse fibroblasts were infected with MCMV at an MOI of 0.5 PFU/cell and centrifuged at 800x*g* for 30 mins, and incubated at 37°C. For *in vivo* infections, mice were infected with $1x10^6$ PFU and sacrificed on day 3, tissues harvested, and the viral titers were assessed using plaque-forming assays (Brune et al., 2001).

3.3.4 Flow cytometry and antibodies

Flow cytometry was performed as previously described (Chen et al., 2015). Clr-b mAb (4A6) has previously been described (Carlyle et al., 2004). All other mAb clones were purchased from eBioscience or Sigma-Aldrich and are has follows: NK1.1/NKR-P1C^{B6} (PK136); NKp46 (29A1.4); CD3ε (145-C11); FcγRII/III (2.4G2); FLAG (M2); streptavidin, SA-PE/APC (Thermo Fisher Scientific). The NKR-P1B^{B6} mAb and hybridoma (2D12) were a kind gift from Drs. Koho Izuka and Wayne Yokoyama (Iizuka et al., 2003).

3.3.5 RNA Isolation, cDNA synthesis and PCR cloning

RNA was isolated using Total RNA isolation kit with gDNA removal (Norgen Biotek) and reverse transcription reactions were done using Superscript III cDNA synthesis kit (Thermo Fisher Scientific). Quantitative RT-PCR was performed on a CFX-96 PCR Detection System (Bio-Rad) using 20-50 ng of cDNA, and PerfeCTa qPCR mix (Quanta Biosciences). The primers used can be found in **Appendix 3.1**.

PCR cloning of m02 and m145 family members was done using gene-specific primers with appropriate restriction enzyme sites, cDNA from MCMV-GFP infected NIH3T3, amplified with Q5 high-fidelity PCR system (New England Biolabs), and cloned into the pIRES2-EGFP

vector (Clontech). The summary of primers can be found in **Appendix 3.1**. The $m12^{C4A}$ gene was synthesized by conducting *in situ* mutagenesis using primers found in **Appendix 3.1**. The $m12^{G4}$ gene was synthesized using GeneArt services from Thermo Fisher Scientific (Burlington, ON). Cloning of the Nkrp1 genes was mediated by PCR using gene specific primers (**Appendix 3.1**), the novel FVB-strain sequences and novel splice variants have been deposited in GenBank, and have the accession numbers, KX443605-KX443630.

3.3.6 Immunoprecipitations and Western Blotting

N-terminally FLAG-tagged constructs of m12 were generated using primers in (**Appendix 3.1**) and cloned into pIRES2-EGFP vector. These constructs were transfected into either HEK293T or NIH3T3 cells and immunoprecipitations were done using FLAG mAb bound to Protein A/G agarose beads in 1% NP-40 buffer. The isolates were ran on SDS-PAGE and transferred to Immobilon PVDF membrane (EMD Millipore) and blotted for αFLAG-HRP conjugated antibody (Cell Signal Technologies) and developed with Immobilon ECL reagent.

3.3.7 RNA-Sequencing and Analysis

Total RNA from either mock-infected, MCMV-GFP or MW97.01 infected NIH3T3 cells using mirVana kit (Thermo Fisher Scientific). These samples were quality checked using an Agilent Bioanalyzer 2100 and confirmed to have RNA integrity values of >9, then used to create a cDNA library for SOLiD RNA-Sequencing. Reads were mapped on mouse genome (Build 37.2) using GeneSifter software (Geospiza) and gene expression is described as RPKM values. For analysis of viral transcripts, raw data was mapped onto the MCMV Smith reference genome (accession number GU305914) using TopHat algorithm and Cufflinks was applied to report RPKM values. Mapped reads were visualized using the Integrative Genome Browser (IGV version 2.3.34, Broad Institute, https://www.broadinstitute.org/igv/).

3.3.8 BWZ Reporter Cell Assays

The ectodomains of the mouse NKR-P1 genes were PCR amplified from d6 LAK cDNA (see **Appendix 3.1** for primers) and cloned into a type-II MSCV vector to make chimeric receptors with intracellular CD3ζ domains. MCMV m12-CD3ζ chimeric reporters were constructed by cloning the ectodomain of m12 into a type-I MSCV vector. Retroviruses

produced with these constructs were used to transduce BWZ.36 cells, and then sorted for GFP^+ expression. All reporters were sorted to have matched GFP expression. Reporter assays were done by co-culturing reporter cells ($5x10^4$) with serially diluted amounts of stimulators in 96-well plates. Stimulators used were either MCMV-infected, mock-infected, or cells transfected with plasmids using Lipofectamine^{2000} (Thermo Fisher Scientific). Positive control cells were stimulated with 10 ng/mL PMA plus 0.5 μM ionomycin. These cells were incubated overnight, washed with PBS, then resuspended in 150 μL of 1X CPRG buffer (90 mg/L chlorophenol-red-β-D-galactopyranoside (Roche), 9 mM MgCl2, 0.1% NP-40, in PBS), incubated at room temperature, then analyzed using a Varioskan microplate reader (Thermo Fisher Scientific), using OD 595-655.

3.3.9 Chromium release assays

Splenic lymphokine-activated killer (LAK) effector cells were generated by harvesting spleens from mice, processing into single cell suspensions, ACK lysed (Thermo Fisher Scientific), then grown in 10% complete RPMI 1640 media supplemented with 2500 U/mL human rIL-2 (Proleukin; Novartis). On day 4, these cells were FACS sorted for $CD3^-NKp46^+$ NK cells subsetted based upon NKR-P1B expression, and used as effectors in ^{51}Cr-release assays on day 6 or 7. Target cells were labeled with 50 μCi $Na_2{}^{51}CrO_4$ (Perkin Elmer) in FCS for 1 hr at 37°C, washed, plated in 96-well V-bottom plates in serial dilutions with effector cells at corresponding ratios, and incubated at 37°C for 4 hrs. Supernatants (100 μl) were then transferred to scintillation plates (LumaPlate-96; Perkin Elmer), dried overnight, and counted using a Top Count NXT microplate Scintillation Counter (Packard Instrument Company). Percent specific lysis values were calculated relative to maximum release (2% Triton-X100) and spontaneous release (media) values.

3.3.11 Bioinformatic analysis

Mapped RNA-Seq reads were loaded visualized on the IGV Genome Browser using the MCMV Smith reference genome (accession number GU305914). Membrane topology was determined using the TMpred server (http://www.ch.embnet.org/software/TMPRED_form.html). The SignalP 4.1 Server (http://www.cbs.dtu.dk/services/SignalP/) was used for identification of

predicted signal peptides. Detection of ORF start site was achieved using NetStart 1.0 Prediction Server (http://www.cbs.dtu.dk/services/NetStart/).

3.3.12 Statistical Analysis

Data were analyzed using GraphPad Prism 5, using either a paired Student's two-tailed t-test, or one-way/two-way ANOVA with Tukey post hoc tests, where applicable. See figure legends for details.

3.4 Results

3.4.1 MCMV encodes an NKR-P1B decoy immunoevasin

The murine NKR-P1B-ligand, Clr-b (*Clec2d*), is rapidly lost in response to cellular infection by diverse viruses, including cytomegaloviruses (RCMV, MCMV) and poxviruses (Vaccinia, Ectromelia) (Aguilar et al., 2015; Voigt et al., 2007; Williams et al., 2012). Recently, we demonstrated that fibroblasts infected with MCMV and treated with blocking Clr-b mAb also induced an alternate Clr-b-independent NKR-P1B-ligand, although we could not resolve whether this ligand was of host or viral origin (Aguilar et al., 2015). To extend these results, we infected target cells with different MCMV strains and used them as stimulator cells for BWZ.CD3ζ/NKR-P1B^{129} (BWZ.P1B^{129}) reporter cell assays. As shown in **Figure 3.1**, mock-treated NIH3T3 cells or cells exposed to UV-irradiated MCMV strongly stimulated BWZ.P1B^{129} reporter cells, a stimulus blocked using Clr-b mAb (4A6), while weaker stimulation was observed upon live MCMV^{Smith} infection, which could not be blocked using Clr-b mAb (**Fig. 3.1A,B,C**) (Aguilar et al., 2015). Thus, live MCMV infection is required to both downregulate host Clr-b and to induce an alternative Clr-b-independent ligand.

To confirm this signal was Clr-b-independent, we generated Clr-b-deficient NIH3T3 cells (NIH3T3.ΔClrb) by CRISPR/Cas9-mediated genome editing using sgRNA to target the Clr-b (*Clec2d*) locus. Only MCMV-infected (but not mock-treated) NIH3T3.ΔClrb cells stimulated BWZ.P1B^{129} reporter cells (**Fig. 3.1D,E**). Employing another approach, we compared MCMV infection of primary adult ear fibroblasts (AEF) from B6 WT and B6.*Clrb*$^{-/-}$ mice (Kartsogiannis et al., 2008); here, BWZ.P1B^{129} reporter cells responded only to infected (but not mock-treated) B6.*Clrb*$^{-/-}$ AEF, whereas WT AEF behaved similarly to NIH3T3 cells (**Fig. 3.2A,B**). Notably,

Figure 3.1

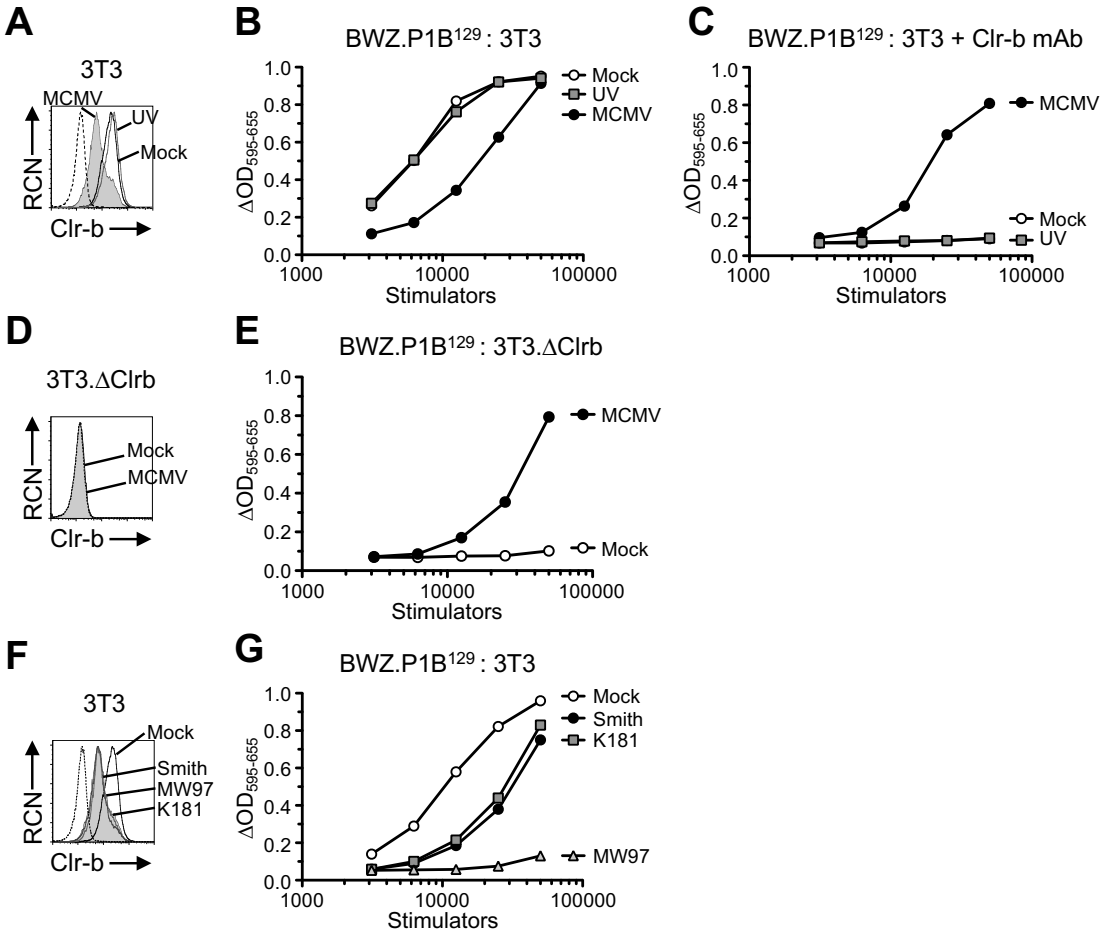

Figure 3.1. MCMV infection induces a Clr-b-independent NKR-P1B ligand. Mouse fibroblasts, NIH3T3, were infected with MCMV (MOI of 0.5 PFU/cell) overnight, and then used as stimulators to CD3ζ-NKR-P1B129 bearing BWZ reporter cells (BWZ.P1B^{129}). (**A**) Cell surface expression of Clr-b on mock, MCMV-infected, or UV-treated MCMV infected cells. BWZ assays with corresponding stimulators (**B**) in absence of antibody block, and (**C**) BWZ assays in the presence of 4A6 (αClr-b mAb, 10 μg/ml). (**D**) Cell surface stains and (**E**) BWZ reporter assays with MCMV infected NIH3T3.ΔClr-b. (**F**) Cell surface expression and (**G**) BWZ assays with fibroblasts infected with different laboratory MCMV strains (Smith, K181 and MW97.01). Data representative of at least 3 independent experiments.

Figure 3.2

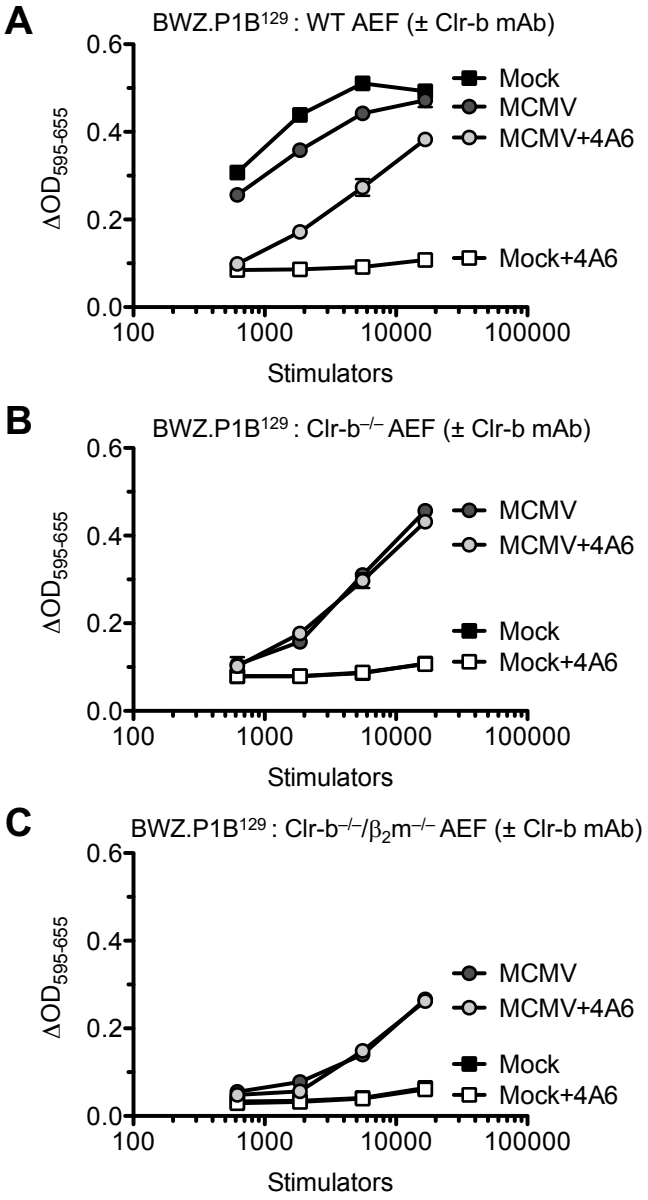

Figure 3.2. MCMV encodes a Clr-b and β_2m–independent NKR-P1B decoy. Adult ear fibroblasts (AEFs) from (**A**) WT/B6, (**B**) Clr-b$^{-/-}$, and (**C**) Clr-b$^{-/-}$/β_2m$^{-/-}$ mice were infected with MCMV^{Smith} and used as stimulators in BWZ assay with BWZ.NKR-P1B^{129} reporters in the absence, or presence of anti-Clr-b mAb (4A6).

similar results were observed upon MCMV infection of primary Clrb$^{-/-}$/β_2m$^{-/-}$ AEF cells (**Fig. 3.2C**), and rat embryonic fibroblast (REF) cells. Thus, a Clr-b/β_2m-independent NKR-P1B-ligand is induced upon MCMV infection of mouse and xenogeneic rat fibroblasts.

Since NKR-P1B is inhibitory, these results suggest that MCMV may encode a decoy immunoevasin. To test this, we analyzed distinct MCMV strains and large genomic deletion mutants to determine if any isolates lacked the NKR-P1B reporter signal upon infection of NIH3T3 fibroblasts. The MCMV^{Smith} and MCMV^{K181} strains both generated strong BWZ.P1B^{129} reporter signals; however, none of the mutants tested nor the parental BAC-generated MCMV^{MW97} strain elicited significant BWZ.P1B^{129} reporter responses (**Fig. 3.1F,G**). Unfortunately, this prevented the use of MCMV^{MW97} mutants to identify the putative immunoevasin gene. On the other hand, this suggested that MCMV^{MW97} may possess a polymorphism or loss-of-function mutation that abrogated BWZ.P1B^{129} reporter cell recognition.

3.4.2 The MCMV m02 family member, m12, directly interacts with the NKR-P1B receptor

To take advantage of the discrepancy between the MCMV strains, we conducted unbiased whole transcriptome RNA-Sequencing (RNA-Seq) using MCMV-infected NIH3T3 cells to identify differences between MCMV^{Smith} and MCMV^{MW97}. RNA-Seq reads were then mapped to the MCMV genome sequence using TopHat analysis (which can detect splicing events) and visualized using the IGV browser. Previous work has shown that RCMV-E encodes a spliced gene, *rctl*, with similar genetic structure to the rat Clr-11 homolog (*Clec2d11*) (Voigt et al., 2007); however, no spliced C-type lectin-like homologs could be found in the MCMV transcriptome.

Since numerous MCMV immunoevasin genes are located near the left or right genomic termini, such as the m02 or the m145 families, we next analyzed differences within these regions (**Fig. 3.3A,B**). Within the m145 family, few differences in transcript expression or genetic polymorphisms were noted between the two MCMV strains (**Appendix 3.2; Apendix 3.3**). In contrast, the m02 family displayed significantly more differences in transcript profiles and single nucleotide polymorphisms (SNP). To validate these functionally, we cloned MCMV^{Smith} m145 and m02 family members into the pIRES2-EGFP mammalian expression vector, then tested them individually using human 293T transfectants as stimulators for BWZ.P1B^{B6} reporter cells.

Figure 3.3

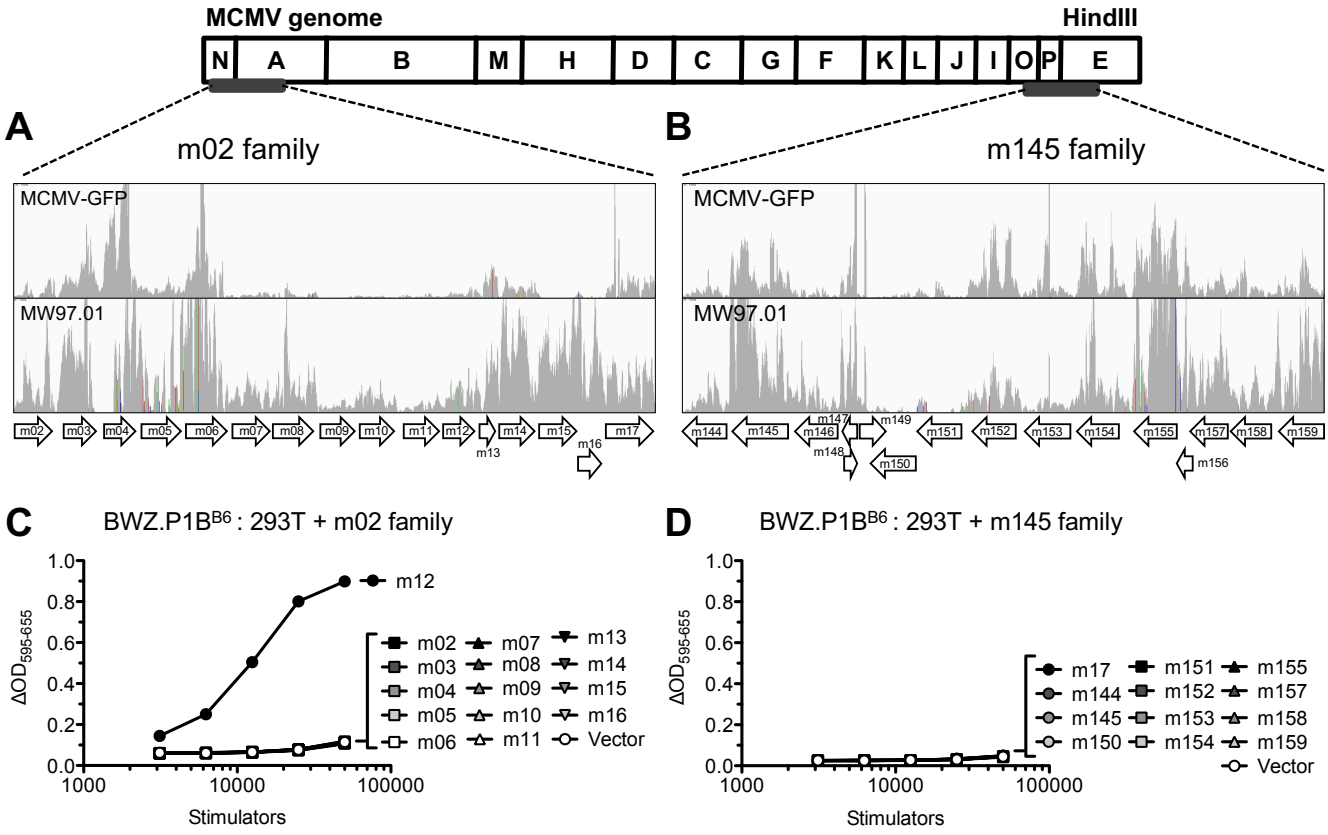

Figure 3.3. The NKR-P1B receptor recognizes the MCMV m02 family member, m12. RNA-Seq was prepared from RNA of fibroblasts infected with either MCMV-GFP (Smith strain) or MCMV$^{MW97.01}$ and mapped to MCMV genome. Histograms from MCMV-GFP (top) and MW97.01 (bottom) reads mapped to the (**A**) m02 and (**B**) m145 regions. BWZ assays using BWZ.NKR-P1B^{B6} reporters stimulated by HEK293T cells transfected with members of the (**C**) m02 or the (**D**) m145 families. SNPs are shown as different colored line in histograms. Data representative of at least 3 independent experiments.

while none of the m145 family gene products yielded positive results, a single gene product in the m02 family, m12, was capable of directly stimulating BWZ.P1B^{B6} (but not parental BWZ–) reporter cells (**Fig. 3.3C,D**). Thus, m12 is an NKR-P1B decoy ligand.

3.4.3 m12 is a glycosylated type-I transmembrane protein

We next characterized the topology, localization, and functional expression of m12. Notably, the m02 family encodes type-I TM proteins, but previous studies showed that tagged m12^{HA} protein was largely retained intracellularly in transient transfectants (Oliveira et al., 2002). In addition, m12 was predicted to differ from the prototypical m04 family ORF structure according to amino acid sequence alignments (Berry et al., 2014). A predicted 20 residue TM domain was identified 10 amino acids from the m12 C-terminus (**Fig. 3.4A**), yet SignalP predicted that m12 lacked an N-terminal signal peptide, when assessed from the annotated start (ATG) codon (Rawlinson et al., 1996). Interestingly, an additional in-frame ATG codon was identified 96 nucleotides downstream of the annotated start site, which highlighted a canonical signal peptide (when analyzed by SignalP) and a predicted translational start site (according to the NetStart server).

To validate the second ATG translational initiation site, we generated several m12 constructs, including: (i) native m12 ORF, m12^{ATG1} and m12^{ATG2}; (ii) N-terminal tagged m12 ORF, with a FLAG tag inserted either after the predicted native signal peptide (m12$^{NSP\text{-}FLAG}$), or following a preprotrypsin signal peptide (m12$^{PSP\text{-}FLAG}$); and (iii) a C-terminal HA-tagged m12 ORF (m12$^{C\text{-}HA}$). These constructs were then analyzed using 293T transient transfectants, flow cytometry, and BWZ.P1B^{129} reporter cell assays (**Fig. 3.4B,C**).

Notably, cell surface m12^{FLAG} was detected on transfectants using ATG2 and both signal peptides (m12$^{NSP\text{-}FLAG}$, m12$^{PSP\text{-}FLAG}$), confirming a type-I TM topology (**Fig. 3.4B**). In addition, all of the m12 constructs stimulated BWZ.P1B^{B6} reporter cells, with m12^{ATG1} yielding the weakest signal (**Fig. 3.4C**). The weaker ligand function of m12^{ATG1} relative to m12^{ATG2} could be due to less efficient folding or signal peptide cleavage, or competitive translation initiation. In keeping with a type-I TM orientation, the m12$^{C\text{-}HA}$ construct could only be detected intracellularly, yet retained BWZ.P1B^{B6} reporter stimulation. Collectively, these results suggest that ATG2 is preferred, the native signal peptide is cleaved, and m12 is expressed as a functional type-I TM cell surface protein.

Figure 3.4

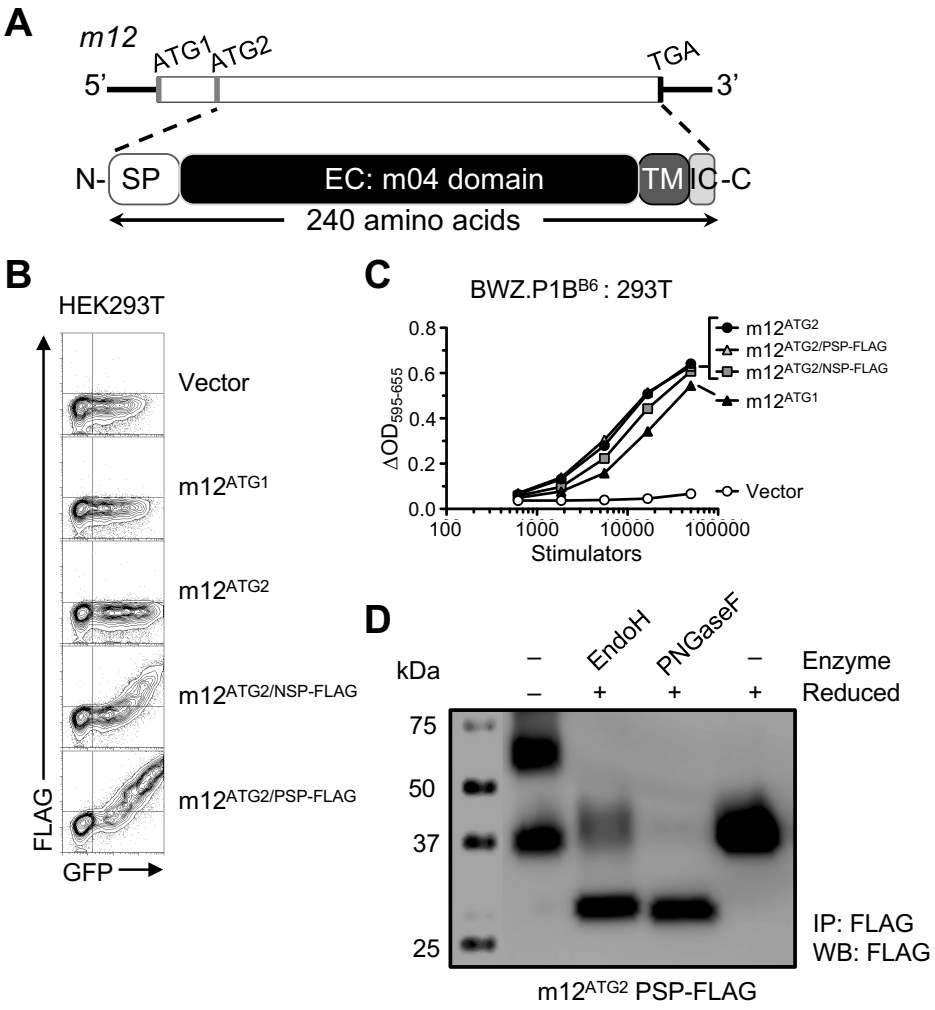

Figure 3.4. m12 is a type-I transmembrane protein. (**A**) Structure of the m12 gene with translational start sites and stop codon labeled (top), and domain structure of the m12 protein (bottom). SP, signal peptide; EC, extracellular domain; TM, transmembrane domain; IC, intracellular domain. (**B**) Cell surface expression of m12 N-terminally tagged-FLAG (NT-FLAG) constructs cloned into pIRES2-EGFP and transfected into HEK293T. (**C**) Stimulation of BWZ.NKR-P1B^{B6} cells by different m12 NT-FLAG constructs. (**D**) Immunoprecipation of NT-FLAG tagged m12^{ATG2} PSP transfected into HEK293T and isolated under different conditions and immunoblotted for FLAG expression. Non-R, non-reduced. Data representative of at least 3 independent experiments.

To assess m12 biochemically, we next conducted immunoprecipitation and Western blot analysis of 293T transfectants. Under non-reducing conditions, the m12 protein exists both as a ~35-40 kDa monomer and a ~60-75 kDa dimer (**Fig. 3.4D**). Under reducing conditions, only a single band of ~40 kDa was observed. Enzymatic digestion using endoglycosidase-H (EndoH) revealed a ~40 kDa EndoH-resistant band and a ~28 kDa EndoH-sensitive band, while treatment with peptide-N-glycosidase-F (PNGaseF) demonstrated a single band at ~28 kDa, in accordance with a predicted size of 24.6 kDa. These data suggest that m12 is a highly N-linked glycosylated type-I TM protein.

3.4.4 Recognition of m12 by the prototypical NK1.1 antigen, the stimulatory NKR-P1C receptor

It was previously shown that the RCMV-E RCTL immunoevasin could weakly engage the stimulatory rNKR-P1A$^{WAG/SD}$ alleles, in addition to the inhibitory rNKR-P1B$^{WAG/SD}$ alleles, suggestive of host counter-evolution during pathogen infection (Voigt et al., 2007). Therefore, we tested whether m12 was capable of interacting with paralogous host receptor isoforms and alleles. To this end, BWZ reporter cells bearing CD3ζ-fusion NKR-P1A/B/C/F/G receptors were constructed from the FVB, B6, and 129/BALB-strain alleles. Notably, the NKR-P1B$^{129/BALB}$ alleles are identical, as are the NKR-P1B$^{Sw/SJL/FVB}$ alleles (Carlyle et al., 1999; Zhang et al., 2012). Sequence analyses confirmed previous work suggesting that NKR-P1F/G are closely related, whereas NKR-P1A/B/C form a separate clade (**Fig. 3.5A**). In general, the FVB alleles more closely resemble the BALB/129 alleles versus those of B6, especially concerning the NKR-P1A/B/C clade (**Fig. 3.5A**).

We next tested BWZ.NKR-P1 type-II TM reporter cells stimulated using 293T transfectants of the m12^{Smith} allele (**Fig. 3.5**). Notably, the stimulatory NKR-P1A, NKR-P1F, and inhibitory NKR-P1G receptors did not appreciably recognize m12^{Smith}, while all inhibitory NKR-P1B receptor alleles recognized m12^{Smith} (**Fig. 3.5B,D,F**). Remarkably, the m12^{Smith} immunoevasin also significantly interacted with the stimulatory NKR-P1C^{B6} receptor, demonstrating that m12^{Smith} is a much-anticipated natural ligand for the prototypical NK1.1 antigen (Glimcher et al., 1977; Koo and Peppard, 1984; Ryan et al., 1992) (**Fig. 3.5C**). Interestingly, the NK1.1^{-} NKR-P1C^{FVB} allele also recognized m12^{Smith}, but the NK1.1^{-} NKR-P1C$^{129/BALB}$ allele did not (**Fig. 3.5C,E,G**), demonstrating that paralogous stimulatory

Figure 3.5

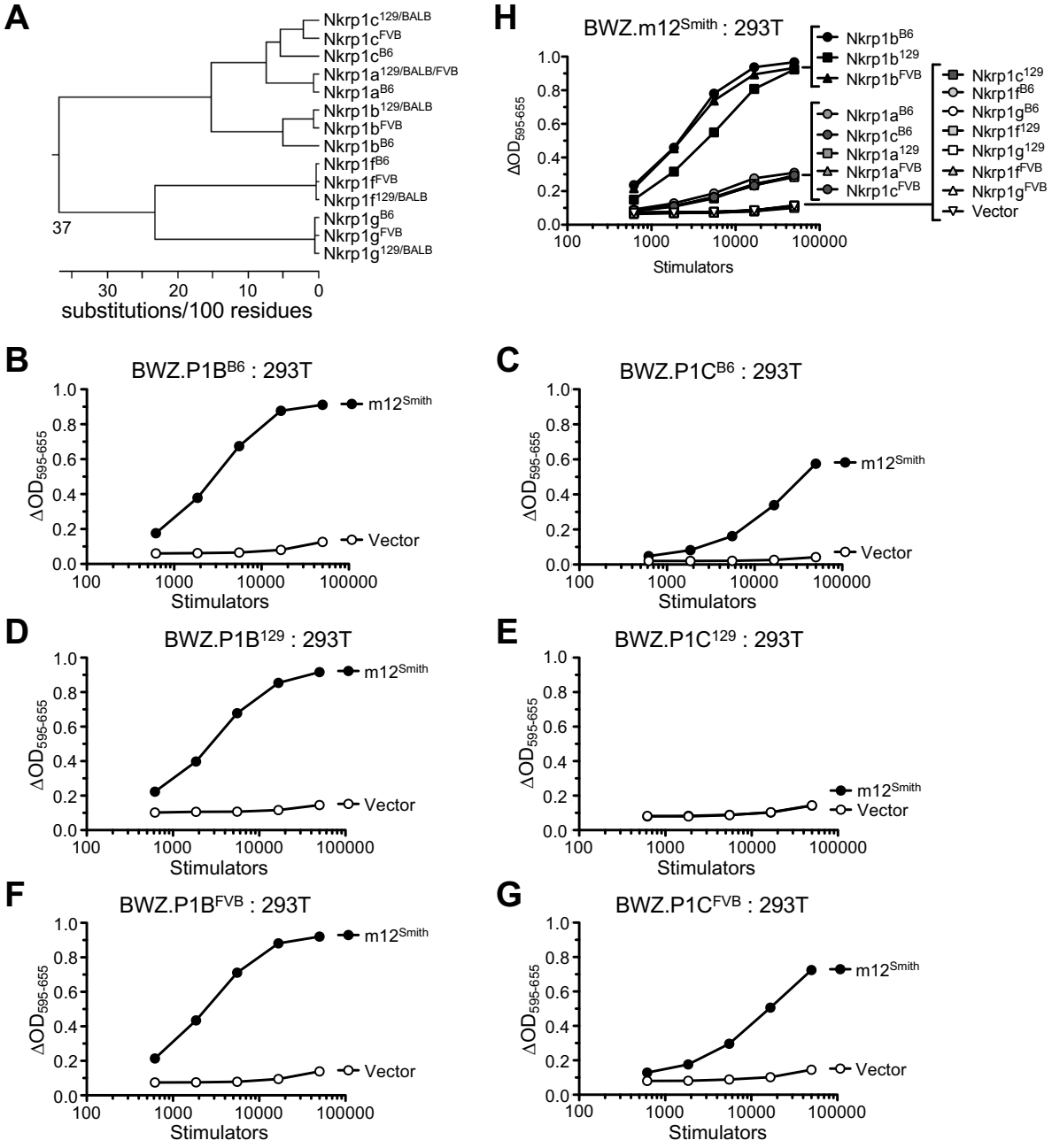

Figure 3.5. Recognition of m12 by the stimulatory NKR-P1C/NK1.1 receptor. (**A**) Phylogenetic tree of the NKR-P1 family of proteins from B6, 129/BALBc, and FVB using ClustalW alignment. HEK293T cells transfected with $m12^{Smith}$ were co-cultured with BWZ reporters bearing (**B**) NKR-P1B^{B6}, (**C**) NKR-P1C^{B6}, (**D**) NKR-P1B^{129}, (**E**) NKR-P1C^{129}, (**F**) NKR-P1B^{FVB}, or (**G**) NKR-P1C^{FVB}. (**H**) BWZ reporters bearing chimeric m12-CD3ζ receptors co-cultured with HEK293T cells transfected with NKR-P1 receptors from B6, 129, or FVB strains. Data representative of at least 3 independent experiments.

recognition of m12^{Smith} is not unique to B6 mice, yet 129/BALB mice may be more susceptible to NKR-P1B-mediated inhibition. Notably, of all tested NKR-P1:immunoevasin combinations, m12^{Smith} was the sole MCMV-encoded NKR-P1 ligand, as no further interactions were observed between NKR-P1 and m02 or m145 family members (**Fig. 3.6**; **Fig. 3.7**).

To confirm these results reciprocally, we also generated BWZ.m12^{Smith} type-I TM reporter cells (using the PSP-FLAG-m12^{Smith} ectodomain fused to the CD8α/CD3ζ TM/cytosolic domains) (Mesci and Carlyle, 2007). BWZ.m12^{Smith} reporter cells were then used to semi-quantitatively assess interactions with all NKR-P1 alleles using 293T transfectants (**Fig. 3.5H**). Using this approach, BWZ.m12^{Smith} reporters recognized NKR-P1B^{B6,129,FVB}, NKR-P1A$^{B6,129/FVB}$, and NKR-P1C^{B6,FVB}, but not NKR-P1C^{129} (where BALB/129 alleles are identical); however, the stimulatory NKR-P1A/C paralogs interacted with m12^{Smith} more weakly than the inhibitory NKR-P1B counterparts in this cellular context. Interestingly, splice variants of NKR-P1B^{FVB} and NKR-P1C^{B6,FVB} maintained stimulation of BWZ.m12^{Smith} reporters, but more extensive deletions lacked function (**Fig. 3.8A**). To confirm that weaker stimulation by NKR-P1C^{B6,FVB} was not due to inefficient surface expression hindered by a charged transmembrane (R) residue (which facilitates FcRγ adaptor association) (Arase et al., 1997), we generated reciprocal domain swaps of NKR-P1B^{B6} and NKR-P1C^{B6}; however, these stimulated the m12^{Smith} reporters similarly to native isoforms (**Fig. 3.8B**), and exhibited similar cell surface staining using PK136 and 2D12 mAb (**Fig. 3.8C**). Interestingly, upon overexpression in 293T cells, PK136 mAb weakly recognized NKR-P1A$^{B6,129/FVB}$, NKR-P1B^{129}, and NKR-P1C^{FVB}, in addition to strongly recognizing NKR-P1C^{B6} and NKR-P1B^{FVB} (Carlyle et al., 1999), while 2D12 mAb was specific for NKR-P1B^{B6} (**Fig. 3.9**) (Iizuka et al., 2003). Collectively, dual recognition of m12 by paralogous NKR-P1 receptors with opposing signals suggests that NKR-P1:m12 interactions are evolving under selection pressures driven by host-pathogen interactions.

3.4.5 Direct interaction between NKR-P1B/C and m12 proteins

To determine whether m12 was capable of directly binding to NKR-P1 proteins, we expressed soluble m12 and NKR-P1 receptor ectodomains and assessed their interaction by surface plasmon resonance (SPR). Using this approach, m12 bound with similar affinity to the inhibitory NKR-P1B^{B6} (K_d = 5.8 μM) and stimulatory NKR-P1C^{B6} (K_d = 4.1 μM) receptors (**Fig. 3.10A**). However, as observed using reporter cell assays, m12 recognition was found to be highly

Figure 3.6

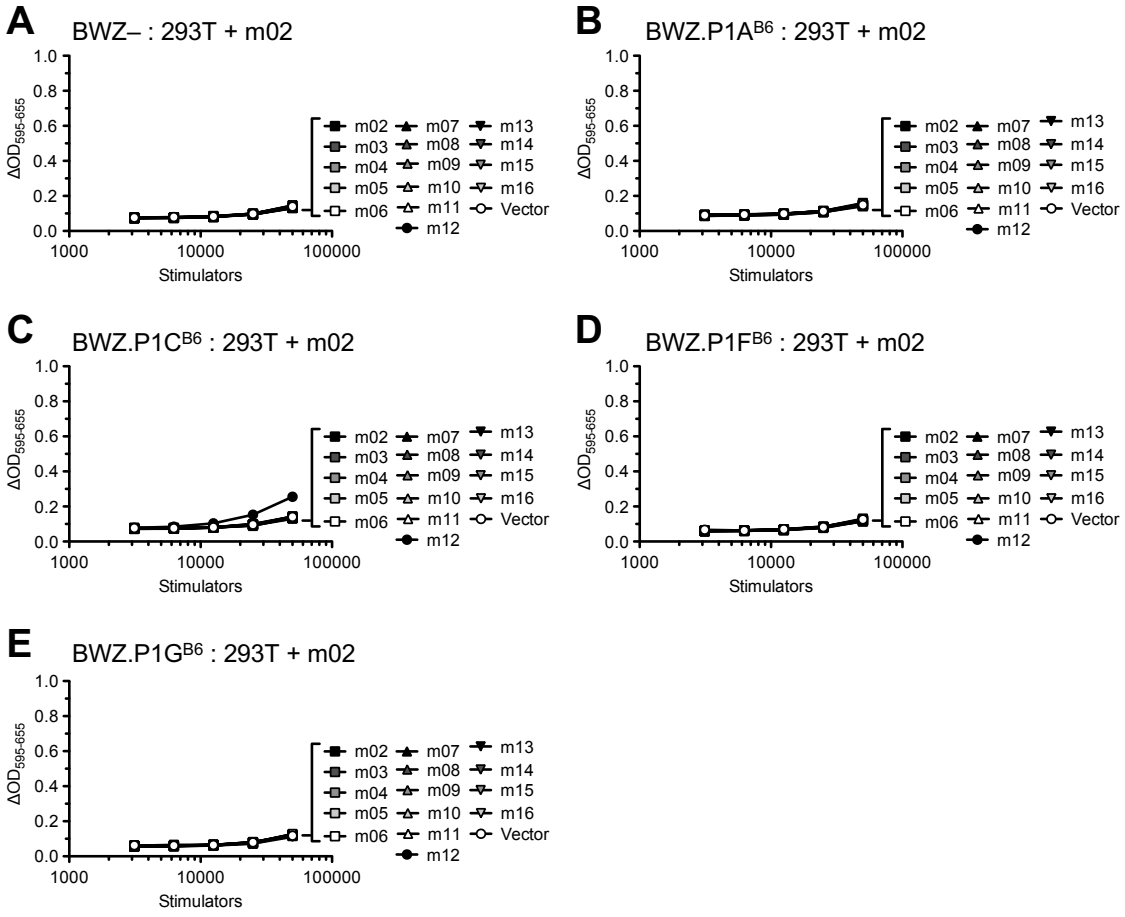

Figure 3.6. Complete analysis of m02 family members using BWZ reporter assays. HEK293T cells were transfected with m02 family members (m02-m16) and 24 hours later were used as stimulators in BWZ assays using (**A**) parental BWZ–, (**B**) BWZ.NKR-P1A^{B6}, (**C**) BWZ.NKR-P1C^{B6}, (**D**) BWZ.NKR-P1F^{B6}, and (**E**) BWZ.NKR-P1G^{B6} reporters.

Figure 3.7

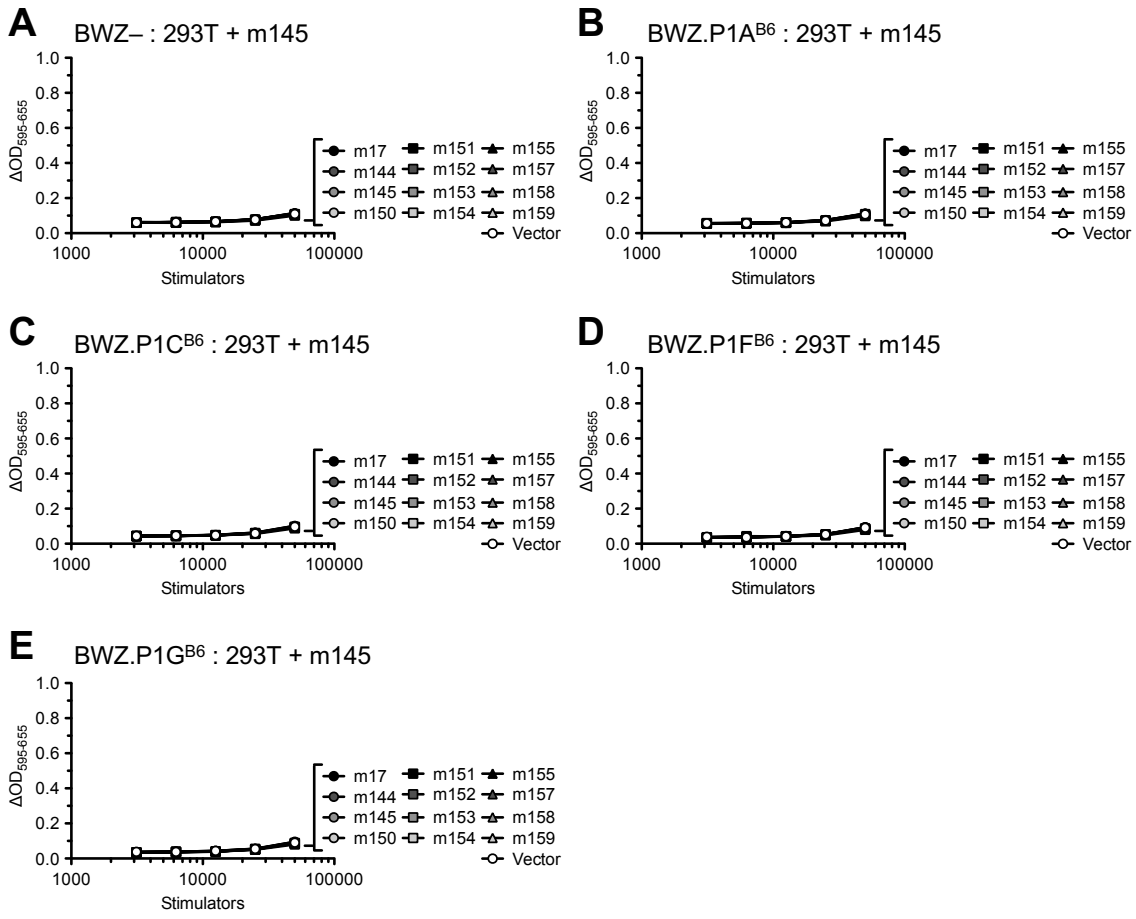

Figure 3.7. Complete analysis of m145 family members using BWZ reporter assays. HEK293T cells were transfected with m145 family members and 24 hours later were used as stimulators in BWZ assays using (**A**) parental BWZ–, (**B**) BWZ.NKR-P1A^{B6}, (**C**) BWZ.NKR-P1C^{B6}, (**D**) BWZ.NKR-P1F^{B6}, and (**E**) BWZ.NKR-P1G^{B6} reporters.

Figure 3.8

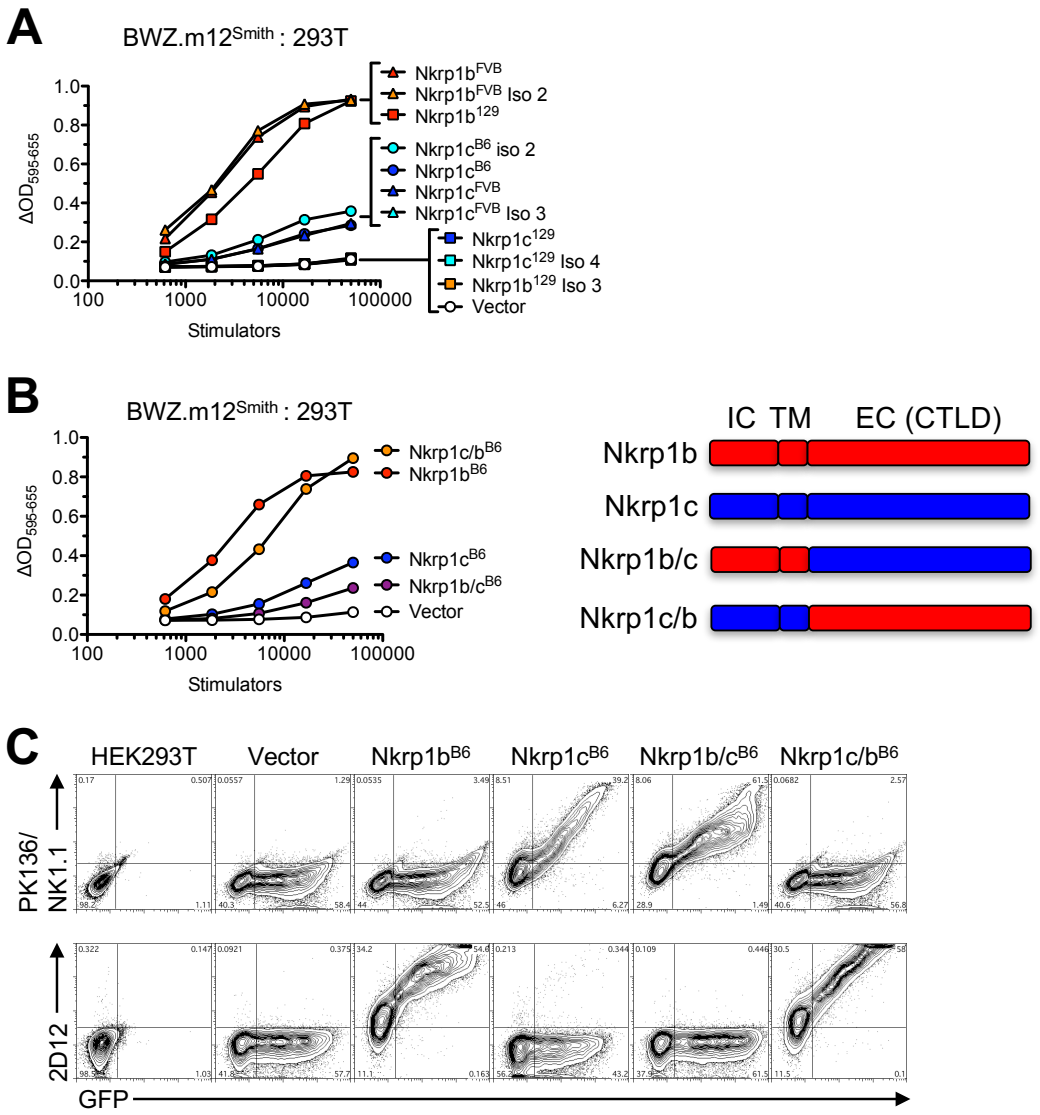

Figure 3.8. Certain Nkrp1 isoforms retain ability to bind the m12 ligand. (**A**) Nkrp1 isoforms were cloned into pIRES2-EGFP using cDNA from B6, 129, and FVB splenic LAK, transfected into HEK293T cells, and used as stimulators against BWZ.m12^{Smith} reporters. (**B**) Intracellular (IC) and extracellular (EC) domain swaps of NKR-P1B^{B6} and NKR-P1C^{B6} were constructed (right) and tested in their ability to stimulate BWZ.m12^{Smith} reporters upon transfection into HEK293T (left). (**C**) Cell surface expression of NKR-P1B/C^{B6} domain swap constructs using α-NKR-P1B mAb (2D12) and α-NKR-P1C mAb (PK136/NK1.1)

Figure 3.9

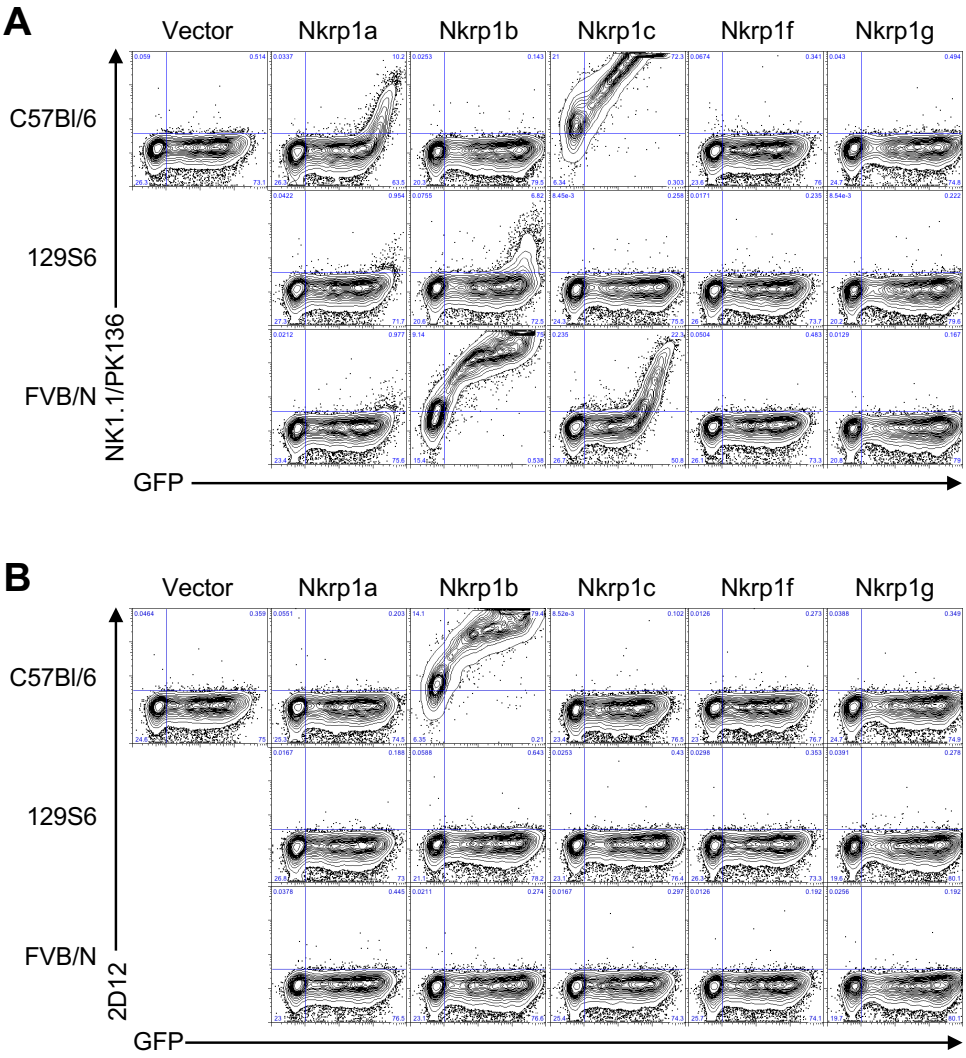

Figure 3.9. Cross-reactivity of NK1.1/PK136 and 2D12 antibodies with the NKR-P1 family of receptors. Clones of the Nkrp1 family (a-g) from C57Bl/6, 129S9, and FVB/N strains were transfected into HEK293T cells, and analyzed by flow cytometry 48 hours post transfection. (**A**) Staining by anti-NKR-P1C^{B6} mAb, NK1.1/PK136. (**B**) Staining by the anti-NKR-P1B^{B6} mAb, 2D12.

Figure 3.10

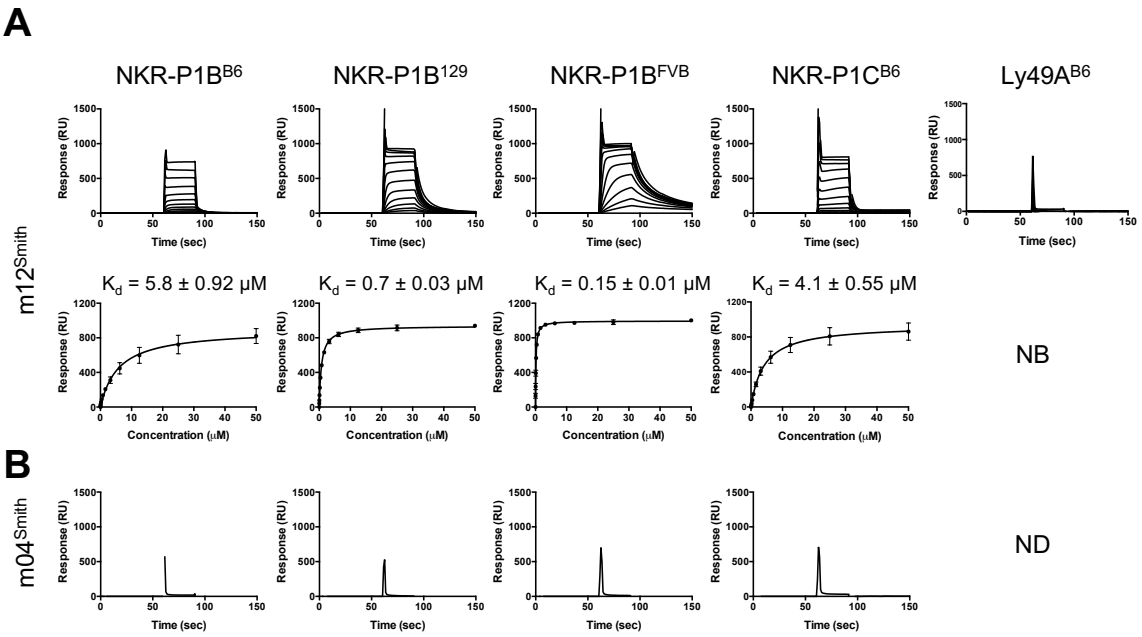

Figure 3.10. Binding of m12 to NKR-P1 receptors. Sensograms and equilibrium binding curves (where appropriate) are shown for the binding of $m12^{Smith}$ (0.025-50 μM) and $m04^{Smith}$ (100 μM) to various NKR-P1 or Ly49 receptors as indicated. Equilibrium dissociation constants (K_d) were calculated form two independent measurements. Error bars represent the standard error of the mean. NB: No binding, ND: not determined.

allele-sensitive, with m12 binding to NKR-P1B^{129} and NKR-P1B^{FVB} with affinities 8-fold (K_d = 0.7 μM) and 40-fold (K_d = 0.15 μM) higher than observed for NKR-P1B^{B6} (**Fig. 3.10A**). Notably, m12 did not bind to the structurally related Ly49A^{B6} receptor. In addition, despite injection at high concentration (100 μM), m04 did not bind appreciably to any NKR-P1 alleles tested (**Fig. 3.10B**). Together, these results demonstrate the allelic and isoform specificity of the direct m12:NKR-P1 interaction.

3.4.6 A single SNP in m12^{Smith} versus m12^{MW97} impacts NKR-P1B immunoevasin function

Despite differential stimulation of BWZ.P1B^{129,B6} reporter cells by NIH3T3 fibroblasts infected using MCMV^{Smith} versus MCMV^{MW97} (**Fig. 3.1G**), quantitation of m12 transcripts by qRT-PCR revealed similar mRNA levels between the two viruses (**Fig. 3.11A**). This is in accordance with integrated quantitation of RNA-Seq read profiles (Juranic Lisnic et al., 2013; Marcinowski et al., 2012). However, a single G271A SNP was observed in m12^{MW97} that resulted in a non-conservative E91K charge substitution. Of note, m12^{K181} is identical to m12^{Smith} in both sequence and BWZ.P1B^{129,B6} reporter cell stimulation (**Fig. 3.1G)**.

To determine whether this allelic m12 SNP affected immunoevasin function, we compared BWZ.P1B^{B6} reporter stimulation by m12^{MW97} versus m12^{Smith} in 293T transfectants; indeed, m12^{MW97} was recognized more weakly than m12^{Smith} and host Clr-b (**Fig. 3.11B**). This suggests that m12^{Smith} is a superior NKR-P1B immunoevasin versus m12^{MW97}, at least in B6 mice.

We next extended these results using cytotoxicity assays. Here, we generated stable retroviral transductant YAC-1 and BWZ.36 (BW) target cells expressing native m12^{Smith}, m12^{MW97}, or host Clr-b (indexed via IRES-GFP levels; **Fig. 3.12A,D**). As observed using 293T transfectants, BWZ.NKR-P1 reporter analyses using YAC-1 and BW stimulators show that BWZ.P1B^{B6} cells recognize m12^{Smith} more strongly than m12^{MW97} (**Fig. 3.12B,E**), while BWZ.P1B^{FVB} cells recognize m12^{Smith} and m12^{MW97} similarly (**Fig. 3.13A,D**). In contrast, unlike 293T.NKR-P1/m12 transient transfectant data (**Fig. 3.5C,H**; **Fig. 3.8B**), we could not detect stimulation of BWZ.P1C^{B6} reporter cells using YAC-1.m12^{Smith} or BW.m12^{Smith} stable transductants (**Fig. 3.12C,F**), perhaps due to lower stable expression levels. In any case, strong

Figure 3.11

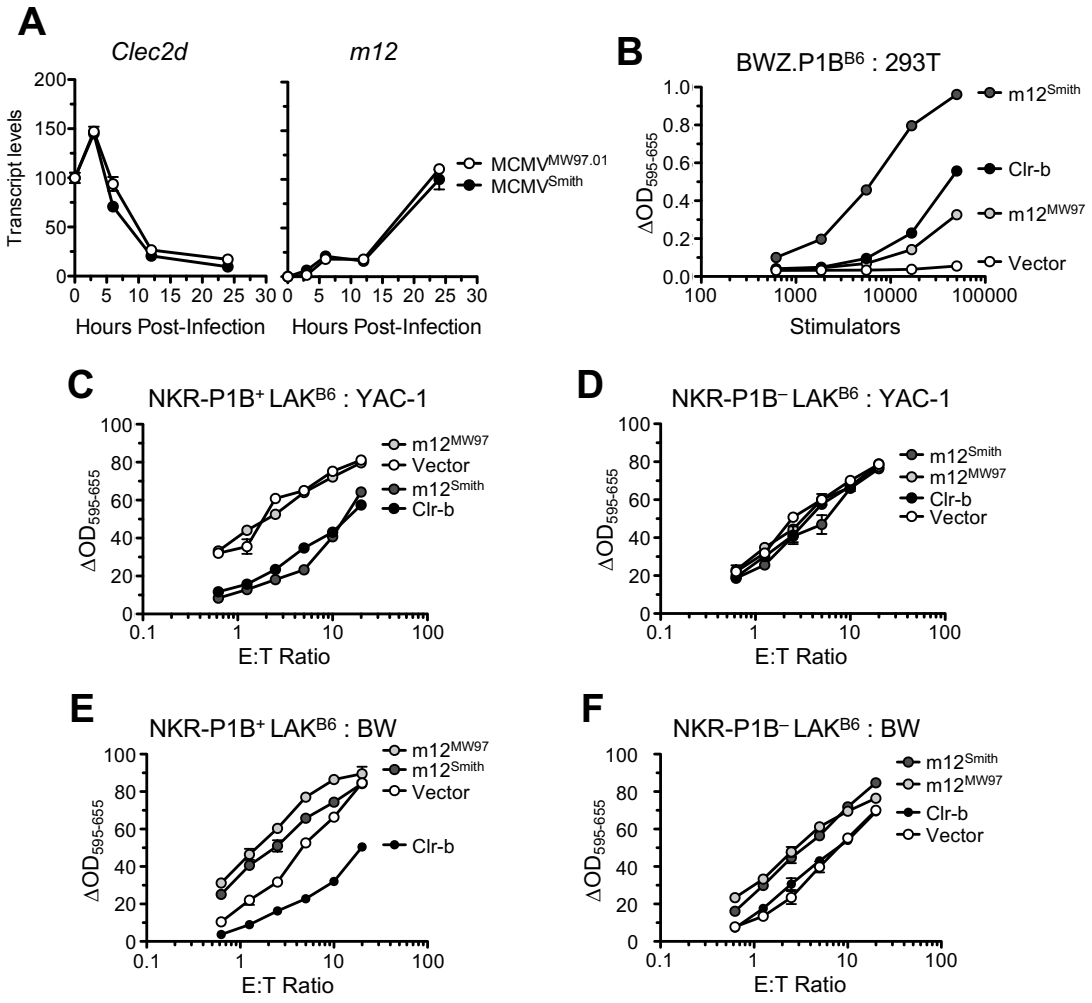

Figure 3.11. A SNP between Smith and MW97.01 strains results in differential NKR-P1B stimulation. (**A**) Transcript expression of m12 during MCMV infection of NIH3T3 with either $MCMV^{Smith}$ or $MCMV^{MW97.01}$. (**B**) HEK293T transfected with m12 from Smith and MW97.01 strains tested in BWZ assays with BWZ.NKR-P1B^{B6} reporters. Clr-b and vector serve as positive and negative controls respectively. YAC-1 cells transduced with $m12^{Smith}$, $m12^{MW97.01}$, Clr-b or empty MSCV (vector) used as targets in killing assays against sorted (**C**) NKp46^{+}NKR-P1B^{+} or (**D**) NKp46^{+}NKR-P1B^{-} LAK. BWZ.36 cells transduced with $m12^{Smith}$, $m12^{MW97.01}$, Clr-b or empty MSCV (vector) used as targets in killing assays against sorted (**E**) NKp46^{+}NKR-P1B^{+} or (**F**) NKp46^{+}NKR-P1B^{-} LAK. Data representative of at least 2 independent experiments.

Figure 3.12

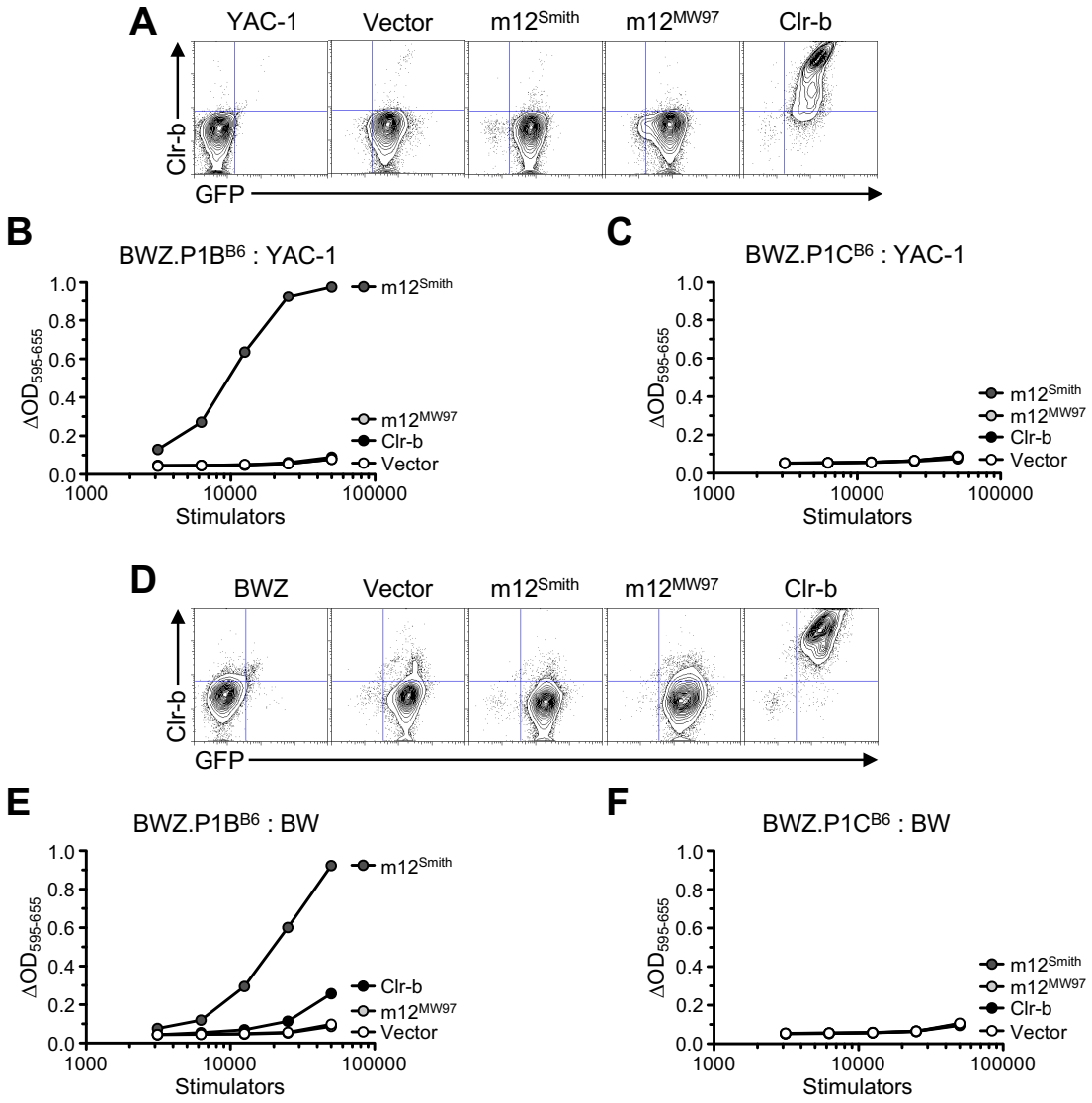

Figure 3.12. Generation of YAC-1 and BWZ.36 transductants. YAC-1 cells were transduced with pMSCV2.2-IRES-EGFP retrovirus encoding m12^{Smith}, m12$^{MW97.01}$, Clr-b, or parental empty vector, and sorted for matching GFP levels. These YAC-1 cells were analyzed by (**A**) flow cytometry by staining for Clr-b expression, and assessed in ability to stimulate (**B**) BWZ.NKR-P1B^{B6} and (**C**) BWZ.NKR-P1C^{B6} reporters. Similarly, BWZ.36 cells were transduced with MSCV retroviruses, sorted for matching GFP levels, assessed by (**D**) flow cytometry, and in BWZ assays using (**E**) BWZ.NKR-P1B^{B6} and (**F**) BWZ.NKR-P1C^{B6} reporters.

Figure 3.13

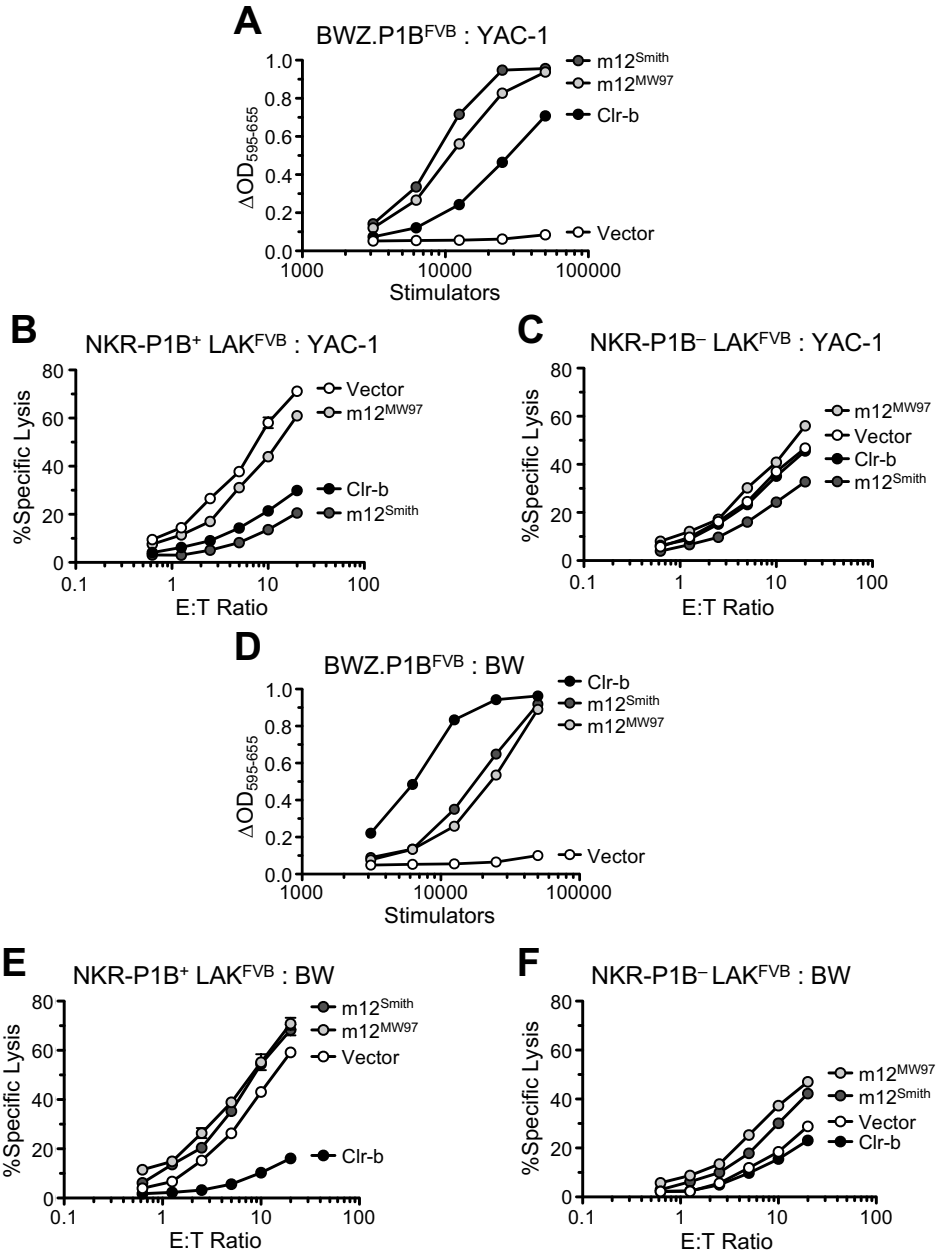

Figure 3.13. Analysis of YAC-1 and BW transductants in the FVB/N strain. YAC-1.MSCV transductants were used as stimulators in BWZ assay with (**A**) BWZ.NKR-P1B^{FVB} reporters, and in ^{51}Cr-release assays as targets against (**B**) NKR-P1B^{+} or (**C**) NKR-P1B^{-} FVB splenic NK-LAKs. Similarly, BW.MSCV transductants were used as stimulators to (**D**) BWZ.NKR-P1B^{FVB} reporters, and in ^{51}Cr-release assays as targets against (**E**) NKR-P1B^{+} or (**F**) NKR-P1B^{-} FVB splenic NK-LAKs.

NKR-P1B:m12^{Smith} inhibition should be evident in B6-strain NK cytotoxicity assays, perhaps overriding NKR-P1C:m12^{Smith} activation.

To test this, YAC-1 and BW transductants were incubated as targets with sorted NKp46^{+}NKR-P1B^{+} or NKp46^{+}NKR-P1B^{-} B6-strain lymphokine-activated killer (NK-LAK) effectors in ^{51}Cr-release cytotoxicity assays. As shown in **Figure 3.11**, YAC-1.m12^{MW97} target cells were killed equivalently to control YAC-1.vector targets, while both YAC-1.m12^{Smith} and YAC-1.Clr-b target cells significantly inhibited NKR-P1B^{+} NK-LAK cell cytoxicity (**Fig. 3.11C**). Importantly, inhibition by m12^{Smith} and host Clr-b was mediated via the NKR-P1B^{B6} receptor, as it was not observed using NKR-P1B^{-} NK-LAK effectors (**Fig. 3.11D**). In contrast, using BW transductants, only BW.Clr-b targets efficiently inhibited NKR-P1B^{+} NK-LAK cytotoxicity relative to control BW.vector targets, while BW.m12^{MW97} and to a certain extent BW.m12^{Smith} targets were killed more efficiently than controls (**Fig. 3.11E**). Interestingly, the weak stimulation of cytotoxicity observed for BW.m12^{Smith} and BW.m12^{MW97} targets was NKR-P1B-independent, as it was also observed using NKR-P1B^{-} NK-LAK effectors; here, cytotoxicity of control BW.vector and BW.Clr-b targets was also similar, since NKR-P1B inhibition is absent (**Fig. 3.11F**). This suggests that the two m12 alleles may be weakly recognized by the NKR-P1A/C^{B6} stimulatory receptors (present on NKR-P1B^{-} effectors), but only in the context of BW (not YAC-1) target cells. This highlights a potential requirement for tumour cell context or expression levels in the recognition of m12 by NKR-P1A/C, one involving m12-dependent but NKR-P1B-independent stimulation.

At present, we cannot rule out differential expression levels/avidity, endogenous *cis/trans* interactions, alternative receptor-ligand interactions, or glycosylation as possible m12 co-factors affecting BW versus YAC-1 cytotoxicity. Notably, however, similar results were observed using sorted FVB-strain NKR-P1B^{+} and NKR-P1B^{-} NK-LAK effectors, partitioned using NK1.1 mAb (PK136), which recognizes NKR-P1B^{FVB} (but not NKR-P1C^{FVB}) (Carlyle et al., 1999) (**Fig. 3.13A-F**). The similar recognition of m12^{Smith} and m12^{MW97} using BWZ.P1B^{FVB} reporters, but strong inhibition of cytotoxicity only by m12^{Smith}, suggests differential recognition of the m12 alleles by other stimulatory receptors, such as the NKR-P1A/C paralogs.

Taken together, these data demonstrate that an allelic m12^{MW97} SNP results in inefficient NKR-P1B immunoevasin function, while the m12^{Smith} immunoevasin is capable of effective inhibition of both B6 and FVB NK-LAK effectors using YAC-1 targets. In contrast, a role for

counterbalancing NKR-P1B inhibitory signals was observed using BW targets, whereby both the $m12^{Smith}$ and $m12^{MW97}$ alleles weakly augmented cytotoxicity independent of NKR-P1B, suggesting co-engagement by paralogous stimulatory NKR-P1A/C receptors.

3.4.7 Two m12-allelic MCMV and an m12-deficient mutant show non-redundant immunoevasin function *in vitro* and differential NKR-P1B-dependent virulence *in vivo*

To confirm an immunoevasin role for m12, we generated two m12-modified variants of the parental $MCMV^{MW97}$ strain. To this end, both m12-deficient (Δm12) and $m12^{Smith}$-revertant ($m12^{Smith}$) mutants of the parental $MCMV^{MW97}$ virus ($m12^{MW97}$) were generated, purified, and compared *in vitro* and *in vivo*. The genotypes of these viruses were confirmed by sequencing and showed no alterations in growth kinetics in tissue culture (J. Reichel, data not shown). *In vitro* characterization revealed that all three MCMV variants similarly downregulated host Clr-b upon infection of NIH3T3 cells (**Fig. 3.14A**). Using infected NIH3T3 cells directly, the $m12^{Smith}$-revertant virus stimulated $BWZ.P1B^{B6}$ reporters similarly to the original $MCMV^{Smith}$ virus, while the Δm12-mutant, parental $MCMV^{MW97}$, and mock-infected NIH3T3 cells lacked significant stimulation (**Fig. 3.15A**; note that in the absence of overexpression, $m12^{MW97}$ and endogenous Clr-b only weakly stimulate $BWZ.P1B^{B6}$ reporters). In contrast, using $BWZ.P1B^{129}$ reporters, strong stimulation was observed with $MCMV^{Smith}$ virus, $m12^{Smith}$-revertant virus, and mock-infected NIH3T3 cells, compared with weak stimulation using parental $MCMV^{MW97}$, and no stimulation using Δm12-mutant MCMV (**Fig. 3.15B**). Finally, using $BWZ.P1B^{FVB}$ reporter cells, stimulation was observed using mock-infected cells, $m12^{Smith}$-revertant virus, $MCMV^{Smith}$, and $MCMV^{MW97}$, but not the Δm12-mutant virus (**Fig. 3.15C**). The Clr-b-independent nature of these responses was also confirmed using blocking Clr-b mAb, as well as using mutant NIH3T3.ΔClrb cells infected with each of the MCMV strains (**Fig. 3.14B,C,D**). Additionally, as previously reported (Aguilar et al., 2015), signals were not detected using any other BWZ.NKR-P1 reporters mixed with MCMV-infected stimulators (**Chapter 2**). Together, these data demonstrate that m12 is a non-redundant NKR-P1B decoy immunoevasin, and that the $m12^{G271A}$ SNP (E91K polymorphism) identified between $MCMV^{Smith}$ and $MCMV^{MW97}$ is responsible for the differential stimulation of BWZ.P1B reporter cells.

Figure 3.14

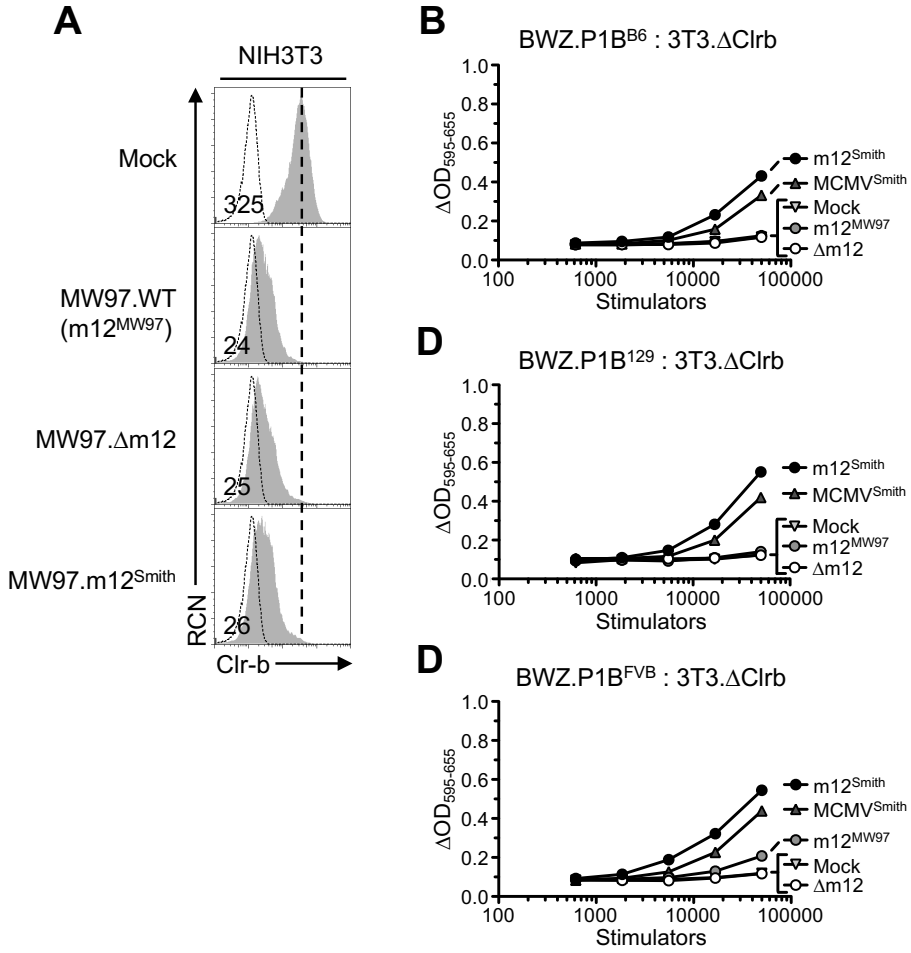

Figure 3.14. MW97.01 m12 variants retain ability to downregulate Clr-b and differentially stimulate NKR-P1B reporters. (**A**) NIH3T3 cells were infected with MW97.m12 MCMV viruses (MOI = 0.5), and assessed for cell surface Clr-b expression 24 hrs post-infection by flow cytometry. NIH3T3.ΔClr-b fibroblasts were infected with MW97 viruses and used as stimulators to (**B**) BWZ.NKR-P1B^{B6}, (**C**) BWZ.NKR-P1B^{129}, and (**D**) BWZ.NKR-P1B^{FVB} reporters.

Figure 3.15

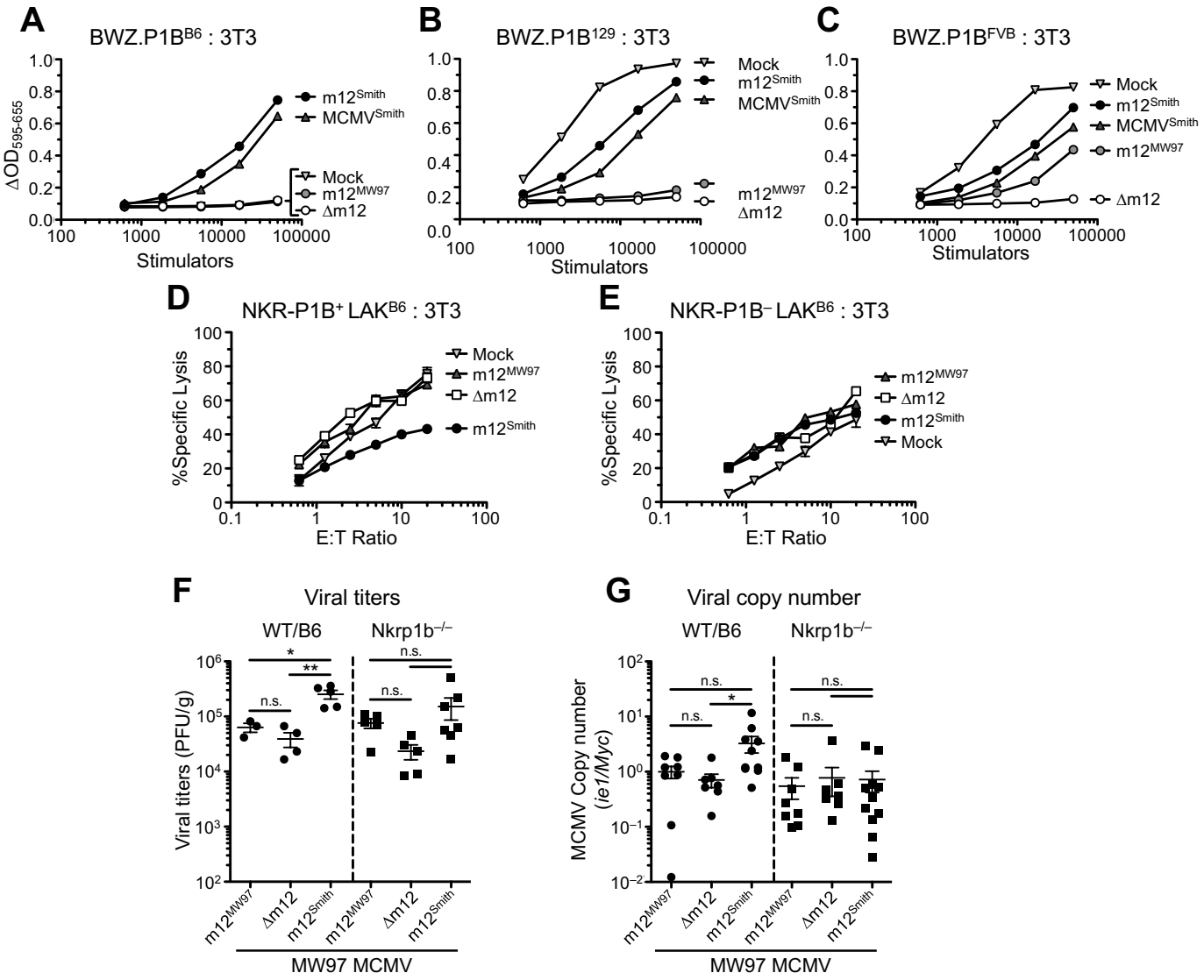

Figure 3.15. Expression of m12^{Smith} inhibits NK response during MCMV infection. NIH3T3 fibroblasts were infected with MCMV^{Smith}, or MW97 variants MW97.WT (m12^{MW97}), MW97.Δm12 (Δm12), MW97.m12^{Smith} (m12^{Smith}) and used as stimulators in BWZ assays with (**A**) BWZ.NKR-P1B^{B6}, (**B**) BWZ.NKR-P1B^{129}, (**C**) BWZ.NKR-P1B^{FVB} reporters. NIH3T3 fibroblasts infected the MW97 variants were used as targets in ^{51}Cr-release assay using (**D**) NKR-P1B^{+} and (**E**) NKR-P1B$^{–}$ sorted B6 splenic NK-LAK cells. (**F**) Viral titers in spleens WT, Clr-b$^{–/–}$ and Nkrp1b$^{–/–}$ mice *in vivo* infected with MW97 variants 3 days post-infection with 1x10^6 PFU. (**G**) MCMV copy numbers (*ie1/Myc*) normalized to infections with MW97.m12^{MW97} and WT mice (Note: this is a combination of infections with 1x10^6 and 1x10^5 PFU/mouse).

To further confirm these results, we conducted ^{51}Cr-release cytotoxicity assays using sorted B6-strain NKR-P1B^{+} and NKR-P1B^{-} NK-LAK effectors and MCMV-infected NIH3T3 targets. Notably, mock, MCMV^{MW97}, and Δm12-infected NIH3T3 targets were efficiently lysed, whereas m12^{Smith}-infected targets displayed significantly lower cytotoxicity in response to NKR-P1B^{+} effectors (**Fig. 3.15D**). Importantly, inhibition by m12^{Smith} was NKR-P1B-dependent, as it was not observed using NKR-P1B^{-} NK-LAK; interestingly, NKR-P1B^{-} NK-LAK displayed slightly lower cytotoxicity overall (Aust et al., 2009), yet all MCMV-infected NIH3T3 targets exhibited slightly elevated (m12-independent) cytotoxicity versus mock-infected controls (**Fig. 3.15E**). These data reveal that m12^{Smith}, but not m12^{MW97}, is directly capable of inhibiting B6-strain NK cytotoxicity in an NKR-P1B-dependent manner upon live MCMV infection.

To evaluate m12 immunoevasin function *in vivo*, the three variant MCMV^{MW97} strains were used to infect B6-strain WT, B6.*Clrb*$^{-/-}$, and B6.*Nkrp1b*$^{-/-}$ mice, then MCMV virulence was evaluated 3 days later using plaque assays and quantitative real-time PCR (qPCR) for viral genomic copy numbers in infected spleens. As expected, due to weak interaction between m12^{MW97} and NKR-P1B^{B6}, no significant difference was observed between the parental MCMV^{MW97} and Δm12-mutant viruses in B6 WT mice *in vivo* (**Figure 3.15F**); remarkably, however, the m12^{Smith}-revertant virus displayed significantly higher splenic viral titers (PFU) and viral genomic copy numbers in B6 WT mice (**Figure 3.15F,G**). Importantly, the enhanced virulence of the m12^{Smith} allele *in vivo* was NKR-P1B-dependent and Clr-b-independent, as it was not observed using B6-strain Nkrp1b$^{-/-}$ mice (**Figure 3.15F,G**), yet Clr-b$^{-/-}$ mice displayed a similar trend to WT B6 mice. Notably, increased virulence of MCMV^{Smith} *in vivo* has been previously observed using WT B6 mice relative to B6.*Nkrp1b*$^{-/-}$ mice (Rahim et al., 2016). This finding is confirmed to be m12-dependent here using three MCMV^{MW97}-strain variants, where the m12^{Smith}-revertant virus exhibits enhanced virulence versus parental MCMV^{MW97} and Δm12-mutant MCMV, in WT B6 but not B6.*Nkrp1b*$^{-/-}$ mice. These findings confirm a non-redundant NKR-P1B immunoevasin function for m12 *in vivo*.

3.4.8 Wild-derived MCMV isolates demonstrate host-driven evolution of the m12 gene product

Collectively, the above results show that two m12 allelic variants differentially modulate NK cell recognition via paralogous NKR-P1B and NKR-P1C alleles, supporting the existence of

both host- and pathogen-driven evolutionary selection pressures. Since NKR-P1B and NKR-P1C are polymorphic between mouse strains, we investigated whether additional m12 polymorphisms also exist in wild-derived MCMV isolates. Thus far, the $m12^{MW97}$ gene product displays a loss-of-function SNP resulting in diminished interaction with NKR-$P1B^{B6,129}$ in comparison to the $m12^{Smith}$ allele. To extend this finding, we searched databases to compare m12 sequences from additional MCMV strains, including the Smith, K181, MW97.01, WP15B, C4A, C4B, C4C, C4D, G4, AA18d, N1, and NO7 isolates (Smith et al., 2013); notably, with the exception of K181 and WP15B, each of the other strains differed from the $m12^{Smith}$ allele by at least 1 amino acid substitution (MW97.01, C4A/D/B), with extensive polymorphisms observed for some wild-derived isolates (G4), including loss of signal peptide (AA18d), and premature truncations in the m04-like domain (C4C,N1,NO7) (**Fig. 3.16A**; **Fig. 3.17**).

To assess these functionally, we cloned unique m12 gene products using viral gDNA templates, *in situ* mutagenesis, or *de novo* gene synthesis, then tested their recognition using BWZ.NKR-P1 reporters and 293T.m12 transfectant stimulators. Not surprisingly, we observed differences in recognition amongst all MCMV m12 alleles when tested against the different NKR-P1B and NKR-P1C alleles (**Fig. 3.16B-G**). The $m12^{C4A}$ variant has an A34V substitution, yet engaged all NKR-P1B alleles similarly to $m12^{Smith}$ (**Fig. 3.16B,D,F**). The $m12^{MW97}$ variant, as observed previously, has an E91K substitution and engaged NKR-$P1B^{B6}$ much less efficiently than $m12^{Smith}$, yet this difference was reduced using the NKR-$P1B^{129}$ allele, and absent using the NKR-$P1B^{FVB}$ allele (**Fig. 3.16B,D,F**). The highly diversified $m12^{G4}$ variant was not recognized by NKR-$P1B^{B6}$, interacted with NKR-$P1B^{129}$ similarly to $m12^{MW97}$, and interacted with NKR-$P1B^{FVB}$ less well than other m12 variants (**Fig. 3.16B,D,F**).

When tested against the NKR-P1C paralogs, all m12 variants interacted with NKR-$P1C^{B6}$ to some extent, although $m12^{G4}$ recognition was very weak (**Fig. 3.16C**). None of the m12 variants were found to interact with NKR-$P1C^{129}$ (**Fig. 3.16E**), which may not be functionally expressed (due to lack of a conserved cysteine residue in the C-type lectin-like ectodomain, C122S). In contrast, NKR-$P1C^{FVB}$ was stimulated strongly by $m12^{Smith}$ and $m12^{C4A}$, but very weakly by $m12^{MW97}$ and $m12^{G4}$ (**Fig. 3.16G**), suggesting this may impact or even reverse differential $m12^{Smith}$ versus $m12^{MW97}$ immunoevasin function *in vivo*. Interestingly, Clr-b also weakly stimulated NKR-$P1C^{FVB}$ reporters (**Fig. 3.16G**), demonstrating that Clr-b represents a second "self" ligand for the activating NKR-P1C receptor in the FVB strain. These data provide

Figure 3.16

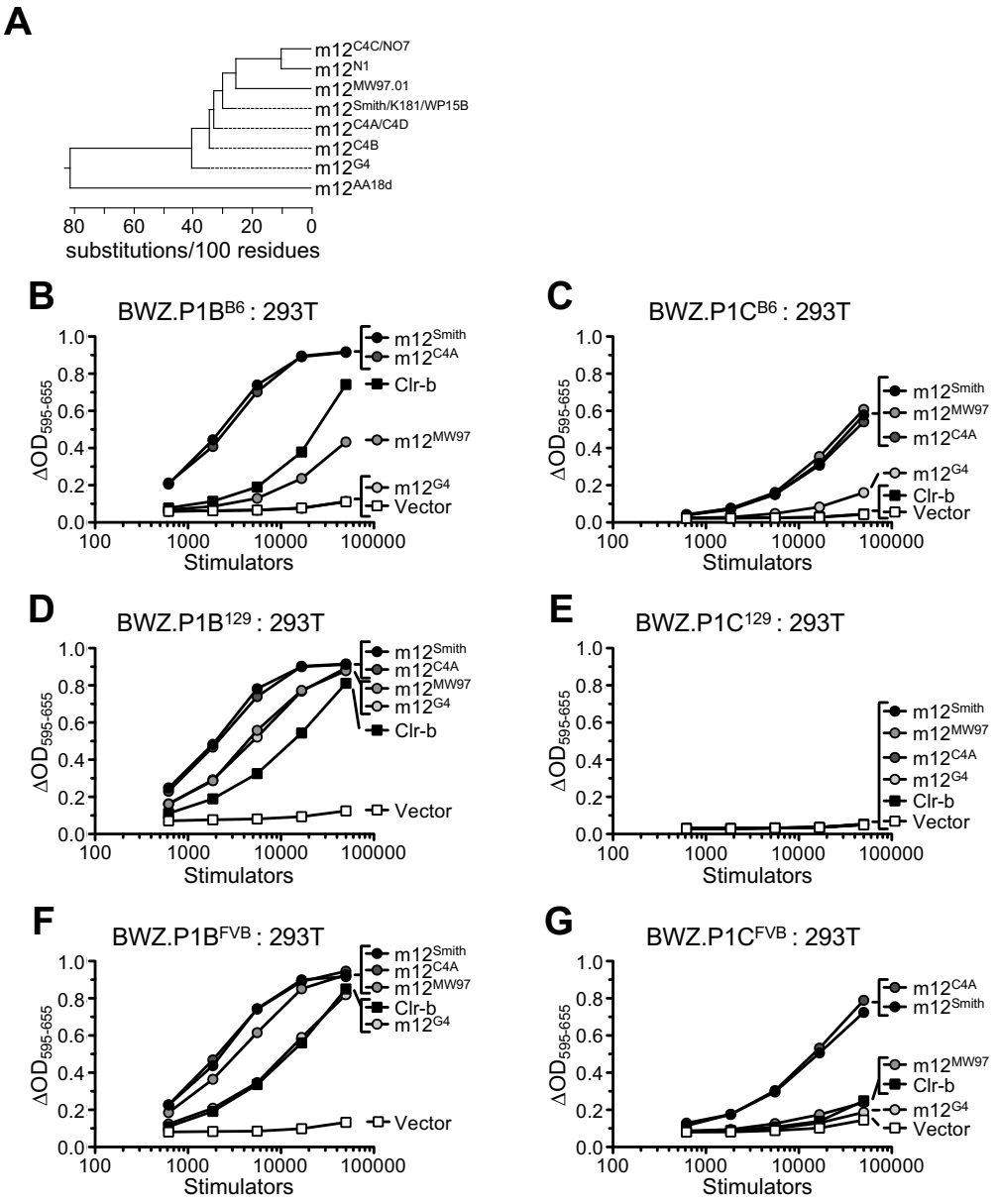

Figure 3.16. Wild isolates of MCMV are suggestive of host driven evolution of m12 gene. (**A**) Phylogenetic tree showing variance in m12 alleles from sequenced MCMV genomes (Smith, K181, MW97.01, WP15B, C4A, C4B, C4C, C4D, G4, AA18d, NO7, and N1). Unique m12 alleles (Smith, MW97.01, C4A and G4) were cloned into pIRES2-EGFP vector, transfected into HEK293T, and used to stimulate (**B**) BWZ.NKR-P1B^{B6}, (**C**) BWZ.NKR-P1C^{B6}, (**D**) BWZ.NKR-P1B^{129}, (**E**) BWZ.NKR-P1C^{129}, (**F**) BWZ.NKR-P1B^{FVB}, (**G**) BWZ.NKR-P1C^{FVB}. Data are representative of at least 3

Figure 3.17

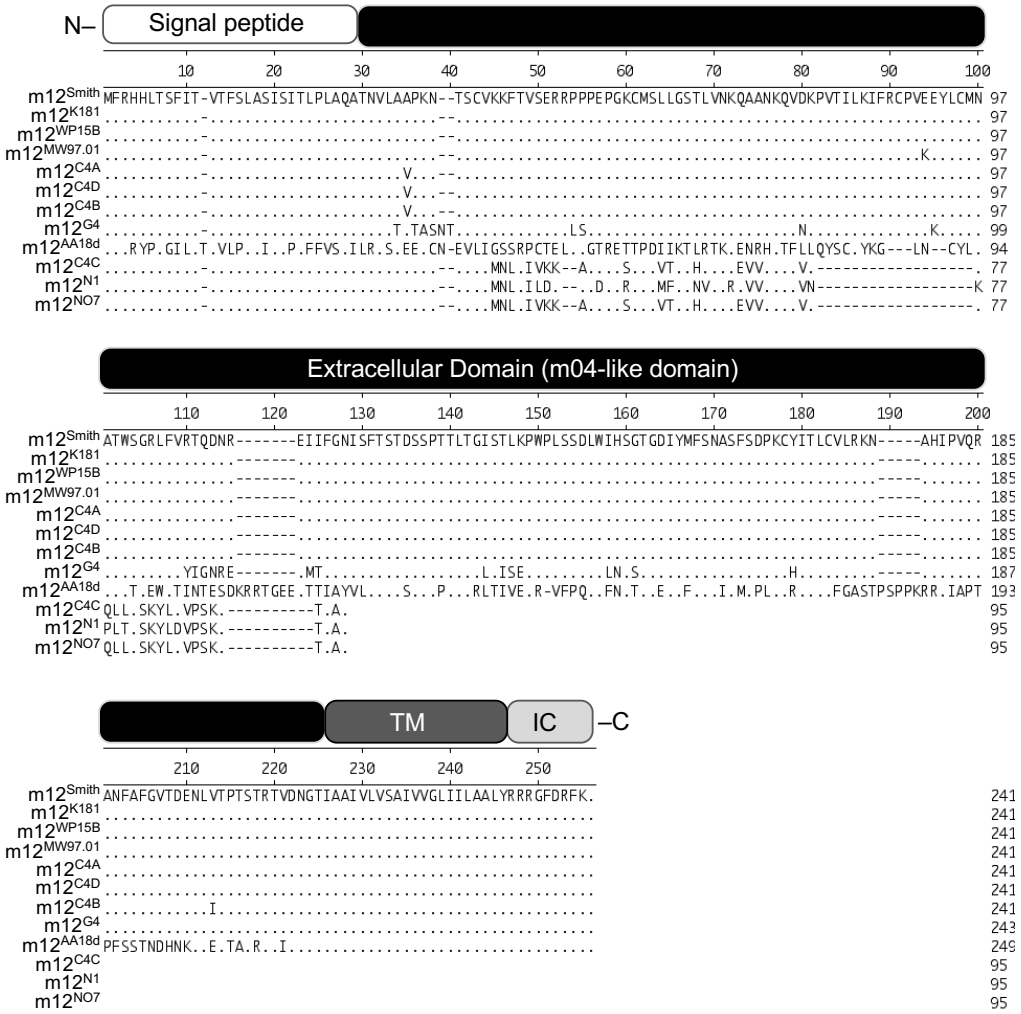

Figure 3.17. Protein alignments of m12 variants from sequenced MCMV genomes. Amino acid sequence of m12 from laboratory strain (Smith, K181, and MW97.01) and wild-type MCMV variants (WP15B, C4A, C4B, C4C, C4D, G4, AA18d, N1 and NO7) were obtained and aligned using ClustalW method. The protein domains are labeled above the amino acid sequence; TM, transmembrane domain; IC, intracellular domain.

further evidence of the existence of host/pathogen-driven evolution of the viral m12 glycoprotein and reciprocal host adaptation of the NKR-P1B/C paralogs. These findings also further validate the hypothesis that the NKR-P1B and NKR-P1C receptors have been co-evolving as a paired receptor clade to recognize similar host and viral ligands.

3.5 Discussion

There have been numerous strategies described for different cytomegaloviruses to evade host NK cell-mediated recognition. Here, we provide evidence that the MCMV m12 glycoprotein functions as a decoy immunoevasin to subvert NK cell-mediated cytotoxicity by direct interaction with the inhibitory NKR-P1B receptor, while the host Clr-b ligand is lost upon MCMV infection by an unknown mechanism (Aguilar et al., 2015). In addition, we provide evidence of co-evolution at the host-pathogen interface, with host adaptation of the NKR-P1A and NKR-P1C (NK1.1) stimulatory receptor paralogs to directly recognize the m12 decoy, as well as the existence of wild-derived viral m12 immunoevasin alleles that may have evolved to escape direct NKR-P1-mediated NK cell activation.

We previously reported a functionally analogous situation in the RCMV-English model, whereby the RCTL immunoevasin served as a decoy ligand for some inhibitory rNKR-P1B alleles (to replace downregulated host rClr11/*Clec2d11*) (Voigt et al., 2007). RCTL was also shown to weakly interact with stimulatory rNKR-P1A paralogs, while RCMV-Maastricht lacked the *rctl* gene. More recently, xenogeneic MCMV or RCMV infection were found to trigger a rapid loss of the host NKR-P1B-ligands, mClr-b and rClr-11 (Aguilar et al., 2015). These observations are suggestive of a conserved host innate pattern recognition response that promotes Clr-b loss in response to virus infection, including MCMV (Aguilar et al., 2015), RCMV (Aguilar et al., 2015; Voigt et al., 2007), poxviruses (Williams et al., 2012), and some RNA viruses (A. Mesci and J. Ma, unpublished data). In addition, this “missing-self” response may be conserved during cellular pathologies, such as transformation and genotoxic stress (Carlyle et al., 2004; Fine et al., 2010). Thus, the NKR-P1:Clr recognition system may play a crucial role in NK cell immunosurveillance of pathological target cells. The conserved use of immunoevasins by MCMV and RCMV to subvert NKR-P1B-mediated NK sensing highlight its role in immunity to

infectious disease, and suggest that similar mechanisms may operate during HCMV infection of human cells, including HCMV-encoded NKR-P1A immunoevasins.

The identification of the distantly Ig-related m02-family member, m12, as a *bona fide* NKR-P1A/B/C ligand is somewhat unexpected given the putative type-II TM C-type lectin-like homology exhibited by the RCMV RCTL gene product, which shares ~60% amino acid identity with the host ligand, rClr11, and a spliced gene structure similar to the host gene (*rClec2d11*) (Voigt et al., 2007). On the other hand, m12, like the other m02 family members, is encoded as a single ORF in the MCMV genome, and adopts a type-I transmembrane topology with an m04-related Ig-like domain. Thus, RCMV and MCMV appear to have employed convergent evolutionary tactics to subvert NKR-P1B-mediated self-nonself discrimination.

An initial study describing m12 demonstrated that it was largely retained intracellularly upon overexpression (Oliveira et al., 2002). Recently, however, structural determination of the m04 ectodomain suggested that, unlike most m02 family members, the m12 protein may not adopt a characteristic m04-like (Ig-like) fold (Berry et al., 2014). However, identification of an in-frame downstream translational start codon (ATG2) suggests that it may be preferred to the annotated translational initiation site (ATG1), as supported by our bioinformatic, biochemical, and expression data. In particular, ATG2 initiation generates a signal peptide with a type-I TM fold more related to the m04 structure. In addition, tagged m12 protein employing ATG2 is detected at the cell surface in a type-I TM topology.

In addition, our mining of the MCMV transcriptome by RNA-Seq provided valuable SNP data to identify polymorphisms between MCMV-GFP (Smith strain) and the BAC-derived isolate (MW97.01 strain). Ultimately, a combination of BWZ.NKR-P1 reporter analysis using m02/m145-family transfectants uniquely identified $m12^{Smith}$ as a viral NKR-P1B ligand. To our knowledge, this is the first description of an m02 family member directly engaging an NKR in isolation, in addition to the known m04/MHC-I complexes shown to bind Ly49P/L/D2/W, the m157 interaction with Ly49H/C/I paralogs, and the m144 orphan ligand, presumed to bind an inhibitory NKR (Arase et al., 2002; Berry et al., 2013; Farrell et al., 1997; Kielczewska et al., 2009; Pyzik et al., 2011). In addition, this work has identified m12 as the first natural (viral) ligand for the prototypical NK1.1 antigen, the stimulatory NKR-$P1C^{B6}$ orphan receptor, and host Clr-b as a second "self" ligand for the $NK1.1^{-}$ activating NKR-$P1C^{FVB}$ allele. Whether additional endogenous NK1.1 ligands exist is currently unknown.

The rodent *Klrb1* genes display considerable polymorphism. Previous polymorphism index and sequence analyses have revealed two antigenic and phylogenetic clusters in mice and rats: the NKR-P1A/B/C and NKR-P1F/G clades (Carlyle et al., 2008; Kirkham and Carlyle, 2014; Kveberg et al., 2009). Strikingly, the NKR-P1B and NKR-P1C receptors appear to have undergone parallel divergence characteristic of paired recognition receptors, leading to the hypothesis that they are under selective pressure, within the constraints imposed by both endogenous self ligands and exogenous viral ligands. This is also evident for NKR-P1F and NKR-P1G, which share overlapping self ligands (Clr-d,g), as well as unique self ligands (Clr-c and Clr-f, respectively) (Chen et al., 2011). Divergence at the *Nkrp1b* locus appears to have maintained host Clr-b recognition across mouse strains, while acquiring strain-dependent polymorphisms to avert viral decoy/surrogate ligand immunoevasins. Alternatively, the *Nkrp1c* locus appears to have co-evolved in certain mouse strains to facilitate direct recognition of a viral decoy, while at the same time minimizing host Clr-b ligand recognition, at least within the context of balanced opposition to *Nkrp1b* polymorphisms. Here, we confirm the above hypotheses by demonstrating a direct strain-dependent interaction between m12 and the inhibitory NKR-P1B and stimulatory NKR-P1C (and to some extent, NKR-P1A) receptors, with the stimulatory interactions of lower apparent avidity (at least in a cellular context). These interactions are specific, as they are not observed using the NKR-P1F/G receptors. As mentioned above, these findings are also exciting in terms of historical significance, since they identify a long-anticipated natural ligand of the first NK cell marker in mice, NK1.1, and they also explain how such polymorphisms and alloantigenic reactivity evolved between mouse strains in the first place. This dichotomy in MCMV-encoded ligands for paired NK cell receptors has previously been documented for m157 (recognized by inhibitory Ly49C/I; stimulatory Ly49H), RCTL (inhibitory rNKR-P1B; stimulatory rNKR-P1A), and m04 (inhibitory Ly49A/G2; stimulatory Ly49P/L/D2/W, in the context of certain H-2 haplotypes). Thus, many self-specific inhibitory NKR have been targeted by CMV immunoevasins, which in turn are recognized by paired host stimulatory receptors, with ensuing strain-specific co-evolution over time. It is possible that host strains/alleles exist that more strongly bind m12 via NKR-P1C and not NKR-P1B, much like how Ly49H (*Cmv1*) became a dominant NK cell receptor for MCMV resistance in the B6 strain. Such strains may be difficult to identify, however, as m157 mutants spontaneously arise during Ly49H-mediated selection *in vivo* (Voigt et al., 2003). These findings may also shed light on the

concept of NK cell memory, whereby Ly49H-mediated NK cell memory may be mediated not only by Ly49H:m157 interactions, but rather integrated signals from a number of immunoevasins interacting with both stimulatory and variegated inhibitory NK receptors (Rahim et al., 2016).

Interestingly, m12 from several MCMV strains exhibits reciprocal polymorphism, albeit less drastic than observed for the host *Klrb1b/c* loci. Surprisingly, the laboratory strains (Smith, K181, and MW97.01) do not differ significantly from most wild-derived isolates (WP15B, C4A, C4B, and C4D). In fact, only single amino acid substitutions were found between them (except for an additional V213I substitution in C4B), yet these were sufficient for $m12^{MW97}$ to display a loss-of-function phenotype for NKR-$P1B^{B6}$ recognition. In contrast, the wild-derived $m12^{G4}$ has 26 substitutions relative to $m12^{Smith}$, yet retained NKR-$P1B^{129}$ and NKR-$P1B^{FVB}$ recognition. These SNP also caused variable interactions with NKR-$P1C^{B6,FVB}$, while all m12 variants were recognized by NKR-$P1B^{B6,FVB}$ (although $m12^{G4}$ was severely impacted), yet no m12 alleles interacted with NKR-$P1C^{129}$ (thus, the protein may not be correctly folded at the cell surface due to an otherwise conserved C122S structural residue substitution). These findings may partially underlie the unique susceptibility of the BALB/c and 129S6 strains to MCMV, whereby counterbalancing of NKR-P1B-mediated inhibition via NKR-P1C activation may not occur; in addition, 129 mice possess signaling defects (Taylor et al., 2002).

The results of this study have several implications. First, they strengthen the notion that surface Clr-b is a marker of cellular health or integrity that once compromised, promotes NKR-P1B-mediated "missing-self" NK recognition. This explains why Clr-b is rapidly lost with a short half-life and why $MCMV^{Smith}$ and $RCMV^{English}$ encode NKR-P1B decoy immunoevasins to subvert NK cells early during infection (Aguilar et al., 2015; Voigt et al., 2007). In humans, the NKR-P1A:LLT1 receptor-ligand pair are likely orthologous to some rodent NKR-P1:Clr interaction(s). NKR-P1A (CD161) is inhibitory and variegated, being expressed on ~60% of human NK cells, thus resembling NKR-P1B in function and expression. LLT1 has more restricted expression than Clr-b, and is induced rather than lost in response to PRR agonists and infection (Aguilar et al., 2015; Germain et al., 2011). Whether LLT1 similarly behaves as a rheostat to detect viral infection or cellular stress requires further investigation. Since two rodent CMV have evolved NKR-P1 decoy evasins, HCMV or other DNA viruses (*i.e.*, herpesviruses, poxviruses, etc.) may similarly encode immunoevasins that target the NKR-P1A receptor.

Poxviruses do encode orphan C-type lectin-like gene products; however, none have yet been shown to interact with human NKR-P1A (*KLRB1*), LLT1 (*CLEC2D*), or the related stimulatory NKp80 (*KLRF1*) and NKp65 (*KLRF2*) receptors. In fact, the m02 gene family has only been described in MCMV, although other herpesviruses encode gene products with IgV-like folds. Thus, these findings may have clinical implications in infectious disease, especially since CMV are progressively being considered as vaccine candidates for antigen delivery.

Taken together, this work broadens our understanding of the evolution of the NKR-P1 recognition system in self-nonself discrimination and innate immunity to infectious diseases. It also highlights the resourcefulness of viral evolution to circumvent host recognition.

Chapter 4

The m153 gene product stabilizes expression of the inhibitory NKR-P1B ligand, Clr-b, during murine cytomegalovirus infection

Oscar A. Aguilar, Mir Munir A. Rahim, Isabella S. Sampaio, Jackeline D. Samaniego, Branka Popović, Mulualem E. Tilahun, Astrid Krmpotić, David H. Margulies, David S.J. Allan, Andrew P. Makrigiannis, Stipan Jonjić, James R. Carlyle

Experiments were designed and conducted by O.A.A. with guidance from D.S.J.A, A.P.M., S.J., and J.R.C. *In vivo* experiments were performed by M.M.A.R. with assistance from O.A.A. O.A.A. received assistance with *in vitro* experiments from I.S.S., J.D.S., B.P., and A.K. This project was funded by grants to D.H.M., A.P.M., S.J., and J.R.C.

This work has not been published.

4 MCMV m153 stabilizes host Clr-b expression

4.1 Abstract

Natural killer (NK) cells are a subset of innate lymphoid cells (ILC) capable of recognizing stressed and infected cells through multiple germline-encoded receptor-ligand interactions. Missing-self recognition involves NK cell sensing of the loss of host-encoded inhibitory ligands on target cells, including MHC class I (MHC-I) molecules and other MHC-I-independent ligands. Murine cytomegalovirus (MCMV) infection promotes a rapid loss of the inhibitory NKR-P1B ligand, Clr-b, on infected cells. Here, we provide evidence that an MCMV m145 family member, m153, functions to stabilize cell surface Clr-b during MCMV infection. Ectopic expression of m153 in fibroblasts significantly augments Clr-b cell surface levels. Moreover, infections using *m153*-deficient MCMV mutants (Δm144-m158; Δm153) show an accelerated and exacerbated Clr-b downregulation. Importantly, enhanced loss of Clr-b by MCMV-Δm153 mutants reverted to wild-type levels upon exogenous m153 complementation in fibroblasts. While the effects of m153 on Clr-b levels are independent of *Clec2d* transcription, imaging experiments reveal that the m153 and Clr-b proteins only minimally co-localize within the same subcellular compartments, and tagged versions of the proteins were refractory to co-immunoprecipitation using gentle detergents. Indeed, a prominent intracellular vesicular localization of m153 suggests that its effects on Clr-b stabilization may be indirect. Surprisingly, the MCMV Δm153-mutant possesses enhanced virulence *in vivo*, independent of both Clr-b and NKR-P1B, suggesting that m153 may modulate other Clr or activating NK cell receptor-ligand interactions.

4.2 Introduction

Viruses are known to employ a variety of non-redundant and sometimes complementary immunoevasin strategies to circumvent host innate and adaptive immune recognition. Herpesviruses contain large dsDNA genomes that readily accommodate numerous immunoevasin genes. Cytomegaloviruses (CMV) are a family of β-herpesviruses with strict species specificity that have intimately co-evolved with their hosts, and as such, have evolved various mechanisms to subvert detection or evade immune effector mechanisms. These viruses

contain ~200 open reading frames (ORF), ~70 of which are conserved core genes, plus numerous genes that are dispensable for replication and thought to alter the host response to the virus (Rawlinson et al., 1996).

Murine cytomegalovirus (MCMV) has been used as a rodent model to study human CMV (HCMV) infection and immune sequelae, as both viruses display similar cellular tropism and pathogenesis. These viruses are well tolerated in immune-competent hosts, where they usually establish chronic or latent infections, but they can also cause congenital defects in newborns, and severe pathologies in immunocompromised individuals, such as cancer patients undergoing chemotherapy, transplant patients, individuals with congenital immunodeficiencies, or AIDS patients (Griffiths et al., 2015; Krmpotic et al., 2003). Both viruses also employ structurally divergent yet evolutionarily convergent mechanisms to evade immune recognition. For this reason, the study of individual MCMV immunoevasin gene products has been used to infer similar functionality of HCMV genes, although each virus does employ some unique mechanisms.

MHC-independent receptor-ligand interactions have also been shown to play a role in CMV detection. The NKR-P1 receptor family recognizes genetically linked C-type lectin-related (Clr) ligands, and consists of five members in mice, including three stimulatory isoforms (NKR-P1A/C/F) and two inhibitory isoforms (NKR-P1B/G), where NKR-P1D represents an NKR-$P1B^{B6}$ allele, and NKR-P1E is a pseudogene, at least in some inbred strains (Kirkham and Carlyle, 2014). Using reporter cell assays, it has been shown that mouse NKR-P1F recognizes Clr-c/d/g, NKR-P1G recognizes Clr-d/f/g, and NKR-P1B/D recognize Clr-b (Carlyle et al., 2004; Chen et al., 2011; Iizuka et al., 2003). While NKR-P1A/C remain orphan receptors, they likely recognize foreign viral and/or host induced-self ligands. Importantly, Clr-b has been shown to represent a marker of healthy cells that is commonly lost or downregulated during cellular pathologies. As such, the NKR-P1B:Clr-b axis has been shown to play a role in missing-self recognition in tumour immunosurveillance, transplantation, genotoxic and cellular stress, and viral (poxvirus and cytomegalovirus) infection (Aguilar et al., 2015; Carlyle et al., 2004; Chen et al., 2015; Fine et al., 2010; Rahim et al., 2015; Voigt et al., 2007; Williams et al., 2012). Moreover, RCMV encodes a Clr-like gene product, RCTL, which targets rat NKR-P1B to subvert NK cell-mediated innate immunity (Voigt et al., 2007).

To extend this work, we investigated whether MCMV, in addition to RCMV, also targets the NKR-P1:Clr recognition system. Here, we show that MCMV stabilizes Clr-b expression on infected cells. These effects were attributed to expression of an m145 family member, m153. Expression of m153 in mouse fibroblasts augmented Clr-b expression, whereas infection using m153-deficient viruses (Δm144-m158; Δm153) resulted in accelerated and more substantial Clr-b loss. However, it remains unclear how m153 directly or indirectly interacts with Clr-b, whether it also targets another Clr family member, or if it interacts with other host proteins. Notably, m153 tetramers identify a candidate receptor on dendritic cells (DC) and a subset of mouse ILC. Finally, using wild-type (WT) B6, B6.*Nkrp1b*$^{-/-}$, and B6.*Clr-b*$^{-/-}$ mice, we demonstate that the *in vivo* function of m153 is NKR-P1B/Clr-b-independent and that the immunoevasin negatively affects MCMV virulence in B6 mice, possibly via interaction with an activating NKR.

4.3 Materials and Methods

4.3.1 Animals

C57BL/6 mice were obtained from Jackson laboratories. B6.*Clr-b*$^{-/-}$ mice were provided by Dr. M.T. Gillespie (Monash University, Australia) (Chen et al., 2015; Kartsogiannis et al., 2008). B6.*Nkrp1b*$^{-/-}$ mice were generated as described previously (Rahim et al., 2015). All animals were maintained in accordance with approved animal care protocols at Sunnybrook Research Institute or the University of Ottawa.

4.3.2 Cells and Viruses

Mouse embryonic fibroblasts (NIH3T3) were obtained from the ATCC. Human embryonic kidney cells (HEK293T) were obtained from Dr. D.H. Raulet (University of California, Berkeley, CA). C57BL/6 mouse embryonic fibroblasts (MEF) were provided by Dr. T.W. Mak (University of Toronto, Canada). Cells were cultured in complete DMEM-HG, supplemented with 2 mM glutamine, 100 U/ml penicillin, 100 μg/ml streptomycin, 50 μg/ml gentamicin, 110 μg/ml sodium pyruvate, 50 μM 2-mercaptoethanol, 10 mM HEPES, and 10% FBS.

MCMV-MW97.01 (WT) isolate was generated using BAC-technology of a cloned MCMV-Smith genome (Wagner et al., 1999). The MCMV-Δ1 and -Δ6 viruses were generated as described previously. The m153-deficient MCMV virus (Δm153) was constructed by removing

the m153 gene using ET-cloning from the full-length MCMV BAC pSM3fr (Wagner and Koszinowski, 2004). All viruses were passaged and titered using MEF cells as described (Brune et al., 2001). Unless otherwise noted, all MCMV infections were done by exposing cells to 0.5 PFU/cell followed by centrifugal enhancement at 800 *g* for 30 mins.

4.3.3 Generation of Dox-Inducible Cell Lines

The pTRIPZ-Empty vector was generated by inserting the multiple cloning site from pEGFP-N1 (AgeI to XhoI; Clontech) and placing it into the parental pTRIPZ lentiviral vector (Thermo Scientific) that was digested with AgeI and XhoI. Similarly, the pTRIPZ-m153$^{N\text{-}HA}$ vector was constructed by PCR amplification of the m153$^{N\text{-}HA}$ cDNA using 5'-AgeI and 3'-XhoI primers and subcloning into the digested pTRIPZ vector. Likewise, the pTRIPZ-Clr-b$^{C\text{-}FLAG}$ was synthesized by a similar approach using the Clr-b cDNA. All PCR primers are listed in **Appendix 4.1**. These vectors were triple transfected into HEK293T cells with packaging vectors (8.2VPR + VSV-G env) to generate lentiviral supernatants, which were then used to transduce NIH3T3 fibroblasts. Transduced cells were selected using media containing 2.5 μg/ml puromycin (Sigma-Aldrich).

4.3.4 Flow Cytometry and Antibodies

Cells were stained in flow buffer (HBSS, 0.5% BSA and 0.03% NaN_3) on ice with primary monoclonal antibodies (mAb) for 25-30 min, or secondary streptavidin (SA) conjugates for 15-20 min, washed, then analyzed using a FACSCalibur flow cytometer (BD Biosciences). Live cells were gated using propidium iodide exclusion. Data were analyzed using FlowJo software (Treestar). Biotinylated Clr-b mAb (4A6; rat IgM) was described previously (Carlyle et al., 2004). Anti-m153 mAb (clone m153.16) was provided by Dr. Stipan Jonjić and has been previously described (Mans et al., 2007). Biotin-conjugated H-2D^{q}L^q mAb (KH117, mouse IgG2a) was purchased from BD Pharmingen, purified pan-Rae1 mAb (186107, rat IgG2a) was purchased from R&D Systems, SA-APC was purchased from Thermo Fisher Scientific. Anti-FLAG (M2 mAb) was purchased from Sigma-Aldrich and anti-HA (C29F4 mAb) was purchased from Cell Signaling Technologies.

4.3.5 RNA Isolation, Cloning and qRT-PCR

Total RNA isolation was performed using total RNA isolation kit (Norgen Biotek), then quantitated (Nanodrop) and assessed for integrity on a 1% agarose gel using EtBr. First strand cDNA synthesis was accomplished using the Superscript III kit (Life Technologies). Cloning of MCMV-encoded genes was performed using cDNA from MCMV-infected NIH3T3 cells, Q5 PCR kit (NEB), and gene-specific primers (**Appendix 3.3** and **Appendix 4.1**), followed by cloning into the pIRES2-EGFP vector (Clontech). Quantitative real-time RT-PCR (qRT-PCR) was performed on a CFX-96 System (BioRad) using 20-50 ng of cDNA, PerfeCTa mix (Quanta), and gene-specific primers designed using Primer-Blast (www.ncbi.nlm.nih.gov/tools/primer-blast). Data was analyzed using CFX Manager software (BioRad).

4.3.6 Immunoprecipitation, Western blot, and Immunofluorescence

Immunoprecipitations (IP) were performed by transfecting NIH3T3.Clr-b$^{C\text{-}FLAG}$ cells with pIRES2-EGFP vector containing either m153$^{N\text{-}HA}$ or empty control followed by addition of lysis buffer (0.5% NP-40, 50 mM Tris-HCl, 150 mM NaCl, 10% glycerol), centrifugation to remove cell debris, pre-clearing of lysates, and immunoprecipitation using specific antibodies bound to protein A/G beads. Following IP, lysates were incubated with 2X Laemmli buffer, boiled, run on SDS-PAGE gels and transferred to PVDF membranes (Millipore) for immunoblotting using FLAG-HRP or HA-HRP mAb conjugates (Cell Signal Technologies).

Immunofluorescence experiments were performed by transfection of NIH3T3 fibroblasts (grown on poly-L-lysine treated coverslips) with pEGFP-N1/C1 or pmCherry-N1/C1 vectors (Clontech) containing Clr-b or m153 fused in-frame with either EGFP or mCherry. Briefly, since m153 is a type I transmembrane protein it was cloned N-terminally relative to fluorophore whereas Clr-b, being a type II transmembrane protein was cloned C-terminally relative to fluorophore. After 48 hours, cells were fixed, stained with DAPI, mounted onto microscope slides, and imaged for fluorescence using an Axiovert 200M wide-field fluorescence microscope (Zeiss).

4.3.7 BWZ Reporter Cell Assays

BWZ.CD3ζ/NKR-P1B reporter cells were generated as previously described (Chen et al., 2011). BWZ assays were performed by co-culturing stimulator cells in 3-fold dilutions with reporter cells (5x10^4/well) in 96-well flat-bottom plates overnight at 37°C. Positive control cells

were incubated with 10 ng/ml PMA plus 0.5 μM ionomycin. Cells were subsequently washed using PBS, and resuspended in 100 μl of 1X CPRG buffer (90 mg/L chlorophenol-red-β-D-galactopyranoside (Roche), 9 mM $MgCl_2$, 0.1% NP-40, in PBS), incubated at room temperature, and analyzed using a Varioskan microplate reader (Thermo Scientific) using absorbance readings of $OD_{595\text{-}655}$.

4.3.8 Chromium Release Assays

Cytotoxicity assays were performed as previously described (Chen et al., 2015). B6 Splenic lymphokine activated killer (LAK) effector cells were cultured in 10% complete RPMI 1640 supplemented with 2,500 U/ml human rIL-2 (Proleukin; Novartis). On day 4, these cells were FACS sorted for $CD3^{-}NKp46^{+}$ and further sorted for NKR-$P1B^{+/-}$ expression and used as effectors in ^{51}Cr-release assays on day 7. Target cells were incubated with 50 μCi $Na_2{}^{51}CrO_4$ (PerkinElmer) in FBS at 37ºC for 1 hr, washed, plated in V-bottom plated in combination with serially diluted effectors, and incubated for 4 hrs at 37ºC. Supernatants (100 μl) were transferred to LumaPlate-96 scintillation plates (PerkinElmer), dried, and counted using Top Count NXT Microplate Scintillation Counter (Packard Instrument Company). Percent specific lysis values were calculated relative to maximum release (2% Triton X-100) and spontaneous release (media) values.

4.3.9 Statistical Analysis

All data were analyzed using Prism 5 (GraphPad), employing either a paired Student's two-tailed *t*-test, or one/two-way ANOVA analysis applying Bonferroni's post-hoc tests (see figure legends). Graphs show mean values ± SEM; *$p<0.05$, **$p<0.01$, ***$p<0.001$. Data are representative of at least 3 independent experiments.

4.4 Results

4.4.1 An MCMV m145 family member stabilizes Clr-b expression during MCMV infection

We have previously demonstrated that MCMV infection promotes a rapid loss of the inhibitory NKR-P1B ligand, Clr-b, on mouse fibroblasts (Aguilar et al., 2015). In addition, a Clr-

b-independent NKR-P1B-ligand was also found to be induced during MCMV infection, subsequently identified as the MCMV m12 IgV-like decoy ligand (Aguilar et al., 2017), which is similar in function to the Clr-like immunoevasin (RCTL) encoded by RCMV (Voigt et al., 2007). In an attempt to uncover the MCMV gene product(s) responsible for Clr regulation, we utilized two MCMV regional genomic deletion mutants (MCMV-Δ1, Δm02-m16; MCMV-Δ6, Δm144-m158) to compare their phenotypes relative to the wild-type (WT) $MCMV^{MW97}$ parental strain. Interestingly, all three viruses promoted loss of Clr-b expression on infected NIH3T3 fibroblasts, yet a more pronounced Clr-b downregulation was consistently observed using the MCMV-Δ6 virus, which is missing most of the m145 gene family (Δm144-m158) (**Fig. 4.1A,B**). In contrast, the MCMV-Δ1 mutant lacking the m02 gene family and several other genes (Δm02-m16) yielded a phenotype similar to WT $MCMV^{MW97}$ (**Fig. 4.1A,B**). The difference in magnitude of Clr-b downregulation promoted by the MCMV-Δ6 virus was statistically significant upon analysis of both cell surface Clr-b median fluorescence intensity (MFI; **Fig. 4.1C**), as well as the percentage of cells that had fully lost Clr-b surface protein (%Clr-b^{-}, **Fig. 4.1D**).

As controls, we also investigated MHC-I (H-$2D^{q}L^{q}$) and NKG2D-ligand (pan-Rae-1α-ε family) cell surface expression on infected NIH3T3 fibroblasts. Notably, the MCMV-Δ1 mutant was partially deficient in MHC-I downregulation (likely due to the loss of m06), while the MCMV-Δ6 mutant was surprisingly more efficient at promoting MHC-I loss (despite the loss of m152; **Fig. 4.2A,B**), suggestive of an additional gene in this region that modulates MHC-I expression, or an effect unique to NIH3T3 cells or the H-2^{q} haplotype. On the other hand, the MCMV-Δ1 virus maintained its ability to internalize Rae-1 family proteins, as expected, while the MCMV-Δ6 virus further upregulated Rae-1 ligands (likely due to loss of m152; **Fig. 4.2A,C**). To determine the temporal stage of MCMV infection underlying these differences, we infected NIH3T3 fibroblasts over an extended time course, and observed that the MCMV-Δ6 virus promoted both a more rapid and exacerbated loss of Clr-b expression, detectable as early as 12 hours post-infection (**Fig. 4.3**). These results suggest that a gene in the m144-m158 region counteracts MCMV infection-mediated Clr-b loss, akin to the positive regulation of MHC-I surface expression by the m04 glycoprotein, which antagonizes the functions of m06 and m152 for certain MHC-I alleles (Kleijnen et al., 1997).

Figure 4.1

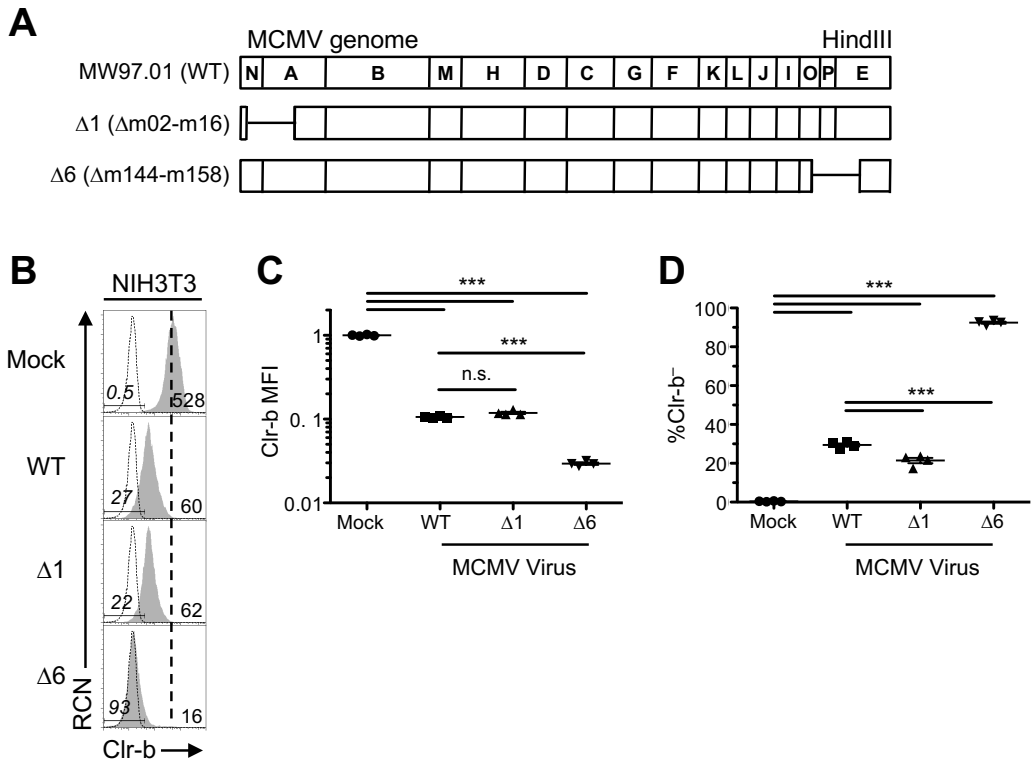

Figure 4.1. Infection with MCMV deficient in m145 family members reveals Clr-b modulation. (**A**) MCMV genomic map demonstrating location of missing genes in the mutant MCMV viruses (Δ1 and Δ6). Labels correspond to the HindIII digestion map. NIH3T3 fibroblasts were infected with WT MCMV (MW97.01), Δ1 (Δm02-m16) or Δ6 (Δm144-m158) mutants at an MOI of 0.5 PFU/cell, and analyzed by flow cytometry 24 hours post infection. (**B**) Representative histograms of Clr-b surface expression. Numbers on the right represent mean fluorescence intensity whereas the ones on the left represent the %Clr-b^{-}. Shaded histogram shows sample stain whereas dotted histogram represents unstained sample. Vertical dotted line symbolizes mock MFI levels. (**C**) Quantitation of Clr-b MFI and (**D**) quantitation of %Clr-b^{-}. Data was analyzed using 1-way ANOVA and are representative of 3 independent experiments.

Figure 4.2

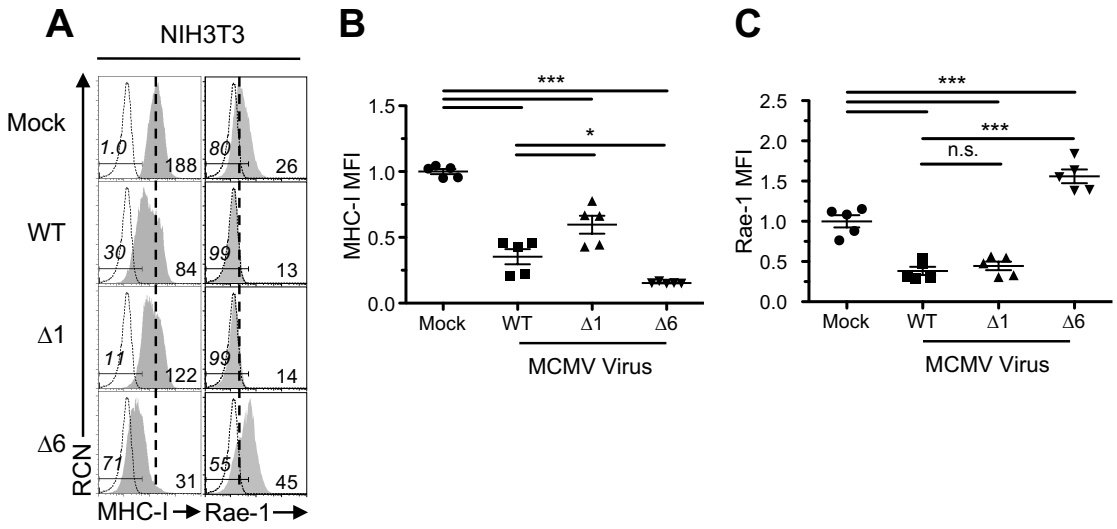

Figure 4.2. Modulation of MHC-I and Rae-1 cell surface expression upon infection with MCMV mutant viruses. NIH3T3 fibroblasts were infected with MCMV viruses (WT, Δ1, or Δ6; MOI = 0.5 PFU/cell), and analyzed for cell surface expression. 24 hours post infection. (**A**) Representative histograms of MHC-I (H-2D^{q}L^{q}; left) and Rae-1 (α–ε; right). (**B**) Quantitation of MHC-I expression. (**C**) Quantitation of Rae-1 expression. Data were analyzed using 1-way ANOVA and are representative of 3 independent experiments.

Figure 4.3

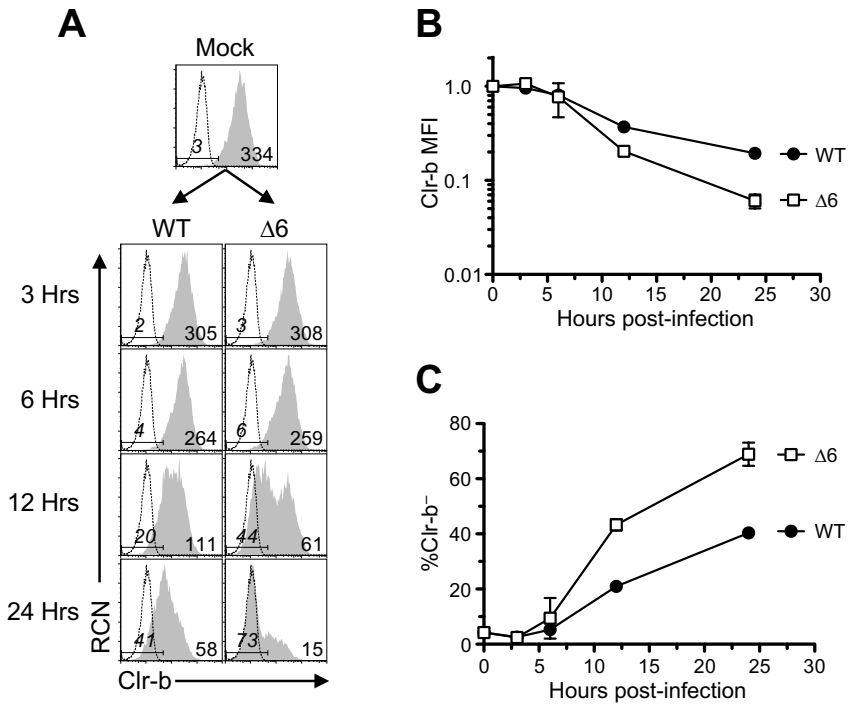

Figure 4.3. MCMV infection with MCMV-Δ6 virus reveals a more pronounced Clr-b downregulation at early time points of infection. NIH3T3 fibroblasts were infected with WT MCMV or D6 mutant at an MOI of 0.5 PFU/cell and analyzed by flow cytometry at different time points within a 24 hours infection timecourse. (**A**) Representative histograms of Clr-b surface expression. Vertical dotted line symbolizes mock MFI. (**B**) Quantitation of Clr-b MFI and (**D**) quantitation of %Clr-b$^-$ of values in **A**. Data are representative of 3 independent experiments.

4.4.2 The m153 glycoprotein sustains Clr-b cell surface expression

In order to identify candidate MCMV genes responsible for Clr-b modulation, we cloned and overexpressed individual MCMV cDNA gene products (in the pIRES2-EGFP reporter vector) and assessed their effects on cell surface Clr-b levels. To this end, we tested the majority of the m145 family members in the *m144-m158* region (m145, m146, m150, m151, m152, m153, m154, m155, m157, and m158), in addition to m144 (which has been shown to negatively modulate NK cell function (Farrell et al., 1997)), m159, and m17 (a distal m145 family member). Notably, these MCMV gene products are all related and are predicted to form MHC-I-like folds (Smith et al., 2002), with m144 and m159 being more divergent from the m145 family, based on ClustalW analysis (**Fig. 4.4A**). Following transfection of these candidate genes into NIH3T3 fibroblasts, expression of surface Clr-b, MHC-I, and pan-Rae-1 levels were assessed by flow cytometry, using IRES-EGFP fluorescence as a marker for transfected cells (**Fig. 4.4B,C**). Interestingly, m153 was the sole gene product found to increase Clr-b cell surface expression, and although modest, this effect was reproducible and statistically significant (**Fig. 4.4B,C**). In contrast, the empty vector and other candidate gene products promoted a slight Clr-b downregulation at high GFP levels, an effect that may be due to innate recognition of high levels of cytosolic pDNA or induction of cellular stress (**Fig. 4.4B**). Importantly, none of the m02 family members appeared to modulate Clr-b expression (**Fig. 4.5**). As previously described, we observed that m152 altered MHC-I and Rae-1 expression (**Fig. 4.6A,B**). Therefore, the m153 gene product is likely responsible for sustaining Clr-b levels following infection by WT $MCMV^{MW97}$, an effect lost upon infection using MCMV-Δ6 mutant virus, which lacks m153.

To confirm this, we extended analysis using an m153-deficient MCMV mutant (Δm153). Upon infection of mouse NIH3T3 fibroblasts at different multiplicities of infection (MOI) and comparison to WT MCMV, the Δm153 and MCMV-Δ6 mutant viruses were found to promote exacerbated yet overlapping levels of Clr-b downregulation (**Fig. 4.7A**). Furthermore, the extent of Clr-b loss correlated well with viral MOI, revealing greater Clr-b downregulation (MFI) and increased percentages of cells completely lacking Clr-b expression (%Clr-b^{-}) at higher MOI (**Fig. 4.7B,C**). Quantitative qRT-PCR analysis of *m153* mRNA levels revealed that m153 expression peaked during the early phase of infection (around 3-6 hours), and thus represents an early (E, β) gene (**Fig. 4.7D**). As controls, MHC-I and Rae-1 levels were found to remain

Figure 4.4

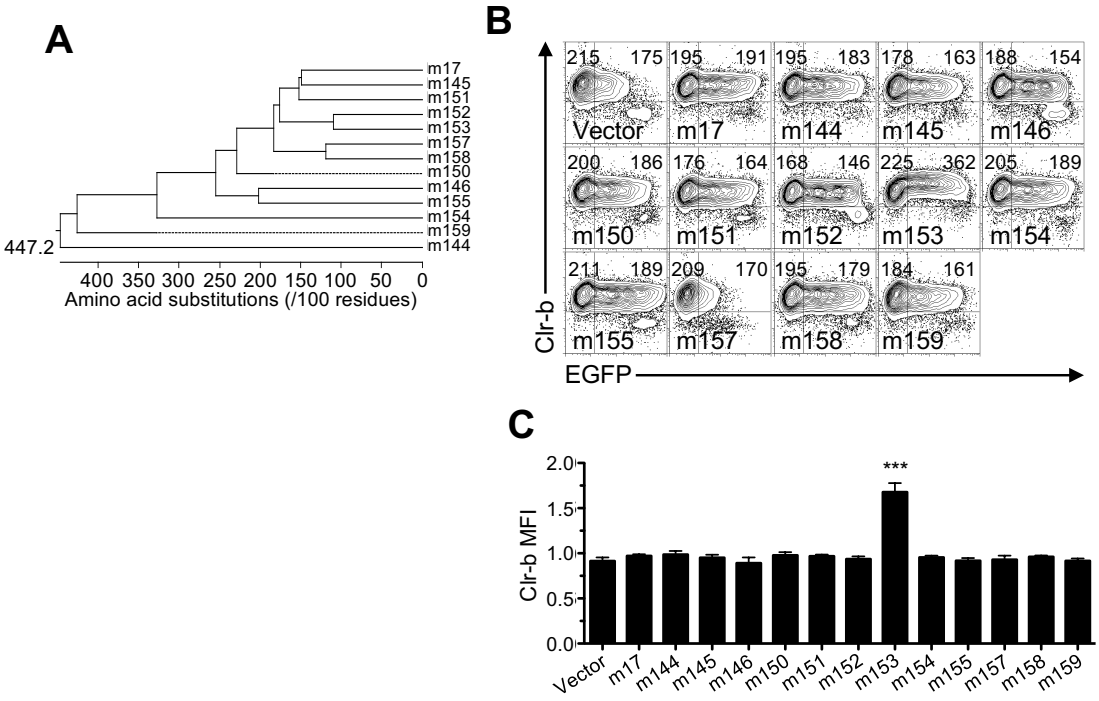

Figure 4.4. Ectopic expression of m153 in mouse fibroblasts increases cell surface Clr-b. (**A**) Analysis of the m145 family amino acid sequences using ClustalW. (**B**) NIH3T3 cells were transfected with MCMV MHC-I-like ORFs and analyzed for Clr-b cell surface expression 48 hours post-transfection. Numbers on the left and right represent MFI values of GFP^- and GFP^+ populations, respectively. (**C**) Quantitations of expression of cell surface markers in **B**. Data was analyzed using 1-way ANOVA and are representative of 3 independent experiments.

Figure 4.5

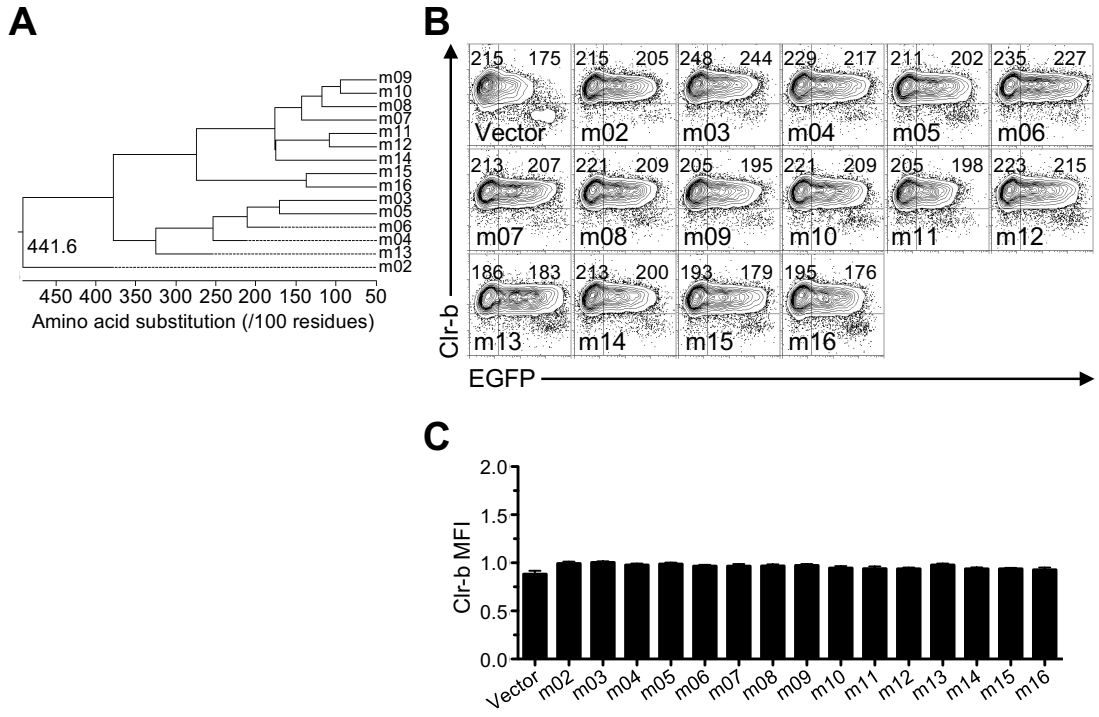

Figure 4.5. Ectopic expression of m02 family of immunoevasins does not affect Clr-b expression. (**A**) Analysis of the m02 family amino acid sequences using ClustalW. (**B**) NIH3T3 cells were transfected with m02 ORFs and analyzed for Clr-b cell surface expression 48 hours post-transfection. Numbers on the left and right represent MFI values of GFP^- and GFP^+ populations, respectively. (**C**) Quantitations of expression of cell surface markers in **B**. Data was analyzed using 1-way ANOVA and are representative of 3 independent experiments.

Figure 4.6

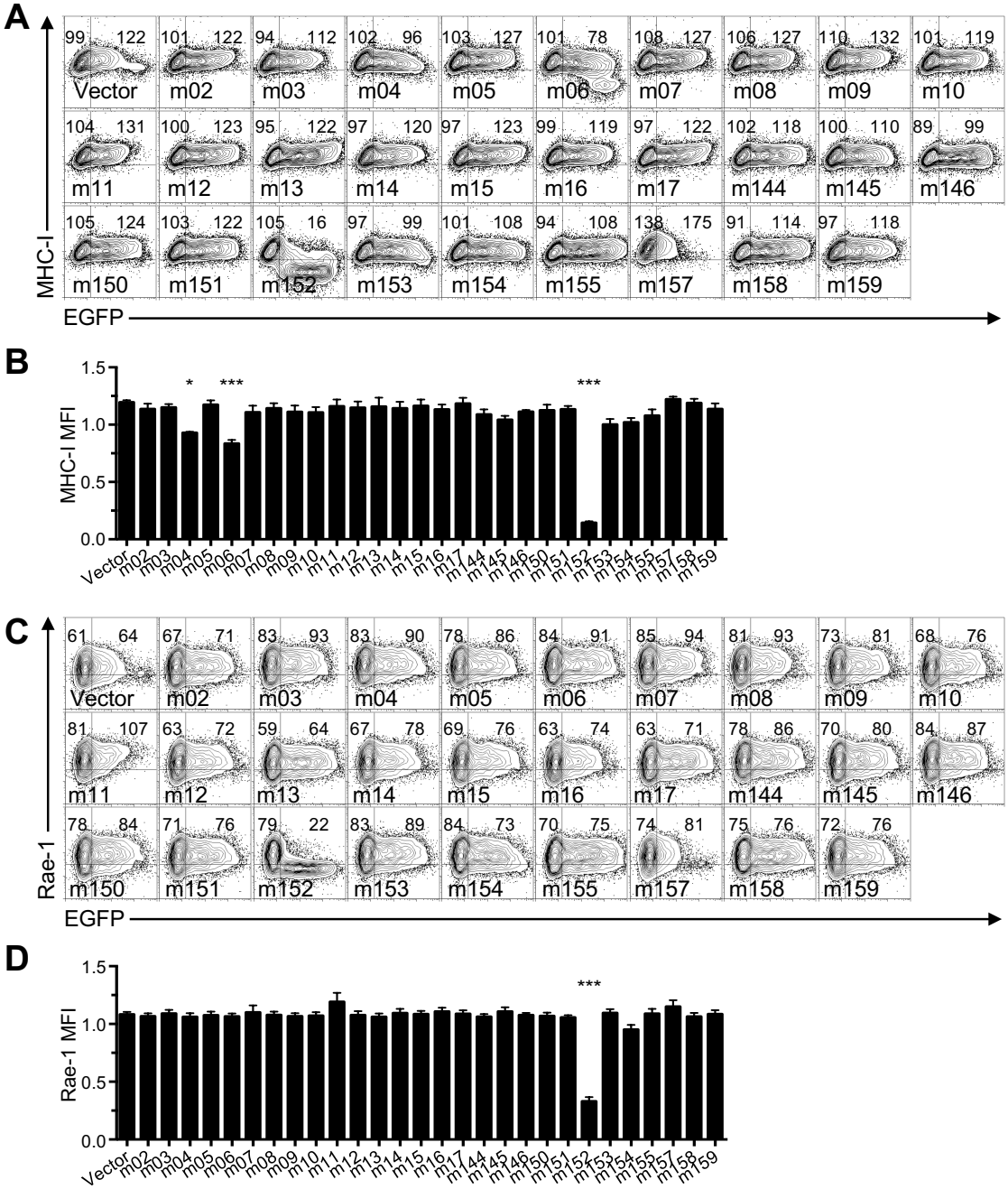

Figure 4.6. Ectopic expression of m02 and m145 family members confirms effects of certain immunoevasins on MHC-I and Rae-1 expression. (**A**) Representative flow plots of MHC-I expression upon transfection. (**B**) Quantitation of (A). (**C**) Represenative flow plots of Rae-1 expression. (**D**) Quantitations of (C). All data are representative of at least 3 independent experiments and were analyzed using 1-way ANOVA.

Figure 4.7

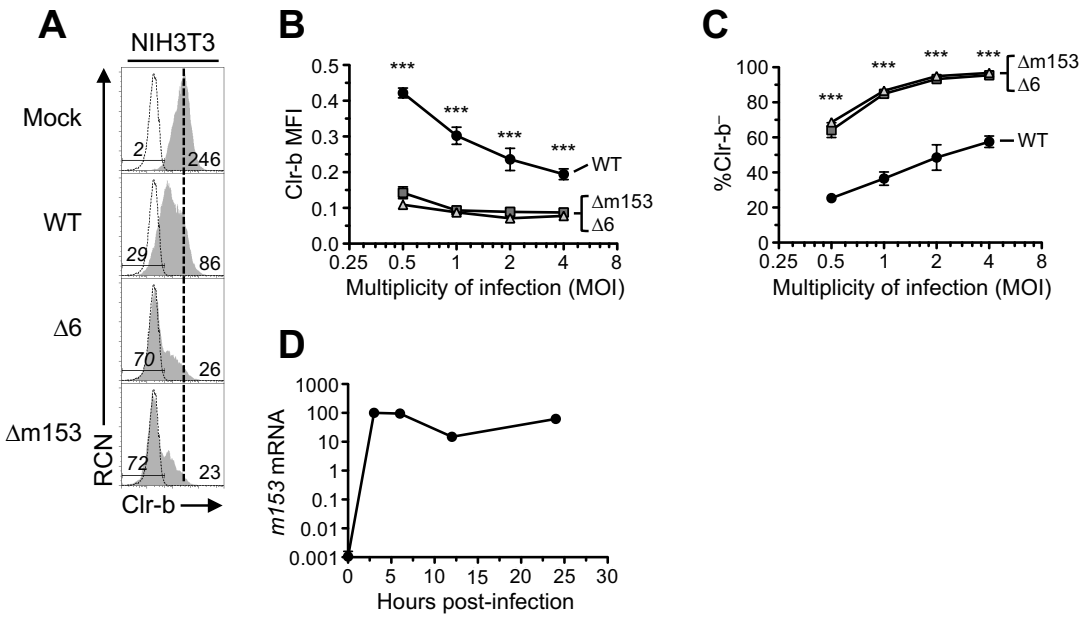

Figure 4.7. Infections with MCMV deficient in m153 recapitulates Clr-b phenotype observed with Δ6 virus. NIH3T3 cells were infected with MCMV viruses (WT, Δ6, or Δm153) at different MOI and assessed for cell surface Clr-b expression by flow cytometry 24 hours post infection. (**A**) Histograms showing Clr-b expression at the different MOIs. Numbers of the right show MFI, whereas the ones on the left show the %Clr-b^{-} cells, according to gate. Vertical dotted line symbolizes mock MFI. (**B**) Quantitation of Clr-b MFI. (**C**) Quantitation of %Clr-b^{-} cells. (**D**) Transcript levels of m153 measured during timecourse of MCMV infection. Data was analyzed using 2-way ANOVA and are representative of 3 independent experiments.

unaltered upon Δm153 infection (**Fig. 4.8**). These data demonstrate that m153 selectively sustains cell surface Clr-b levels during MCMV infection.

4.4.3 Exogenous m153 complementation upon MCMV-Δm153 infection rescues Clr-b levels

To further determine the effects of m153 expression on Clr-b levels, we generated stable NIH3T3 transductants possessing Tet (Dox)-inducible m153 expression. To monitor cell surface m153 levels, we cloned the m153 cDNA with an N-terminal HA-tag ($m153^{HA}$) into a modified pTRIPZ Tet-On lentiviral vector and used this construct to stably transduce NIH3T3 fibroblasts. Interestingly, in comparison to control cells transduced using the empty vector (NIH3T3.Empty), transductants expressing m153 (NIH3T3.$m153^{HA}$) constitutively expressed higher basal levels of cell surface Clr-b, even in the absence of doxycycline (Dox) treatment (**Fig. 4.9A,B**, ~2.3-fold increase). This effect was likely due to leaky $m153^{HA}$ expression by the minimal Tet-On promoter, since we could detect $m153^{HA}$ transcripts and cell surface staining (by both HA-tag and a new m153 mAb) in the absence of Dox treatment (**Fig. 4.10**). In addition, NIH3T3 cells transduced with the parental pTRIPZ vector revealed leaky RFP reporter expression in the absence of Dox induction. However, in agreement with the lack of an observed diagonal correlation between Clr-b and EGFP levels in m153 transient transfection assays (**Fig. 4.4B**), we observed no further increase in Clr-b expression in stable NIH3T3.$m153^{HA}$ transductants upon titrated Dox treatment. In contrast, HA-tag expression increased dramatically at the cell surface of NIH3T3.$m153^{HA}$ transductants upon titrated Dox induction, demonstrating that the $m153^{HA}$ protein was strongly induced (**Fig. 4.10**). Taken together, these findings suggest that low levels of m153 protein are sufficient to increase Clr-b cell surface expression.

To determine if low-level m153 expression was sufficient to exogenously complement and stabilize Clr-b levels following infection with the MCMV-Δm153 and MCMV-Δ6 mutants, we infected NIH3T3.$m153^{HA}$ and control NIH3T3.Empty transductants and compared Clr-b levels to cells infected with WT $MCMV^{MW97}$. As expected, infections at different MOI revealed that NIH3T3.Empty transductants behaved similarly to parental NIH3T3 cells, in that MCMV-Δm153 and MCMV-Δ6 mutants had a more pronounced Clr-b loss relative to WT MCMV infection, as determined by both Clr-b MFI levels (**Fig. 4.9C**) and %Clr-b^- cells (**Fig. 4.9D**). In

Figure 4.8

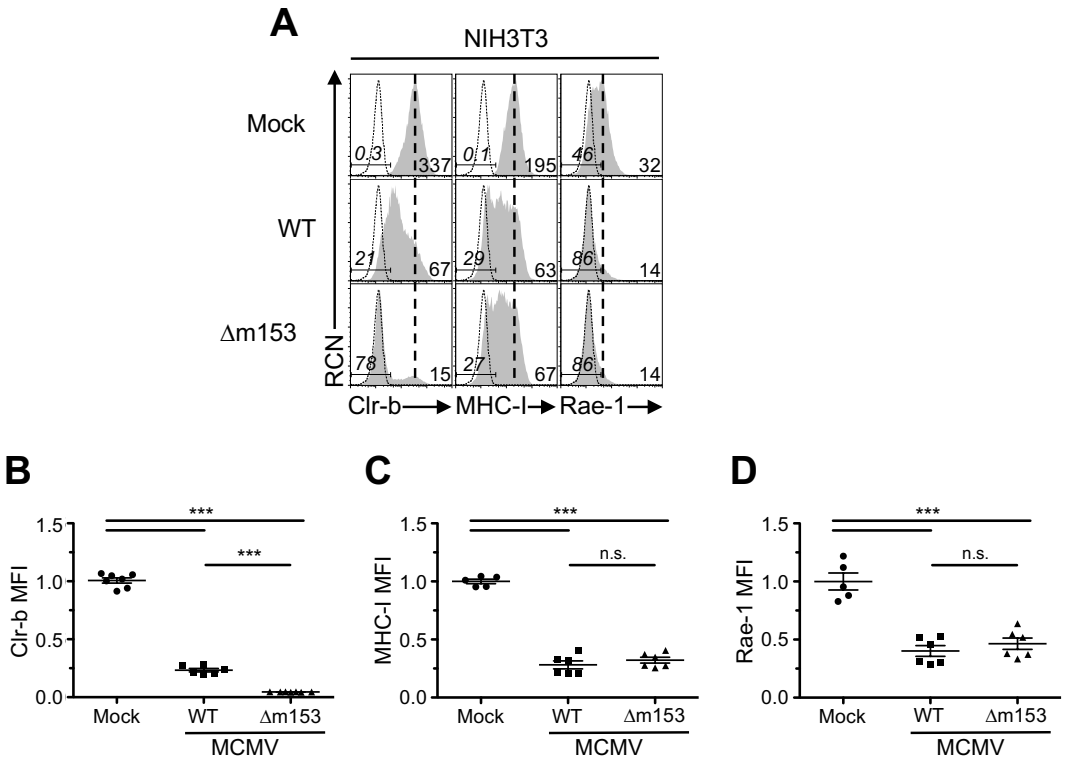

Figure 4.8. Infection with MCMV Δm153 virus does not alter MHC-I or Rae-1 expression. NIH3T3 fibroblasts were infected with WT MCMV or Δm153 mutant at an MOI of 0.5 PFU/cell and analyzed by flow cytometry 24 hours later. (**A**) Histograms of cell surface expression of Clr-b (left), MHC-I (middle), and Rae-1 (right). Vertical dotted line symbolizes mock MFI, whereas numbers on the left represent the %marker⁻ cells in gate, and numbers on the right represent MFI values. Quantitations of cell surface levels of (**B**) Clr-b, (**C**) MHC-I, and (**D**) Rae-1 expression. Data was analyzed using 1-way ANOVA and are representative of 3 independent experiments

Figure 4.9

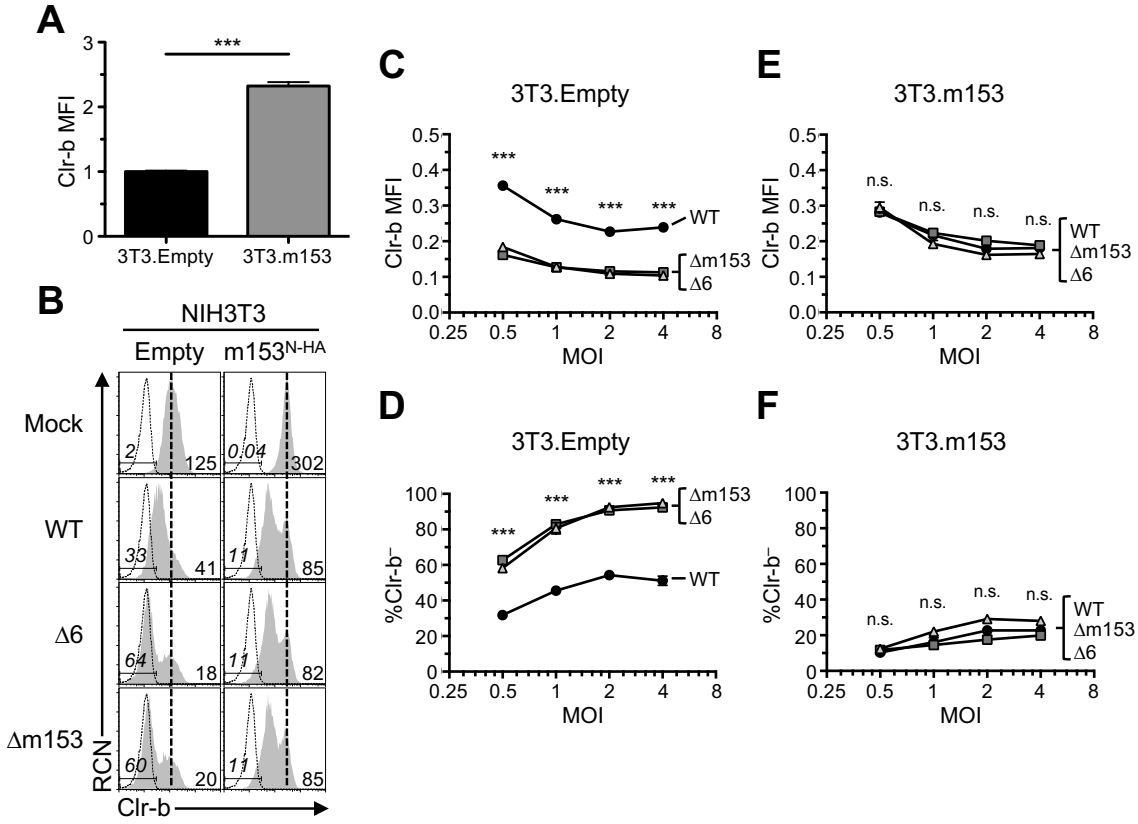

Figure 4.9. Complementation of m153 abrogates Clr-b loss observed in Δm153 virus. NIH3T3 cells were transduced with pTRIPZ lentivirus expressing m153 or empty vector and infected with MCMV viruses. (**A**) Comparison of the Clr-b expression on resting cell. (**B**) Histograms of Clr-b levels on NIH3T3.Empty (left) and NIH3T3.m153 fibroblasts (right) upon infection with MCMV viruses (WT, Δ6, or Δm153). Numbers of the right show MFI, whereas the ones on the left show the %Clr-b^{-} cells, according to gate. Vertical dotted line symbolizes mock MFI. Analysis of NIH3T3.Empty cells by (**C**) quantitation of Clr-b MFI and (**D**) quantitation of %Clr-b^{-} cells at different MOI. Analysis of NIH3T3.m153$^{N\text{-}HA}$ cells by (**E**) quantitation of Clr-b MFI and (**F**) quantitation of %Clr-b^{-} cells at different MOI. Data was analyzed using 2-way ANOVA and are representative of 3 independent experiments.

Figure 4.10

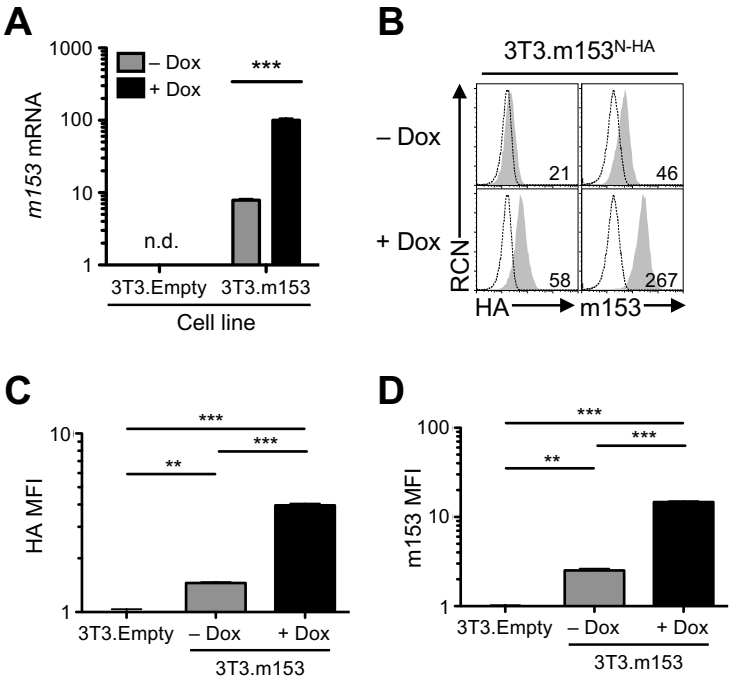

Figure 4.10. Leaky expression of m153 in pTRIPZ transduced NIH3T3.m153$^{N\text{-}HA}$ cells. (**A**) *m153* transcripts in NIH3T3.m153$^{N\text{-}HA}$ cells in the presence and absence of dox, with NIH3T3.Empty as controls. (**B**) Cell surface expression of m153 by detection using α-HA (left) and α-m153 (right). Shaded histogram shows sample stain whereas dotted histogram represents NIH3T3.Empty negative controls. Numbers in the right show the MFI values. Quantitations using (**C**) HA and (**D**) m153 stains. Data were analyzed using 1-way ANOVA and are representative of 3 independent experiments.

contrast, NIH3T3.m153^{HA} transductants uniformly expressed similar Clr-b levels regardless of infection using the WT MCMV^{MW97}, MCMV-Δm153, or MCMV-Δ6 mutants, across all MOI tested (**Fig. 4.9E,F**). Similar results were also observed in the presence of Dox treatment. These data confirm that the presence of m153 stabilizes Clr-b expression and antagonizes MCMV infection-mediated Clr-b downregulation.

4.4.4 m153 may stabilize Clr-b surface levels by an indirect mechanism

Collectively, the above findings suggest that m153 sustains Clr-b surface protein expression in a non-linear manner. To gain insight into the mechanism, we first assessed whether transcriptional regulation was involved. Here, we measured Clr-b (*Clec2d*) transcript levels during MCMV infection with WT MCMV^{MW97} or MCMV-Δm153, and observed similar losses of Clr-b mRNA following infection (**Fig. 4.11A**). We also observed similar steady-state *Clec2d* mRNA levels in stable NIH3T3.m153^{HA} and control NIH3T3.Empty transductants, both in the absence and presence of Dox induction (**Fig. 4.11B**). These findings demonstrate that m153 does not modulate Clr-b at the transcript level.

Since both MHC-I molecules and NKG2D-ligands are targeted by multiple non-redundant MCMV gene products, most of which involve direct interactions, and both Clr-b and m153 can be expressed at the cell surface, we tested whether m153 may stabilize Clr-b expression by a direct mechanism. Since previous attempts to immunoprecipitate (IP) Clr-b protein using 4A6 mAb (rat IgMκ) have been unsuccessful, we generated stable NIH3T3 transductants that expressed a Clr-b cDNA with a C-terminal FLAG-tag (NIH3T3.Clr-b^{FLAG}) using the inducible pTRIPZ lentiviral vector. Using these cells, Clr-b^{FLAG} protein could be visualized upon FLAG-tag immunoprecipitation (IP) followed by anti-FLAG Western blot (WB) upon Dox induction (**Fig. 4.11C**, left lanes). Therefore, we next transiently co-transfected these cells with the m153^{HA} construct, or control Empty vector, to determine if IP for Clr-b^{FLAG} could co-IP m153^{HA}. However, FLAG-tag IP followed by anti-HA WB failed to detect any m153^{HA} protein, even though HA-tag IP followed by anti-HA WB of the same cells was able to detect m153^{HA} (**Fig. 4.11D**). Reciprocally, HA-tag IP followed by anti-FLAG WB failed to detect any Clr-b^{FLAG} protein (**Fig. 4.11C**, right lanes). These results suggest that either the two proteins do not interact

Figure 4.11

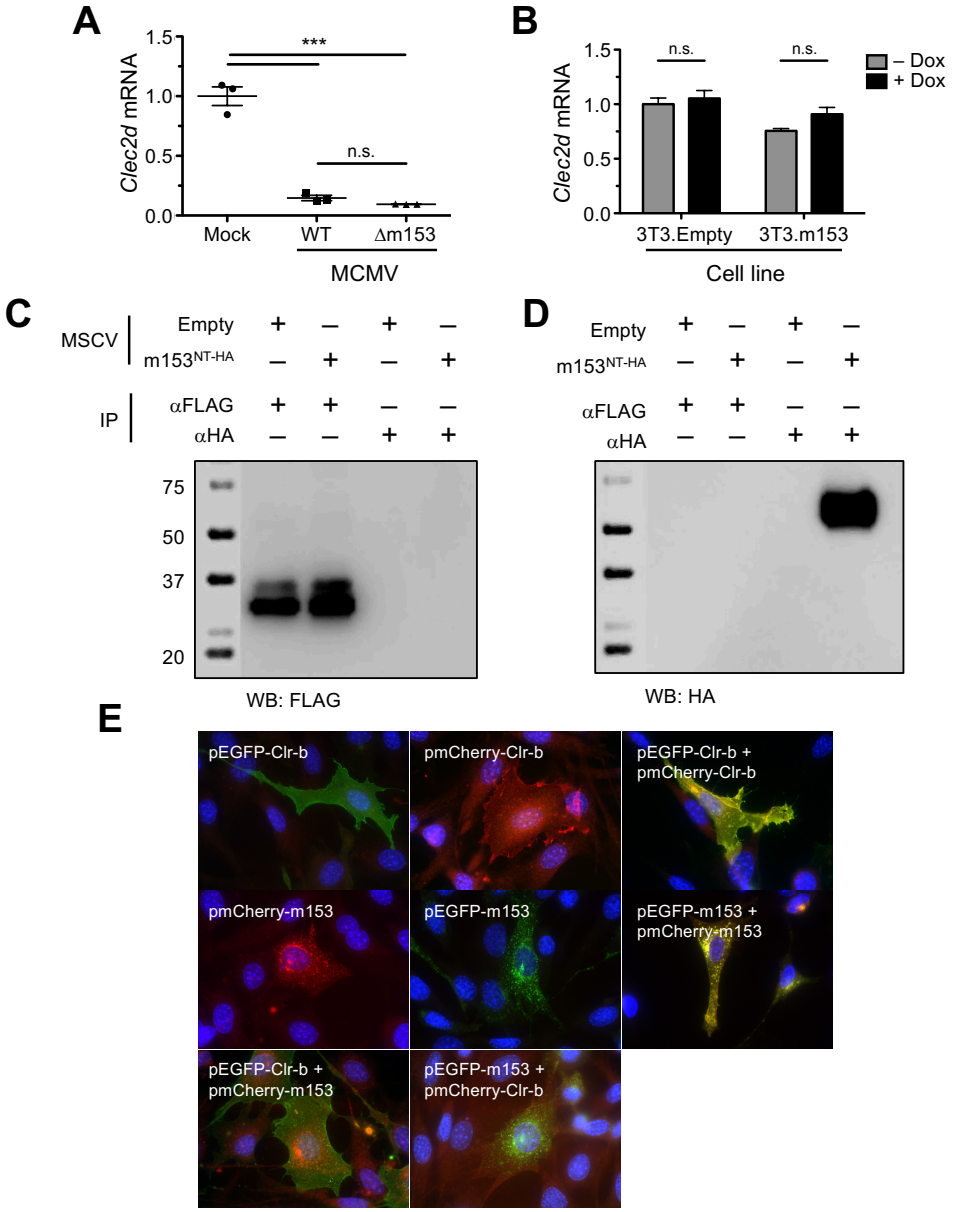

Figure 4.11. Clr-b modulation by m153 is post-transcriptional, with unknown protein interactions. (**A**) *Clec2d* transcript levels in NIH3T3 cells infected with WT or Δm153 virus and in (**B**) NIH3T3 cells transduced with $m153^{N\text{-}HA}$ or empty control pTRIPZ vector. Immunoprecipitations using α-FLAG or α-HA mAb from lysates of NIH3T3.Clr-$b^{C\text{-}FLAG}$ cells transfected with $m153^{N\text{-}HA}$ or empty control vector. These lysates were immunoblotted for α-FLAG (**C**) or α-HA (**D**). (**E**) NIH3T3 cells were transfected with constructs of m153 and Clr-b fused to either EGFP or mCherry, and analyzed for cellular localization using fluorescence microscopy 48 hours post transfection. All data are representative of at least 3 independent experiments.

directly, or the IP conditions may disrupt non-covalent (direct or indirect) interactions between Clr-b and m153. However, similar experiments using a milder detergent, digitonin, also failed to detect an interaction.

Next, we attempted to visualize whether Clr-b and m153 may co-localize to the same subcellular compartments upon overexpression. To this end, we generated vectors encoding N-terminal (cytosolic) EGFP or mCherry fusion proteins of Clr-b^{FLAG} (Clr-b$^{FLAG\text{-}Fluor}$) and C-terminal (cytosolic) EGFP or mCherry fusion proteins of m153^{HA} (m153$^{HA\text{-}Fluor}$), then analyzed transient NIH3T3 transfectants using fluorescence microscopy. Upon visualization, m153 constructs (m153$^{HA\text{-}EGFP/mCherry}$) were primarily detected in intracellular vesicles, whereas Clr-b constructs (Clr-b$^{FLAG\text{-}EGFP/mCherry}$) were detected more diffusely throughout the cell and at the cell surface; notably, this was reproducible independent of the fluorophore combinations used (**Fig. 4.11E**, upper left and middle images). To validate co-localization, we co-transfected NIH3T3 cells with constructs encoding each protein fused to two independent fluorophores; importantly, these showed overlapping expression, as expected (**Fig. 4.11E**, right images). In contrast, co-transfection of NIH3T3 cells with constructs encoding the two proteins fused to alternate fluorophores revealed limited co-localization of m153^{HA} and Clr-b^{FLAG} (**Fig. 4.11E**, bottom/lower images). Although ambiguous, these results suggest that m153 and Clr-b largely fail to co-localize to the same subcellular compartments upon transfection; as such, they may not directly interact with one another in a heteromeric complex, or m153 may target alternative Clr family members, or other proteins.

Nonetheless, to further investigate interaction between m153 and Clr-b at the post-translational level, we conducted differential MCMV infections of our stable NIH3T3.Clr-b^{FLAG} transductants. Here, basal endogenous Clr-b expression in the absence of Dox induction is similar to parental NIH3T3 cells, while a ~15-fold increase in Clr-b levels was detected using 4A6 mAb upon Dox induction (**Fig. 4.12A**). Upon infection using WT MCMV^{MW97} or MCMV-Δm153, uninduced NIH3T3.Clr-b^{FLAG} cells downregulated Clr-b levels similar to parental NIH3T3 cells, with the Δm153-mutant promoting exacerbated Clr-b loss (**Fig. 4.12A**). Moreover, in the presence of Dox induction, the ability of m153 to sustain Clr-b expression was clearly evident, as only a ~4-fold reduction in Clr-b MFI levels was observed using WT MCMV^{MW97}, while a ~70-fold reduction was observed using the Δm153-mutant (**Fig. 4.12A,B**). This was further evident when comparing the percentage of cells that had completely lost Clr-b

Figure 4.12

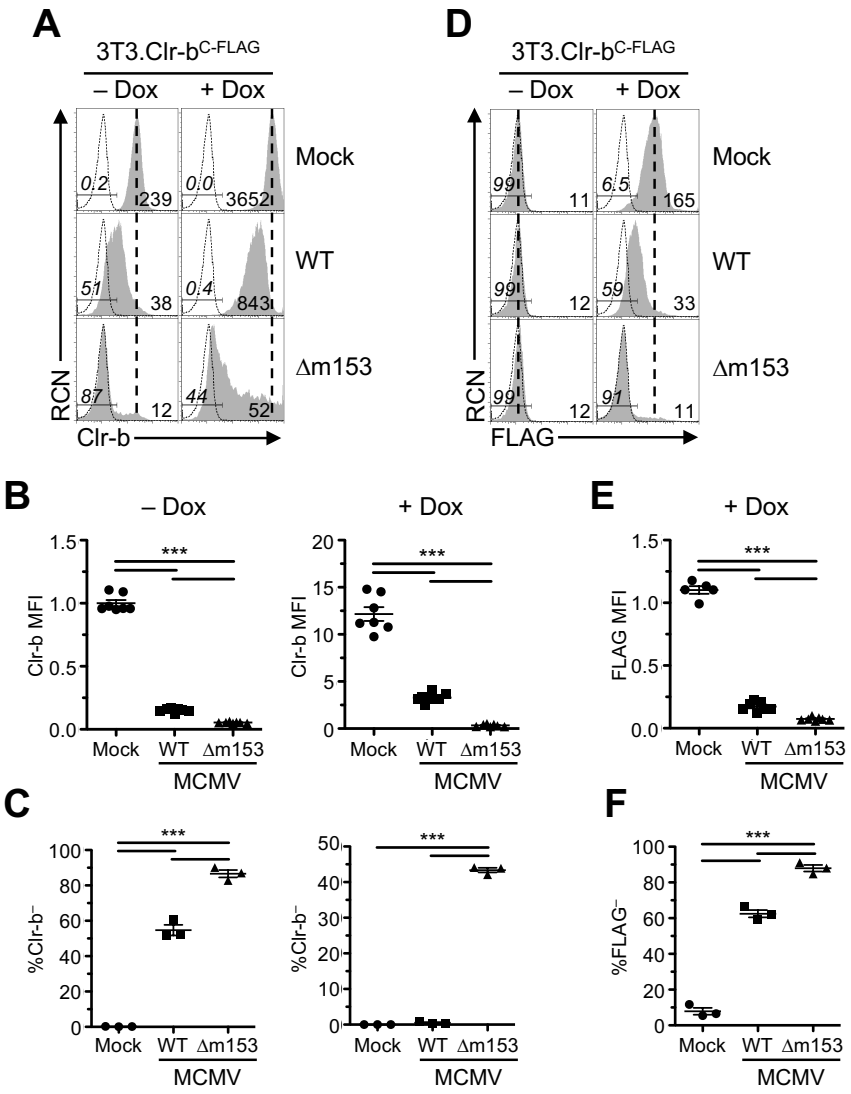

Figure 4.12. Prominent Clr-b loss in cells overexpressing Clr-b when infected with MCMV lacking m153. NIH3T3.Clr-b fibroblasts were cultured in absence or presence of dox and infected with either WT or Δm153 MCMV virus and analyzed using flow cytometry 24 hrs post-infection. (**A**) Clr-b cell surface expression measured by α-Clr-b mAb, 4A6. Vertical dotted line symbolizes mock MFI, whereas numbers on the left represent the %Clr-b$^-$ cells in gate, and numbers on the right represent MFI values. (**B**) Quantitation of Clr-b MFI in (A), normalized to Clr-b levels on resting uninduced cells. (**C**) Measurements of %Clr-b$^-$ cells with different viruses in A. (**D**) Clr-b cell surface expression measured by α-FLAG mAb, M2. (**E**) Quantitation of Clr-b MFI in (D). (**F**) Measurements of %Clr-b$^-$ cells with different viruses in (D). Data was analyzed using 1-way ANOVA and are representative of 3 independent experiments

expression (%Clr-b$^-$ cells), where the Δm153 mutant approached ≥40% Clr-b$^-$ cells, a magnitude not seen using WT MCMV^{MW97} (**Fig. 4.12C**).

Using the same cells, we also analyzed ectopic Clr-b^{FLAG} expression in the absence of endogenous Clr-b using FLAG mAb. While minimal basal FLAG-tag staining was observed on uninduced NIH3T3.Clr-b^{FLAG} cells, Dox induction promoted high levels of the exogenous Clr-b^{FLAG} protein (**Fig. 4.12D**). Following infection, Clr-b downregulation was clearly exacerbated using the Δm153-mutant in comparison to WT MCMV^{MW97} (**Fig. 4.12D,E,F**). These results demonstrate the efficacy of MCMV infection in promoting a loss of cell surface Clr-b protein, and highlight the clear impact of m153 in stabilizing Clr-b levels during MCMV infection.

4.4.5 Functional characterization of m153-induced Clr-b modulation

In order to test the functional role of m153, we first assessed NKR-P1B:Clr-b interactions in the context of m153 expression via BWZ reporter cell assays using stimulator cells varying in m153 expression. Briefly, BWZ.P1B reporter cells induce NFAT-driven β-galactosidase (*LacZ*) activity upon ligation of a CD3ζ/NKR-P1B chimeric fusion receptor by cognate Clr-b ligand, relative to parental BWZ.36 cells. Interestingly, a subtle difference in BWZ.P1B reporter activity could be detected between NIH3T3.m153^{HA} versus NIH3T3.Empty cells, both basally (no Dox induction, endogenous Clr-b) and upon MCMV infection (**Fig. 4.13A**). However, no difference was observed between the WT MCMV^{MW97} and Δm153-mutant viruses in this context. To vary the stimulator cells, we next used inducible NIH3T3.Clr-b^{FLAG} stimulator cells infected using either WT MCMV^{MW97} or Δm153-mutant MCMV (**Fig. 4.13B**). Using this approach, the functional effect of m153 in sustaining Clr-b levels was revealed, whereby a significant increase in BWZ.P1B reporter cell activity was observed using WT-infected versus Δm153-infected stimulator cells.

We next tested the MCMV variants in NK cellular cytotoxicity assays. To this end, we sorted NKR-P1B$^+$ and NKR-P1B$^-$ splenic NK-LAK (NKp46$^+$) effectors for use in ^{51}Cr-release cytotoxicity assays against MCMV-infected NIH3T3 target cells. In agreement with a previous report, NKR-P1B$^+$ NK-LAK displayed slightly higher levels of cytotoxicity in general compared to NKR-P1B$^-$ NK-LAK (Aust et al., 2009). Interestingly, cytotoxicity of WT MCMV-infected NIH3T3 cells was similar to mock-infected NIH3T3 target cells, while cytotoxicity of Δm153-infected targets was augmented (**Fig. 4.13C**). Surprisingly, this result was consistent regardless

Figure 4.13

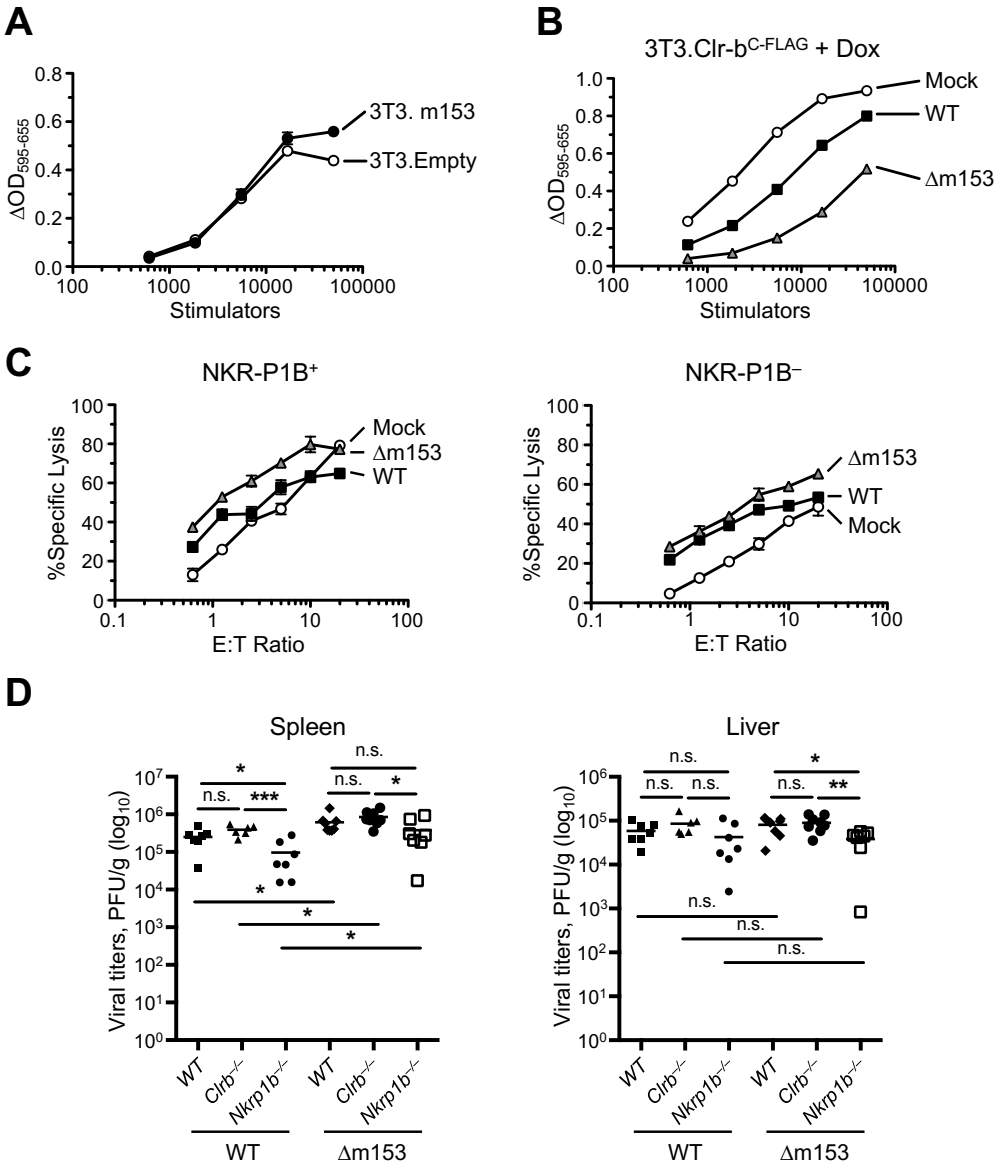

Figure 4.13. Functional characterization reveals additional modes of immunomodulation for m153. (**A**) NIH3T3.Empty and NIH3T3.m153 cells were co-cultured with BWZ.NKR-P1B reporter cells to measure receptor-ligand interactions using BWZ assay. (**B**) BWZ assay using WT MCMV-infected or Δm153-infected NIH3T3.Clr-b$^{C\text{-}FLAG}$ cells. (**C**) ^{51}Cr-release assay using NKR-P1B^{+} (left) and NKR-P1B^{-} splenic NKp46^{+}CD3^{-} LAKs (right) measuring ability to kill MCMV infected NIH3T3 cells. (**D**) In vivo MCMV infection using WT or Δm153 viruses on WT/B6, Clrb$^{-/-}$, and Nkrp1b$^{-/-}$ mice measuring viral titers in spleen and liver 3 days post infection. All data are representative of at least 3 independent experiments.

of NKR-P1B receptor expression on the NK-LAK effectors, although the magnitude was more pronounced using NKR-P1B^{+} NK-LAK. Together, these results demonstrate that expression of m153 protects infected cells from NK-mediated cytotoxicity *in vitro*.

To determine the role of m153 *in vivo*, and in the context of NKR-P1B:Clr-b interactions, we utilized cohorts of WT B6 mice, ligand-deficient B6.Clr-b$^{-/-}$ mice, and receptor-deficient B6.Nkrp1b$^{-/-}$ mice, and infected all three cohorts using either WT MCMV^{MW97} or Δm153-mutant MCMV. As shown previously (Rahim et al., 2016), infection using WT MCMV^{Smith} demonstrates that Nkrp1b$^{-/-}$ mice possess significantly lower splenic viral titers compared to WT B6 mice, while Clr-b$^{-/-}$ mice show a trend (albeit not significant) towards higher PFU titers (**Fig. 4.13D**); this was subsequently shown to be due to a role for NKR-P1B in immune evasion via the MCMV m12 immunoevasin during MCMV^{Smith} infection, an effect which was less significant using MCMV^{MW97} virus (Aguilar et al., 2017). Interestingly, infection using Δm153-mutant MCMV resulted in a similar overall phenotype among the three host cohorts, with significantly lower viral titers in Nkrp1b$^{-/-}$ mice, and an insignificant trend towards higher titers in Clr-b$^{-/-}$ mice, versus WT B6 mice. Unexpectedly, however, splenic viral titers in all three host strains were elevated using Δm153-mutant versus WT MCMV^{MW97} (**Fig. 4.13D**). These results demonstrate that, while m153 stabilizes Clr-b levels during MCMV infection, it appears to be deleterious for overall viral fitness in the B6 host strain, similar to m157. Thus, the elevated viral titers seen using the Δm153-mutant suggest that m153 may engage an unknown stimulatory receptor; while this could involve alternative NKR-P1:Clr family interactions, we cannot rule out the involvement of other receptor-ligand systems. Nonetheless, the reduced viral titers observed in Nkrp1b$^{-/-}$ mice in this study and elsewhere (Rahim et al., 2016), are consistent with the effects of the Clr-b-independent MCMV m12 decoy ligand recognized by the inhibitory NKR-P1B receptor (Chapter 3) (Aguilar et al., 2017). In contrast, the trend towards higher viral titers in Clr-b$^{-/-}$ mice suggests a more complex, perhaps m153-independent role for Clr-b in restraining viral fitness, perhaps due to NK cell education effects (Chen et al., 2015). Collectively, these data suggest that MCMV employs multiple strategies to modulate NKR-P1B:Clr-b interactions, in addition to multiple roles for m153 in regulating viral fitness *in vivo*, in turn making it difficult to decipher the direct influence of m153 in isolation.

4.4.6 Alleles of m153 reveal role for host-driven viral evolution

An analysis of m153 genes from different wild-derived MCMV isolates reveal that although all of the viral strains encode functional m153 gene product ORF, many of these have polymorphisms in their extracellular domains (**Fig. 4.14**). As seen in Chapter 3, this scenario is commonly observed when viral gene products are adapting to maintain host strain-dependent immune evasion (gain-of-function), or avert being directly recognized by host activating receptors (loss-of-function). Therefore, in accordance with the *in vivo* data (**Fig. 4.13D**), these findings suggest that m153 likely interacts with additional host molecules during MCMV infection that may be either advantageous or deleterious to viral fitness or host resistance.

4.4.7 m153 tetramers bind DC and a subset of ILC cell lines *in vitro*

To examine direct interactions between the m153 gene product and cellular receptors or ligands *in trans*, we utilized m153 tetramer reagents to stain various cell lines *in vitro*. Interestingly, m153 tetramers reproducibly stained the DC2.4 dendritic cell line at high levels, as well as staining a subset of the mouse ILC3-like MNK-3 cell line at lower levels (**Fig. 4.15**). These findings suggest that additional interactions between m153 and an unknown receptor or ligand on innate DC and ILC may influence the immune response to MCMV *in vivo*. The generation of a cDNA library from DC2.4 cells, combined with the use of m153 tetramers should facilitate the cloning of this putative m153 receptor.

4.5 Discussion

Beta-herpesviruses dedicate a significant portion of their genome to encode viral immunoevasin genes that subvert host immune recognition. Here, we report that the viral MHC-I homolog, m153, plays a role in limiting the downregulation of the host inhibitory NKR-P1B-ligand, Clr-b, during MCMV infection. Host cells infected with m153-deficient (Δm153) MCMV display an exacerbated "missing-self" loss of Clr-b surface expression, with faster kinetics and to a greater extent than WT MCMV. In addition, cells overexpressing m153 have increased basal levels of Clr-b compared to control cells. Despite efforts here to identify a direct mechanism, the effect of m153 on Clr-b expression appears to be indirect, as the two proteins fail to interact upon co-IP, and they co-localize only minimally upon transfection. However, the effect of m153 on Clr-b levels is independent of transcription and likely post-translational in nature, and m153

Figure 4.14

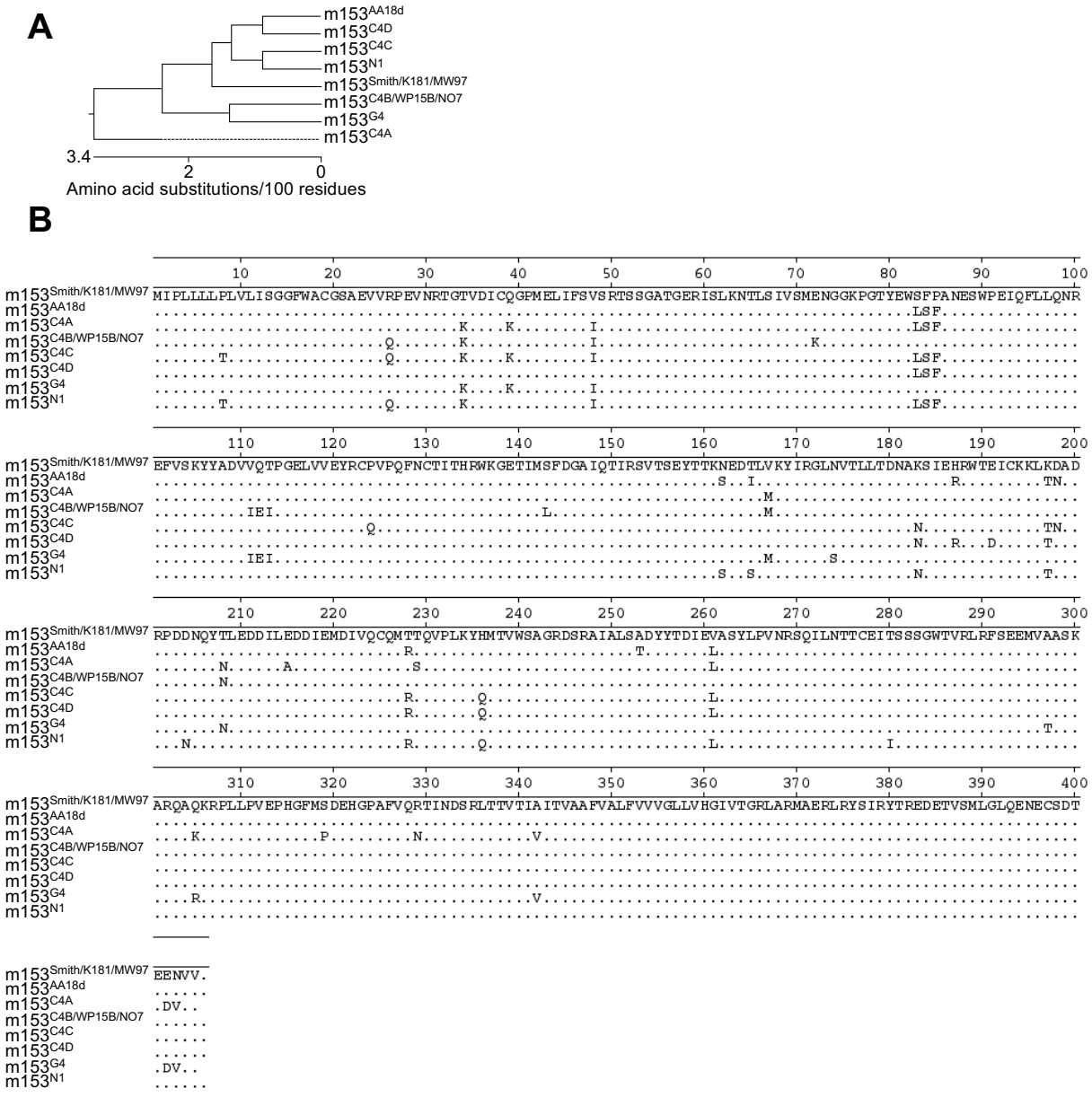

Figure 4.14. Analysis of m153 alleles from wild isolates of MCMV. (**A**) Phylogenetic tree and (**B**) amino acid comparison of m153 protein sequences aligned using ClustalW.

Figure 4.15

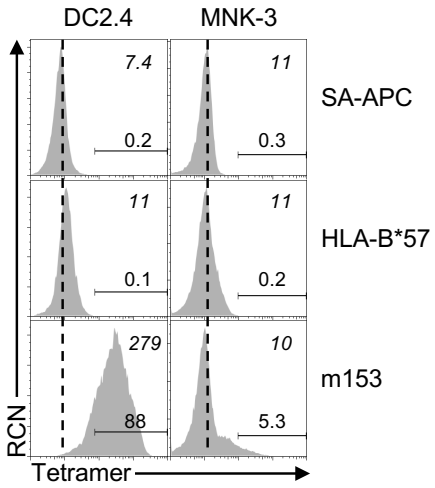

Figure 4.15. Tetramers of m153 reveal presence of an interacting partner on DC and ILC3 cell lines. Tetramers of m153 and HLA-B*57 were used to stain the DC2.4 and MNK-3 cell lines, DC and ILC3 lines respectively. Numbers in italics on the top right corner represent MFI values; numbers on above gates represent positive gated cell percentages; Dotted line line represents negative control MFI values. Data representative of 2 independent experiments.

expression does functionally modulate NKR-P1B:Clr-b interactions in the recognition of MCMV-infected cells.

Previous work has shown that Clr-b is lost in response to a number of cellular pathologies. These include transformation, genotoxic and cellular stress, and viral infection (Carlyle et al., 2004; Fine et al., 2010). The latter finding has been documented in a variety of infection models, including poxviruses (Vaccinia, Ectromelia) (Williams et al., 2012), RCMV-English (Voigt et al., 2007), MCMV (Aguilar et al., 2015), and also RNA viruses (unpublished observations). Thus, Clr-b appears to be a "healthy-self" marker on normal cells, and Clr-b downregulation appears to be a host response to viral infection that promotes "missing-self" recognition via loss of NKR-P1B inhibition. In support of this hypothesis, both RCMV and MCMV appear to have encoded viral immunoevasins that act as surrogate ligands to functionally engage NKR-P1B and circumvent this "missing-self" NK cell recognition mechanism (Aguilar et al., 2015; Voigt et al., 2007). In turn, cell surface Clr-b expression appears to be regulated by sensors that detect cellular "fitness" versus pathology, and thus the ligand behaves as an innate relay mechanism to alert NK cells. This "missing-self" role is also consistent with reports of short-lived *Clec2d* transcripts, as well as Clr-b protein, in the absence of constitutive or basal nascent transcription in healthy cells (Aguilar et al., 2015; Martick et al., 2008).

Our results show that MCMV Δm153 mutants downregulate Clr-b more efficiently, suggesting that m153 functions to prevent host-mediated Clr-b loss. However, the mechanism behind Clr-b stabilization by m153 remains ambiguous. We hypothesized that m153 may function similarly to the m04 gene product (gp34 glycoprotein), perhaps binding directly to Clr-b and escorting it to the cell surface, in order to maintain inhibitory signals via NKR-P1B. However, direct protein-protein interactions and substantial direct cellular co-localization could not be demonstrated between m153 and Clr-b. The fact that MCMV-Δm153 is capable of enhancing Clr-b downregulation, even on cells that express ectopic Clr-b^{FLAG}, demonstrates that this mechanism is likely post-translational in nature. Thus, m153 might interfere with the host ubiquitin-proteasomal degradation or autophagic internalization machinery, thereby preventing loss of "self" ligands from the cell surface upon infection. However, similar stabilization effects on MHC-I or Rae-1 expression were not observed upon transfection of m153, or upon infection with Δm153-mutant MCMV.

Alternatively, it is possible that the physiological function of m153 may be to target another Clr family member, which in turn interacts with Clr-b (e.g., via Clr heterodimerization); here, the observed positive Clr-b stabilization by m153, which is subtle, limited and non-linear, might be an indirect result of negative destabilization of another Clr by m153, for example by preventing induction of stimulatory Clr-c,d,g ligands (recognized by NKR-P1F). In support of this hypothesis, Clr-b/Clr-g heterodimers have been detected upon co-transfection, and Clr-g overexpression has been found to negatively regulate Clr-b expression at the cell surface, presumably by forming heterodimers over homodimers (unpublished findings). In addition, previous work has shown that *ex vivo* hematopoietic cells from B6.Clr-b$^{-/-}$ mice, but not WT B6 mice, spontaneously upregulate a stimulatory NKR-P1F ligand in reporter cell assays, suggesting that the mere absence of Clr-b may destabilize Clr-b/Clr-g heterodimers, in turn enforcing the formation of Clr-g homodimers recognized by NKR-P1F (Chen et al., 2015). This mechanism has been hypothesized to be partially responsible for the hyporesponsiveness of Clr-b$^{-/-}$ NK cells (Chen et al., 2015) – not only are they not educated via NKR-P1B, they may also be tolerized to chronic ectopic stimulatory NKR-P1F ligands, similar to the negative effects observed for NKG2D function upon transgenic overexpression of ectopic Rae-1ε ligand (Tripathy et al., 2008). In turn, this suggests that the loss of Clr-b upon MCMV infection may also spontaneously enforce the expression of stimulatory Clr homodimers, thereby promoting NK cell activation. Notably, significant polymorphism in the Clr-c gene product (another NKR-P1F ligand) has been observed between the B6, BALB/c, and 129-strain alleles (Chen et al., 2011), localized to the Clr-c membrane-proximal region; this is suggestive of host adaptation to evolutionary pressure from a viral immunoevasin, one which might intracellularly retain Clr-c,d,g. We are currently investigating this hypothesis further.

In keeping with an indirect effect, attempts to decipher the significance of m153 stabilization on Clr-b ligand function were ambiguous. Mouse fibroblasts infected with MCMV Δm153-mutant virus were more effectively killed by NK-LAK in comparison to WT MCMV; however, this was observed using both NKR-P1B^{+} and NKR-P1B^{-} effectors, implying that additional factors are involved and that the effect may be independent of the NKR-P1B:Clr-b axis. In addition, surprisingly, MCMV infections in B6-strain mice *in vivo* revealed elevated, not diminished, splenic viral titers upon infection with Δm153-mutant MCMV (versus WT virus), and this effect was independent of the host genotype, being similar for WT, Nkrp1b$^{-/-}$, and Clr-

$b^{-/-}$ animals. This suggests that the loss of m153 (a putative immunoevasin) from MCMV increased viral fitness. In contrast, for both WT MCMV and Δm153-mutant MCMV, Nkrp1b$^{-/-}$ mice displayed lower viral titers compared to WT B6 mice (Rahim et al., 2016), suggestive of the existence of a viral decoy ligand (i.e., MCMV m12; Chapter 3) (Aguilar et al., 2017), while Clr-b$^{-/-}$ mice exhibited a trend towards increased viral titers, suggestive of hyporesponsive NK cell function (Chen et al., 2015). The results of cytotoxicity assays, and the increased Δm153-mutant viral titers *in vivo*, reveal the possibility that m153 may interfere with host innate immunity via other mechanisms, in addition to Clr-b modulation. Previous work in the Margulies lab has demonstrated that m153 is capable of forming homodimers (Mans et al., 2007), which may interact with an unidentified receptor/ligand found on CD11c^{+} dendritic cells, monocytes, and NK cells (Mans, 2008). In concordance with this, they found that stimulator cells from different mouse strains exhibit differential m153 reporter cell responses. Furthermore, polymorphisms in m153 alleles exist amongst wild-derived MCMV isolates (**Fig.4.14**), suggestive of viral evolution under selective pressure to evade host innate immune recognition. Unfortunately, in the absence of further information regarding these putative alternative interactions, it is not possible to decipher the independent role that m153 plays in NK cell recognition via the NKR-P1B:Clr-b interaction. Notably, however, the m153 tetramer staining reported here for DC2.4 dendritic cells (DC) and MNK-3 innate lymphoid cells (ILC) *in vitro* is consistent with the expression of a candidate m153 receptor or ligand on these innate immune cell types. Further expression cloning efforts using m153 tetramers and DC2.4 cDNA libraries, or other high throughput differential display technologies such as RNA-Seq, should reveal the identity of this host protein.

In conclusion, these findings reveal a novel putative immune evasion mechanism by which MCMV targets the host innate immune response, and suggests that the B6-strain host may have adapted to avert the m153 evasion strategy. MCMV employs numerous genes that function to modulate MHC-I recognition, but the MHC-I-independent mechanisms are still being investigated. Here, we demonstrate that MCMV utilizes m153 to interfere with host-mediated "missing-self" Clr-b downregulation, thereby impairing NK cell recognition via NKR-P1B. The human genome encodes a single conserved inhibitory NKR-P1 family member, NKR-P1A (CD161; *KLRB1*), suggesting that HCMV or other viruses may also employ analogous

mechanisms to evade NK cell recognition by modulating expression of the NKR-P1A ligand, LLT-1.

Chapter 5

Discussion

Oscar A. Aguilar

This work has not been published.

5.1 Thesis Goals

The innate immune system plays a pivotal role in detecting and mounting an appropriate host response to invading pathogens. Within the cellular milieu, NK cells are frontline sentinels in recognizing the cytopathological effects of intracellular pathogens, in particular viruses. The complexity of NK cell recognition and regulation continues to become more evident as interest increases in this field. It was first proposed that NK cells are regulated by inhibitory receptors that recognize "healthy-self" MHC-I molecules, in turn capable of performing "missing-self" recognition upon the loss of these ligands. Since then, stimulatory receptors for "induced-self" MHC-I-related ligands have been identified, as well as other families of MHC-I-independent inhibitory and stimulatory receptors that function in parallel. Many of these MHC-I-independent receptor-ligand interactions had previously been ignored; however, in recent years, there has been an expansion in the number and diversity of cognate receptors and unique binding partners discovered. In addition, it is becoming increasingly clear that under pathological states, many if not all of these interactions can be modulated in order to evade immune recognition; in this sense, the study of immunoevasins enlightens us about normal immune function, since pathogens have evolved over millennia to figure out how to circumvent normal immune function and self-nonself discrimination. Examples of this even extend beyond pathogen evolution to cancer detection, and include the shedding of soluble NKG2D ligands and immunoediting of NK ligands by tumour cells (Groh et al., 2002; Salih et al., 2002; Waldhauer and Steinle, 2008; Wu et al., 2004). Viruses are the most widely documented and genomically compact pathogens that modulate innate immunity and NK cell ligand expression in order to successfully evade recognition. For instance, there exist numerous examples of how viruses modulate MHC-I recognition by encoding viral immunoevasins that target antigen presentation, or alternatively act as decoy inhibitory ligands for these receptors. However, MHC-I recognition is only one of the many axes that NK cells utilize in discriminating between "self" and "altered/non-self". These include the CD94/NKG2 heterodimers, NKG2D homodimer, NKp46 natural cytotoxicity receptor, 2B4 SLAM-family receptor, DNAM-1 Ig-like receptor, amongst others, all of which are becoming increasingly studied and shown to be part of the arsenal of viral immune evasion strategies. In light of this, the goal of this thesis was to further elucidate the importance of the MHC-I-independent NKR-P1B:Clr-b missing-self axis of NK recognition in the context of CMV infection in rodents, in order to document and draw parallels to human health and pathogenesis.

5.2 Viral infection-mediated loss of the inhibitory NK ligand, Clr-b

In Chapter 2 of this thesis, we highlight the consequences of MCMV infection on expression of the inhibitory NKR-P1B ligand, Clr-b. We demonstrate that cross-species infection of MCMV and RCMV infection of healthy rat and mouse fibroblasts results in a conserved mClr-b/rClr-11 loss, and that this occurs at the cell surface as well as transcript levels. Although not demonstrated, we also discuss how this might represent a cellular response to infection by a number of viruses, including DNA herpesviruses (MCMV, RCMV) and poxviruses (Vaccinia, Ectromelia), as well as RNA viruses (such as influenza and EMCV; A. Mesci and J. Ma unpublished observations). Here, we also provided evidence that the effective half-life of Clr-b at the cell surface is quite short; thus, we postulate that this marker of healthy-self serves as a steady-state indicator of cellular fitness. Previously, it was demonstrated that the Clr-b gene (*Clec2d*) 3'UTR encodes a discontinuous hammerhead ribozyme (HHR) motif that at the transcript level is capable of self-cleavage upon formation of an active secondary RNA structure in the presence of divalent cations alone (Martick et al., 2008). This HHR ribozyme is present in mouse Clr-b (*Clec2d*), the rat Clr-11 homolog (*Clec2d11*), the mouse Clr-a gene product (*Clec2e*), the less well studied rat *Clec2d9/10* gene products, and it is conserved across numerous other species that encode *Clec2*-like genes, such as the tree shrew, hedgehog, horse, elephant, cow, dog, and even platypus, but not in humans (Scott et al., 2009). Thus, since Clr-b transcript and cell surface expression are tightly regulated in rodents, this mechanism further highlights how divergent Clr-b homologs in many species may be used to sense the "real-time" health status of targets under surveillance to NK cells. Notably, in humans, this mechanism may have been functionally replaced by alternative splicing of the LLT1 gene product (*CLEC2D*) (Germain et al., 2010; Martick et al., 2008).

On the hypothetical basis that the Clr-b loss is a consequence of pathogen insult, we hypothesized that innate immune sensors could be potentially responsible for initializing the signaling cascades that resulted in Clr-b downregulation. However, despite our efforts using shRNA screening, KO cell lines, and PRR agonists, we were not fully capable of characterizing the innate mechanisms that resulted in the observed Clr-b loss phenotype. The only agonists that resulted in Clr-b downregulation in isolation were adenosine phosphate agonists (AMP, ADP, ATP) and the potassium ionophore, nigericin. Interestingly, the adenosine oligophosphate

analogs had different effects at different concentrations. Therefore, whether the phenotype is a result of activation of the P2X7-family of purinergic receptors, AMPK-dependent mechanisms (AMP/ADP/ATP-regulated), or other nucleotide metabolism receptors (CD39, CD73 ectonucleases), the underlying mechanism remains to be determined. The effects of nigericin similarly deserve to be followed up in light of a potential inflammasome-independent activation or potentiation pathway.

Despite not being able to provide a single candidate agonistic immunoregulatory pathway for pathogenic Clr-b downregululation, an induced gene product must play a role, as blocking translation elongation via cycloheximide appears to abrogate Clr-b loss. Thus, whether it is a viral gene product or a host factor that is produced in response to infection remains to be determined. However, recent work in our laboratory does demonstrate that the immediate early gene product , *ie3* (M122) of MCMV (but not *ie1,2*) can partially promote Clr-b downregulation in isolation upon overexpression, and this effect is dependent upon direct and indirect repression of nascent *Clec2d* transcription (Kirkham et al., 2017). Thus, it is possible that host transcriptional integrity in general (the shutoff of host gene transcription by viruses) or specific *ie3* expression itself is recognized as a "pattern of pathogenesis" (Vance et al., 2009), in turn resulting in Clr-b modulation to alert immune recognition. However, the Clr-b loss observed using *ie3* overexpression is only partial (~2-3-fold), and thus there likely are other factors at play, including generalized host transcription shutdown, which by proxy results in Clr-b loss. An unbiased approach may elucidate some of these host factors. To date, we have attempted using an shRNA lentiviral screen to generate a partial list of candidates involved in Clr-b/*Clec2d* expression; however, knockdown approaches may not be optimal since gene expression is not fully abrogated and there exist off-target considerations. These limitations could be averted using a whole genome CRISPR/Cas9 sgRNA-mediated gene editing library comparing MCMV infection with normal cell health. However, the complexity observed in this study supports the notion that there is a great deal of redundancy or multiplicity of factors that impact the host innate immune sensors and pathways, which can result in conflicting results. Nevertheless, given our current technologies, high throughput screens might represent the best unbiased approach to identify candidate gene products or pathways.

5.3 Targeting of the prototypical NKR-P1 family by a viral immunoevasin

In Chapter 3 of this thesis, we identify an IgV-like m02-family, NKR-P1B-decoy ligand utilized by MCMV to circumvent and inhibit NK cell recognition of infected cells. Importantly, this ligand, the MCMV m12 gene product, was subsequently discovered to bind the stimulatory orphan receptors, NKR-P1A and NKR-P1C (the prototypical NK1.1 alloantigen), resolving an over 4-decade search for physiological or natural NK1.1 ligands. Additionally, we have revealed that there exist polymorphisms amongst wild-derived MCMV isolates in the m12 gene, including some viral isolates that completely lack functional m12 genes (loss-of-function alleles). This is corroborated by previous findings that the NKR-P1B and NKR-P1C genetic loci (*Klrb1b/*c) display similarly extensive polymorphisms, localized to their mAb-binding extracellular domains, in turn suggesting that viral versus host-driven reciprocal evolution pressures are responsible for this allelic diversity. These findings advance not only our knowledge about NK cell recognition of MCMV-infected cells, but they also enlighten us as to mechanisms of co-evolutionary immune evasion strategies, as well as host-pathogen interplay between the NKR-P1 receptors and the MCMV m12 decoy. Despite these advances, there remains a number of outstanding questions regarding this immunoevasin strategy. First, although we describe the kinetics of the *m12* transcript expression, the absolute cell surface expression of this decoy remains to be determined by means such as NKR-P1B tetramers (Aguilar et al., 2017), and/or m12 mAb, which we have now successfully generated (Aguilar *et al.*, manuscript in preparation). In addition, ongoing efforts to elucidate X-ray co-crystallographic structures of m12 bound to the NKR-P1A/B/C-family of receptors and their respective functionally discrepant alleles would be beneficial to understanding the underlying strategy that MCMV in general, and MCMV m12 in particular, utilize to target immune evasion pathways, specifically the highly polymorphic and alloantigenic NKR-P1 receptor family. For instance, it was recently revealed that m157 targets the stalk region of the Ly49H/C/I receptors (Berry et al., 2013); thus, whether m12 uses a similar approach or targets the C-type lectin-like ectodomain would be of great interest (Aguilar et al., 2017). A co-crystal structure may also reveal why the E91K SNP between the MCMV^{Smith} and MCMV^{MW97} alleles results in differential NKR-P1B^{B6} recognition, versus that of NKR-P1B^{129} and NKR-P1B^{FVB} (Aguilar et al., 2017).

A notable phenotype that also remains to be explored is the discrepancy between the NKR-P1C^{B6} and m12^{Smith} biophysical SPR protein-protein interaction results, and the cellular BWZ reporter assay results; in particular, according to SPR affinity measurements, m12^{Smith}

bound with similar strength to NKR-P1B^{B6} and NKR-P1C^{B6}, whereas in a cellular context, BWZ.m12^{Smith} reporters respond much weaker in terms of cellular avidity to NKR-P1C^{B6} transfectants than to NKR-P1B^{B6}-bearing stimulator cells (Aguilar et al., 2017). This result may be explained by differences in post-translational modifications (including glycosylation), differences in threshold cell surface expression levels, *cis-trans* receptor-ligand interactions on BWZ reporter cells, or involvement of other unknown regulatory factors in this interaction. Follow-up studies of viral clearance of MCMV mutants containing additional m12 alleles utilized to infect different mouse strains would further elucidate the viral evolution patterns observed evolutionarily and would have great implications on how host strains in turn adapt evolutionarily to develop resistance to diverse CMV pathogen isolates (Aguilar et al., 2017). On this point, it would be interesting to analyze the *Nkrp1* genes of wild-derived (non-inbred) mice, where the m12-null wild-derived MCMV isolates were originally isolated, since we predict that some mouse strains captured on Australian island reserves may actually possess dominant NKR-P1A or NKR-P1C activating receptors that may have evolved to result in stronger MCMV resistance, akin to the evolution of the Ly49H activating receptor in the B6 inbred strain (Smith et al., 2013). In such a case, it would be interesting to determine if such a dominant stimulatory NKR-P1A/C-directed response also results in NK cell memory, similar to that observed for the Ly49H$^+$ subset in B6 mice (however, this may be difficult, given that NKR-P1A/C are expressed on ~95-100% of NK cells in B6 mice). This might help elucidate the molecular signaling mechanisms involved in NK cell memory, since Ly49H utilizes different adaptor signaling pathways compared to NKR-P1C (DAP12 versus FcRγ, respectively). In B6 mice, it has been suggested that the m12^{Smith} allele may have an influence in generating NK cell memory, where Ly49H$^+$NKR-P1B$^+$ NK cells appear to be suppressed in their ability to generate memory NK cells (Rahim et al., 2016). This study also brings into question why the BALB/c and 129S6 mouse strains have lost functional NKR-P1C expression and the resulting ability to recognize m12$^{Smith/MW97}$ altogether. We have previously suggested that this may be due to loss of a key structural cysteine residue (C122S substitution in Nkrp1c$^{BALB/129}$) that may prevent proper folding of the C-type lectin-like domain; however, these studies are ongoing. Importantly, NKR-P1 family members are expressed on a number of innate and adaptive lymphocyte populations including invariant NKT cells (NK1.1$^+$), subsets of ILC (which highly express NKR-P1B in particular), γδ T cell subsets, as well as activated conventional CD8$^+$ αβ T cells and some CD4$^+$

T cell subsets; thus, whether m12 affects host responses in these cells remains to be determined. Nevertheless, this makes m12 a potential 'blanket' immunoevasin capable of directly targeting or being temporally recognized by a number of innate and adaptive immune cell subsets.

In summary, the results from this chapter identifies the very first MCMV m02 family member capable of directly engaging NK receptors and prompts further investigation into the molecular and functional consequences of these interactions.

5.4 Modulation of the host ligand, Clr-b by a viral immunoevasin

In Chapter 4 of this thesis, we identify an MCMV-encoded gene product that positively regulates and stabilizes Clr-b expression, whilst MCMV infection in general results in rapid Clr-b loss. This project was initiated as a consequence of searching for potential NKR-P1B decoy ligands, such as m12 (Chapter 3), keeping in mind that CMV have been demonstrated to modulate NK ligands during infection. Therefore, MCMV mutant viruses were screened to determine if any virally encoded genes affected Clr-b surface expression (using 4A6 mAb and BWZ.P1B reporter cell assays). Using the MCMV large regional genomic deletion mutants, and cellular expression cloning, we discovered that m153, an m145 family member, stabilizes Clr-b cell surface expression during MCMV infection. We revealed that the absence of m153 during infection resulted in a more pronounced Clr-b loss. However, despite efforts to determine whether m153 directly interacted with Clr-b (using co-immunoprecipitations and confocal fluorescence imaging), we were not able to conclusively confirm any direct protein-protein interactions. This could be due to a weak non-covalent interaction that is lost during immunoprecipitation using detergents, or perhaps may involve a heteromeric multi-protein complex that might similarly be disrupted during protein isolation. Nevertheless, we demonstrate that the effect of m153 on Clr-b expression is transcriptionally independent, and likely post-translational in nature. Several avenues can be utilized to determine the mechanism by which m153 is influencing Clr-b. For instance, Clr-b and m153 can be individually immunoprecipitated from fibroblasts using the approach outlined in Chapter 4, followed by mass spectrometry, in order to identify whether these proteins interact using this more sensitive technique. This approach could also potentially reveal other unknown binding partners that might be used to compare whether there exist any complementary candidate interacting molecules, or perhaps cellular pathways that might shed light on potential regulatory mechanisms.

Interestingly, MCMV infections of WT, Clr-b$^{-/-}$ and Nkrp1b$^{-/-}$ mice *in vivo* revealed that an m153-deficient virus, MCMV Δm153, resulted in higher viral titers, irrespective of host mouse strain genotype, highlighting the possibility in turn that m153 expression may directly result in immune cell activation during the acute phase of infection. Thus, in addition to the described effects that m153 has on sustaining Clr-b levels, it may also have Clr-b-independent effects during MCMV infection that appear to play a more prominent balanced role *in vivo*. Further evidence for this can be attributed to the Margulies lab finding that m153 directly binds an unknown receptor/ligand that is expressed on dendritic cells, monocytes, and NK cells (Mans, 2008). Therefore, identifying this candidate receptor/ligand would allow us to directly investigate the role that m153 plays in modulating Clr-b versus other immunoregulatory mechanisms during infection. Importantly, the m153 gene is polymorphic across wild-derived isolates of MCMV, further providing evidence for host-driven evolutionary selection pressures, as in seen with m12 (Chapter 3). Indeed, searching for polymorphisms in the host receptors may directly assist in identifying the candidate receptor/ligand. In addition, m153-tetramers can be a useful tool to functionally screen and expression clone cDNA libraries prepared from DC (e.g., DC2.4), monocyte, or NK/ILC (e.g., MNK-3) cell lines. (Krmpotic et al., 2002)

The work outlined in this chapter further elucidates the pathways by which MCMV modulates MHC-I-independent NK recognition. This places m153 as an immunomodulatory m145 member, along with m145, m152, m154, m155, and m157 (Arapovic et al., 2009b; Arase et al., 2002; Hasan et al., 2005; Krmpotic et al., 2002; Krmpotic et al., 2005; Zarama et al., 2014; Ziegler et al., 1997).

5.5 General Conclusions

In summary, the work described in this thesis is outlined graphically in **Figure 5.1**, healthy cells possess abundant expression of the inhibitory NK ligand, Clr-b, in order to promote "healthy-self" inhibition, as well as to invoke "missing-self" NK cell recognition via NKR-P1B disinhibition (**Fig. 5.1A**). Upon MCMV infection, the infected cell (via innate pattern recognition or viral immune modulation) loses Clr-b at the cell surface and transcript levels, resulting in loss of NKR-P1B-mediated inhibitory signaling (**Fig. 5.1B**). However, MCMV has evolved several non-redundant mechanisms to circumvent this strategy. Firstly, MCMV encodes an immunoevasin, m12, that serves as a direct NKR-P1B "decoy" ligand, in turn resulting in NK

Figure 5.1

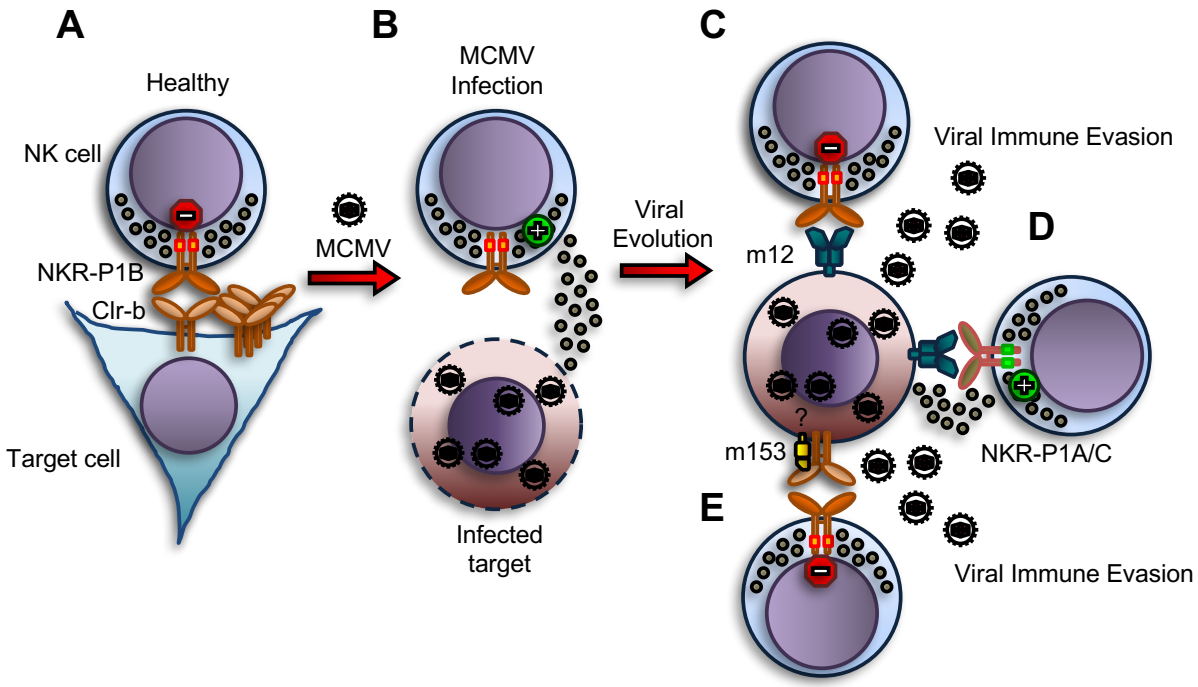

Figure 5.1. Model of MCMV modulation through the NKR-P1 axis of NK recognition. (**A**) Healthy target cells are protected from NK cell activation by expressing abundant levels of Clr-b at the cells surface. (**B**) MCMV infection results in loss of Clr-b at the cell surface resulting in NKR-P1B dependent missing-self recognition. (**C**) MCMV evolved a viral decoy, m12, that directly engages NKR-P1B and inhibits NK cells. (**D**) Host also has adapted stimulatory molecules to recognize the m12 ligand thereby controlling MCMV infection. (**E**) MCMV also encodes m153, a gene that stabilizes Clr-b expression upon infection through an unknown mechanism, but likely inhibits NKR-P1B-mediated missing-self.

inhibition in the absence of lost self Clr-b ligand (**Fig. 5.1C**). Secondly, MCMV also encodes a second immunoevasin, m153, that stabilizes host "self" Clr-b expression upon MCMV infection (**Fig. 5.1D**). Importantly, with respect to m12 decoy inhibition, the host has evolved counter-measures that involve stimulatory NKR-P1A/C paralogous receptors that directly recognize m12 on infected cells, thus serving as surrogate "T-cell receptor-like" MCMV antigen-specific receptors (**Fig. 5.1E**).

5.6 Implications for Human Health

The findings in this thesis prompt investigations into the human setting. Rodent CMV viruses have long been used as a tool to study the pathologies of HCMV in humans. Indeed, although many immunomodulatory genes are not genetically or structurally conserved between M/RCMV and HCMV, HCMV functionally utilizes similar mechanisms to evade NK cell recognition. For instance, although HCMV does not contain structural homologs to the m02 or m145 family of genes, it does encode the convergent US and UL immunoevasin families, and indeed the MHC-I retention originally described for the MCMV m06 and m152 immunoevasins has also been observed for the HCMV US2, US3, US6, US10 and US11 proteins (Lin et al., 2007; Lisnic et al., 2015). In humans, NKR-P1A (CD161/*KLRB1*) is a single inhibitory NKR-P1 family member with LLT-1/*CLEC2D* as its sole ligand (although NKp65/*KLR-F2* and NKp80/*KLR-F1* are suspected divergent activating family members with genetically linked ligands, CLEC2A/B, respectively). However, due to limited availability of reagents, we are not certain whether LLT1 is as broadly expressed as Clr-b, or whether LLT1 is only expressed in hematopoietic compartments. Due to these limitations, it is currently unknown if viruses modulate host LLT1 ligand expression and/or NKR-P1A receptor function. However, given previous findings in the lab (RCMV RCTL:rNKR-P1A/B) and the findings in this thesis (MCMV m12:mNKR-P1A/B/C), the investigation of whether HCMV encodes an NKR-P1A decoy to subvert NK recognition is merited. This work is of urgent importance, as HCMV is currently being used a potential viral vector to deliver vaccines; thus, understanding the immune evasion strategies of this human virus will result in improved safety and efficacy in vaccine clinical trials.

References

Ablasser, A., Goldeck, M., Cavlar, T., Deimling, T., Witte, G., Rohl, I., Hopfner, K.P., Ludwig, J., and Hornung, V. (2013). cGAS produces a 2'-5'-linked cyclic dinucleotide second messenger that activates STING. Nature *498*, 380-384.

Aguilar, O.A., Berry, R., Rahim, M.M.A., Reichel, J.J., Popovic, B., Tanaka, M., Fu, Z., Balaji, G.R., Lau, T.N.H., Tu, M.M.*, et al.* (2017). A viral immunoevasin controls innate immunity by targeting the prototypical killer cell receptor family. Cell *169*, 58-71 e14.

Aguilar, O.A., Mesci, A., Ma, J., Chen, P., Kirkham, C.L., Hundrieser, J., Voigt, S., Allan, D.S., and Carlyle, J.R. (2015). Modulation of Clr Ligand Expression and NKR-P1 Receptor Function during Murine Cytomegalovirus Infection. J Innate Immun *7*, 584-600.

Aldemir, H., Prod'homme, V., Dumaurier, M.J., Retiere, C., Poupon, G., Cazareth, J., Bihl, F., and Braud, V.M. (2005). Cutting edge: lectin-like transcript 1 is a ligand for the CD161 receptor. J Immunol *175*, 7791-7795.

Allan, D.S., Kirkham, C.L., Aguilar, O.A., Qu, L.C., Chen, P., Fine, J.H., Serra, P., Awong, G., Gommerman, J.L., Zuniga-Pflucker, J.C.*, et al.* (2015). An in vitro model of innate lymphoid cell function and differentiation. Mucosal Immunol *8*, 340-351.

Andrews, D.M., Sullivan, L.C., Baschuk, N., Chan, C.J., Berry, R., Cotterell, C.L., Lin, J., Halse, H., Watt, S.V., Poursine-Laurent, J.*, et al.* (2012). Recognition of the nonclassical MHC class I molecule H2-M3 by the receptor Ly49A regulates the licensing and activation of NK cells. Nat Immunol *13*, 1171-1177.

Arapovic, J., Lenac Rovis, T., Reddy, A.B., Krmpotic, A., and Jonjic, S. (2009a). Promiscuity of MCMV immunoevasin of NKG2D: m138/fcr-1 down-modulates RAE-1epsilon in addition to MULT-1 and H60. Mol Immunol *47*, 114-122.

Arapovic, J., Lenac, T., Antulov, R., Polic, B., Ruzsics, Z., Carayannopoulos, L.N., Koszinowski, U.H., Krmpotic, A., and Jonjic, S. (2009b). Differential susceptibility of RAE-1 isoforms to mouse cytomegalovirus. J Virol *83*, 8198-8207.

Arase, H., Arase, N., and Saito, T. (1996). Interferon gamma production by natural killer (NK) cells and NK1.1+ T cells upon NKR-P1 cross-linking. J Exp Med *183*, 2391-2396.

Arase, H., Mocarski, E.S., Campbell, A.E., Hill, A.B., and Lanier, L.L. (2002). Direct recognition of cytomegalovirus by activating and inhibitory NK cell receptors. Science *296*, 1323-1326.

Arase, N., Arase, H., Park, S.Y., Ohno, H., Ra, C., and Saito, T. (1997). Association with FcRgamma is essential for activation signal through NKR-P1 (CD161) in natural killer (NK) cells and NK1.1+ T cells. J Exp Med *186*, 1957-1963.

Aust, J.G., Gays, F., Mickiewicz, K.M., Buchanan, E., and Brooks, C.G. (2009). The expression and function of the NKRP1 receptor family in C57BL/6 mice. J Immunol *183*, 106-116.

Babic, M., Pyzik, M., Zafirova, B., Mitrovic, M., Butorac, V., Lanier, L.L., Krmpotic, A., Vidal, S.M., and Jonjic, S. (2010). Cytomegalovirus immunoevasin reveals the physiological role of "missing self" recognition in natural killer cell dependent virus control in vivo. J Exp Med *207*, 2663-2673.

Bando, J.K., and Colonna, M. (2016). Innate lymphoid cell function in the context of adaptive immunity. Nat Immunol *17*, 783-789.

Bartel, Y., Bauer, B., and Steinle, A. (2013). Modulation of NK cell function by genetically coupled C-type lectin-like receptor/ligand pairs encoded in the human natural killer gene complex. Front Immunol *4*, 362.

Berry, R., Ng, N., Saunders, P.M., Vivian, J.P., Lin, J., Deuss, F.A., Corbett, A.J., Forbes, C.A., Widjaja, J.M., Sullivan, L.C.*, et al.* (2013). Targeting of a natural killer cell receptor family by a viral immunoevasin. Nat Immunol *14*, 699-705.

Berry, R., Vivian, J.P., Deuss, F.A., Balaji, G.R., Saunders, P.M., Lin, J., Littler, D.R., Brooks, A.G., and Rossjohn, J. (2014). The structure of the cytomegalovirus-encoded m04 glycoprotein, a prototypical member of the m02 family of immunoevasins. J Biol Chem *289*, 23753-23763.

Beziat, V., Dalgard, O., Asselah, T., Halfon, P., Bedossa, P., Boudifa, A., Hervier, B., Theodorou, I., Martinot, M., Debre, P.*, et al.* (2012). CMV drives clonal expansion of NKG2C+ NK cells expressing self-specific KIRs in chronic hepatitis patients. Eur J Immunol *42*, 447-457.

Bezman, N.A., Kim, C.C., Sun, J.C., Min-Oo, G., Hendricks, D.W., Kamimura, Y., Best, J.A., Goldrath, A.W., Lanier, L.L., and Immunological Genome Project, C. (2012). Molecular definition of the identity and activation of natural killer cells. Nat Immunol *13*, 1000-1009.

Biron, C.A., Byron, K.S., and Sullivan, J.L. (1989). Severe herpesvirus infections in an adolescent without natural killer cells. N Engl J Med *320*, 1731-1735.

Bottino, C., Castriconi, R., Pende, D., Rivera, P., Nanni, M., Carnemolla, B., Cantoni, C., Grassi, J., Marcenaro, S., Reymond, N.*, et al.* (2003). Identification of PVR (CD155) and Nectin-2 (CD112) as cell surface ligands for the human DNAM-1 (CD226) activating molecule. J Exp Med *198*, 557-567.

Braud, V.M., Allan, D.S., O'Callaghan, C.A., Soderstrom, K., D'Andrea, A., Ogg, G.S., Lazetic, S., Young, N.T., Bell, J.I., Phillips, J.H.*, et al.* (1998). HLA-E binds to natural killer cell receptors CD94/NKG2A, B and C. Nature *391*, 795-799.

Brown, M.G., Dokun, A.O., Heusel, J.W., Smith, H.R., Beckman, D.L., Blattenberger, E.A., Dubbelde, C.E., Stone, L.R., Scalzo, A.A., and Yokoyama, W.M. (2001). Vital involvement of a natural killer cell activation receptor in resistance to viral infection. Science *292*, 934-937.

Brune, W., Hengel, H., and Koszinowski, U.H. (2001). A mouse model for cytomegalovirus infection. Curr Protoc Immunol *Chapter 19*, Unit 19 17.

Carayannopoulos, L.N., Naidenko, O.V., Fremont, D.H., and Yokoyama, W.M. (2002). Cutting edge: murine UL16-binding protein-like transcript 1: a newly described transcript encoding a high-affinity ligand for murine NKG2D. J Immunol *169*, 4079-4083.

Carlyle, J.R., Jamieson, A.M., Gasser, S., Clingan, C.S., Arase, H., and Raulet, D.H. (2004). Missing self-recognition of Ocil/Clr-b by inhibitory NKR-P1 natural killer cell receptors. Proc Natl Acad Sci U S A *101*, 3527-3532.

Carlyle, J.R., Martin, A., Mehra, A., Attisano, L., Tsui, F.W., and Zuniga-Pflucker, J.C. (1999). Mouse NKR-P1B, a novel NK1.1 antigen with inhibitory function. J Immunol *162*, 5917-5923.

Carlyle, J.R., Mesci, A., Fine, J.H., Chen, P., Belanger, S., Tai, L.H., and Makrigiannis, A.P. (2008). Evolution of the Ly49 and Nkrp1 recognition systems. Semin Immunol *20*, 321-330.

Cerwenka, A., Bakker, A.B., McClanahan, T., Wagner, J., Wu, J., Phillips, J.H., and Lanier, L.L. (2000). Retinoic acid early inducible genes define a ligand family for the activating NKG2D receptor in mice. Immunity *12*, 721-727.

Cerwenka, A., and Lanier, L.L. (2016). Natural killer cell memory in infection, inflammation and cancer. Nat Rev Immunol *16*, 112-123.

Chan, C.J., Martinet, L., Gilfillan, S., Souza-Fonseca-Guimaraes, F., Chow, M.T., Town, L., Ritchie, D.S., Colonna, M., Andrews, D.M., and Smyth, M.J. (2014). The receptors CD96 and CD226 oppose each other in the regulation of natural killer cell functions. Nat Immunol *15*, 431-438.

Chee, M.S., Bankier, A.T., Beck, S., Bohni, R., Brown, C.M., Cerny, R., Horsnell, T., Hutchison, C.A., 3rd, Kouzarides, T., Martignetti, J.A.*, et al.* (1990). Analysis of the protein-coding content of the sequence of human cytomegalovirus strain AD169. Curr Top Microbiol Immunol *154*, 125-169.

Chen, P., Aguilar, O.A., Rahim, M.M., Allan, D.S., Fine, J.H., Kirkham, C.L., Ma, J., Tanaka, M., Tu, M.M., Wight, A.*, et al.* (2015). Genetic investigation of MHC-independent missing-self recognition by mouse NK cells using an in vivo bone marrow transplantation model. J Immunol *194*, 2909-2918.

Chen, P., Belanger, S., Aguilar, O.A., Zhang, Q., St-Laurent, A., Rahim, M.M., Makrigiannis, A.P., and Carlyle, J.R. (2011). Analysis of the mouse 129-strain Nkrp1-Clr gene cluster reveals conservation of genomic organization and functional receptor-ligand interactions despite significant allelic polymorphism. Immunogenetics *63*, 627-640.

Child, S.J., Hanson, L.K., Brown, C.E., Janzen, D.M., and Geballe, A.P. (2006). Double-stranded RNA binding by a heterodimeric complex of murine cytomegalovirus m142 and m143 proteins. J Virol *80*, 10173-10180.

Cooper, M.A., Elliott, J.M., Keyel, P.A., Yang, L., Carrero, J.A., and Yokoyama, W.M. (2009). Cytokine-induced memory-like natural killer cells. Proc Natl Acad Sci U S A *106*, 1915-1919.

Corbett, A.J., Coudert, J.D., Forbes, C.A., and Scalzo, A.A. (2011). Functional consequences of natural sequence variation of murine cytomegalovirus m157 for Ly49 receptor specificity and NK cell activation. J Immunol *186*, 1713-1722.

Daley-Bauer, L.P., Roback, L.J., Wynn, G.M., and Mocarski, E.S. (2014). Cytomegalovirus hijacks CX3CR1(hi) patrolling monocytes as immune-privileged vehicles for dissemination in mice. Cell Host Microbe *15*, 351-362.

Davis-Poynter, N., Yunis, J., and Farrell, H.E. (2016). The Cytoplasmic C-Tail of the Mouse Cytomegalovirus 7 Transmembrane Receptor Homologue, M78, Regulates Endocytosis of

the Receptor and Modulates Virus Replication in Different Cell Types. PLoS One *11*, e0165066.

Davis-Poynter, N.J., Lynch, D.M., Vally, H., Shellam, G.R., Rawlinson, W.D., Barrell, B.G., and Farrell, H.E. (1997). Identification and characterization of a G protein-coupled receptor homolog encoded by murine cytomegalovirus. J Virol *71*, 1521-1529.

De Obaldia, M.E., and Bhandoola, A. (2015). Transcriptional regulation of innate and adaptive lymphocyte lineages. Annu Rev Immunol *33*, 607-642.

Desrosiers, M.P., Kielczewska, A., Loredo-Osti, J.C., Adam, S.G., Makrigiannis, A.P., Lemieux, S., Pham, T., Lodoen, M.B., Morgan, K., Lanier, L.L.*, et al.* (2005). Epistasis between mouse Klra and major histocompatibility complex class I loci is associated with a new mechanism of natural killer cell-mediated innate resistance to cytomegalovirus infection. Nat Genet *37*, 593-599.

Diefenbach, A., Hsia, J.K., Hsiung, M.Y., and Raulet, D.H. (2003). A novel ligand for the NKG2D receptor activates NK cells and macrophages and induces tumor immunity. Eur J Immunol *33*, 381-391.

Dokun, A.O., Kim, S., Smith, H.R., Kang, H.S., Chu, D.T., and Yokoyama, W.M. (2001). Specific and nonspecific NK cell activation during virus infection. Nat Immunol *2*, 951-956.

Dolken, L., Perot, J., Cognat, V., Alioua, A., John, M., Soutschek, J., Ruzsics, Z., Koszinowski, U., Voinnet, O., and Pfeffer, S. (2007). Mouse cytomegalovirus microRNAs dominate the cellular small RNA profile during lytic infection and show features of posttranscriptional regulation. J Virol *81*, 13771-13782.

Dorsch-Hasler, K., Keil, G.M., Weber, F., Jasin, M., Schaffner, W., and Koszinowski, U.H. (1985). A long and complex enhancer activates transcription of the gene coding for the highly abundant immediate early mRNA in murine cytomegalovirus. Proc Natl Acad Sci U S A *82*, 8325-8329.

Ettinger, J., Geyer, H., Nitsche, A., Zimmermann, A., Brune, W., Sandford, G.R., Hayward, G.S., and Voigt, S. (2012). Complete genome sequence of the english isolate of rat cytomegalovirus (Murid herpesvirus 8). J Virol *86*, 13838.

Farrell, H.E., Vally, H., Lynch, D.M., Fleming, P., Shellam, G.R., Scalzo, A.A., and Davis-Poynter, N.J. (1997). Inhibition of natural killer cells by a cytomegalovirus MHC class I homologue in vivo. Nature *386*, 510-514.

Fine, J.H., Chen, P., Mesci, A., Allan, D.S., Gasser, S., Raulet, D.H., and Carlyle, J.R. (2010). Chemotherapy-induced genotoxic stress promotes sensitivity to natural killer cell cytotoxicity by enabling missing-self recognition. Cancer Res *70*, 7102-7113.

Fuchs, A., Cella, M., Giurisato, E., Shaw, A.S., and Colonna, M. (2004). Cutting edge: CD96 (tactile) promotes NK cell-target cell adhesion by interacting with the poliovirus receptor (CD155). J Immunol *172*, 3994-3998.

Germain, C., Bihl, F., Zahn, S., Poupon, G., Dumaurier, M.J., Rampanarivo, H.H., Padkjaer, S.B., Spee, P., and Braud, V.M. (2010). Characterization of alternatively spliced transcript variants of CLEC2D gene. J Biol Chem *285*, 36207-36215.

Germain, C., Meier, A., Jensen, T., Knapnougel, P., Poupon, G., Lazzari, A., Neisig, A., Hakansson, K., Dong, T., Wagtmann, N.*, et al.* (2011). Induction of lectin-like transcript 1 (LLT1) protein cell surface expression by pathogens and interferon-gamma contributes to modulate immune responses. J Biol Chem *286*, 37964-37975.

Glimcher, L., Shen, F.W., and Cantor, H. (1977). Identification of a cell-surface antigen selectively expressed on the natural killer cell. J Exp Med *145*, 1-9.

Greene, T.T., Tokuyama, M., Knudsen, G.M., Kunz, M., Lin, J., Greninger, A.L., DeFilippis, V.R., DeRisi, J.L., Raulet, D.H., and Coscoy, L. (2016). A Herpesviral induction of RAE-1 NKG2D ligand expression occurs through release of HDAC mediated repression. Elife *5*.

Griffiths, P., Baraniak, I., and Reeves, M. (2015). The pathogenesis of human cytomegalovirus. J Pathol *235*, 288-297.

Groh, V., Wu, J., Yee, C., and Spies, T. (2002). Tumour-derived soluble MIC ligands impair expression of NKG2D and T-cell activation. Nature *419*, 734-738.

Hanke, T., Takizawa, H., McMahon, C.W., Busch, D.H., Pamer, E.G., Miller, J.D., Altman, J.D., Liu, Y., Cado, D., Lemonnier, F.A.*, et al.* (1999). Direct assessment of MHC class I binding by seven Ly49 inhibitory NK cell receptors. Immunity *11*, 67-77.

Hasan, M., Krmpotic, A., Ruzsics, Z., Bubic, I., Lenac, T., Halenius, A., Loewendorf, A., Messerle, M., Hengel, H., Jonjic, S.*, et al.* (2005). Selective down-regulation of the NKG2D ligand H60 by mouse cytomegalovirus m155 glycoprotein. J Virol *79*, 2920-2930.

Henry, S.C., Schmader, K., Brown, T.T., Miller, S.E., Howell, D.N., Daley, G.G., and Hamilton, J.D. (2000). Enhanced green fluorescent protein as a marker for localizing murine cytomegalovirus in acute and latent infection. J Virol Methods *89*, 61-73.

Hoglund, P., and Brodin, P. (2010). Current perspectives of natural killer cell education by MHC class I molecules. Nat Rev Immunol *10*, 724-734.

Hou, S., Hyland, L., Ryan, K.W., Portner, A., and Doherty, P.C. (1994). Virus-specific CD8+ T-cell memory determined by clonal burst size. Nature *369*, 652-654.

Iizuka, K., Naidenko, O.V., Plougastel, B.F., Fremont, D.H., and Yokoyama, W.M. (2003). Genetically linked C-type lectin-related ligands for the NKRP1 family of natural killer cell receptors. Nat Immunol *4*, 801-807.

Jarahian, M., Fiedler, M., Cohnen, A., Djandji, D., Hammerling, G.J., Gati, C., Cerwenka, A., Turner, P.C., Moyer, R.W., Watzl, C.*, et al.* (2011). Modulation of NKp30- and NKp46-mediated natural killer cell responses by poxviral hemagglutinin. PLoS Pathog *7*, e1002195.

Jonjic, S., Mutter, W., Weiland, F., Reddehase, M.J., and Koszinowski, U.H. (1989). Site-restricted persistent cytomegalovirus infection after selective long-term depletion of CD4+ T lymphocytes. J Exp Med *169*, 1199-1212.

Jonjic, S., Pavic, I., Polic, B., Crnkovic, I., Lucin, P., and Koszinowski, U.H. (1994). Antibodies are not essential for the resolution of primary cytomegalovirus infection but limit dissemination of recurrent virus. J Exp Med *179*, 1713-1717.

Jordan, S., Krause, J., Prager, A., Mitrovic, M., Jonjic, S., Koszinowski, U.H., and Adler, B. (2011). Virus progeny of murine cytomegalovirus bacterial artificial chromosome pSM3fr show reduced growth in salivary Glands due to a fixed mutation of MCK-2. J Virol *85*, 10346-10353.

Juranic Lisnic, V., Babic Cac, M., Lisnic, B., Trsan, T., Mefferd, A., Das Mukhopadhyay, C., Cook, C.H., Jonjic, S., and Trgovcich, J. (2013). Dual analysis of the murine cytomegalovirus and host cell transcriptomes reveal new aspects of the virus-host cell interface. PLoS Pathog *9*, e1003611.

Kalejta, R.F. (2008). Tegument proteins of human cytomegalovirus. Microbiol Mol Biol Rev *72*, 249-265, table of contents.

Karlhofer, F.M., and Yokoyama, W.M. (1991). Stimulation of murine natural killer (NK) cells by a monoclonal antibody specific for the NK1.1 antigen. IL-2-activated NK cells possess additional specific stimulation pathways. J Immunol *146*, 3662-3673.

Karre, K., Ljunggren, H.G., Piontek, G., and Kiessling, R. (1986). Selective rejection of H-2-deficient lymphoma variants suggests alternative immune defence strategy. Nature *319*, 675-678.

Kartsogiannis, V., Sims, N.A., Quinn, J.M., Ly, C., Cipetic, M., Poulton, I.J., Walker, E.C., Saleh, H., McGregor, N.E., Wallace, M.E.*, et al.* (2008). Osteoclast inhibitory lectin, an immune cell product that is required for normal bone physiology in vivo. J Biol Chem *283*, 30850-30860.

Keil, G.M., Ebeling-Keil, A., and Koszinowski, U.H. (1987). Sequence and structural organization of murine cytomegalovirus immediate-early gene 1. J Virol *61*, 1901-1908.

Kielczewska, A., Pyzik, M., Sun, T., Krmpotic, A., Lodoen, M.B., Munks, M.W., Babic, M., Hill, A.B., Koszinowski, U.H., Jonjic, S.*, et al.* (2009). Ly49P recognition of cytomegalovirus-infected cells expressing H2-Dk and CMV-encoded m04 correlates with the NK cell antiviral response. J Exp Med *206*, 515-523.

Kiessling, R., Klein, E., Pross, H., and Wigzell, H. (1975a). "Natural" killer cells in the mouse. II. Cytotoxic cells with specificity for mouse Moloney leukemia cells. Characteristics of the killer cell. Eur J Immunol *5*, 117-121.

Kiessling, R., Klein, E., and Wigzell, H. (1975b). "Natural" killer cells in the mouse. I. Cytotoxic cells with specificity for mouse Moloney leukemia cells. Specificity and distribution according to genotype. Eur J Immunol *5*, 112-117.

Kim, S., Poursine-Laurent, J., Truscott, S.M., Lybarger, L., Song, Y.J., Yang, L., French, A.R., Sunwoo, J.B., Lemieux, S., Hansen, T.H.*, et al.* (2005). Licensing of natural killer cells by host major histocompatibility complex class I molecules. Nature *436*, 709-713.

Kirkham, C.L., Aguilar, O.A., Yu, T., Tanaka, M., Mesci, A., Chu, K.L., Fine, J.H., Mossman, K.L., Bremner, R., Allan, D.S.*, et al.* (2017). Interferon-dependent induction of Clr-b during MCMV infection protects bystander cells from NK cells via NKR-P1B-mediated inhibition. J Innate Immun.

Kirkham, C.L., and Carlyle, J.R. (2014). Complexity and Diversity of the NKR-P1:Clr (Klrb1:Clec2) Recognition Systems. Front Immunol *5*, 214.

Kleijnen, M.F., Huppa, J.B., Lucin, P., Mukherjee, S., Farrell, H., Campbell, A.E., Koszinowski, U.H., Hill, A.B., and Ploegh, H.L. (1997). A mouse cytomegalovirus glycoprotein, gp34,

forms a complex with folded class I MHC molecules in the ER which is not retained but is transported to the cell surface. EMBO J *16*, 685-694.

Klenerman, P., and Oxenius, A. (2016). T cell responses to cytomegalovirus. Nat Rev Immunol *16*, 367-377.

Koo, G.C., and Peppard, J.R. (1984). Establishment of monoclonal anti-Nk-1.1 antibody. Hybridoma *3*, 301-303.

Krmpotic, A., Bubic, I., Polic, B., Lucin, P., and Jonjic, S. (2003). Pathogenesis of murine cytomegalovirus infection. Microbes Infect *5*, 1263-1277.

Krmpotic, A., Busch, D.H., Bubic, I., Gebhardt, F., Hengel, H., Hasan, M., Scalzo, A.A., Koszinowski, U.H., and Jonjic, S. (2002). MCMV glycoprotein gp40 confers virus resistance to CD8+ T cells and NK cells in vivo. Nat Immunol *3*, 529-535.

Krmpotic, A., Hasan, M., Loewendorf, A., Saulig, T., Halenius, A., Lenac, T., Polic, B., Bubic, I., Kriegeskorte, A., Pernjak-Pugel, E*., et al.* (2005). NK cell activation through the NKG2D ligand MULT-1 is selectively prevented by the glycoprotein encoded by mouse cytomegalovirus gene m145. J Exp Med *201*, 211-220.

Kumar, V., and McNerney, M.E. (2005). A new self: MHC-class-I-independent natural-killer-cell self-tolerance. Nat Rev Immunol *5*, 363-374.

Kung, S.K., Su, R.C., Shannon, J., and Miller, R.G. (1999). The NKR-P1B gene product is an inhibitory receptor on SJL/J NK cells. J Immunol *162*, 5876-5887.

Kurz, S.K., and Reddehase, M.J. (1999). Patchwork pattern of transcriptional reactivation in the lungs indicates sequential checkpoints in the transition from murine cytomegalovirus latency to recurrence. J Virol *73*, 8612-8622.

Kveberg, L., Dai, K.Z., Inngjerdingen, M., Brooks, C.G., Fossum, S., and Vaage, J.T. (2011). Phylogenetic and functional conservation of the NKR-P1F and NKR-P1G receptors in rat and mouse. Immunogenetics *63*, 429-436.

Kveberg, L., Dai, K.Z., Westgaard, I.H., Daws, M.R., Fossum, S., Naper, C., and Vaage, J.T. (2009). Two major groups of rat NKR-P1 receptors can be distinguished based on chromosomal localization, phylogenetic analysis and Clr ligand binding. Eur J Immunol *39*, 541-551.

Kveberg, L., Sudworth, A., Todros-Dawda, I., Inngjerdingen, M., and Vaage, J.T. (2015). Functional characterization of a conserved pair of NKR-P1 receptors expressed by NK cells and T lymphocytes in liver and gut. Eur J Immunol *45*, 501-512.

Lanier, L.L. (2005). NK cell recognition. Annu Rev Immunol *23*, 225-274.

Lanier, L.L. (2008). Evolutionary struggles between NK cells and viruses. Nat Rev Immunol *8*, 259-268.

Lanier, L.L., Chang, C., and Phillips, J.H. (1994). Human NKR-P1A. A disulfide-linked homodimer of the C-type lectin superfamily expressed by a subset of NK and T lymphocytes. J Immunol *153*, 2417-2428.

Lawson, C.M., Grundy, J.E., and Shellam, G.R. (1988). Antibody responses to murine cytomegalovirus in genetically resistant and susceptible strains of mice. J Gen Virol *69 (Pt 8)*, 1987-1998.

Lee, S.H., Girard, S., Macina, D., Busa, M., Zafer, A., Belouchi, A., Gros, P., and Vidal, S.M. (2001). Susceptibility to mouse cytomegalovirus is associated with deletion of an activating natural killer cell receptor of the C-type lectin superfamily. Nat Genet *28*, 42-45.

Leibelt, S., Friede, M.E., Rohe, C., Gutle, D., Rutkowski, E., Weigert, A., Kveberg, L., Vaage, J.T., Hornef, M.W., and Steinle, A. (2015). Dedicated immunosensing of the mouse intestinal epithelium facilitated by a pair of genetically coupled lectin-like receptors. Mucosal Immunol *8*, 232-242.

Lenac Rovis, T., Kucan Brlic, P., Kaynan, N., Juranic Lisnic, V., Brizic, I., Jordan, S., Tomic, A., Kvestak, D., Babic, M., Tsukerman, P.*, et al.* (2016). Inflammatory monocytes and NK cells play a crucial role in DNAM-1-dependent control of cytomegalovirus infection. J Exp Med *213*, 1835-1850.

Lenac, T., Budt, M., Arapovic, J., Hasan, M., Zimmermann, A., Simic, H., Krmpotic, A., Messerle, M., Ruzsics, Z., Koszinowski, U.H.*, et al.* (2006). The herpesviral Fc receptor fcr-1 down-regulates the NKG2D ligands MULT-1 and H60. J Exp Med *203*, 1843-1850.

Li, T., Chen, J., and Cristea, I.M. (2013a). Human cytomegalovirus tegument protein pUL83 inhibits IFI16-mediated DNA sensing for immune evasion. Cell Host Microbe *14*, 591-599.

Li, X., Shu, C., Yi, G., Chaton, C.T., Shelton, C.L., Diao, J., Zuo, X., Kao, C.C., Herr, A.B., and Li, P. (2013b). Cyclic GMP-AMP synthase is activated by double-stranded DNA-induced oligomerization. Immunity *39*, 1019-1031.

Liao, N.S., Bix, M., Zijlstra, M., Jaenisch, R., and Raulet, D. (1991). MHC class I deficiency: susceptibility to natural killer (NK) cells and impaired NK activity. Science *253*, 199-202.

Lin, A., Xu, H., and Yan, W. (2007). Modulation of HLA expression in human cytomegalovirus immune evasion. Cell Mol Immunol *4*, 91-98.

Lisnic, B., Lisnic, V.J., and Jonjic, S. (2015). NK cell interplay with cytomegaloviruses. Curr Opin Virol *15*, 9-18.

Little, S.P., Jofre, J.T., Courtney, R.J., and Schaffer, P.A. (1981). A virion-associated glycoprotein essential for infectivity of herpes simplex virus type 1. Virology *115*, 149-160.

Lodoen, M., Ogasawara, K., Hamerman, J.A., Arase, H., Houchins, J.P., Mocarski, E.S., and Lanier, L.L. (2003). NKG2D-mediated natural killer cell protection against cytomegalovirus is impaired by viral gp40 modulation of retinoic acid early inducible 1 gene molecules. J Exp Med *197*, 1245-1253.

Lodoen, M.B., Abenes, G., Umamoto, S., Houchins, J.P., Liu, F., and Lanier, L.L. (2004). The cytomegalovirus m155 gene product subverts natural killer cell antiviral protection by disruption of H60-NKG2D interactions. J Exp Med *200*, 1075-1081.

Loewendorf, A., Kruger, C., Borst, E.M., Wagner, M., Just, U., and Messerle, M. (2004). Identification of a mouse cytomegalovirus gene selectively targeting CD86 expression on antigen-presenting cells. J Virol *78*, 13062-13071.

Malmberg, K.J., Beziat, V., and Ljunggren, H.G. (2012). Spotlight on NKG2C and the human NK-cell response to CMV infection. Eur J Immunol *42*, 3141-3145.

Mans, J. (2008). Characterization of mouse cytomgelaovirus MHC-1 homologs (Doctoral dissertation) (Johannesburg: University of Witwatersrand), pp. 190.

Mans, J., Natarajan, K., Balbo, A., Schuck, P., Eikel, D., Hess, S., Robinson, H., Simic, H., Jonjic, S., Tiemessen, C.T.*, et al.* (2007). Cellular expression and crystal structure of the murine cytomegalovirus major histocompatibility complex class I-like glycoprotein, m153. J Biol Chem *282*, 35247-35258.

Marcinowski, L., Lidschreiber, M., Windhager, L., Rieder, M., Bosse, J.B., Radle, B., Bonfert, T., Gyory, I., de Graaf, M., Prazeres da Costa, O.*, et al.* (2012). Real-time transcriptional profiling of cellular and viral gene expression during lytic cytomegalovirus infection. PLoS Pathog *8*, e1002908.

Mariathasan, S., Newton, K., Monack, D.M., Vucic, D., French, D.M., Lee, W.P., Roose-Girma, M., Erickson, S., and Dixit, V.M. (2004). Differential activation of the inflammasome by caspase-1 adaptors ASC and Ipaf. Nature *430*, 213-218.

Marks, J.R., and Spector, D.H. (1984). Fusion of the termini of the murine cytomegalovirus genome after infection. J Virol *52*, 24-28.

Martick, M., Horan, L.H., Noller, H.F., and Scott, W.G. (2008). A discontinuous hammerhead ribozyme embedded in a mammalian messenger RNA. Nature *454*, 899-902.

Melnychuk, R.M., Smith, P., Kreklywich, C.N., Ruchti, F., Vomaske, J., Hall, L., Loh, L., Nelson, J.A., Orloff, S.L., and Streblow, D.N. (2005). Mouse cytomegalovirus M33 is necessary and sufficient in virus-induced vascular smooth muscle cell migration. J Virol *79*, 10788-10795.

Mesci, A. (2011). The Role of NKR-P1B:Clr-b Recognition in NK cell-mediated Immunity to Cytomegalovirus Infection (University of Toronto, 2011.), pp. 197 leaves.

Mesci, A., and Carlyle, J.R. (2007). A rapid and efficient method for the generation and screening of monoclonal antibodies specific for cell surface antigens. J Immunol Methods *323*, 78-87.

Mesci, A., Ljutic, B., Makrigiannis, A.P., and Carlyle, J.R. (2006). NKR-P1 biology: from prototype to missing self. Immunol Res *35*, 13-26.

Messerle, M., Buhler, B., Keil, G.M., and Koszinowski, U.H. (1992). Structural organization, expression, and functional characterization of the murine cytomegalovirus immediate-early gene 3. J Virol *66*, 27-36.

Messerle, M., Keil, G.M., and Koszinowski, U.H. (1991). Structure and expression of murine cytomegalovirus immediate-early gene 2. J Virol *65*, 1638-1643.

Mintern, J.D., Klemm, E.J., Wagner, M., Paquet, M.E., Napier, M.D., Kim, Y.M., Koszinowski, U.H., and Ploegh, H.L. (2006). Viral interference with B7-1 costimulation: a new role for murine cytomegalovirus fc receptor-1. J Immunol *177*, 8422-8431.

Misra, V., Muller, M.T., Chantler, J.K., and Hudson, J.B. (1978). Regulation of murine cytomegalovirus gene expression. I. Transcription during productive infection. J Virol *27*, 263-268.

Moon, H.M., Sapienza, V.J., Carp, R.I., and Kim, K.S. (1976). DNA synthesis in mouse embryo fibroblast cells infected with murine cytomegalovirus. Virology *75*, 376-383.

Muller, M., Misra, V., Chantler, J.K., and Hudson, J.B. (1978). Murine cytomegalovirus gene expression during nonproductive infection in Go-phase 3T3 cells. Virology *90*, 279-287.

Muller, M.T., and Hudson, J.B. (1977). Cell cycle dependency of murine cytomegalovirus replication in synchronized 3T3 cells. J Virol *22*, 267-272.

Murphy, K., Travers, P., Walport, M., and Janeway, C. (2012). Janeway's immunobiology, 8th edn (New York: Garland Science).

O'Leary, J.G., Goodarzi, M., Drayton, D.L., and von Andrian, U.H. (2006). T cell- and B cell-independent adaptive immunity mediated by natural killer cells. Nat Immunol *7*, 507-516.

Oliveira, S.A., Park, S.H., Lee, P., Bendelac, A., and Shenk, T.E. (2002). Murine cytomegalovirus m02 gene family protects against natural killer cell-mediated immune surveillance. J Virol *76*, 885-894.

Orr, M.T., and Lanier, L.L. (2011). Inhibitory Ly49 receptors on mouse natural killer cells. Curr Top Microbiol Immunol *350*, 67-87.

Orr, M.T., Murphy, W.J., and Lanier, L.L. (2010). 'Unlicensed' natural killer cells dominate the response to cytomegalovirus infection. Nat Immunol *11*, 321-327.

Parikh, B.A., Piersma, S.J., Pak-Wittel, M.A., Yang, L., Schreiber, R.D., and Yokoyama, W.M. (2015). Dual Requirement of Cytokine and Activation Receptor Triggering for Cytotoxic Control of Murine Cytomegalovirus by NK Cells. PLoS Pathog *11*, e1005323.

Parvatiyar, K., Zhang, Z., Teles, R.M., Ouyang, S., Jiang, Y., Iyer, S.S., Zaver, S.A., Schenk, M., Zeng, S., Zhong, W.*, et al.* (2012). The helicase DDX41 recognizes the bacterial secondary messengers cyclic di-GMP and cyclic di-AMP to activate a type I interferon immune response. Nat Immunol *13*, 1155-1161.

Paust, S., and von Andrian, U.H. (2011). Natural killer cell memory. Nat Immunol *12*, 500-508.

Pinto, A.K., Munks, M.W., Koszinowski, U.H., and Hill, A.B. (2006). Coordinated function of murine cytomegalovirus genes completely inhibits CTL lysis. J Immunol *177*, 3225-3234.

Plougastel, B., Dubbelde, C., and Yokoyama, W.M. (2001a). Cloning of Clr, a new family of lectin-like genes localized between mouse Nkrp1a and Cd69. Immunogenetics *53*, 209-214.

Plougastel, B., Matsumoto, K., Dubbelde, C., and Yokoyama, W.M. (2001b). Analysis of a 1-Mb BAC contig overlapping the mouse Nkrp1 cluster of genes: cloning of three new Nkrp1 members, Nkrp1d, Nkrp1e, and Nkrp1f. Immunogenetics *53*, 592-598.

Pyzik, M., Charbonneau, B., Gendron-Pontbriand, E.M., Babic, M., Krmpotic, A., Jonjic, S., and Vidal, S.M. (2011). Distinct MHC class I-dependent NK cell-activating receptors control cytomegalovirus infection in different mouse strains. J Exp Med *208*, 1105-1117.

Rahim, M.M., Chen, P., Mottashed, A.N., Mahmoud, A.B., Thomas, M.J., Zhu, Q., Brooks, C.G., Kartsogiannis, V., Gillespie, M.T., Carlyle, J.R., *et al.* (2015). The mouse NKR-P1B:Clr-b recognition system is a negative regulator of innate immune responses. Blood *125*, 2217-2227.

Rahim, M.M., Wight, A., Mahmoud, A.B., Aguilar, O.A., Lee, S.H., Vidal, S.M., Carlyle, J.R., and Makrigiannis, A.P. (2016). Expansion and Protection by a Virus-Specific NK Cell Subset Lacking Expression of the Inhibitory NKR-P1B Receptor during Murine Cytomegalovirus Infection. J Immunol *197*, 2325-2337.

Raulet, D.H. (2003). Roles of the NKG2D immunoreceptor and its ligands. Nat Rev Immunol *3*, 781-790.

Raulet, D.H., and Vance, R.E. (2006). Self-tolerance of natural killer cells. Nat Rev Immunol *6*, 520-531.

Raulet, D.H., Vance, R.E., and McMahon, C.W. (2001). Regulation of the natural killer cell receptor repertoire. Annu Rev Immunol *19*, 291-330.

Rawlinson, W.D., Farrell, H.E., and Barrell, B.G. (1996). Analysis of the complete DNA sequence of murine cytomegalovirus. J Virol *70*, 8833-8849.

Rebsamen, M., Heinz, L.X., Meylan, E., Michallet, M.C., Schroder, K., Hofmann, K., Vazquez, J., Benedict, C.A., and Tschopp, J. (2009). DAI/ZBP1 recruits RIP1 and RIP3 through RIP homotypic interaction motifs to activate NF-kappaB. EMBO Rep *10*, 916-922.

Reddehase, M.J. (2002). Antigens and immunoevasins: opponents in cytomegalovirus immune surveillance. Nat Rev Immunol *2*, 831-844.

Reddehase, M.J., Jonjic, S., Weiland, F., Mutter, W., and Koszinowski, U.H. (1988). Adoptive immunotherapy of murine cytomegalovirus adrenalitis in the immunocompromised host: CD4-helper-independent antiviral function of CD8-positive memory T lymphocytes derived from latently infected donors. J Virol *62*, 1061-1065.

Reddehase, M.J., Weiland, F., Munch, K., Jonjic, S., Luske, A., and Koszinowski, U.H. (1985). Interstitial murine cytomegalovirus pneumonia after irradiation: characterization of cells that limit viral replication during established infection of the lungs. J Virol *55*, 264-273.

Reusch, U., Muranyi, W., Lucin, P., Burgert, H.G., Hengel, H., and Koszinowski, U.H. (1999). A cytomegalovirus glycoprotein re-routes MHC class I complexes to lysosomes for degradation. EMBO J *18*, 1081-1091.

Riddell, S.R., Watanabe, K.S., Goodrich, J.M., Li, C.R., Agha, M.E., and Greenberg, P.D. (1992). Restoration of viral immunity in immunodeficient humans by the adoptive transfer of T cell clones. Science *257*, 238-241.

Rosen, D.B., Bettadapura, J., Alsharifi, M., Mathew, P.A., Warren, H.S., and Lanier, L.L. (2005). Cutting edge: lectin-like transcript-1 is a ligand for the inhibitory human NKR-P1A receptor. J Immunol *175*, 7796-7799.

Rosen, D.B., Cao, W., Avery, D.T., Tangye, S.G., Liu, Y.J., Houchins, J.P., and Lanier, L.L. (2008). Functional consequences of interactions between human NKR-P1A and its ligand LLT1 expressed on activated dendritic cells and B cells. J Immunol *180*, 6508-6517.

Rutkowski, E., Leibelt, S., Born, C., Friede, M.E., Bauer, S., Weil, S., Koch, J., and Steinle, A. (2016). Clr-a: A Novel Immune-Related C-Type Lectin-like Molecule Exclusively Expressed by Mouse Gut Epithelium. J Immunol.

Ryan, J.C., Turck, J., Niemi, E.C., Yokoyama, W.M., and Seaman, W.E. (1992). Molecular cloning of the NK1.1 antigen, a member of the NKR-P1 family of natural killer cell activation molecules. J Immunol *149*, 1631-1635.

Salih, H.R., Rammensee, H.G., and Steinle, A. (2002). Cutting edge: down-regulation of MICA on human tumors by proteolytic shedding. J Immunol *169*, 4098-4102.

Sanderson, S., and Shastri, N. (1994). LacZ inducible, antigen/MHC-specific T cell hybrids. Int Immunol *6*, 369-376.

Schwartzberg, P.L., Mueller, K.L., Qi, H., and Cannons, J.L. (2009). SLAM receptors and SAP influence lymphocyte interactions, development and function. Nat Rev Immunol *9*, 39-46.

Scott, W.G., Martick, M., and Chi, Y.I. (2009). Structure and function of regulatory RNA elements: ribozymes that regulate gene expression. Biochim Biophys Acta *1789*, 634-641.

Serafini, N., Vosshenrich, C.A., and Di Santo, J.P. (2015). Transcriptional regulation of innate lymphoid cell fate. Nat Rev Immunol *15*, 415-428.

Shellam, G.R., Redwood, A.J., Smith, L.M., and Gorman, S. (2007). Murine cytomegaloviruses and other herpesviruses. In The mouse in biomedical research, J.G. Fox, ed. (Amsterdam ; Boston, MA: Elsevier/Academic Press).

Sherrill, J.D., Stropes, M.P., Schneider, O.D., Koch, D.E., Bittencourt, F.M., Miller, J.L., and Miller, W.E. (2009). Activation of intracellular signaling pathways by the murine cytomegalovirus G protein-coupled receptor M33 occurs via PLC-{beta}/PKC-dependent and -independent mechanisms. J Virol *83*, 8141-8152.

Smith, H.R., Heusel, J.W., Mehta, I.K., Kim, S., Dorner, B.G., Naidenko, O.V., Iizuka, K., Furukawa, H., Beckman, D.L., Pingel, J.T.*, et al.* (2002). Recognition of a virus-encoded ligand by a natural killer cell activation receptor. Proc Natl Acad Sci U S A *99*, 8826-8831.

Smith, L.M., McWhorter, A.R., Shellam, G.R., and Redwood, A.J. (2013). The genome of murine cytomegalovirus is shaped by purifying selection and extensive recombination. Virology *435*, 258-268.

Smith, M.G. (1954). Propagation of salivary gland virus of the mouse in tissue cultures. Proc Soc Exp Biol Med *86*, 435-440.

Smith, M.G. (1956). Propagation in tissue cultures of a cytopathogenic virus from human salivary gland virus (SGV) disease. Proc Soc Exp Biol Med *92*, 424-430.

Spits, H., Bernink, J.H., and Lanier, L. (2016). NK cells and type 1 innate lymphoid cells: partners in host defense. Nat Immunol *17*, 758-764.

Spreu, J., Kuttruff, S., Stejfova, V., Dennehy, K.M., Schittek, B., and Steinle, A. (2010). Interaction of C-type lectin-like receptors NKp65 and KACL facilitates dedicated immune recognition of human keratinocytes. Proc Natl Acad Sci U S A *107*, 5100-5105.

Sun, J.C., Beilke, J.N., and Lanier, L.L. (2009). Adaptive immune features of natural killer cells. Nature *457*, 557-561.

Sun, J.C., and Lanier, L.L. (2011). NK cell development, homeostasis and function: parallels with CD8(+) T cells. Nat Rev Immunol *11*, 645-657.

Sweet, C. (1999). The pathogenicity of cytomegalovirus. FEMS Microbiol Rev *23*, 457-482.

Tahara-Hanaoka, S., Shibuya, K., Onoda, Y., Zhang, H., Yamazaki, S., Miyamoto, A., Honda, S., Lanier, L.L., and Shibuya, A. (2004). Functional characterization of DNAM-1 (CD226) interaction with its ligands PVR (CD155) and nectin-2 (PRR-2/CD112). Int Immunol *16*, 533-538.

Taylor, M.A., Ward, B., Schatzle, J.D., and Bennett, M. (2002). Perforin- and Fas-dependent mechanisms of natural killer cell-mediated rejection of incompatible bone marrow cell grafts. Eur J Immunol *32*, 793-799.

Tokuyama, M., Lorin, C., Delebecque, F., Jung, H., Raulet, D.H., and Coscoy, L. (2011). Expression of the RAE-1 family of stimulatory NK-cell ligands requires activation of the PI3K pathway during viral infection and transformation. PLoS Pathog *7*, e1002265.

Tripathy, S.K., Keyel, P.A., Yang, L., Pingel, J.T., Cheng, T.P., Schneeberger, A., and Yokoyama, W.M. (2008). Continuous engagement of a self-specific activation receptor induces NK cell tolerance. J Exp Med *205*, 1829-1841.

Tsutsui, Y., Kosugi, I., and Kawasaki, H. (2005). Neuropathogenesis in cytomegalovirus infection: indication of the mechanisms using mouse models. Rev Med Virol *15*, 327-345.

Valchanova, R.S., Picard-Maureau, M., Budt, M., and Brune, W. (2006). Murine cytomegalovirus m142 and m143 are both required to block protein kinase R-mediated shutdown of protein synthesis. J Virol *80*, 10181-10190.

Vance, R.E., Isberg, R.R., and Portnoy, D.A. (2009). Patterns of pathogenesis: discrimination of pathogenic and nonpathogenic microbes by the innate immune system. Cell Host Microbe *6*, 10-21.

Vance, R.E., Jamieson, A.M., and Raulet, D.H. (1999). Recognition of the class Ib molecule Qa-1(b) by putative activating receptors CD94/NKG2C and CD94/NKG2E on mouse natural killer cells. J Exp Med *190*, 1801-1812.

Vance, R.E., Kraft, J.R., Altman, J.D., Jensen, P.E., and Raulet, D.H. (1998). Mouse CD94/NKG2A is a natural killer cell receptor for the nonclassical major histocompatibility complex (MHC) class I molecule Qa-1(b). J Exp Med *188*, 1841-1848.

Veillette, A. (2006). NK cell regulation by SLAM family receptors and SAP-related adapters. Immunol Rev *214*, 22-34.

Verma, S., Loewendorf, A., Wang, Q., McDonald, B., Redwood, A., and Benedict, C.A. (2014). Inhibition of the TRAIL death receptor by CMV reveals its importance in NK cell-mediated antiviral defense. PLoS Pathog *10*, e1004268.

Vink, C., Beuken, E., and Bruggeman, C.A. (2000). Complete DNA sequence of the rat cytomegalovirus genome. J Virol *74*, 7656-7665.

Vivier, E., Tomasello, E., Baratin, M., Walzer, T., and Ugolini, S. (2008). Functions of natural killer cells. Nat Immunol *9*, 503-510.

Vivier, E., van de Pavert, S.A., Cooper, M.D., and Belz, G.T. (2016). The evolution of innate lymphoid cells. Nat Immunol *17*, 790-794.

Voigt, S., Mesci, A., Ettinger, J., Fine, J.H., Chen, P., Chou, W., and Carlyle, J.R. (2007). Cytomegalovirus evasion of innate immunity by subversion of the NKR-P1B:Clr-b missing-self axis. Immunity *26*, 617-627.

Voigt, S., Sandford, G.R., Ding, L., and Burns, W.H. (2001). Identification and characterization of a spliced C-type lectin-like gene encoded by rat cytomegalovirus. J Virol *75*, 603-611.

Voigt, V., Forbes, C.A., Tonkin, J.N., Degli-Esposti, M.A., Smith, H.R., Yokoyama, W.M., and Scalzo, A.A. (2003). Murine cytomegalovirus m157 mutation and variation leads to immune evasion of natural killer cells. Proc Natl Acad Sci U S A *100*, 13483-13488.

Wagner, F.M., Brizic, I., Prager, A., Trsan, T., Arapovic, M., Lemmermann, N.A., Podlech, J., Reddehase, M.J., Lemnitzer, F., Bosse, J.B.*, et al.* (2013). The viral chemokine MCK-2 of murine cytomegalovirus promotes infection as part of a gH/gL/MCK-2 complex. PLoS Pathog *9*, e1003493.

Wagner, M., Gutermann, A., Podlech, J., Reddehase, M.J., and Koszinowski, U.H. (2002). Major histocompatibility complex class I allele-specific cooperative and competitive interactions between immune evasion proteins of cytomegalovirus. J Exp Med *196*, 805-816.

Wagner, M., Jonjic, S., Koszinowski, U.H., and Messerle, M. (1999). Systematic excision of vector sequences from the BAC-cloned herpesvirus genome during virus reconstitution. J Virol *73*, 7056-7060.

Wagner, M., and Koszinowski, U.H. (2004). Mutagenesis of viral BACs with linear PCR fragments (ET recombination). Methods Mol Biol *256*, 257-268.

Waldhauer, I., and Steinle, A. (2008). NK cells and cancer immunosurveillance. Oncogene *27*, 5932-5943.

Walker, J.A., Barlow, J.L., and McKenzie, A.N. (2013). Innate lymphoid cells--how did we miss them? Nat Rev Immunol *13*, 75-87.

Walton, S.M., Mandaric, S., Torti, N., Zimmermann, A., Hengel, H., and Oxenius, A. (2011). Absence of cross-presenting cells in the salivary gland and viral immune evasion confine cytomegalovirus immune control to effector CD4 T cells. PLoS Pathog *7*, e1002214.

Welte, S., Kuttruff, S., Waldhauer, I., and Steinle, A. (2006). Mutual activation of natural killer cells and monocytes mediated by NKp80-AICL interaction. Nat Immunol *7*, 1334-1342.

Williams, K.J., Wilson, E., Davidson, C.L., Aguilar, O.A., Fu, L., Carlyle, J.R., and Burshtyn, D.N. (2012). Poxvirus infection-associated downregulation of C-type lectin-related-b prevents NK cell inhibition by NK receptor protein-1B. J Immunol *188*, 4980-4991.

Wu, J.D., Higgins, L.M., Steinle, A., Cosman, D., Haugk, K., and Plymate, S.R. (2004). Prevalent expression of the immunostimulatory MHC class I chain-related molecule is counteracted by shedding in prostate cancer. J Clin Invest *114*, 560-568.

Yokoyama, W.M., and Plougastel, B.F. (2003). Immune functions encoded by the natural killer gene complex. Nat Rev Immunol *3*, 304-316.

Yu, X., Harden, K., Gonzalez, L.C., Francesco, M., Chiang, E., Irving, B., Tom, I., Ivelja, S., Refino, C.J., Clark, H.*, et al.* (2009). The surface protein TIGIT suppresses T cell activation by promoting the generation of mature immunoregulatory dendritic cells. Nat Immunol *10*, 48-57.

Zarama, A., Perez-Carmona, N., Farre, D., Tomic, A., Borst, E.M., Messerle, M., Jonjic, S., Engel, P., and Angulo, A. (2014). Cytomegalovirus m154 hinders CD48 cell-surface expression and promotes viral escape from host natural killer cell control. PLoS Pathog *10*, e1004000.

Zhang, Q., Rahim, M.M., Allan, D.S., Tu, M.M., Belanger, S., Abou-Samra, E., Ma, J., Sekhon, H.S., Fairhead, T., Zein, H.S.*, et al.* (2012). Mouse Nkrp1-Clr gene cluster sequence and expression analyses reveal conservation of tissue-specific MHC-independent immunosurveillance. PLoS One *7*, e50561.

Zhou, H., Kartsogiannis, V., Hu, Y.S., Elliott, J., Quinn, J.M., McKinstry, W.J., Gillespie, M.T., and Ng, K.W. (2001). A novel osteoblast-derived C-type lectin that inhibits osteoclast formation. J Biol Chem *276*, 14916-14923.

Zhou, H., Kartsogiannis, V., Quinn, J.M., Ly, C., Gange, C., Elliott, J., Ng, K.W., and Gillespie, M.T. (2002). Osteoclast inhibitory lectin, a family of new osteoclast inhibitors. J Biol Chem *277*, 48808-48815.

Ziegler, H., Thale, R., Lucin, P., Muranyi, W., Flohr, T., Hengel, H., Farrell, H., Rawlinson, W., and Koszinowski, U.H. (1997). A mouse cytomegalovirus glycoprotein retains MHC class I complexes in the ERGIC/cis-Golgi compartments. Immunity *6*, 57-66.

Zimmermann, A., Trilling, M., Wagner, M., Wilborn, M., Bubic, I., Jonjic, S., Koszinowski, U., and Hengel, H. (2005). A cytomegaloviral protein reveals a dual role for STAT2 in IFN-{gamma} signaling and antiviral responses. J Exp Med *201*, 1543-1553.

Zook, E.C., and Kee, B.L. (2016). Development of innate lymphoid cells. Nat Immunol *17*, 775-782.

Appendices

Appendix 3.1. PCR primer list for Chapter 3.

Cloning of m02 family		
Gene	**Primer**	**Sequence (5'-3')**
m02	m02 Fwd	aaaactgcagATGGCAGCCGCTGTCGGGAGACGAGC
	m02 Rev	tccccccgggTCAACCGTCTCGAGCGTAGTCTCCG
m03	m03 Fwd	aaaactgcagATGACGATCGGTCGTGTAAGTTATCC
	m03 Rev	tccccccgggTTATCTATGGCTGTCGATCAGAATGG
m04	m04 Fwd	aaaactgcagATGTCTCTCACACATCGGCCGTTGTTGG
	m04 Rev	tccccccgggTTAGTTACTCTTAAGCGGTTTGAAGTTCGAGC
m05	m05 Fwd	aaaactgcagATGTGGCTTAGCGTGTGTCCATGTACC
	m05 Rev	tccccccgggTTAGTCTAAGATCTCGATGCTCTCC
m06	m06 Fwd	aaaactgcagATGCCCAGTTGGAGCGATACGTTGAC
	m06 Rev	tccccccgggTTATTTGGTAAGCAAGGGGGAAGTGAG
m07	m07 Fwd	aaaactgcagATGAGGGGATATACGGGCGATACGATGG
	m07 Rev	tccccccgggTTACATACTCACCGCAGGTGTGGGCGGTGACAGG
m08	m08 Fwd	aaaactgcagATGCGTCTCTATCTTGATCTATCACAG
	m08 Rev	tccccccgggTTAAGACGCAGGAGAGGATGTTGTACGGAGAGGC
m09	m09 Fwd	aaaactgcagATGAAACTCTTTTTCTCGAGTCGTCTG
	m09 Rev	tccccccgggTTAAGACGCACGAGATGCCGTTGAACGG
m10	m10 Fwd	aaaactgcagATGAAAGTCTCTCCAGATCGTCTGTTGC
	m10 Rev	tccccccgggTCACAACACACTGGTTGGTGGGGAATTCAGCG
m11	m11 Fwd	aaaactgcagATGGCTCACCGCTACCTGGGGAGATCGC
	m11 Rev	tccccccgggTTATGCAGCACTGGTTGATATGTGTAACGG
m12	m12 atg1 Fwd	aaaactgcagATGTCCACTTTTAGATGGTCGTCG
	m12 atg2 Fwd	aaaactgcagATGTTCCGTCACCACCTGACGTCG
	m12 Rev	tccccccgggTCATTTGAAGCGGTCGAAACCTCTGC
m13	m13 Fwd	aaaactgcagATGCGGACGATGTCTTTGTCGAAGTCAACG
	m13 Rev	tccccccgggCTAGCGGTTGCGGATTGCGGCACCG
m14	m14 Fwd	aaaactgcagATGCGTCGTCTGGGTATAGTTATTGTCATCG
	m14 Rev	tccccccgggTTATGACGAATGCTGACACATTTTCCGG
m15	m15 Fwd	aaaactgcagATGTACCGTCACGTCGGATATATCTTAC
	m15 Rev	tccccccgggTTAGATGAATATATAGATCCATAGG
m16	m16 Fwd	aaaactgcagATGGATCTATATATTCATCTAAAAATAATGAC
	m16 Rev	tccccccgggTTATGATAAAAGTATTGCGTATAAGACAC
Cloning of m145 family		
Gene	**Primer**	**Sequence (5'-3')**
m17	m17 Fwd	aacgcgaagctagcATGGGGACGGGAGGAAAGGCGG
	m17 Rev	aacgcgaaggatccTCAGACTTGGGGCAGACGCTGA
m144	m144 Fwd	aaacgcctcgagATGAGGGCTCTGGCGCTGAT
	m144 Rev	aaacgcggatccTCAAATGCTGGGATCTGGGA
m145	m145 Fwd	cgcccggaattcATGGACCGTCGGGTGGTCTCATACC

	m145 Rev	aacgcgaaggatccTCACGCCTCTATCGTCTTATACC
m146	m146 Fwd	aacgcgaagctagcATGACGACGCCGAGTCCGATTCGCG
	m146 Rev	aacgcgaaggatccTCACACGCACACGCAAGGCATTGG
m150	m150 Fwd	gcgaagctagcATGTGTATTGTCGCGGTTCTC
	m150 Rev	gcgaaggatccgaattcTCACACGTCCGTGCTCGACTCGCC
m151	m151 Fwd	gcgaagctagcATGATTGGCGTGATACGTGCGC
	m151 Rev	gcgaaggatccgaattcTTATCGAAAGCTGAGCTCGCTGTGG
m152	m152 Fwd	aacgcgaagctagcATGCTGGGCGCTATCACCTACTTGC
	m152 Rev	aacgcgaaggatccTCACCACACGCGGCAGTTGATG
m153	m153 Fwd	aaacgcctcgagATGATTCCCCTTCTCCTTCTG
	m153 Rev	aaacgcggatccTCACACCACATTCTCCTCCG
m154	m154 Fwd	gcgaagctagcATGCGGGCGATGTTACGGATATATGC
	m154 Rev	gcgaaggatccgaattcTCACACATAAGACTCGTCATAACC
m155	m155 Fwd	gcgaagctagcATGTCTGTACGAGTATGTGCTCTCC
	m155 Rev	gcgaaggatccgaattcTCATTTGTAGACGGGCGGGACGCTC
m157	m157 Fwd	aacgcgaagctagcATGGTCATCGTCCCCCTAGT
	m157 Rev	aacgcgaaggatccTCAAACGACCAGACGCATAA
m158	m158 Fwd	aacgcgaagctagcATGTTGTCGAGGTGGGGAACGCTGG
	m158 Rev	aacgcgaaggatccTCAGATTCTCCTGCGTTTCACACG
m159	m159 Fwd	aacgcgaagctagcATGTGGACGACGTCGTATTTTTTAATCGG
	m159 Rev	aacgcgaaggatccTCAGAGATCAGAGCACATAGTTTTCAATCG

Cloning of NKR-P1 Receptors

Gene	**Primer**	**Sequence (5'-3')**
NKR-P1A	Nkrp1a$^{B6/129/FVB}$ Fwd	gaattcctcgagATGGACACAGCAAGGGTCTA
	Nkrp1a$^{B6/129/FVB}$ Rev	aaaactgcagTCAGTGTCCATAACCCACATAG
NKR-P1B	Nkrp1b$^{B6/129/FVB}$ Fwd	gaattcctcgagATGGATTCAACAACACTGGTCTATGCAGA
	Nkrp1b^{B6} Rev	aaaactgcagTCAGGAGTCATTACACGGGGTTTCATGG
	Nkrp1b$^{129/FVB}$ Rev	aaaactgcagTCAGGAGTCATTACTCGGGGTT
NKR-P1C	Nkrp1c^{B6} Fwd	gaattcctcgagATGGACACAGCAAGTATCTACC
	Nkrp1c$^{129/FVB}$ Fwd	gaattcctcgagATGGACACAGCAAGGGTCTA
	Nkrp1c^{B6} Rev	aaaactgcagTCAGGAGTCATTACTCGGGG
	Nkrp1c$^{129/FVB}$ Rev	aaaactgcagTCAGGAGTCATTACTTGGGGTT
NKR-P1F	Nkrp1f$^{B6/129/FVB}$ Fwd	gaattcctcgagATGGACACATCAAAGGTCCATGG
	Nkrp1f$^{B6/FVB}$ Rev	aaaactgcagTCAGACATGTATCAGGGTCTT
	Nkrp1f^{129} Rev	aaaactgcagTCAGACATGTAGCAGGGTCTT
NKR-P1G	Nkrp1g$^{B6/129/FVB}$ Fwd	gaattcctcgagATGGATGCACCAGTGCTCTATGC
	Nkrp1g$^{B6/FVB}$ Rev	aaaactgcagTCAGACGTGTTTCAGTGTCTT
	Nkrp1g^{129} Rev	aaaactgcagTCAGATGTGTTTCAGTGTCTT

Construction of type-II NKR-P1 Reporters

Gene	**Primer**	**Sequence (5'-3')**
NKR-P1A	Nkrp1a$^{129/FVB}$ EC Fwd	gaattcctcgagCGAGTCCTAATACAAAAACC

	Nkrp1a$^{129/FVB}$ EC Rev	ataagaatgcggccgcTCAGTGTCCATAACCCACATAG
NKR-P1B	Nkrp1b$^{B6/FVB}$ EC Fwd	gaattcctcgagTCAGTACAAAAATCATCAGTAC
	Nkrp1b^{B6} EC Rev	ataagaatgcggccgcTCAGGAGTCATTACACGGG
	Nkrp1b^{FVB} EC Rev	ataagaatgcggccgcTCAGGAGTCATTACTCGGGGTT
NKR-P1C	Nkrp1c^{B6} EC Fwd	gaattcctcgagCGAGTCTTAGTACAAAAACC
	Nkrp1c$^{129/FVB}$ EC Fwd	gaattcctcgagCGAGTCCTAATACAAAAACC
	Nkrp1c^{B6} EC Rev	ataagaatgcggccgcTCAGGAGTCATTACTCGGG
	Nkrp1c$^{129/FVB}$ EC Rev	ataagaatgcggccgcTCAGGAGTCATTACTTGGGGTTTCA
NKR-P1F	Nkrp1f^{FVB} EC Fwd	gaattcctcgagAGATTCCTAGTGCAAAAACC
	Nkrp1f^{FVB} EC Rev	ataagaatgcggccgcTCAGACATGTATCAGGGTCTTTTGG
NKR-P1G	Nkrp1g^{FVB} EC Fwd	gaattcctcgagCAAAAACCTCTAATAGAAAAATGC
	Nkrp1g^{FVB} EC Rev	ataagaatgcggccgcTCAGACGTGTTTCAGTGTCTTTTGG

Note: Additional primers have previously been described in Chen *et al*. 2011, *Immunogenetics*

Construction of type-I m12 Reporters

Gene	Primer	Sequence (5'-3')
m12 EC	m12 Fwd	gaattcctcgagATGTTCCGTCACCACCTGACGTCG
	m12 NF-PSP Fwd	gaattcctcgagATGTCTGCACTTCTGATCCTAGCTCTTGTTGG
	m12 EC Rev	ataagaatgcggccgcCGTGCCGTTATCTACTGTTCGTGTCGATGTTGG

N-terminally FLAG tagging of m12

Gene	Primer	Sequence (5'-3')
NT - FLAG	m12 NF FPATG	aaaactgcagATGGACTACAAGGACGACGACGACAAGGGATCAGGATCAA TGTTCCGTCACCACCTGACGTCG
NSP 1	m12 NF_NSP_F1	atcgataacgttaccgctagcacaggcaGACTACAAGGACGACGACGACAAGGGATC AGGATCAacgaatgttcttgctgcacc
NSP 2	m12 NF_NSP_F2P	aaaactgcagATGTTCCGTCACCACCTGACGTCGtttatcaccgtcacattctcgctcgcatcg atatcgataacgttaccgctag
PSP 1	m12 NF_PSP_F1	GCCGTTGCTGACTACAAGGACGACGACGACAAGGGATCAGGATCAac gaatgttcttgctgcacc
PSP 2	m12 NF_PSP_F2P	aaaactgcagATGTCTGCACTTCTGATCCTAGCTCTTGTTGGAGCTGCCGTT GCTGACTACAAGGA

Construction of m12 C4A variant

Gene	Primer	Sequence (5'-3')
m12 C4A	m12 C4A F1	TCGCATCGATATCGATAACGTTACCGCTAGCACAGGCAACGAATGTT CTTGCTGtACCAA
	m12 C4A F2	aaaactgcagATGTTCCGTCACCACCTGACGTCGTTTATCACCGTCACATTC TCGCTCGCATCGATATCGA

qRT-PCR primers

Gene	Primer	Sequence (5'-3')
m12	m12 qPCR Fwd	CGTGAATAAACAAGCCGCGA
	m12 qPCR Rev	TCTCTGTTGTCCTGTGTGCG
ie1/3	ie1/3 qPCR Fwd	CCCCTCGAGGACACACAATG
	ie1/3 qPCR Rev	GTTCTCATCCAAGTGACGGC

Clec2d	Clec2d qPCR Fwd	AGCTCCTCAGCTCTGAGATGTGTG
	Clec2d qPCR Rev	AGGGGAGATGGTTCCGTGCCTTT
Tbp	Tbp qPCR Fwd	AGAGCCACGGACAACTGCGTTG
	Tbp qPCR Rev	CTGGGAAGCCCAACTTCTGCAC

Appendix 3.2. RPKM values of viral gene expression 24 hours post-infection in NIH3T3.

	RPKM Values	
Gene	**MCMV-GFP**	**MW97.01**
m01	648.43	669.93
m02	1733.68	3174.85
m03	6577.96	6560.36
m04	18718.41	5835.71
m05	2251.15	4168.92
m06	10223.22	9663.51
m07	792.98	2337.72
m08	936.81	3577.21
m09	99.25	823.01
m10	349.20	1774.58
m11	517.32	832.18
m12	1206.27	2383.49
m13	4912.69	4795.42
m14	2554.60	7442.80
m15	159.84	8700.37
m16	317.61	7201.19
m17	4953.73	3801.70
m18	2441.09	1116.93
m19	11309.51	3951.73
m20	6626.82	2941.24
m21	3277.63	1991.01
m22	1755.96	2100.75
M23	403.68	1688.10
m23.1	1332.51	338.23
M24	807.57	1052.26
M25	6233.25	4729.28
m25.1	5730.54	10488.75
m25.2	6363.36	8812.59
m25.3	7868.86	8660.07
m25.4	1050.63	11345.79
M26	2855.97	2639.96
M27	1103.74	591.68
M28	7059.57	3511.79
m29	7938.82	5890.48
m29.1	8657.63	4598.29
m30	965.92	3209.28
M31	943.16	2658.94
M32	12714.17	6700.88

M34	2135.06	2415.40
M35	2136.04	2029.55
M37	8595.53	3345.92
M38	6540.54	3678.17
m39	2769.15	3142.50
m40	2775.49	1286.70
m41	17075.34	7135.01
m42	4168.49	2618.39
M43	14785.95	18930.66
M44	13709.46	27155.73
m45.1	1910.54	2286.86
M46	1904.35	3078.09
m48.1	36283.10	59279.11
m48.2	38079.95	61784.46
M49	9843.50	14433.92
M50	1121.78	5021.19
M51	989.36	1276.57
M52	2111.48	2012.02
M53	14946.46	5422.19
M55	23767.36	17983.28
M56	9811.82	7886.85
m58	478.93	394.96
m59	608.91	449.05
M69	245.83	1296.36
m69.1	496.00	893.45
M70	473.17	520.75
M71	3728.12	1763.61
M72	12457.60	5082.29
M73	27422.69	15302.34
m74	4391.26	8994.57
M75	2292.27	2136.23
M76	3158.74	3499.53
M77	1803.61	2537.67
M78	16157.64	19863.52
M79	3913.45	1967.23
M80	11702.22	9981.45
M82	462.27	11541.02
M83	1573.97	9502.71
M84	1013.22	5305.13
M85	6316.45	7779.06
M87	2751.32	2755.57
M88	5225.81	2127.53
m90	3451.79	3401.70

M91	4964.18	1294.29
M92	4161.55	2847.11
M93	15491.38	6053.51
M94	71835.49	21225.33
M95	8452.04	2659.91
M96	14606.97	5556.95
M97	6084.93	4089.11
M98	10154.20	6224.36
M99	21807.23	11707.21
M100	4421.04	4468.95
M102	1976.77	913.67
M103	1737.37	3047.99
M104	969.24	975.12
M105	212.19	678.30
m106	1746.26	10241.06
m107	758.79	1097.79
m108	807.63	1265.53
M114	3506.45	7211.36
M115	1744.35	7040.02
M116	2518.07	15557.55
m117	159.65	462.08
m117.1	429.43	319.25
m119.1	3854.00	10206.46
m119.2	23251.24	37881.42
m119.3	10754.20	22989.07
m119.4	675.42	1983.74
m119.5	956.23	2433.74
m120	1157.14	2589.04
M121	1006.00	2036.36
m123.1	1939.95	2568.53
m123Ex2	1334.61	17695.88
m124	2027.66	2604.08
m124.1	2139.53	2825.48
m125	189.48	462.56
m126	651.76	606.24
m127	961.96	466.29
m128Ex3	14168.10	1558.68
m129	1735.75	975.14
m130	854.40	876.75
m131	1745.78	5204.26
m134	346.21	842.75
m135	329.48	689.94
m136	499.92	1020.31

m137	1127.55	465.67
m138	9058.16	11828.90
m139	1556.04	1936.82
m140	1246.91	1584.31
m141	948.10	549.25
m142	4596.51	1686.06
m143	2271.68	787.06
m144	1229.17	979.22
m145	4793.37	6019.59
m146	806.72	1286.90
m147	8479.73	4861.80
m148	9795.94	4901.75
m149	1647.88	711.07
m150	393.19	126.85
m151	820.54	265.23
m152	5332.65	1753.75
m153	3713.57	668.97
m154	4819.35	2765.75
m155	8033.29	8851.13
m156	4393.81	4630.81
m157	2068.70	3224.77
m158	1900.56	1436.99
m159	2357.08	4094.72
m160	9475.34	9128.93
m161	9764.30	6796.84
m162	8741.80	5591.35
m163	4804.45	6466.56
m164	2925.58	1529.13
m165	1402.98	627.56
m166	6583.85	3190.94
m167	2232.83	776.97
m168	109476.50	136174.82
m169	115203.56	116098.37
m170	225.54	261.80

Appendix 3.3. SNP analysis between MCMV-GFP and MW97.01 viral transcripts.

Chromosome	Position	Reference	SNP	Quality	Genome	Gene Region
GU305914.1	238	T	A	91.28	MCMV-GFP	left terminal
GU305914.1	251	T	A	140.03	MCMV-GFP	left terminal
GU305914.1	289	T	G	142.03	MCMV-GFP	left terminal
GU305914.1	1395	G	C	624.77	MCMV-GFP	m02
GU305914.1	1401	G	A	376.78	MCMV-GFP	m02
GU305914.1	1496	G	A	1039.77	MCMV-GFP	m02
GU305914.1	1527	C	T	421.77	MCMV-GFP	m02
GU305914.1	1603	C	T	107.28	MCMV-GFP	m02
GU305914.1	1755	A	G	1305.77	MCMV-GFP	m02
GU305914.1	2923	C	T	839.77	MW97.01	m03
GU305914.1	2935	A	G	1411.77	MW97.01	m03
GU305914.1	3020	A	T	539.77	MW97.01	m03
GU305914.1	3023	A	G	424.77	MW97.01	m03
GU305914.1	3061	T	A	904.77	MW97.01	intergenic
GU305914.1	3620	A	G	3787.77	MW97.01	m04
GU305914.1	3638	T	G	1716.77	MW97.01	m04
GU305914.1	3649	C	A	2363.77	MW97.01	m04
GU305914.1	3717	T	C	2187.77	MW97.01	m04
GU305914.1	3727	G	C	1240.77	MW97.01	m04
GU305914.1	4272	C	T	6349.77	MW97.01	m05
GU305914.1	4294	C	T	930.77	MW97.01	m05
GU305914.1	4404	C	T	1522.77	MW97.01	m05
GU305914.1	4456	G	C	908.77	MW97.01	m05
GU305914.1	4520	A	G	451.77	MW97.01	m05
GU305914.1	4628	G	A	3175.77	MW97.01	m05
GU305914.1	4668	G	C	1986.77	MW97.01	m05
GU305914.1	4716	C	T	1159.77	MW97.01	m05
GU305914.1	4717	G	A	1159.77	MW97.01	m05
GU305914.1	4822	G	A	233.84	MW97.01	m05
GU305914.1	4913	G	A	871.8	MW97.01	m05
GU305914.1	4940	G	A	922.28	MW97.01	m05
GU305914.1	5072	C	T	3378.77	MW97.01	m05
GU305914.1	5103	A	G	2566.77	MW97.01	m05
GU305914.1	5133	C	A	691.77	MW97.01	m05
GU305914.1	5147	C	T	1276.77	MW97.01	m05
GU305914.1	5261	A	T	7693.77	MW97.01	intergenic
GU305914.1	5277	C	A	7021.77	MW97.01	intergenic
GU305914.1	5593	G	A	12882.77	MW97.01	m06
GU305914.1	5638	C	T	11253.77	MW97.01	m06
GU305914.1	6502	T	C	62.74	MCMV-GFP	m07

GU305914.1	6542	A	G	331.78	MCMV-GFP	m07
GU305914.1	6571	A	G	152.03	MCMV-GFP	m07
GU305914.1	7420	C	T	236.84	MCMV-GFP	intergenic
GU305914.1	7740	C	A	376.78	MCMV-GFP	m08
GU305914.1	8232	A	C	290.78	MCMV-GFP	m08
GU305914.1	8326	A	G	276.8	MCMV-GFP	m08
GU305914.1	8339	C	T	641.77	MCMV-GFP	m08
GU305914.1	8445	T	C	646.77	MCMV-GFP	m08
GU305914.1	8486	A	G	1261.77	MCMV-GFP	m08
GU305914.1	8895	G	C	62.74	MCMV-GFP	m09
GU305914.1	8994	A	G	62.74	MCMV-GFP	m09
GU305914.1	9135	A	G	107.28	MCMV-GFP	m09
GU305914.1	12052	G	A	5989.77	MW97.01	m12
GU305914.1	12900	C	T	5365.77	MCMV-GFP	m13
GU305914.1	13177	C	A	1491.77	MCMV-GFP	m14
GU305914.1	13502	A	G	1682.77	MCMV-GFP	m14
GU305914.1	13543	A	G	2074.77	MCMV-GFP	m14
GU305914.1	13685	T	G	2047.77	MCMV-GFP	m14
GU305914.1	13751	A	G	265.94	MCMV-GFP	m14
GU305914.1	13754	C	T	277.8	MCMV-GFP	m14
GU305914.1	14052	C	G	1100.77	MCMV-GFP	intergenic
GU305914.1	14940	A	G	196.9	MCMV-GFP	m15
GU305914.1	15032	A	C	1498.77	MCMV-GFP	m15
GU305914.1	15101	G	A	817.8	MCMV-GFP	m16
GU305914.1	15133	G	T	241.84	MCMV-GFP	m16
GU305914.1	15361	G	A	152.03	MCMV-GFP	m16
GU305914.1	15592	C	T	62.74	MCMV-GFP	m16
GU305914.1	15734	C	A	1190.77	MCMV-GFP	intergenic
GU305914.1	15982	A	C	62.74	MCMV-GFP	m17
GU305914.1	16006	C	T	376.78	MCMV-GFP	m17
GU305914.1	18442	T	G	3647.77	MCMV-GFP	m18
GU305914.1	19229	C	T	107.28	MCMV-GFP	m18
GU305914.1	19896	T	C	286.8	MCMV-GFP	m18
GU305914.1	21692	G	A	2122.77	MCMV-GFP	m20
GU305914.1	21770	T	G	2859.77	MCMV-GFP	m20
GU305914.1	21831	G	C	556.77	MCMV-GFP	m20
GU305914.1	22058	C	T	46.31	MCMV-GFP	m20
GU305914.1	22222	T	C	617.77	MCMV-GFP	m20
GU305914.1	22231	A	T	653.78	MCMV-GFP	m20
GU305914.1	22737	G	C	4010.77	MCMV-GFP	m20/m21
GU305914.1	24338	A	C	259.56	MCMV-GFP	M23
GU305914.1	25281	T	C	331.78	MCMV-GFP	M24
GU305914.1	25301	C	T	196.9	MCMV-GFP	M24

GU305914.1	27030	G	A	644.77	MCMV-GFP	M25
GU305914.1	27798	G	T	107.28	MCMV-GFP	M25
GU305914.1	27918	T	G	653.78	MCMV-GFP	M25
GU305914.1	28047	G	A	693.1	MCMV-GFP	M25
GU305914.1	28137	A	G	1071.77	MCMV-GFP	M25
GU305914.1	28797	G	A	286.8	MCMV-GFP	M25
GU305914.1	28820	T	A	376.78	MCMV-GFP	intergenic
GU305914.1	28844	A	C	376.78	MCMV-GFP	intergenic
GU305914.1	28863	C	T	457.77	MCMV-GFP	intergenic
GU305914.1	29231	G	A	3734.77	MCMV-GFP	m25.1/m25.2
GU305914.1	29423	T	C	4776.77	MCMV-GFP	m25.1/m25.2
GU305914.1	29492	G	A	2439.77	MCMV-GFP	m25.1/m25.2
GU305914.1	29731	C	T	614.77	MCMV-GFP	m25.1/m25.2
GU305914.1	30088	G	A	455.77	MCMV-GFP	m25.1/m25.2
GU305914.1	30095	C	T	466.77	MCMV-GFP	m25.1/m25.2
GU305914.1	30214	T	C	98.89	MCMV-GFP	m25.1/m25.2
GU305914.1	30289	T	C	7275.77	MCMV-GFP	m25.1/m25.3/m25.4
GU305914.1	30443	T	C	501.77	MCMV-GFP	m25.1/m25.3/m25.4
GU305914.1	33616	T	C	312.78	MCMV-GFP	M27
GU305914.1	34140	A	C	522.77	MCMV-GFP	M27
GU305914.1	34861	G	A	856.77	MCMV-GFP	M28
GU305914.1	34867	T	C	686.77	MCMV-GFP	M28
GU305914.1	34900	G	A	505.77	MCMV-GFP	M28
GU305914.1	35044	G	C	3101.77	MCMV-GFP	M28
GU305914.1	35176	T	C	1775.77	MCMV-GFP	M28
GU305914.1	35224	A	G	1341.77	MCMV-GFP	M28
GU305914.1	35944	G	C	4150.77	MCMV-GFP	m29
GU305914.1	36900	A	T	2062.77	MCMV-GFP	m30
GU305914.1	37213	T	C	107.28	MCMV-GFP	m30
GU305914.1	40003	C	T	4579.77	MW97.01	M32
GU305914.1	41971	C	A	1314.77	MCMV-GFP	intergenic
GU305914.1	42604	A	C	1783.77	MCMV-GFP	intergenic
GU305914.1	43271	T	C	1166.77	MCMV-GFP	M34
GU305914.1	43283	G	A	991.77	MCMV-GFP	M34
GU305914.1	44580	T	A	594.77	MCMV-GFP	M34
GU305914.1	49931	C	A	8471.77	MCMV-GFP	M37
GU305914.1	51521	T	C	6672.77	MCMV-GFP	M38
GU305914.1	51701	G	A	4048.77	MCMV-GFP	M38
GU305914.1	55972	C	A	47.77	MW97.01	M43
GU305914.1	64840	A	C	43.77	MCMV-GFP	intergenic
GU305914.1	69989	A	G	152.03	MCMV-GFP	intergenic
GU305914.1	69989	A	G	320.78	MW97.01	intergenic
GU305914.1	69997	T	C	184.9	MCMV-GFP	intergenic

GU305914.1	69997	T	C	376.78	MW97.01	intergenic
GU305914.1	70159	G	A	152.03	MW97.01	intergenic
GU305914.1	71530	T	C	331.78	MCMV-GFP	intergenic
GU305914.1	71530	T	C	942.77	MW97.01	intergenic
GU305914.1	71585	C	A	538.77	MCMV-GFP	intergenic
GU305914.1	71585	C	A	1221.77	MW97.01	intergenic
GU305914.1	71675	T	C	920.77	MCMV-GFP	intergenic
GU305914.1	71675	T	C	1216.77	MW97.01	intergenic
GU305914.1	72179	T	C	374.78	MCMV-GFP	intergenic
GU305914.1	72179	T	C	386.77	MW97.01	intergenic
GU305914.1	72238	G	A	546.77	MCMV-GFP	intergenic
GU305914.1	72238	G	A	1087.77	MW97.01	intergenic
GU305914.1	72364	A	G	947.78	MCMV-GFP	intergenic
GU305914.1	72364	A	G	2311.77	MW97.01	intergenic
GU305914.1	72418	G	A	754.77	MCMV-GFP	intergenic
GU305914.1	72418	G	A	2092.77	MW97.01	intergenic
GU305914.1	72531	A	G	1375.77	MCMV-GFP	intergenic
GU305914.1	72531	A	G	1711.77	MW97.01	intergenic
GU305914.1	72928	G	A	833.77	MCMV-GFP	intergenic
GU305914.1	72928	G	A	2113.77	MW97.01	intergenic
GU305914.1	75584	G	A	481.9	MCMV-GFP	M50
GU305914.1	75584	G	A	1883.77	MW97.01	M50
GU305914.1	75907	G	A	367.78	MCMV-GFP	M50
GU305914.1	75907	G	A	917.77	MW97.01	M50
GU305914.1	75943	T	A	691.77	MW97.01	M50
GU305914.1	75997	G	A	556.77	MCMV-GFP	M50
GU305914.1	75997	G	A	1076.77	MW97.01	M50
GU305914.1	76113	G	A	1947.77	MCMV-GFP	M50
GU305914.1	76113	G	A	4933.77	MW97.01	M50
GU305914.1	77761	A	G	145.41	MCMV-GFP	M52
GU305914.1	77761	A	G	641.28	MW97.01	M52
GU305914.1	77769	A	T	46.77	MCMV-GFP	M52
GU305914.1	77800	A	G	201.78	MW97.01	M52
GU305914.1	78932	T	C	3968.77	MCMV-GFP	M53
GU305914.1	78932	T	C	4453.77	MW97.01	M53
GU305914.1	79373	A	G	2584.77	MCMV-GFP	M53
GU305914.1	79373	A	G	1941.77	MW97.01	M53
GU305914.1	80122	A	C	2171.77	MCMV-GFP	intergenic
GU305914.1	80122	A	C	3163.77	MW97.01	intergenic
GU305914.1	81309	G	A	1190.77	MCMV-GFP	intergenic
GU305914.1	81309	G	A	1086.77	MW97.01	intergenic
GU305914.1	81357	G	T	1747.77	MCMV-GFP	intergenic
GU305914.1	81357	G	T	1558.77	MW97.01	intergenic

GU305914.1	81760	T	C	482.9	MCMV-GFP	intergenic
GU305914.1	81760	T	C	3374.77	MW97.01	intergenic
GU305914.1	81961	G	A	1841.77	MCMV-GFP	intergenic
GU305914.1	81961	G	A	3584.77	MW97.01	intergenic
GU305914.1	82635	A	C	152.03	MW97.01	intergenic
GU305914.1	83122	T	G	13983.77	MCMV-GFP	M55
GU305914.1	83122	T	G	19428.77	MW97.01	M55
GU305914.1	83801	G	A	365.78	MCMV-GFP	M55
GU305914.1	83801	G	A	488.77	MW97.01	M55
GU305914.1	83883	G	A	2514.77	MCMV-GFP	M55
GU305914.1	83883	G	A	4001.77	MW97.01	M55
GU305914.1	83904	G	T	556.77	MCMV-GFP	M55
GU305914.1	83904	G	T	601.77	MW97.01	M55
GU305914.1	83925	C	T	887.77	MCMV-GFP	M55
GU305914.1	83925	C	T	1270.77	MW97.01	M55
GU305914.1	84283	C	G	482.77	MCMV-GFP	M55
GU305914.1	84283	C	G	2220.77	MW97.01	M55
GU305914.1	84417	A	G	151.9	MCMV-GFP	M55
GU305914.1	84417	A	G	249.56	MW97.01	M55
GU305914.1	84567	C	T	11125.77	MCMV-GFP	M55
GU305914.1	84567	C	T	22890.77	MW97.01	M55
GU305914.1	84634	C	T	9524.77	MCMV-GFP	M55
GU305914.1	84634	C	T	20122.77	MW97.01	M55
GU305914.1	84702	G	A	2934.77	MCMV-GFP	M55
GU305914.1	84702	G	A	5030.77	MW97.01	M55
GU305914.1	84714	C	T	1851.77	MCMV-GFP	M55
GU305914.1	84714	C	T	2875.77	MW97.01	M55
GU305914.1	84867	A	G	2246.77	MCMV-GFP	M55
GU305914.1	84867	A	G	3765.77	MW97.01	M55
GU305914.1	84888	T	C	688.77	MCMV-GFP	M55
GU305914.1	84888	T	C	357.98	MW97.01	M55
GU305914.1	84926	T	C	2482.77	MCMV-GFP	M55
GU305914.1	84926	T	C	1497.77	MW97.01	M55
GU305914.1	84990	A	G	6651.77	MCMV-GFP	M55
GU305914.1	84990	A	G	11683.77	MW97.01	M55
GU305914.1	85158	T	C	13025.77	MCMV-GFP	M55
GU305914.1	85158	T	C	20834.77	MW97.01	M55
GU305914.1	85182	C	T	9811.77	MCMV-GFP	M55
GU305914.1	85182	C	T	14959.77	MW97.01	M55
GU305914.1	85223	T	C	37.77	MCMV-GFP	M55
GU305914.1	85224	T	C	120.77	MCMV-GFP	M55
GU305914.1	85224	T	C	414.77	MW97.01	M55
GU305914.1	85230	T	C	52.77	MCMV-GFP	M55

GU305914.1	85230	T	C	49.77	MW97.01	M55
GU305914.1	85250	T	C	852.77	MCMV-GFP	M55
GU305914.1	85250	T	C	862.78	MW97.01	M55
GU305914.1	85272	G	A	3196.77	MCMV-GFP	M55
GU305914.1	85272	G	A	6119.77	MW97.01	M55
GU305914.1	85308	A	G	4789.77	MCMV-GFP	M55
GU305914.1	85308	A	G	7414.77	MW97.01	M55
GU305914.1	85353	A	G	426.77	MCMV-GFP	M55
GU305914.1	85353	A	G	474.77	MW97.01	M55
GU305914.1	85410	T	C	1375.77	MCMV-GFP	M55
GU305914.1	85410	T	C	1163.89	MW97.01	M55
GU305914.1	85475	C	A	3950.77	MCMV-GFP	M55
GU305914.1	85475	C	A	6118.77	MW97.01	M55
GU305914.1	85523	C	T	3398.77	MCMV-GFP	M55
GU305914.1	85523	C	T	6439.77	MW97.01	M55
GU305914.1	85536	T	C	3509.77	MCMV-GFP	M55
GU305914.1	85536	T	C	5602.77	MW97.01	M55
GU305914.1	87763	G	A	236.84	MCMV-GFP	M56
GU305914.1	87763	G	A	1437.77	MW97.01	M56
GU305914.1	89134	G	A	4808.77	MCMV-GFP	intergenic
GU305914.1	89134	G	A	4558.77	MW97.01	intergenic
GU305914.1	89798	T	C	1737.77	MCMV-GFP	intergenic
GU305914.1	89798	T	C	3490.77	MW97.01	intergenic
GU305914.1	90978	G	A	6479.77	MCMV-GFP	intergenic
GU305914.1	90978	G	A	14783.77	MW97.01	intergenic
GU305914.1	94538	A	G	436.77	MCMV-GFP	intergenic
GU305914.1	94538	A	G	2290.77	MW97.01	intergenic
GU305914.1	94659	A	G	556.77	MCMV-GFP	intergenic
GU305914.1	94659	A	G	681.77	MW97.01	intergenic
GU305914.1	94681	A	G	646.77	MCMV-GFP	intergenic
GU305914.1	94681	A	G	781.77	MW97.01	intergenic
GU305914.1	94710	C	T	98.89	MCMV-GFP	intergenic
GU305914.1	94710	C	T	87.82	MW97.01	intergenic
GU305914.1	94717	A	G	55.31	MCMV-GFP	intergenic
GU305914.1	94717	A	G	219.77	MW97.01	intergenic
GU305914.1	94811	T	C	196.9	MW97.01	intergenic
GU305914.1	94838	C	T	376.78	MCMV-GFP	intergenic
GU305914.1	94838	C	T	736.77	MW97.01	intergenic
GU305914.1	95146	C	T	470.77	MCMV-GFP	intergenic
GU305914.1	95146	C	T	1340.77	MW97.01	intergenic
GU305914.1	95358	G	A	142.03	MCMV-GFP	intergenic
GU305914.1	95358	G	A	406.77	MW97.01	intergenic
GU305914.1	95374	A	G	132.03	MCMV-GFP	intergenic

GU305914.1	95374	A	G	376.78	MW97.01	intergenic
GU305914.1	95424	C	T	245.74	MW97.01	intergenic
GU305914.1	95475	G	T	196.9	MW97.01	intergenic
GU305914.1	95578	C	T	227.1	MW97.01	intergenic
GU305914.1	95607	G	T	62.74	MW97.01	intergenic
GU305914.1	95611	G	T	98.28	MW97.01	intergenic
GU305914.1	95682	T	C	143.03	MW97.01	intergenic
GU305914.1	99869	A	C	107.28	MCMV-GFP	M70
GU305914.1	99869	A	C	816.77	MW97.01	M70
GU305914.1	103872	T	C	405.77	MW97.01	M72
GU305914.1	103881	G	A	93.96	MW97.01	M72
GU305914.1	103932	T	C	476.77	MW97.01	M72
GU305914.1	104022	T	A	2562.77	MW97.01	M72
GU305914.1	104106	A	G	2422.77	MW97.01	M72
GU305914.1	104287	A	G	11563.77	MW97.01	M72/M73
GU305914.1	104399	A	G	4059.77	MW97.01	M73
GU305914.1	104763	T	C	1201.77	MW97.01	m74
GU305914.1	104786	T	C	489.77	MW97.01	m74
GU305914.1	104818	C	T	152.03	MW97.01	m74
GU305914.1	104848	C	G	492.79	MW97.01	m74
GU305914.1	104864	A	G	268.56	MW97.01	m74
GU305914.1	104886	T	C	662.78	MW97.01	m74
GU305914.1	104910	A	C	164.77	MW97.01	m74
GU305914.1	104911	T	C	164.77	MW97.01	m74
GU305914.1	104949	C	T	1881.77	MW97.01	m74
GU305914.1	105033	G	C	321.78	MW97.01	m74
GU305914.1	105042	T	C	367.78	MW97.01	m74
GU305914.1	105138	A	G	4256.77	MW97.01	m74
GU305914.1	105159	A	G	444.22	MW97.01	m74
GU305914.1	105160	T	G	444.22	MW97.01	m74
GU305914.1	106225	A	G	276.94	MW97.01	M75
GU305914.1	106268	G	A	607.77	MW97.01	M75
GU305914.1	106295	T	C	1151.77	MW97.01	M75
GU305914.1	106394	G	T	2982.77	MW97.01	M75
GU305914.1	106412	T	C	4118.77	MW97.01	M75
GU305914.1	106571	G	A	231.84	MW97.01	M75
GU305914.1	106577	G	A	309.78	MW97.01	M75
GU305914.1	106658	A	G	4600.77	MW97.01	M75
GU305914.1	106754	G	A	860.77	MW97.01	M75
GU305914.1	106907	C	T	1450.77	MW97.01	M75
GU305914.1	106955	C	A	1006.77	MW97.01	M75
GU305914.1	106973	C	T	3727.77	MW97.01	M75
GU305914.1	107015	T	C	4774.77	MW97.01	M75

GU305914.1	107125	A	G	4156.77	MW97.01	M75
GU305914.1	107159	T	A	2022.77	MW97.01	M75
GU305914.1	107248	A	C	366.78	MW97.01	M75
GU305914.1	107300	A	G	245.8	MW97.01	M75
GU305914.1	107369	T	C	1299.77	MW97.01	M75
GU305914.1	108311	C	T	232.1	MW97.01	M75
GU305914.1	108565	T	C	2693.77	MW97.01	M76
GU305914.1	108850	T	C	1126.77	MW97.01	M76
GU305914.1	111195	G	A	26301.77	MW97.01	M78
GU305914.1	111998	T	C	1122.77	MW97.01	M78
GU305914.1	112104	C	T	6055.77	MW97.01	M78
GU305914.1	112424	A	C	9527.77	MW97.01	M78
GU305914.1	113163	C	T	411.79	MW97.01	M79
GU305914.1	113193	C	T	107.28	MW97.01	M79
GU305914.1	114348	T	C	152.03	MW97.01	M80
GU305914.1	114789	T	G	1108.77	MW97.01	M80
GU305914.1	115167	C	T	4677.77	MW97.01	M80
GU305914.1	115311	A	C	196.9	MW97.01	M80
GU305914.1	115349	T	C	455.77	MW97.01	M80
GU305914.1	115437	A	G	1526.77	MW97.01	M80
GU305914.1	115503	G	A	4007.77	MW97.01	M80
GU305914.1	115542	A	G	4809.77	MW97.01	M80
GU305914.1	117408	G	C	1379.77	MW97.01	M82
GU305914.1	117495	C	T	1848.77	MW97.01	M82
GU305914.1	117528	G	A	1090.77	MW97.01	M82
GU305914.1	117570	T	C	603.77	MW97.01	M82
GU305914.1	117886	A	G	1571.77	MW97.01	M83
GU305914.1	117907	A	G	7352.77	MW97.01	M83
GU305914.1	118078	T	C	16505.77	MW97.01	M83
GU305914.1	118096	A	G	12588.77	MW97.01	M83
GU305914.1	118146	C	A	3011.77	MW97.01	M83
GU305914.1	118184	G	T	826.77	MW97.01	M83
GU305914.1	118709	G	A	2206.77	MW97.01	M83
GU305914.1	118810	C	G	10721.77	MW97.01	M83
GU305914.1	118855	T	C	181.9	MW97.01	M83
GU305914.1	119260	C	G	363.94	MW97.01	M83
GU305914.1	119262	T	C	363.94	MW97.01	M83
GU305914.1	120408	C	T	806.77	MW97.01	M84
GU305914.1	120624	T	C	310.85	MW97.01	M84
GU305914.1	120990	A	C	895.77	MW97.01	M84
GU305914.1	121083	C	T	896.85	MW97.01	M84
GU305914.1	121185	A	G	2419.77	MW97.01	M84
GU305914.1	121215	C	T	1897.77	MW97.01	M84

GU305914.1	121314	C	T	3469.77	MW97.01	M84
GU305914.1	121384	G	A	1896.77	MW97.01	M84
GU305914.1	121989	G	A	768.78	MW97.01	intergenic
GU305914.1	122611	T	G	10209.77	MW97.01	M85
GU305914.1	131240	A	G	2835.77	MW97.01	M88
GU305914.1	131285	G	C	1976.77	MW97.01	M88
GU305914.1	132742	A	G	1979.77	MW97.01	intergenic
GU305914.1	136546	C	T	1896.77	MW97.01	M94
GU305914.1	136550	T	C	1944.77	MW97.01	M94
GU305914.1	136670	A	C	6475.77	MW97.01	M94
GU305914.1	136733	A	G	5202.77	MW97.01	M94
GU305914.1	136834	A	G	10278.77	MW97.01	M94
GU305914.1	136899	G	C	27664.77	MW97.01	M94
GU305914.1	137020	C	T	70.77	MW97.01	M94
GU305914.1	137021	A	C	70.77	MW97.01	M94
GU305914.1	137032	C	T	773.22	MW97.01	M94
GU305914.1	137112	T	C	7963.77	MW97.01	M94
GU305914.1	137257	G	C	4162.77	MW97.01	M94
GU305914.1	137378	G	A	1866.77	MW97.01	intergenic
GU305914.1	137382	T	G	1191.74	MW97.01	intergenic
GU305914.1	137452	A	C	861.77	MW97.01	intergenic
GU305914.1	137940	C	T	4444.77	MW97.01	intergenic
GU305914.1	140968	T	C	2840.77	MW97.01	M97
GU305914.1	146950	G	A	586.78	MW97.01	M102
GU305914.1	160830	G	A	62.74	MCMV-GFP	intergenic
GU305914.1	161416	A	T	185.9	MCMV-GFP	intergenic
GU305914.1	161965	T	C	884.77	MCMV-GFP	intergenic
GU305914.1	162095	A	G	49.77	MCMV-GFP	m107
GU305914.1	162293	T	G	681.77	MCMV-GFP	m107
GU305914.1	162392	A	G	922.77	MCMV-GFP	m107/m108
GU305914.1	162475	A	G	112.77	MCMV-GFP	m107/m108
GU305914.1	166389	T	C	461.77	MCMV-GFP	M114
GU305914.1	166663	G	T	825.77	MCMV-GFP	M115
GU305914.1	166874	C	T	168.77	MCMV-GFP	M115
GU305914.1	167459	T	C	34.77	MW97.01	M116
GU305914.1	172735	T	C	2030.77	MCMV-GFP	m119.1
GU305914.1	173967	G	A	2386.77	MCMV-GFP	intergenic
GU305914.1	179236	G	A	2288.77	MW97.01	intergenic
GU305914.1	190871	T	C	449.77	MCMV-GFP	m136
GU305914.1	208129	A	G	321.78	MW97.01	m150
GU305914.1	208135	A	G	236.84	MW97.01	m150
GU305914.1	208169	C	G	591.77	MW97.01	m150
GU305914.1	208469	G	A	232.1	MW97.01	m150

GU305914.1	208558	A	G	196.9	MW97.01	m150
GU305914.1	208674	G	C	107.28	MW97.01	m150
GU305914.1	208733	C	G	62.74	MW97.01	m150
GU305914.1	208854	T	C	62.74	MW97.01	m150
GU305914.1	208937	T	C	1361.77	MW97.01	m151
GU305914.1	209086	T	C	1620.77	MW97.01	m151
GU305914.1	209175	C	T	1155.77	MW97.01	m151
GU305914.1	209213	A	G	95.28	MW97.01	m151
GU305914.1	209871	C	T	365.78	MW97.01	m151
GU305914.1	210036	T	C	98.89	MW97.01	m151
GU305914.1	210111	G	A	496.77	MW97.01	intergenic
GU305914.1	210291	G	A	1309.85	MW97.01	intergenic
GU305914.1	210387	A	G	2717.77	MW97.01	m152
GU305914.1	210795	C	T	2370.77	MW97.01	m152
GU305914.1	213992	G	A	276.94	MW97.01	m154
GU305914.1	214019	G	C	331.78	MW97.01	m154
GU305914.1	214323	A	G	698.77	MW97.01	intergenic
GU305914.1	214432	C	T	375.78	MW97.01	intergenic
GU305914.1	214577	G	T	4280.77	MW97.01	m155
GU305914.1	214704	A	G	996.79	MW97.01	m155
GU305914.1	214706	C	T	996.79	MW97.01	m155
GU305914.1	214733	G	A	2207.77	MW97.01	m155
GU305914.1	214821	C	T	2147.77	MW97.01	m155
GU305914.1	214871	T	C	1496.77	MW97.01	m155
GU305914.1	215603	T	C	17357.77	MW97.01	m155
GU305914.1	215627	A	G	13431.77	MW97.01	m155
GU305914.1	215746	A	C	3984.77	MW97.01	m156
GU305914.1	216930	G	T	546.77	MCMV-GFP	m157
GU305914.1	217234	A	G	1621.77	MW97.01	m158
GU305914.1	222767	C	T	3276.77	MW97.01	m164
GU305914.1	227424	A	G	187.9	MW97.01	intergenic
GU305914.1	230177	T	G	152.03	MCMV-GFP	intergenic

Appendix 4.1. PCR primer list for Chapter 4.

Cloning of m02 family and m145 family

Please refer to **Appendix 3.1** for these primer sequences.

N-terminally HA tagging m153

Gene	Primer	Sequence (5'-3')
$m153^{N\text{-}HA}$	m153 NT-HA Fwd1	TTGCTTACCCATACGATGTTCCAGATTACGCTGGATCAGGATCAGAG GTCGTGCGGCCCGAAGT
	m153 NT-HA Xho F2	gcctcgagATGTCTGCACTTCTGATCCTAGCTCTTGTTGGAGCTGCAGTTG CTTACCCATACGATGTT
	m153 NotI R	ggcggccgcTCACACCACATTCTCCTCCGTA

Construction of type-I m153 Reporters

Gene	Primer	Sequence (5'-3')
m153 EC	m153 XhoI ATG Fwd	gctcgagATGATTCCCCTTCTCCTTCTGCCG
	m153 NF-PSP Fwd	gcctcgagATGTCTGCACTTCTGATCCTAGCT
	m153 EC Rev	tagcggccgcGGTCAGTCTCGAATCGTTGATCGTCCTCTGG

Construction of Tet-Inducible pTRIPZ vectors

Gene	Primer	Sequence (5'-3')
m153	m153 NT-HA AgeI-ATG F	ataaccggtcgccaccATGTCTGCACTTCTGATCCTAGC
	m153 XhoI-TGA R	tatctcgagTCACACCACATTCTCCTCCGTATCCG
Clr-b	Clr-b AgeI-ATG F	ataaccggtcgccaccATGTGTGTCACAAAGGCTTCC
	Clr-b C-FLAG XhoI-TGA R	tatctcgagCTACTTGTCGTCGTCGTCCTTGTAGTCTGATCCTGATCCGGAA GGAAAAAAAGGAGTTTGG

Construction of Fusion constructs

Gene	Primer	Sequence (5'-3')
m153	m153 fusion XhoI F	ggactcagatctcgagcgccaccATGTCTGCACTTCTGATCCTAGCTCTTGTTGGA GC
	m153 fusion BamHI R	ggcgaccggtggatccCCTGATCCTGATCCCACCACATTCTCCTCCGTATCCG AGCACTCG
Clr-b	Clr-b fusion XhoI F	atctcgagGATCAGGATCAATGTGTGTCACAAAGGCTTCC
	Clr-b fusion BamHI R	gtggatccTCACTTGTCGTCGTCGTCCTTGTAGTCTGATCCTGATCCGGAA GGAAAAAAAGGAGTTTGGCAGTGG

qRT-PCR primers

Gene	Primer	Sequence (5'-3')
m153	m153 qPCR Fwd	GTGTCAGATGACGACCCAGG
	m153 qPCR Rev	TCTGACTTCTGTTGACCGGC